Tumour-Priming of Human Natural Killer Cells and the Impact of Tumour Microenvironment in Ovarian Cancer

A thesis submitted to University College London for the degree of Doctor of Philosophy

By

Xenia Charalambous

March 2022

Supervisor: Prof Mark W Lowdell

Department of Haematology

University College London, Cancer Institute

Faculty of Medical Sciences

Statement of Originality

I, Xenia Charalambous, confirm that the work presented in this thesis is my own. Where information has been derived from other sources, I confirm that this has been indicated in the thesis.

Abstract

Ovarian cancer is the most deadly gynaecological malignancy due to its asymptomatic nature and late detection. First-line treatments include a combination of surgery and chemotherapy. However, the limitation of current treatments results in relapse with chemoresistant residual tumour cells. The presence of immune cells, including the natural killer (NK) cells in the tumour site and malignant ascites, have diverted the focus towards immunotherapy.

In this project, NK cells derived from ovarian cancer patients (OCPs) were either isolated from the peripheral blood (PB) or the ascites to compare NK cells in circulation and at the tumour site. Subsequently, the OCP-derived NK cells were compared to NK cells isolated from the PB of healthy volunteered donors (HDs). Herein, is the first time to show a comparison of OCP-derived NK cells and HD-derived NK cells using extensive immunophenotypic panels. Results obtained, revealed an activated phenotype of ascites-derived NK cells via downregulation of CD16 and upregulation of CD2 and CD69 surface markers. However, ascites-derived NK cells exhibited impaired cytotoxic function compared to HD-derived NK cells.

Additionally, the downregulation of CD15 levels suggests the potential mechanism behind resistance against NK cell cytotoxicity in ovarian cancer after comparison of the NK cell-resistant SKOV3 and NK cell-sensitive OVCAR3 epithelial ovarian cancer target cells.

Moreover, herein, is the first time to show tumour-induced mediated priming of NK cells using the INB16 cell line, a pharmaceutical-grade subline of the original CTV-1 acute monoblastic leukemic cell line against solid tumours, including ovarian cancer. This resulted in successful NK cell activation via downregulation of CD16 and upregulation of CD69 even in the presence of an immunosuppressive low-oxygen (hypoxic) tumour. It is also the first time to demonstrate the interaction between NK cells and ovarian target cells using novel platforms such as the eSIGHT Live Cell Analyser and z-Movi Cell Avidity Analyser.

Impact Statement

The research presented in this project, has enhanced the understanding on NK cell immunotherapy in ovarian cancer. The pioneer investigation of tumour priming using the INB16 leukaemic target cell line as an alternative priming agent for NK cells, has created the foundation for pivotal studies, future experimental designs and methodological approaches in the academic setting. In addition, the results obtained here, have demonstrated successful enhancement of INB16 tumour-induced mediated priming on NK cell responsiveness against NK-insensitive ovarian cancer target cells as well as against the hypoxic Tumour Microenvironment (TME). Therefore this can encourage its clinical use as a novel therapeutic approach in ovarian cancer as well as in a broader spectrum of malignancies either as a single agent or in combination with other current therapies in the cancer field.

Acknowledgements

Last but not least, a profound thank you to my family and my friends for their continuous support and understanding and for never stop believing in me and lifting me up in moments of doubts and difficulties. Your love was the fuel to carry on with this journey. Thank you also to the new family member, my lovely niece, that came to our lives during this project and made this journey even more unforgettable.

Table of Contents

List of Figures

List of Tables

Abbreviations

ADAM	A Disintegrin And Metalloprotease
ADCC	Antibody Dependent Cellular Cytotoxicity
AICL	Activation-induced C-type Lectin
ALL	Acute Lymphoblastic Leukaemia
AML	Acute Myeloid Leukaemia
ATCC	American Type Culture Collection
BCP	B-cell Precursor
BiKE	Bispecific Killer Engager
BM	Bone Marrow
BRCA1/2	Breast Cancer type 1 or 2
BSA	Bovine Serum Albumin
BSO	Bilateral Salpingo-Oopherectomy
CAF	Cancer-Associated Fibroblast
CAR	Chimeric Antigen RecOCPeptor
CD	Cluster of Differentiation
cGMP	current Good Manufacturing Practice
CHS	Contact Hypersensitivity
CIML	Cytokine-Induced Memory-Like
Clr	C-type lectin-related
CMV	Cytomegalovirus
CO$_2$	Carbon dioxide
CpNK	Co-primed NK cells
CSC	Cancer Stem Cell
CTLA-4	Cytotoxic T-Lymphocyte-associated protein 4
CTLR	C-type Lectin-like Receptor
DC	Dendritic Cell
DMSO	Dimethyl Sulfoxide Solution
DNA	Deoxyribonucleic Acid
DNAM-1	DNAX Accessory Molecule-1
DNFB	2,4-dinitrofluorobenzene
EDTA	ethylenediaminetetraacetic Acid

EOC	Epithelial Ovarian Cancer
EpCAM	Epithelial Cell Adhesion Molecule
FasL	Fas Ligand
FBS	Fetal Bovine Serum
FMO	Fluorescence Minus One
FRα	Folate Receptor alpha
FSC	Forward Scatter
GlyCAM-1	Glycosylation-Dependent Cell Adhesion Molecule
GM-CSF	Granulocyte-Macrophage Colony-Stimulating Factor
GM-CSF	Granulocyte-Macrophage Colony-Stimulating Factor
GSK3	Glycogen Synthase Kinase 3
GvHD	Graft-vs-Host Disease
HBSS	Hank's Balanced Salt Solution
HD	Healthy Donor
HDAC	Histone Deacetylase
HER2	Human Epidermal Growth Factor Receptor 2
HGS	High Grade Serous
HIF	Hypoxia Inducible Factor
HLA	Human Leukocyte Antigen
HLA-DR	Human Leukocyte Antigen – DR isotype
HPC	Hematopoietic Progenitor Cell
HRT	Hormone Replacement Therapy
HSC	Hematopoietic Stem Cell
HSP	Heat Shock Protein
ICAM	Inter-Cellular Adhesion Molecule
ICI	Immune-Checkpoint Inhibitor
IDO	Indoleamine 2,3-Dioxygenase
IFN-γ	Interferon-γ
Ig	Immunoglobulin
IL	Interleukin
ILCs	Innate Lymphoid Cells
ILDR	Immunoglobulin-like Domain-Containing Receptor
ILT	Immunoglobulin-like Transcript

ILT	Immunoglobulin-like Transcript
iNK	Immature Natural Killer Cell
IP	Intraperitoneal
iPSC	Induced Pluripotent Stem Cell
ITAM	Immunoreceptor Tyrosine-based Activation Motif
ITIM	Immune Tyrosine-based Inhibitory Motif
IV	Intravenously
KIR	Killer Cell Immunoglobulin-like Receptors
KIR	Killer Cell Ig-like Receptor
LFA	Lymphocyte Function-associated Antigen
LGS	Low Grade Serous
LIR	Leukocyte Immunoglobulin-like Receptor
mAb	Monoclonal antibody
MAC-1	Macrophage-1-Antigen
MALT	Mucosa-Associated Lymphoid Tissue
MDSC	Myeloid-Derived Suppressor Cell
MHC	Major Histocompatibility Complex
MIC	MHC class I chain-related protein
MMC	Mitomycin C
MMP	Matrix Metalloproteinase
MTOC	Microtubule Organizing Center
NCR	Natural Cytotoxic Receptors
NHSBT	National Health Service Blood and Transplant
NK	Natural Killer
NKC	Natural Killer Gene Complex
NKG	Natural Killer Group
NKR	NK Receptor
NSCL	Non-Small Cell Lung
O/N	Overnight
O$_2$	Oxygen
OCP	Ovarian Cancer Patient
OS	Overall Survival
OXA	Oxazolone

PARP	PolyADP-Ribose Polymerase
PB	Peripheral Blood
PBMC	Peripheral Blood Mononuclear Cell
PBS	Phosphate Buffer Saline
PD-1	Programmed Death-1
PFS	Progression Free Survival
PGE$_2$	Prostaglandin-E2
PMT	Photomultiplier Tubes
pre-NK	Natural Killer Cell Precursor
RAG	Recombination-Activating Gene
RCC	Renal Cell Carcinoma
RFH	Royal Free Hospital
RNA	Ribonucleic Acid
RPMI-	Roswell Park Memorial Institute medium with Glutamax
RT	Room Temperature
RTCA	Real-Time Cell Analysis
SCC	Side Scatter
SCID	Severe Combined Immunodeficiency
SHP	Src Homology containing Phosphatase
SLAM	Lymphocytic Activation Molecule
SLT	Secondary Lymphoid Tissue
SNARE	Soluble N-ethylmaleimide-sensitive-factor Accessory-protein Receptor
SRIR	Self-Recognizing Inhibitory Receptor
TAA	Tumour-Associated Antigen
TAM	Tumour-Associated Marophage
TIGIT	T Cell Immunoglobulin And Immunoreceptor Tyrosine-Based Inhibitory Motif (ITIM) Domain
TIL	Tumour Infiltrating Lymphocyte
TIML	Tumour-Induced Memory-Like
TME	Tumour Microenvironment
TNF-α	Tumour Necrosis Factor-α
TpNK	Tumour-primed NK cells

TRAIL	Tumour Necrosis Factor Related Apoptosis-Inducing Ligand
Treg	Regulatory T cell
TriKE	Trispecific Killer Engager
UCB	Umbilical Cord Blood
ULBP	HCMV UL16-binding protein
VCAM	Vascular Cell Adhesion Protein
VEGF	Vascular Endothelial Growth Factor

Chapter 1   INTRODUCTION

1.1 The Human Immune System

The immune system is the biological defence system of the body comprising of different cells, tissues and organs that orchestrate a dynamic network for the elimination of pathogens, viruses and cancer cells, leaving the healthy host cells intact. The immune system can be divided in two arms of immune responses, the innate and the adaptive, which exhibit variations in their mechanisms of time of response, antigen specificity and components. Despite their different mechanisms of action, these two arms can synergise for an intact fully sufficient immune response (Chaplin, 2010).

1.1.1 Innate Immunity

The innate system is the first line of defence and acts rapidly, within hours, against any pathogen to prevent the spread throughout the body. In order to express its immediate response upon the initial sensitising encounter, it relies on germline-encoded recognition and it is antigen independent. The innate immune system, includes the physical barriers that are constitutively active, such as epithelial cell layers and the mucociliary layer. It also encompasses soluble proteins and bioactive small molecules that are either continuously present in biological fluids, such as the collectins and ficolins in the plasma, or released upon immune cell activation, such as cytokines and chemokines. The innate immune system consists of a vast number of immune cells such as the natural killer (NK) cells, γ/δ T cells and

iNK cells of the lymphoid lineage, as well as, myeloid lineage macrophages, dendritic cells (DCs), neutrophils, mast cells, basophils and eosinophils (Chaplin, 2010).

1.1.2 Adaptive Immunity

The adaptive immune system, is exclusively found in vertebrates, it is more complex than the innate immune system and acts as the second line of defence. It is composed of a smaller number of cells, the B- and T-lymphocytes. They express great antigen specificity, thereby the adaptive immunity is distinctive to the pathogen presented. In comparison to the cells involved in the innate immunity, B- and T- cells exhibit long term response and are long-lived cells that manifest characteristics of the adaptive immunity, such as clonal expansion, antigen specificity and immunological memory. These attributes, facilitate a rapid and effective recognition and elimination after another encounter of the same pathogen. There are two main mechanisms of the adaptive immunity; the humoral and cell-mediated. The humoral immunity is mediated by antibodies against specific antigen, produced by the B- lymphocytes. The cell-mediated immunity is intermediated by T- lymphocytes, where the helper T cells release cytokines that allow the T- lymphocytes to bind to the specific antigens and differentiate into cytotoxic T- cells (Chaplin, 2010).

1.2 Natural Killer Cells

NK cells were first described in 1975 by two concomitant studies as a unique subpopulation of the lymphocytes that lacks detectable surface

markers. These cells were competent to induce spontaneous, natural cell-mediated cytotoxicity against murine tumour cells without prior stimulation. This novel mechanism of cytotoxicity distinct the NK cells from B- or T-lymphocyte cells or macrophages as no prior exposure to antigen or somatic rearrangement of their surface receptors is required (Herberman *et al.*, 1975; Kiessling *et al.*, 1975).

NK cells constitute 5-15% of the circulating lymphocyte population in the peripheral blood (PB) of humans and are found in plenteousness in the bone marrow (BM). They are also present in the liver, uterus, spleen, gut, skin and lung, as well as to a limited extent in secondary lymphoid tissue (SLT), mucosa-associated lymphoid tissue (MALT), and the thymus (Carrega & Ferlazzo, 2012). The NK cells are also distinctive in a phenotypic level from the other lymphocytes, such as B- and T- cells, by their surface expression of CD56, CD16 and absence of CD3 and any of the N- cell related antigens.

NK cells are members of the group 1 innate lymphoid cells (ILCs) due to their key ability to produce interferon-γ (IFN-γ) and tumour necrosis factor-α (TNF-α). However, they are not capable of secreting group 2 cytokines such as IL-5 and IL-13 or group 3 cytokines IL-17 and IL-22 (Spits *et al.*, 2013). NK cells are classified as innate immune cells targeting tumour and virally infected cells via secretion of cytokines and chemokines, as well as, by direct and indirect lysis. Interestingly, NK cells have been reported to express features of the adaptive immune system, such as clonal expansion and immunological memory (Cerwenka & Lanier, 2016; Sun *et al.*, 2011). This will be described thoroughly in section 1.2.5.

1.2.1 Natural Killer Cell Subsets

NK cells are not a homogenous population, as the intensity of CD56 and CD16 surface expressions can further divide the human NK cells into two major subsets, the CD56^{bright} and CD56^{dim} with discrete function and distribution (L. L. Lanier *et al.*, 1986). Historically, the first description of the two subsets was reported by Lanier and colleagues in 1986 (L. L. Lanier *et al.*, 1986). All the different NK cell subsets express genomic, phenotypic and functional variances. A study performed by Wendt and colleagues, using gene chip arrays, reported 473 different transcripts between the two subsets, with 176 wholly expressed in CD56^{dim} and 130 in CD56^{bright} (Wendt *et al.*, 2006). In addition, a more thorough study by Horowitz *et al* using Mass Cytometry, revealed an extensive NK cell repertoire consisting of an estimate of 108,000 to 125,000 total NK cell phenotypes (Horowitz *et al.*, 2013).

1.2.1.1 CD56^{bright} NK Cells

CD56^{bright} NK cells are predominantly found in the SLT and account for around 10% of total circulating NK cells and are considered to be the immature subset. They express low levels of CD16, known as CD56^{bright}/CD16^{dim}, and are principally responsible for secreting immunoregulatory cytokines, such as IFN-γ, TNF-α, TNF-β, IL-10 and granulocyte-macrophage colony-stimulating factor (GM-CSF) (Cooper *et al.*, 2001). The CD56^{bright} subset has limited impact in cytotoxic activity compared to the CD56^{dim} (Cooper *et al.*, 2001). However, upon cytokine stimulation, CD56^{bright} NK cells can express enhanced cytotoxicity effect compared to the CD56^{dim} subset. This is due to their display of high affinity of IL-2 receptor

complex on their cell surface, that allows them to express cytotoxic activity, even with low doses of IL-2 (Caligiuri, 1990). In addition, Fauriat and colleagues demonstrated that CD56^{dim} NK cells expressed higher cytokine and chemokine secretion in comparison to the CD56^{bright} subset, upon target cell recognition (Fauriat *et al.*, 2010).

1.2.1.2 CD56^{dim} *NK Cells*

CD56^{dim} NK cells are the fully matured and most robust NK cell subset in the PB and account for ~90% of the total circulating NK cells. This subset expresses high levels of CD16, known as CD56^{dim}/CD16^{bright}, and higher levels of cytotoxic perforin and granzymes compared to CD56^{bright} subset (Jacobs *et al.*, 2001). CD56^{dim}/CD16^{bright} NK cells are mainly responsible for cytolytic responses and are less involved in cytokine and chemokine production (Cooper *et al.*, 2001). They are capable of inducing both natural cell mediated cytotoxicity and antibody depended cell cytotoxicity (ADCC) and are more efficient on forming conjugates with the target cells (Cooper *et al.*, 2001) (Jacobs *et al.*, 2001). In contrast to CD56^{bright} NK subset, they display intermediate affinity of IL-2 receptor complex on their cell surface and have weak effect in response to high dose of IL-2 in vitro (Caligiuri, 1990).

Another NK subset that is CD56^{-}/CD16^{bright} was reported in patients with chronic infections such as Human Immunodeficiency Virus (HIV) and Hepatitis C Virus (HCV) and represented around 20-40% of the NK population in comparison to healthy individuals. Increase of the CD56^{-}/CD16^{bright} resulted to a reduction of the CD56^{dim}/CD16^{bright} NK subset

whereas the CD56^{bright}/CD16^{dim} NK cell levels remained stable (Hu *et al.*, 1995) (Gonzalez *et al.*, 2009).

1.2.2 Natural Killer Cell Receptors

The NK receptors (NKRs) are essential for the distinguish of normal cells from transformed, stressed or foreign cells and they consist of both activating and inhibitory receptors (Cooper *et al.*, 2001). On the phenotypic characteristics, the NK subtypes have diverse expression levels of activating and inhibitory receptors, adhesion and other molecules, as well chemokine receptors. A summary of the NK cell receptors and adhesion molecules as well as their ligands, can be observed in Table 1-1 (Pegram *et al.*, 2011; Vilgelm & Richmond, 2019).

Table 1-1: Human NK Cell Receptors and Adhesion Molecules

		Specificity
NK Cell Activating Receptors	NKp30	B7-H6
	NKp44	Unknown (Haemagglutinin)
	NKp46	Unknown (Haemagglutinin)
	NKp80	AICL
	2B4	CD48
	CD16	IgG
	NKG2D	MIC-A, -B, ULBPs(1-6)
	DNAM-1	CD122, CD155
NK Cell Inhibitory Receptors	KIR2DL1	HLA-C
	KIR2DL2	
	KIR2DL3	
	KIR2DL4	HLA-G
	KIR3DL1	HLA-B
	KIR3DL2	HLA-C
	LIR2/ILT4	HLA-F
	CD94/NKG2A	HLA-E
NK Cell Chemokine Receptors	CCR1	CCL1
	CCR2	CCL2
	CCR5	CCL3-5,8,11,12
	CCR7	CCL19,21
	CXCR1	CXCL1,6,8
	CXCR3	CXCL9-11
	CXCR4	CXCL12
	CX3CR1	CX3CL1
NK Cell Adhesion and Other Molecules	CD2	LFA-3
	CD11a	ICAMs(1-6)
	CD11c	ICAM-1, VCAM-1
	CD25	Unknown
	CD44	Hyaluronate
	CD49e	Fibronectin
	CD59	C8, C9
	CD62L	GlyCAM-1
	CD69	Unknown

The activating NK cell receptors consist of various categories. These include the natural cytotoxicity receptors (NCRs), C-type lectin-like receptors (CTLRs), immunoglobulin-like domain-containing receptors (ILDRs), signaling lymphocytic activation molecule family (SLAM), those associated with the immunoreceptor Tyrosine-based activation motif (ITAM) and other activating receptors. These receptors are competent of recognising ligands that are expressed on the surface of infected, stressed, transformed, tumour cells as well as normal cells.

The NCRs are among the earliest identified NK cell activating receptors. They are type I transmembrane receptors and consist of the NKp30, NKp44 and NKp46. While NKp46 is particularly expressed in NK cells, the other two are also found on T-cell subsets. Additionally, NKp46 and NKp30 are expressed in both resting and activated NK cells, however, NKp44 is only present on activated NK cells (Moretta *et al.*, 2001). Identification of their ligands has been challenging, except from NKp30, which bind to its ligand B7-H6, presented on the surface of tumour cells (Kaifu *et al.*, 2011).

Natural-killer group 2, member D (NKG2D) is a homodimeric CTLR, a type II transmembrane receptor and it is expressed on the surface of both NK cells and T cells. It requires association with DAP10 or KAP10 adaptor proteins (Moretta *et al.*, 2001). A study conducted by Pende and colleagues demonstrated that NKG2D contribution to NK cell activation is irrespective to the surface expression density of NCRs (Pende *et al.*, 2001). The ligands for

the NKG2D receptor are the MHC class I chain-related protein A (MIC-A) and B (MIC-B) and UL-binding proteins 1-6 (ULBP1-6) expressed on the surface of stressed and tumour cells (Lanier, 2015).

NKp80 is another CTLR, a dimeric type II transmembrane receptor that is expressed on all PB NK cells and meagerly to NK-T cells which are characterised by their CD56+/CD3+ phenotype (Moretta *et al.*, 2001). Unlike NKG2D, NKp80 cannot associate with adaptor proteins due to the lack of charged amino acids on its transmembrane domain. The ligand for this receptor is the activation-induced C-type lectin (AICL) which is expressed in normal cells, such as, monocytes, macrophages and granulocytes, as well as on tumour cells (Akatsuka *et al.*, 2010; Welte *et al.*, 2006).

DNAX Accessory Molecule-1 (DNAM-1) is an ILDR NK activating receptor that is also expressed on CD8+ T-cells and myeloid cells. It recognises the poliovirus receptor (CD155) and nectin adhesion molecule (CD122), both of which are expressed on the surface of tumour and virus-infected cells (Bottino *et al.*, 2003).

CD16, is an FcγRIIIα antibody activating receptor on the surface of the NK cells which is associated with homo- or hetero-dimer ITAMs and/or CD3ζ chains. It is primarily responsible for the ADCC of CD16+ NK cells (Cooper *et al.*, 2001). Uniquely among NK triggering receptors, ligation of CD16 alone is able to activate and trigger resting NK cell whereas all other activating receptors require more than one signal (Bryceson, 2006).

2B4 is also an NK activating receptor derived from the SLAM family of receptors. It is a type I transmembrane receptor that is present on different immune cells. It is bind to another immunoglobulin-molecule, CD48, which is expressed on the hematopoietic cells (Moretta *et al.*, 2001).

In addition to the aforementioned NK cell activating receptors, these cells also expressed other co-stimulatory proteins, including CD2 and CD27.

Both CD56^{bright} and CD56^{dim} NK subsets show similarities and differences on their phenotypic properties for activating receptors. Both subsets express NKp30 and NKG2D whereas the NKp46 activating receptor is expressed in higher frequency on the CD56^{bright} compared to CD56^{dim} (Cooper *et al.*, 2001).

1.2.2.2 Inhibitory Receptors

NK cell inhibitory receptors can be grouped in two main categories; the killer cell Ig-like receptors (KIRs) and the killer cell lectin-like receptors (KLRs) (Biassoni *et al.*, 2001).

KIRs principally recognise and bind to the classical MHC class I human leukocyte antigens (HLAs). They are a type I transmembrane receptors with either two (KIR2DL1-3, KIR2DL4), three (KIR3DL1 and KIR3DL2) or four (leukocyte immunoglobulin-like receptor (LIR)/immunoglobulin-like transcript (ILT), LIR1/ILT2 and LIR2/ILT4) extracellular immunoglobulin-like domains. KIR2DL1-3 and KIR2DL4 domains bind to HLA-C and HLA-G alleles correspondingly, whereas,

KIR3DL1 and KIR3DL2 domains recognise the HLA-B and HLA-A alleles respectively (Biassoni *et al.*, 2001). The LIR2/ILT4 recognises the HLA-F allele, while the LIR1/ILT2 is involved in extensive HLA alleles recognition (Biassoni *et al.*, 2001).

KLR encompasses the CD94/NKG2A heterodimer that recognise the non-classical MHC class I human antigen, HLA-E. It is a type II transmembrane receptor. While NKG2A is expressed in both human and mouse, KIR is expressed merely in human. CD94 can additionally bind to the NKG2C and act as an activating receptor upon HLA class I molecules recognition (Biassoni *et al.*, 2001).

Both KIRs and KLR express ITIMs in their cytoplasmic tails (Biassoni *et al.*, 2001). The inhibitory function of these receptors, requires the co-aggregation with the activating receptors to successfully downmodulate the NK cell function (Biassoni *et al.*, 2001). In order to exhibit their inhibitory signals, the inhibitory receptors are phosphorylated on their ITIMs upon ligand recognition via a potential protein tyrosine kinase, Lck. This has an effect on the activating receptors via two pathways. One pathway involves the recruitment of specific Src homology 2- containing phosphatases (SHP-1 and SHP-2) which are critical for the dephosphorylation of an activating molecule (Vav-1) and the other pathway involves the recruitment of the protein tyrosine kinase, c-Abl, which phosphorylates the small adaptor protein, Crk, and subsequently dissociates it from signalling complexes formed during activation. Vav-1 dephosphorylation and Crk phosphorylation entail the inhibition of activation via actin-dependent signals (Kumar, 2018).

A comparison of the phenotypic expression of inhibitory receptors on the CD56^{bright} and CD56^{dim} NK subsets, shows absence of KIRs and ILT2 on the CD56^{bright} NK cells, but, expression of those receptors on the CD56^{dim} NK cells. However, CD94/NKG2A inhibitory receptor is expressed with higher density on the   CD56^{bright} NK cells (Cooper *et al.*, 2001).

1.2.2.3 Adhesion molecules and Chemokine Receptors

The adhesion molecules of the NK cells include the CD2, CD11a (or lymphocyte function-associated antigen 1, LFA-1), CD11b (or macrophage-1-antigen, MAC-1), CD11c, CD44, CD49e, CD54 (or inter-cellular adhesion molecule -1, ICAM-1), and CD62L (L-selectin) (Poli *et al.*, 2009).

CD56^{bright} NK cells exhibit higher density of CD2, CD11c, CD54 (ICAM-1) and CD62L, while the CD56^{dim} NK cells express higher levels of CD11a (Poli *et al.*, 2009).

Other molecules of NK cells include the CD25, CD55, CD57, CD59, CD69 and Human Leukocyte Antigen–DR isotype (HLA-DR). CD56^{bright} NK subset lacks expression of the NK cell maturation marker, CD57, but displays at a higher level the CD25, CD55 and CD59. Additionally, the HLA-DR is present on CD56^{bright} NK subset but is absent on the CD56^{dim} NK cells (Poli *et al.*, 2009).

The chemokine receptors repertoire vary greatly between the two main NK cell subsets. CD56^{bright} solely express CCR7 and CXCR3, while, CD56^{dim} exclusively displays CXCR1 and CX3CR1 (Poli *et al.*, 2009).

The divergent expression levels of adhesion molecules and chemokine receptors on these NK subsets, result in distinct migratory properties. CD56^{bright} NK cells preferentially migrate to secondary lymphoid organs, while the CD56^{dim} subset migrates to the site of inflammation (Poli *et al.*, 2009).

1.2.3 Natural Killer Cell Development

For more than three decades, it has been largely postulated that the NK cell development process, has been predominantly attained in the BM. This was first identified in late 1970s by BM ablation studies in murine models (Haller & Wigzell, 1977) (Kumar, 1978). Indeed, it has been identified in humans that CD34$^+$ hematopoietic stem cells (HSCs), hematopoietic progenitor cells (HPCs) and a fraction of NK cell precursors (pre-NK) are enriched in the BM (Freud & Caligiuri, 2006). However, Freud and colleagues demonstrated a significant role of SLT in NK cell development process after the detection of CD56^{bright} NK cells on lymph nodes and tonsils (Freud *et al.*, 2005). The pre-NK cells on the SLT express a unique phenotype of CD34$^+$/CD45RA$^+$ (Freud *et al.*, 2005). The CD56^{dim} NK cell subset is primarily detected on the BM, PB and spleen (Freud *et al.*, 2005). Since the identification of these two major NK cell subtypes, it has been suggested that they might represent two sequential stages of the final steps of the NK cell development and maturation and that CD56^{bright} NK cells act as precursors of CD56^{dim} NK subset. This supported by various studies and observations. These include the fact that CD56^{bright} NK cell population is agranular, have longer telomeres and express CD117 (c-kit) which is usually expressed in

immature HPCs. Additionally, *in vitro* IL-15 priming of CD34$^+$ cells has shown to generate CD56^{bright} NK cells and *in vivo* studies after CD34$^+$ cells transplantation demonstrated the presence of CD56^{bright} NK cells at the time of engraftment, while, CD56^{dim} NK subset emerged later following reduction of CD56^{bright} NK population (Jacobs *et al.*, 1992; L L Lanier *et al.*, 1986; Matos, 1993; Mingari *et al.*, 1997; Romagnani *et al.*, 2007)

A complete and continuous *in vivo* process of the human NK cell development stages, as well as, the possibility of migration of human NK cells to other tissues for fully maturation still remain elusive (Freud & Caligiuri, 2006).

1.2.3.1 Stages of NK Cell Development

The combination of CD34, CD117, CD94, CD56 and CD16 antigens have been utilized in distinguishing the different stages of NK cell development. There are five distinct stages; Stage 1 (CD34$^+$/CD117$^-$/CD94$^-$/CD56$^-$/CD16$^-$), Stage 2 (CD34$^+$/CD117$^+$/CD94$^-$/CD56$^-$/CD16$^-$), Stage 3 (CD34$^-$/CD117$^-$/CD94$^-$ CD56$^{+/-}$/CD16$^-$), Stage 4 (CD34$^-$/CD117$^{+/-}$/CD94$^+$/CD56$^+$/CD16$^-$) and stage 5 (CD34$^-$/CD117$^-$/CD94$^{+/-}$/CD56$^+$/CD16$^+$) (Freud & Caligiuri, 2006). A summary of the NK cell development stages can be seen in Figure 1-1.

Stage 1 (pro-NK) in human SLT is identified by multipotent CD34$^+$, CD45RA$^+$, CD117$^-$ and CD94$^-$ cells. They are also characterised by the absence of CD122 expression, and as a result, they lack the capacity to differentiate in response to IL-15. The pro-NK cells express different levels of

CD34 and cells with higher expression levels are also CD10$^+$, resulting in a phenotype closely similar to the BM-derived population (CD34$^+$/CD45RA$^+$/CD117$^-$/CD94$^-$/CD10$^+$) (Galy *et al.*, 1995).

Stage 2 (pre-NK) is marked by the acquisition of CD117 and CD122, that facilitates the IL-15 responsiveness to NK development. CD10 is downregulated in this stage. Lineage plasticity is observed in Stage 2, as pre-NK cells are able to differentiate into other lineages, such as T-cells and DC (Freud & Caligiuri, 2006).

Stage 3 represents the immature NK (iNK) cells in which they lost their multipotency potential due to the loss of CD34 expression and acquisition of CD56 marker (CD34$^-$/CD117$^+$/CD94$^-$/CD56$^+$). They also express the activating cell surface receptors, NKp44 and 2B4. However, iNK cells are still incapable of producing IFN-γ and mediate cellular cytotoxicity. They also lack the expression of other important surface receptors, such as the activating NKG2D, NKp46, CD16 and the inhibitory KIRs and CD94/NKG2 heterodimer (Freud & Caligiuri, 2006).

Stage 4 is characterised by the acquisition of CD94 marker (CD34$^-$/CD117$^{+/-}$/CD94$^+$/CD56$^+$) as well as the other important receptors mentioned above and the development into immature CD56^{bright} NK cells. The NK cell development continues with the final stage that encompasses the CD56^{dim} NK population.

During Stage 5, CD56^{dim} loses the expression of CD117 and CD94 and acquires CD16 marker (CD34$^-$/CD117$^-$/CD94$^-$/CD56$^+$/CD16$^+$) (Freud &

Caligiuri, 2006). Interestingly, Bjorkstrom and colleagues reported that Stage 5 is not the final stage of NK cell development, as the CD56^{dim} population is differentiated further. This includes two additional stages, where on the first step, CD56^{dim} gain NKG2A, CD62L and KIR expression and the final step that involves the loss of NKG2A and CD62L markers, acquisition of the replicative senescence CD57 molecule, increased expression of KIRs and subsequent reduction of its proliferative capacity (Bjorkstrom *et al.*, 2010).
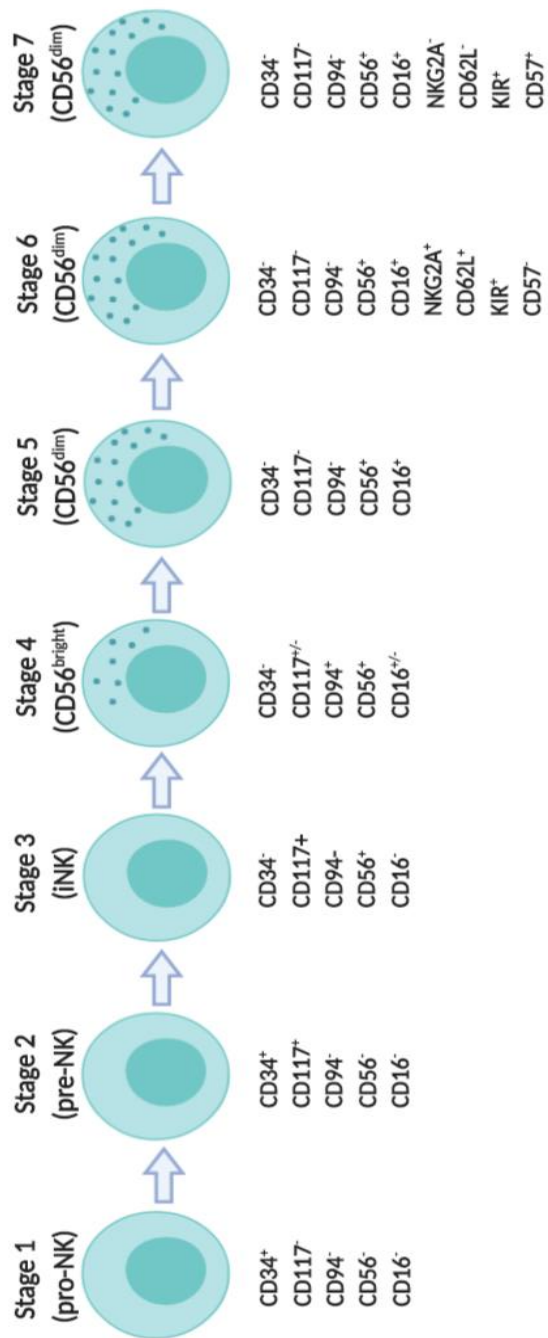
Figure 1-1: NK Cell Development Stages

1.2.4 Natural Killer Cell Education

During the NK cell development and maturation, the gain of functionality occurs through a process known as education or licensing. This process can be grouped into three categories; classical MHC class I dependent, non-classical MHC class I dependent and MHC class I independent (He & Tian, 2017).

In the first group, NK cells express self-recognising inhibitory receptors (SRIRs) that subsequently allows the licensed NK cells to distinguish "self" MHC class I cells from "non-self" cells. This is a feature for both murine and human models. This is achieved through the interaction of KIRs on the NK cells and the classical MHC class I molecules (HLA-A, -B and -C) on the surface of normal cells. However, some mature NK cells lack the expression of inhibitory receptors, resulting in unlicensed NK cells that are hypo-responsive and have a low potential to attack host MHC class I cells (Anfossi *et al.*, 2006).

The non-classical MHC class I dependent NK cell education, is attained by the CD94/NKG2A inhibitory receptor that is capable of recognising non-classical MHC class I molecules (HLA-E). The complete mechanism that determines the differential NK cell education via KIRs or NKG2A is still tenuous (He & Tian, 2017).

The MHC class I independent NK cell education, relies on the presence of SLAM molecules on the NK cell surface (2B4) and its ligand CD48 as well as the presence of TIGIT (T cell immunoglobulin and

immunoreceptor tyrosine-based inhibitory motif (ITIM) domain NK inhibitory receptor and its ligand CD155 on host cells. However the precise mechanism behind this process is still to be determined (Anfossi *et al.*, 2006).

The NK cell education process comprises of four signal models; Arming, Disarming, Rheostat and Confining models.

The Arming Model relies on the expression of inhibitory receptors with ITIM motifs on the surface of the NK cells that consequently induce functionally mature NK cells and renders them responsive via engagement with MHC class I cells. On the contrary, the Disarming Model highlights the lack of NK cell inhibitory receptors and the presence of the activating receptors, leading to a sustain NK cell activation. These NK cells are hypo-responsive or "disarmed" (He & Tian, 2017). The Rheostat Model, is a quantitative process of NK cell responsiveness by establishing the frequency and strength of the inhibitory receptors to interact with host MHC class I cells. Finally, the Confining Model postulates the confinement of NK inhibitory and activating receptors distribution and cell adhesion molecules for the effective NK cell responsiveness (He & Tian, 2017).

1.2.5 Natural Killer Cell Memory

Immunological memory is a characteristic of the adaptive immunity and is referred as the feature of the T- and B- immune cells. It allows these cells to recognise a previously encountered antigen and respond rapidly upon re-stimulation (Cerwenka & Lanier, 2016). This is achieved via the expression of recombination-activating genes (RAGs) on these cells.

Intriguingly, increasing evidence signifies that NK cells share some features of the adaptive immunity such as clonal expansion and immunological memory similarly to T- and B- cells (Cerwenka & Lanier, 2016; Sun *et al.*, 2011).

O'Leary and colleagues were the first to report NK cell antigen-specific responses in a murine model of hapten-induced contact hypersensitivity (CHS) (O'Leary *et al.*, 2006). In this study, mice with T- and B- cell depletion RAG2$^{-/-}$ or severe combined immunodeficiency (SCID) mice were injected with compounds that have the ability to chemically altered proteins, known as haptens. For this study, they specifically used the 2,4-dinitrofluorobenzene (DNFB) or the oxazolone (OXA). Four weeks after the sensitisation, re-challenge occurred using the same or an unrelated hapten. The CHS response occurred only in mice that had been previously sensitised with the same hapten and when NK cells were not depleted. Furthermore, it was demonstrated that liver NK cells and not splenic NK cells were responsible for this antigen-specific memory CHS response and it was CXCR6, NKG2D, IL-12, IFN-α and IFN-γ dependent (O'Leary *et al.*, 2006) (Paust *et al.*, 2010).

In addition to the memory responses to haptens, NK cells also express antigen-specific memory against viruses in both murine and human models. The majority of investigations have been conducted for cytomegalovirus (CMV). Studies in murine CMV (MCMV) demonstrated that LY49H and DNAM-1 activating receptors on the surface of naïve NK cells interacted with their ligands, m157 and CD155 respectively on the MCMV-infected cells. The NK cells were subsequently exposed to clonal expansion using IL-12, -18

and -33 and finally entered a contraction phase that was regulated by the pro-apoptotic factor, Bim, to give rise to MCMV-specific memory NK cells (Cerwenka & Lanier, 2016). For human CMV (HCMV), Guma and colleagues were the first to show that healthy individuals with pre-encounter of HCMV and positive serologically for HCMV, have enhanced expression levels of CD94/NKG2C activating NK cell receptor (Guma, 2004). This receptor bound to the HLA-E molecule on the surface of HCMV-infected fibroblasts in an IL-12 dependent manner, produced by the monocytes, and give rise to memory CD94/NKG2C positive NK cells (Guma, 2004). Additionally, Zhang *et al* reported an antibody dependent memory NK cells in HCMV that expressed low levels of CD16 and recognised HCMV-specific antibodies on the surface of the HCMV-infected fibroblasts (Zhang *et al.*, 2013).

Interestingly, NK cell memory responses have been demonstrated in the absence of a specific antigen via cytokine induction. An *in vitro* exposure of NK cells to the cytokine combination of IL-12, -15 and -18 resulted in the clonal expansion of NK cells population characterised by augmented function via the production of IFN-γ, perforin and granzymes and the increased expression of CD25 molecule. After adoptive transfer of these cytokine-induced NK cells to RAG2$^{-/-}$ mice this NK cell population, persevered long term and maintained their ability to express IFN-γ, perforin and granzymes. The presence of IL-2 or -15 increased further the number of the NK cells and retained their abilities *in vivo* for at least four months (Cooper *et al.*, 2009).

1.2.6 Natural Killer Cell Recognition

Following the discovery of NK cells in 1970s, the understanding of NK cell recognition of target cells from normal cells, was ambiguous. Numerous studies have been performed to postulate the mechanism behind this, and have been evolved through the years and are described below. In comparison to T- and B- cells, this system is more complex in NK cells, as instead of being regulated by a single receptor, it is controlled by the coordination of activating receptors, inhibitory receptors and adhesion molecules (Lanier, 2005).

1.2.6.1 "Missing-self" Hypothesis

The "missing-self" hypothesis was first described in 1980s in which NK cells were capable of recognising and killing cells with low or absent MHC class I expression of MHC class I molecules on their surface. This is a feature of transformed or viral-infected cells (Kärre *et al.*, 1986; Ljunggren & Kärre, 1990). This mechanism relies on the NK inhibitory receptors that bind to the MHC class I molecules on the surface of normal cells and repress the NK cell responses to kill these cells. Therefore, cells with MHC class I expression impairment are inadequate in suppressing the NK cell cytolytic responses.

This has been confirmed in studies using murine models, where syngeneic and allogeneic mice were injected with RBL-5 lymphoma cell line (Kärre *et al.*, 1986). However, lack of MHC class I molecules on the surface of virus-infected or tumour cells was insufficient to induce killing by the NK

cells, leading to the conclusion that the "missing-self" hypothesis was deficient in explaining the NK cell recognition process (Ljunggren & Kärre, 1990).

1.2.6.2 *"Induced-self" Hypothesis*

The "induced-self" hypothesis implies the importance of NK activating receptors. The presence of stress-inducible antigens on the surface of target cells, causes cellular distress and evokes NK cell responses. These "induced-self" molecules are the MIC-A and -B which act as ligands for the NKG2D NK cell activating receptor (Bauer, 1999).

1.2.6.3 *"Altered-self" Hypothesis*

The "altered-self" hypothesis was reported by Iizuka *et al* (2003) in which it was defined an alternative NK gene complex (NKC), the CTLRs, particularly the Nkrp1 family. Unlike other NKC receptors that are capable of recognising MHC class I molecules, these CTLRs engage to cadherins and specific C-type lectin-related (Clr) molecules, leading to an alternate mode of "missing-self" hypothesis (Iizuka *et al.*, 2003). In this study, it was shown that Nkrp1d and Nkrp1f members bound to lectin-like ligands, Clrb and Clrg respectively and affect NK cell responses. As these ligands are solely expressed by DCs and macrophages, this interaction may be applicable to innate immunity during immune responses (Iizuka *et al.*, 2003).

1.2.6.4 *"Dynamic Equilibrium" Hypothesis*

It has been now established that the NK cell recognition and responses are regulated via a dynamic equilibrium of activating and inhibitory

receptors rather than a single type of NK cell receptors, as well as the relative amount of NK cell receptors and their ligands. This is occurred in an MHC class I independent manner (Lanier, 2005). Despite the advanced progress in understanding how NK cells recognise and attack target cells, many questions still remain unanswered.

1.2.7 Natural Killer Cell Activation

The NK cell activation process against target cells, comprises of various sequential steps that can be grouped into 3 main stages; recognition, effector and termination. The principal step for the NK cell activation entails the formation of immunological synapse between the NK cells and the target cell (Orange, 2008). A summary of the stages and steps is illustrated in Figure 1-2. The NK cell activation can occur via two main mechanisms; the natural cytotoxicity and the ADCC.

1.2.7.1 Stages of Natural Killer Cell Activation

The recognition stage, consists of the adhesion, conjugate formation and initial activation signaling. This stage relies on the synergy of activating and co-activating NK cell receptors as well as adhesion molecules, specifically the LFA-1 and MAC-1 molecules (Orange, 2008).

After the formation of immunological synapse and adhesion, this process continues to the effector stage, that is characterised by three key steps. The first step is the actin rearrangement of cell cytoskeleton that facilitates the clustering of receptors and adhesion molecules to generate a robust signaling. The second step includes the movement of microtubule

organizing center (MTOC) and NK lytic granules towards the site of the synapse (polarisation). The last step is the fusion of the NK lytic granules with the plasma membrane for exocytosis (degranulation). The soluble N-ethylmaleimide-sensitive-factor accessory-protein receptor (SNARE) protein family, and perforin are responsible for the coordination of the two distinct membranes fusion of the NK cell and the target cell in a calcium-dependent manner. Once the NK lytic granules enter the target cell, they induced programmed cell death, known as apoptosis. This is driven by the co-engagement of ligands from TNF family on the surface of the NK cells with their receptors on the surface of the target cells. The polarisation and degranulation steps are crucial for the NK cell cytotoxicity (Orange, 2008).

The last stage in the NK cell activation process, entails the NK cell inactivity and detachment. Once the lytic granules have been transferred to the target cell, the NK cell can detached itself from the lysed target cell and restore its cytotoxic potential (Orange, 2008).
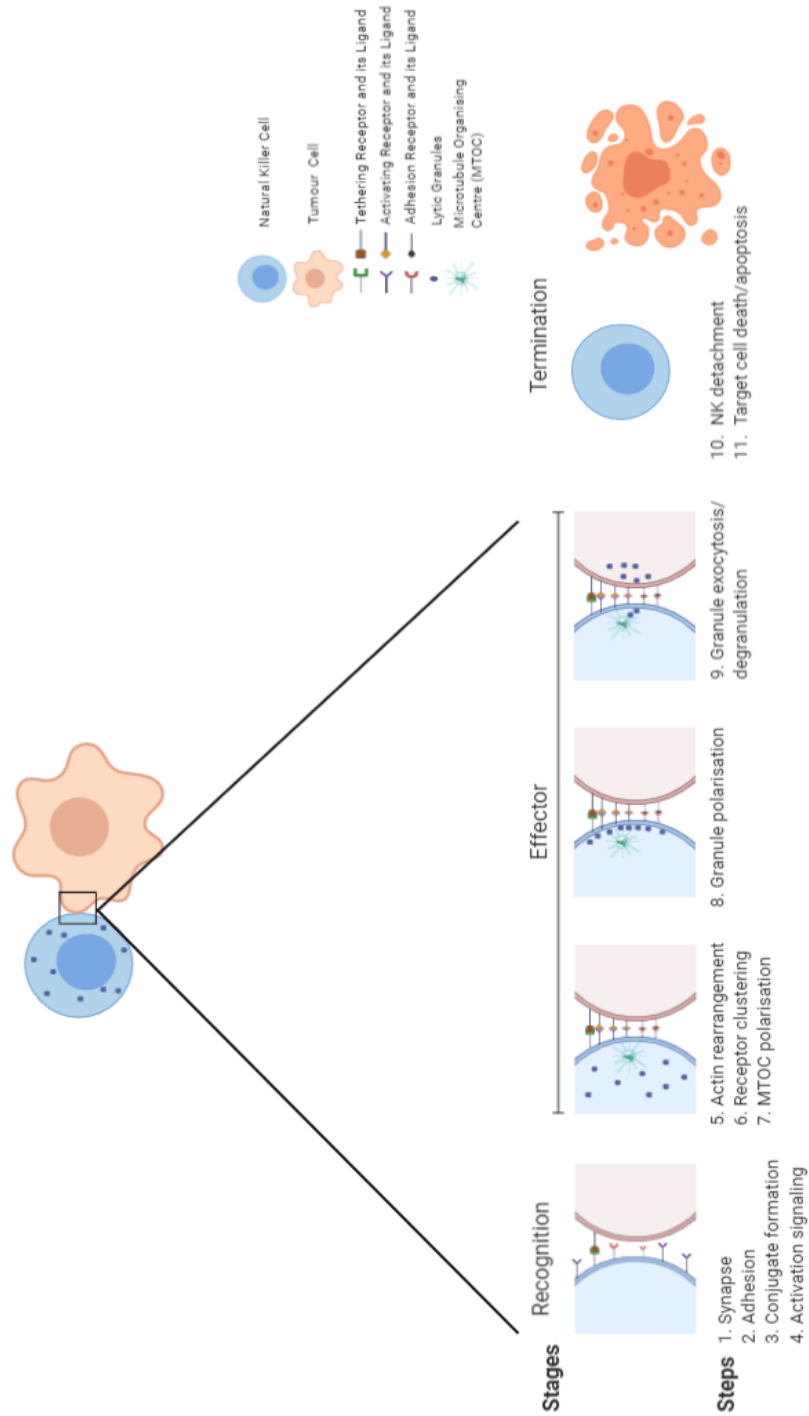
Figure 1-2: Stages and Steps of Natural Killer Cell Activation

1.2.7.2 Natural Cytotoxicity

The NK natural cytotoxicity relies on the interaction of NK cell activating and co-stimulating receptors and their ligands on the surface of the target cell. This includes the NCRs (NK-30, NKp44 and NKp46), NKG2D, 2B4 and DNAM-1. However, NK cell cytotoxicity, cytokine secretion and degranulation responses are achieved only when these receptors were in specific pairwise combination. Bryceson *et al* investigated which combinations of NK activating receptors had the strongest synergistic effects on resting NK cells (rNK), after comparing 2B4, CD2, DNAM-1, NKG2D and NKp46. It was observed that the strongest synergistic combination was achieved between 2B4 and the NKp46, NKG2D and DNAM-1. The NKp46 receptor was able to bind to all the NK cell receptors tested (Bryceson, 2006).

1.2.7.3 Antibody Dependent Cellular Cytotoxicity (ADCC)

The CD16 NK activating receptor and its IgG ligand on the surface of target cells are responsible for the ADCC. It has been shown that it is the only NK cell receptor capable of inducing NK cell activation, cytotoxicity and degranulation in primary rNK cells, without, the requirement of co-engagement with other receptors as seen in NK natural cytotoxicity (Bryceson, 2006). Bryceson and colleagues examined the potential of enhancement of the NK cell responses upon combination of CD16 with either 2B4, CD2, DNAM-1, NKG2D or NKp46 NK cell receptors. It was demonstrated that NK cell cytotoxicity was augmented in all the pairwise combinations, with the exception of the NKp46 (Bryceson, 2006).

1.2.8 Natural Killer Cell Priming

The priming of NK cells is a significant process against target cells that display resistance or low sensitivity to primary rNK cells. This can be achieved by pre-incubation of rNK cells with cytokines, such as IL-2, -12, -15, -18 and -21 (Romee *et al.*, 2014) or with tumour target cells, such as K562 and CTV-1 (Kweon *et al.*, 2019) (North *et al.*, 2007). A detailed description of the NK priming will be reviewed in chapter 5.

The first NK cell priming approach via cytokine activation was established in 1982, using interleukin-2 (IL-2) known as the lymphokine-activated killer (LAK) phenomenon (Grimm, 1982). Its application in clinic had a positive outcome in patients with advanced metastatic cancers (Rosenberg *et al.*, 1985). Since the first use of cytokine-primed NK cells to enhance antitumor responses both *in vitro* and *in vivo*, other cytokines have also been studied either as a single priming agent or in combination. The IL-2 and IL-15 have been the primarily best studied in the cancer field (Romee *et al.*, 2014).

In addition, tumour cell lines have been used as an alternative priming mediated agent for NK cells. Our group had shown the use of a previously defined rNK resistant leukaemic cell line (CTV-1), as an effective NK cell priming agent for the successful elimination of tumour target cells that were previously resistant to primary rNK cells (North *et al.*, 2007). Interestingly, it has been recently reported, by our group, that the cytokine-primed and tumour-primed NK cells exhibit differential phenotypic, transcriptomic and cytokine secretion profiles (Sabry *et al.*, 2019). In addition, Pal *et al* (2017) demonstrated the use of irradiated acute B-cell precursor leukaemia (BCP-

ALL) cell line, NALM-16 or primary BCP-ALL specimens (P3B, P31G) as well as primary acute myeloid leukaemia (AML) specimens (P18R and P84D) to activate the NK cells. They reported tumour-induced memory like NK (TIML-NK) cells that exhibited tumour specific NK cell responsiveness as they only heightened cytotoxicity against the tumour target cells that were also used for NK cell mediated priming (Pal *et al.*, 2017). A thorough description of NK cell priming will be described in chapter 5.

1.2.9 Natural Killer Cell Evasion Strategies by Tumour Cells

The ability of cancer cells to evade or suppress the immune system is a result of cancer immunoediting, which emphasises the dynamic interaction between tumour cells and the immune cells. Cancer immunoediting can be divided into three phases, known as the " three Es"; elimination, equilibrium and escape. In the early phase of tumour formation, the immune system can effectively eliminate the cancer cells. This is followed by a prolonged period of equilibrium, where the tumour cells are not eliminated, but, they are under control by the immune system and this is not clinically detectable. Finally, upon tumour escape from the immune responses, tumour evasion is initiated and cancer becomes clinically detectable (Dunn *et al.*, 2004).

Our group has previously identified that NK-cell mediated lysis is a result of two distinct stages, known as "two-stage hypothesis"; priming and triggering. The priming signal is achieved either by a cytokine or a tumour cell that expresses the ligands for NK cell activating receptors. The triggering signal, requires the co-engagement of additional NK cell activating receptors and co-stimulatory receptors to successfully kill the target cell (North *et al.*,

2007). Interestingly, the "two-stage hypothesis" is a phenomenon of the NK natural cytotoxicity, as the CD16 in ADCC is capable of lysing the target cells by direct triggering of primary rNK cells (Bryceson, 2006).

This "two-stage hypothesis" marks for two NK cell evasion strategies by the tumour cells; the prevention of priming (type 1 evasion) and the prevention of triggering (type 2 evasion). Most tumour cell lines are type I and fail to effectively prime the NK cells, therefore they are not lysed by rNK cells. However, primed-NK cells can efficiently kill these target cells. On the contrary, the NK cell-resistant leukaemic cell line (CTV-1) was shown to successfully prime the rNK cells but fail to trigger (type 2). As a result, this study demonstrated for the first time, the use of a tumour cell line, rather than a cytokine, to essentially mediate NK cell priming and lyse other tumour cells that were previously resistant to NK cell-mediated cytotoxicity (North *et al.*, 2007).

Target cells can evade the NK cell immunosurveillance via direct and indirect mechanisms.

1.2.9.1 Direct Evasion

They are several direct evasion strategies of target cells, including the persistent expression of MIC ligands for NKG2D NK activating receptor, the downregulation or shedding of ligands for NK activating receptors and the release of inhibitory cytokines.

The persistent expression of soluble MIC ligands, sustains the triggering of NKG2D activating receptor on the surface of the NK cells, and

reduces the NK cell cytotoxicity via downregulation of this receptor. This has been reported both *in vitro* and *in vivo* using transgenic murine models. However, cytokine stimulation of these NK cells could restore the expression of the NKG2D activating receptor (Oppenheim *et al.*, 2005).

The downregulation of NK activating receptors such as NKG2D and NCRs (NKp30, NKp44 and NKp46) is a result of three conditions; (i) the release of suppressive cytokines such as the IL-10, TGF-β and indoleamine 2,3-dioxygenase (IDO) by the target cells, (ii) the shedding of soluble ligands and (iii) the downregulation of their ligands on the surface of the target cells via epigenetic gene regulation (Groth *et al.*, 2011). The shedding of soluble activating ligands, such as MICA/B and ULBPs on the surface of the tumour cells is induced by upregulation of matrix metalloproteinases (MMPs) as well as a disintegrin and metalloprotease (ADAMs) families (Groth *et al.*, 2011). Furthermore, the cancer cells display mutations in epigenetic gene regulation by overexpression of histone deacetylases (HDACs). The HDACs have a vital role in cell cycle progression and transcription repression. Therefore, overexpression of the HDACs results to uncontrolled proliferation and survival, key hallmarks of cancer cells as established by Hanahan and Weinberg (Glozak & Seto, 2007) (Hanahan & Robert, 2011). The HDAC activity influences the expression of NKG2D ligands (MICA/B and ULBPs) on the target cells, causing downregulation, that can be reversed upon treatments with HDAC inhibitors (Bhat *et al.*, 2019).

1.2.9.2 Indirect Evasion

The indirect evasion strategy of tumour cells involves the recruitment of other cells in the site of the tumour that generates an immunosuppressive tumour microenvironment (TME) and inhibits the NK cell function. The prominent trait of the TME is hypoxia, which is characterised by the lower than physiological levels of oxygen. This mechanism favors tumour cells evasion by causing immune cell function impairment at the tumour site. A more thorough explanation of the TME immunosuppressive mechanisms, will be given in chapter 6. Additionally, secretion of various inhibitory factors by tumour cells, results in the accumulation of regulatory T (Treg) cells, myeloid-derived suppressor cells (MDSCs), tumour-associated macrophages (TAMs) and cancer-associated fibroblasts (CAFs) within the TME. These tumour-derived factors include TGF-β, Granulocyte-Macrophage Colony-Stimulating Factor (GM-CSF), IL-1β, Vascular Endothelial Growth Factor (VEGF), Prostaglandin-E$_2$ (PGE$_2$), IL-4 and IL-13. Moreover, the tumour-derived factors, inhibit DC function by disrupting its migration to the lymph nodes and its activation that impairs the NK cell priming (Vesely *et al.*, 2011).

1.3 Ovarian Cancer

1.3.1 Epidemiology of Ovarian Cancer

Ovarian cancer is the most lethal gynaecological malignancy and the fourth most common cancer in women in the UK. Ovarian cancer is broadly used term that encompasses also fallopian tube cancer and primary

peritoneal cancer that are all closely related and treated comparably. Each year over 7,400 women are diagnosed and nearly 4,000 of them die from the disease (Cancer Research UK, 2020). The 5-year survival for ovarian cancer is related to patient's age, with the youngest women (15-39) having the highest rate (87%) and the oldest women (80-99) the lowest rate (20%). The overall 5-year survival after age-standardised of ovarian cancer is around 46% and it falls to 35% for 10 years (Cancer Research UK, 2021).

The incidence of ovarian cancer is increased with age as 75% of diagnoses are in post-menopausal women aged over 50. Additionally, family history has a contribution to the aetiology of this disease as women with inherited breast cancer type 1 and breast cancer type 2 (BRCA1 and BRCA2) gene mutations have high risk of developing the disease and accounts for 65-75% of hereditary ovarian cancer. In addition, Lynch syndrome which is an autosomal dominant hereditary disease caused by germline mutations, is also associated with hereditary ovarian cancer and accounts for 10-15% of these cancers. Moreover, the extended use of hormone replacement therapy (HRT), the lifestyle including smoking and obesity as well as endometriosis and previous incidences of cancer like breast and bowel are additional risk factors for ovarian cancer development.

Ovarian tumours express two main pathological types; epithelial and non-epithelial. The non-epithelial type encompasses the germ tumours which account for only 5% of ovarian cancer and the stromal tumours which comprise of benign mature and cancerous immature teratomas. The epithelial ovarian cancer (EOC) is the most common form (90%) with various

histological subtypes including serous, clear cell, endometrioid, carcinosarcoma and undifferentiated. The most common EOC subtype is the serous that can be divided to either high grade serous (HGS) or low grade serous (LGS). Some EOC tumours exhibit an unclear differentiation under microscopical observation, called borderline tumours or tumours of low malignant potential (LMP) (Cancer Research UK, 2021).

1.3.2 Stages and Grades of Ovarian Cancer

The stage of a cancer is defined by the tumour size and the spread to a different site in the body. The ability of the cancer cells to spread from an initial or primary site to a different or secondary site is known as metastasis which is one of the key hallmarks of cancer as determined by Hanahan and Weinberg (2011) (Hanahan & Robert, 2011). The grade of cancer is characterized by the morphology of the tumour cells under a light microscope. The relative survival rate in cancer patients is lessened with the progress of the stage and/or grade of the tumour. A description of ovarian cancer stages and grades can be observed in Table 1-2.

Table 1-2: Stages and Grades of Ovarian Cancer

Stages of Ovarian Cancer			
Stage I	**Stage II**	**Stage III**	**Stage IV**
Ia. Located entirely inside one ovary	**Iia.** Extension of tumour cells to fallopian tubes or womb	**IIIa.** Microscopic tumour cells in the lining of abdomen	**Iva.** Tumour cells spread in the fluid around lungs (pleural effusion)
Ib. Located entirely inside both ovaries	**Iib.** Extension to bowel or bladder	**IIIb.** Tumour of ≤2 cm in the lining of the abdomen	**Ivb.** Tumour cells spread inside lungs, liver and spleen
Ic. Located either in one or both ovaries with some tumour cells on the surface and/or in ascitic fluid	**Iic.** Spread into the ascitic fluid and other pelvic organs	**IIIc.** Tumour cells >2 cm in the lining of the abdomen and in lymph nodes in the upper abdomen	

Grades of Ovarian Cancer	
GX	The grade cannot be evaluated
GB	Borderline tumour-LPM
G1	Well-differentiated cells
G2	Moderately differentiated cells
G3	Poorly differentiated or undifferentiated cells

1.3.3 Therapeutic Approaches Against Ovarian Cancer

The standard treatment for ovarian cancer is surgical debulking and chemotherapy using platinum (Cisplatin, Carboplatin) and taxanes (Paclitaxel, Docetaxel) drugs.

The surgical debulking involves the abdominal hysterectomy, which is either partial (removal of the uterus) or total (removal of both uterus and cervix) as well as the unilateral or bilateral salpingo-oopherectomy (BSO) (removal of single or both ovaries and fallopian tubes) and the omentectomy (removal of the omentum, a fat layer of tissue that covers some abdominal organs).

In the late 1970s the first platinum drug, cisplatin, was used as a single agent for the treatment of ovarian cancer (Rossof *et al.*, 1979; Thigpen *et al.*, 1979). The next generation of studies involved the combination of cisplatin with cyclophosphamide, rather than a single agent, that resulted in increased progression free survival (PFS) and overall survival (OS) (Decker *et al.*, 1982). Few years later, carboplatin was introduced as an analogue of cisplatin either as a single agent or in combination. It expressed similar response rates, however, with significantly improved toxicity profile (Wiltshaw *et al.*, 1983). Taxanes were introduced in the 1990s, and their combination with platinum drugs exhibited superior PFS and OS compared to the platinum/cyclophosphamide. Thenceforth, the combination of platinum and taxanes has been established as the standard care in advanced ovarian cancer (McGuire *et al.*, 1996).

The majority of ovarian cancer patients experience disease recurrence within 5 years and the recurrent ovarian cancer is mainly resistant to the previous chemotherapeutic drugs used for the initial treatment. The tumour sensitivity to platinum treatment is associated with the time of recurrence. Considering the limited availability of chemotherapeutic drugs in ovarian cancer, it is essential to establish alternative therapeutic approaches against ovarian cancer. There are currently new therapies which are aimed against molecular targets and pathways that are required for the tumour growth and survival. These therapeutic drugs include anti-angiogenic therapies (bevacizumab, cediranib and pazopanib, and nintedanib), polyADP-ribose polymerase (PARP) inhibitors (niraparib, rucaparib), epithelial growth factor receptor (EGFR) inhibitors (erlotinib, cetuximab or lapatinib) or folate receptor alpha (FRα) inhibitors (farletuzumab), as well as several immunotherapeutic approaches (Cortez *et al.*, 2018). However, these new approaches show diverse outcomes on the therapeutic potential in ovarian cancer.

1.3.3.1 Immunotherapies in Ovarian Cancer

The first evidence of immunosurveillance in ovarian cancer was reported almost two decades ago, by Zhang and colleagues, where they established the presence of tumour-infiltrating lymphocytes (TILs) and its positive correlation with patient survival (Zhang *et al.*, 2003).

Immunotherapy as an approach against ovarian cancer is based on four aspects on the tumour cells; (i) the expression of tumour-associated antigens (TAAs) such as CA125, human epidermal growth factor receptor 2 (HER2), epithelial cell adhesion molecule (EpCAM), NY-ESO-1 and LAGE-1,

(ii) the presence of TILs, (iii) the expression of peptides/MHC class I molecules on their surface and (iv) the dynamic interaction between cancer cells and immune cells. Immunotherapeutic approaches in ovarian cancer are still in early phases and involved antibody-based vaccines, peptide vaccines, cytokine vaccines, tumour cell vaccines, DC vaccines and heat shock protein (HSP) vaccine (Liu *et al.*, 2010).

1.3.3.2 Natural Killer Cell Immunotherapy in Ovarian Cancer

The current approaches for the enhancement of NK cell cytotoxicity against ovarian cancer cells include cytokine therapy with IL-2 or IL-15, adoptive NK cell transfer and antibody-based immunotherapy (Greppi *et al.*, 2019).

Several clinical trials have been conducted using IL-2 either as a single priming agent or in combination with other therapies which aimed to improve NK cell counts in ovarian cancer patients, however, it resulted in variable levels of clinical success. Similar to IL-2, IL-15 can potently increase NK cell count and enhance NK cell function better than IL-2 with less cytotoxic effects. In addition, *in vivo* studies, using murine model, demonstrated that treatment with IL-15 did not cause capillary leak syndrome, a major side effect of IL-2 administration (Munger *et al.*, 1995). In this regard, several clinical trials, evaluating IL-15 either as monomeric or as superagonist fusion complex (ALT-803) for cytokine-priming of NK cells are ongoing (Greppi *et al.*, 2019).

Adoptive therapy is another approach to enhance the NK cell responses against ovarian tumour cells, in which NK cells previously isolated

from the PB of ovarian cancer patient are cytokine-primed and adoptively transfer back to the same patient. This aims to improve the autologous NK cell function impairment. The first adoptive transfer was achieved in 1990s using high doses of IL-2, however, it demonstrated limited clinical responses and high cytotoxicity profile (Stewart *et al.*, 1990). It has been reported that NK cell activation via different cytokines such as IL-12, -15 and -18, displayed efficient enhancement in NK cell responses even in the presence of ascites. The ascitic fluid acts as a reservoir for malignant cells, immune cells and immunoregulatory factors that facilitates the tumour growth and used as an indicator of peritoneal spread of the cancer cells. It is the primary highlight of the immunosuppressive TME in ovarian cancer (Uppendahl *et al.*, 2019). Additionally, the *ex vivo* inhibition of glycogen synthase kinase 3 (GSK3) kinase in the PB, has been shown to enrich adaptive NK cells and enhanced the production of cytokines, natural cytotoxicity and ADCC upon exposure to ovarian tumour cells (Cichocki *et al.*, 2017).

The antibody-based immunotherapeutic approach in ovarian cancer is capable of effectively enhancing NK cell-mediated anti-tumour responses. This approach involves single antibodies against TAAs on the surface of ovarian cancer cells or new engineered bispecific/trispecific/tetraspecific killer engagers (BiKEs, TriKEs or TetraKEs). Examples of BiKE and TriKE include the crosslink of TAAs such as EpCAM with the CD16 on NK cells, thus activating the ADCC response, whereas, for TriKE it also involves the addition of IL-15 to this crosslink. The TetraKE comprises of EpCAM on cancer cells, CD16 on NK cells, CD133 on cancer stem cells and IL-15. The addition of IL-15, as a cross-linker, not only sustains the ADCC response but

also facilitates the NK expansion, cytokine production and survival of NK cells (Schmohl *et al.*, 2016a). Another promising immunotherapeutic approach to augment the NK cell function is the infusion of engineered immune cells with chimeric antigen receptors (CARs). Although these studies have been broadly performed on T-lymphocytes, recent investigations are focused on NK cells, however, questions remain to be answered for the optimal and successful NK cell anti-tumour activity (Hermanson & Kaufman, 2015).

1.4   Thesis Aims and Hypotheses

The aim of this project was to provide a deeper understanding of the NK cell function impairment in ovarian cancer and establish a potential novel NK immunotherapeutic approach against ovarian cancer.

The hypotheses that have been formulated and examined in this thesis were:

Hypothesis 1:
Natural Killer (NK) cells in the peripheral blood from ovarian cancer patients (OCPs) and NK cells from ascitic fluid at the site of the tumour, show different phenotypic and functional characteristics (Chapter 3).

Hypothesis 2:
NK cells derived from ascites at the tumour site of OCPs demonstrate different genomic, phenotypic and functional characteristics (Chapter 3).

Hypothesis 3:

Sensitivity to NK cell-mediated lysis in ovarian cancer depends on the differential expression of NK ligands and cell surface markers on ovarian cancer cells (Chapter 4).

Hypothesis 4:

Priming of NK cells mediated by either cytokine-induced or tumour-induced agents, can overcome the resistance of ovarian cancer target cells against NK cell cytotoxicity (Chapter 5).

Hypothesis 5:

NK cell priming can overcome the NK-mediated lysis impairment in ovarian cancer patients (Chapter 5).

Hypothesis 6:

NK cell priming improves function of HD- and OCP-derived NK cells to overcome the suppressive factors of the hypoxic TME (Chapter 6).

Chapter 2   METHODS

2.1 Cell Lines and Culture Systems

2.1.1 Cell Lines and Culture Media

All cell lines used for the completion of this project were obtained from American Type Culture Collection (ATCC). Two epithelial ovarian cancer cell lines derived from high-grade serous (HGS) adenocarcinoma , the SKOV3 and OVCAR3 cells were used in this project. The rationale behind this choice of ovarian tumour cells, relies on the fact that the epithelial ovarian tumours as well as the HGS are the most common type and sup-type respectively and therefore the selection of those cell lines for all the investigations, will enable the understanding in ovarian cancer setting to a greater extent.

In addition, K562 leukaemic cells as well as INB16 and RAJI lymphoma cells were also used in this project. All tumour cell lines were used as target cells against the NK effector cells except INB16 cells in which their role was to prime the NK cells. INB16 cell line is a distinct clone derived from the CTV-1 leukaemic cell line (from DSMZ) and it is an ALL cell line with AML tendency due to the presence of CD15 marker.

All the aforementioned cell lines, except the OVCAR3, were cultured in Roswell Park Memorial Institute medium with Glutamax (RPMI-1640; Life Technologies, Paisley, UK) supplemented with 10% foetal bovine serum (FBS) (Gibco, Thermo Fisher), penicillin (100 IU), and streptomycin (100 IU) (Invitrogen, Carlsbad, CA, USA). For OVCAR3 cells, RPMI-1640 medium

with Glutamax was used, supplemented with 20% FBS, penicillin (100IU) and streptomycin (100IU) and 0.01mg/ml bovine insulin (Sigma).

The cells were harvested every 2 to 3 days, depending on culture confluence. For adherent cell lines (SKOV3 and OVCAR3), culture medium was removed from the flasks and cells were washed gently with 7ml of Hank's Balanced Salt Solution (HBSS) (no calcium and no magnesium) (Gibco, ThermoFisher Scientific, UK) to remove any residual medium. Subsequently, Cell Detachment solution (amsbio, UK) was added to the culture flasks (1ml for T25 and 3ml for T75) and the cells were incubated at 37°C in a standard cell culture incubator (Panasonic) with 5% CO_2 and 21% O_2 for 5 minutes. Cells were then removed from the incubator, 6ml of the corresponded supplemented medium were added to the culture flask and cell suspension was transferred to a 50ml polypropylene conical tube for centrifugation at 300 g for 5 minutes at room temperature (RT). The concentration of the pelleted cells was determined and 14,000 cells/cm^2 were seeded in the new culture flasks.

For non-adherent cell lines culture medium in the flasks was mixed gently, removed and finally replaced with fresh culture medium in a volume ratio 1:1.

All cells were in culture for a maximum of 10 passages for adherent cell lines and for a maximum of 3 weeks for non-adherent cell lines at 37°C in humidified air containing 5% CO_2 and 21% O_2 or 5% CO_2 and 1% O_2 for hypoxic experiments.

2.1.2 Cell Concentration and Viability

The concentration and viability of cells were determined prior transferring to new culture flasks, using the Trypan Blue exclusion method under a brightfield microscope. Sample of cells was mixed with 0.4% Trypan Blue solution (Sigma-Aldrich, UK) an azo dye, that penetrates and stains with blue colour only the dead cells due to their cell membrane disruption, whereas the live cells with intact cell membrane remain unstained. Subsequently, 10µl of this mixture was loaded onto a haemocytometer counting chamber (Labtech, UK). The total number of cells across the four sets of 16 squares (1mm^2) was counted as indicated with red in the image below and the mean was calculated.
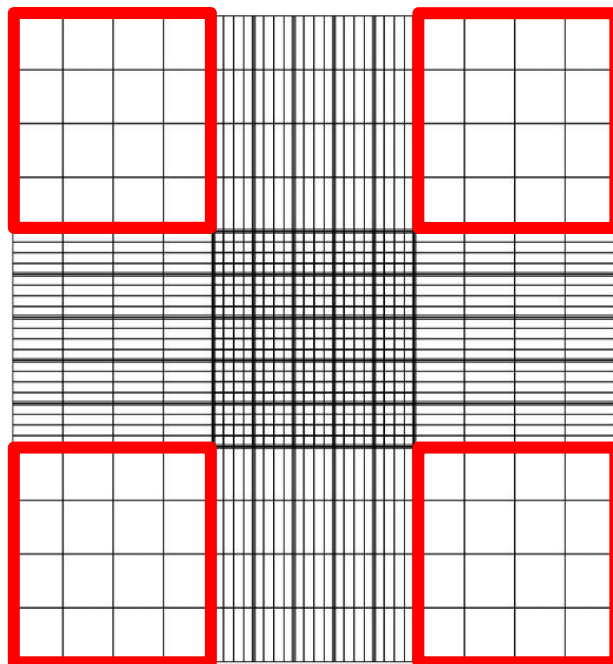
Figure 2-1: Haemocytometer Chamber Grid

The number of live cells as well as the viability were determined using the equations below:

Equation 2-1

$$Cell\ concentration = Mean\ of\ live\ cells\ x\ dilution\ factor\ x\ 10^4$$

Equation 2-2

$$Cell\ viability\ (\%) = \frac{Mean\ of\ live\ cells}{Mean\ of\ total\ cells}\ x\ 10$$

2.1.3 Cell Cryopreservation

The SKOV3 and OVCAR3 epithelial ovarian cancer cell lines were cryopreserved in a cryomix consisting of 5% dimethyl sulfoxide solution (DMSO) (WAK-Chemie Medical Steinbach, Germany) in FBS. For this procedure, cells were resuspended at $3\text{-}4x10^6$/ml of their respective culture media, and 0.5ml was added into a 2ml cryogenic vial (Sigma-Aldrich, UK). Subsequently, 10% of DMSO/FBS stock mix was prepared and 0.5ml was added to the same 2ml cryogenic vial, resulting in a final 1ml mixture consisting of $1.5\text{-}2x10^6$ cells in 5% DMSO/FBS.

For RAJI, K562 and INB16 cell lines, a maximum of $20x10^6$ cells were pipetted into the 2ml cryogenic vials in 10% DMSO/FBS cryomix. Therefore, cells were resuspended in $40x10^6$/ml and 20% DMSO/FBS stock cryomix was prepared. Finally, 1ml of each was added to the 2ml cryogenic vials (Sigma-Aldrich, UK) to result in $20x10^6$ cells in 10% DMSO/FBS cryomix.

All the cryovials were labelled with the name and concentration of the cells, the percentage of the cryomix and the date of cryopreservation. They were then placed inside a freezing container (ThermoFisher Scientific, UK) and stored overnight at -80°C prior transferring them to the liquid nitrogen phase at UCL-RFH Biobank.

2.1.4 Cell Thawing

Cryopreserved cells were gently thawed in a 37°C water bath by keeping the O-ring and cap out of the water to avoid any contamination. The thawed cells were transferred to a 15ml polypropylene conical tube (ThermoFisher Scientific, UK). Subsequently, 9ml of the appropriate supplemented culture medium was added gently to the cells and conical tube was centrifuged at 300g for 5 minutes, RT. Supernatant was discarded, pellet was resuspended in supplemented culture medium and the concentration and viability of the cells were determined as described above in section 2.1.2. Cells were transferred in a T25 culture flask and placed in a standard cell culture incubator (Panasonic) (37°C, 5% CO_2, 21% O_2).

2.2 Natural Killer Cell Isolation

NK cells were obtained from leukocyte cones of healthy donors provided by the National Health Service Blood and Transplant service (NHSBT) or from heparinised blood (Heparin Sodium 1,000IU/ml, Wockhardt, UK) of healthy donors at Royal Free Hospital.

For patient samples, Peripheral Blood Mononuclear Cells (PBMCs) and ascitic fluid were collected. The patient groups used for this study consisted of late stage patients with relapsed ovarian cancer that had already undergone chemotherapeutic cycles and surgical debulking and were currently being provided palliative treatment that included drainage of malignant ascites.

For all the samples, informed consent was provided in accordance with the declaration of Helsinki and the study was approved by the UCL/Royal Free Ethical Review Board, NC.2015.019.

The collected blood was initially diluted (1:1) in HBSS without calcium and magnesium (Gibco, ThermoFisher Scientific, UK). Consequently, Human Lympholyte (Cedarlane, North Carolina) was used to isolate the PBMCs via density gradient centrifugation. This was performed by adding 20ml of Lympholyte to a 50ml polypropylene conical tube and 25ml of diluted blood were transferred slowly to the tube, resulting in two distinct layers. After this step, the tube was centrifuged at 800g for 20 minutes, RT at brake 0 and the PBMC layer was collected and transferred to a new 50ml polypropylene conical tube. Subsequently, the layer was washed with HBSS (no calcium and no magnesium) (Gibco, ThermoFisher Scientific, UK) and centrifuged at 800g for 10 minutes, RT at brake 3. Consequently, pelleted cells were resuspended in supplemented culture medium and the absolute number and viability of PBMCs were determined.

Finally, the NK cells were isolated by either negative selection or positive selection as described below. The reason behind using two different NK cell selection was to establish which NK isolation protocol could result in a higher yield and better purity. The purity of the positive NK isolation technique was found to be lower than that resulting from negative selection. The desired collected cells from the NK positive selection method, were both NK (CD56$^+$/CD3$^-$) and NK-T (CD56$^+$/CD3$^+$) cells, due to the use of the CD56 MicroBeads that bind to any CD56$^+$ cell in the PBMC population

However, the negative selection for the NK isolation, allows the collection of pure untouched NK cell population, as the reagents from this method, bind to all the cells that are not CD56$^+$/CD3$^-$. Figure 2-2 shows that the purity of NK cell positive isolation was 74.83% compared to 97.30% for the negatively-selected NK cells

Therefore, negative selection was chosen as the approach for NK cell isolation.
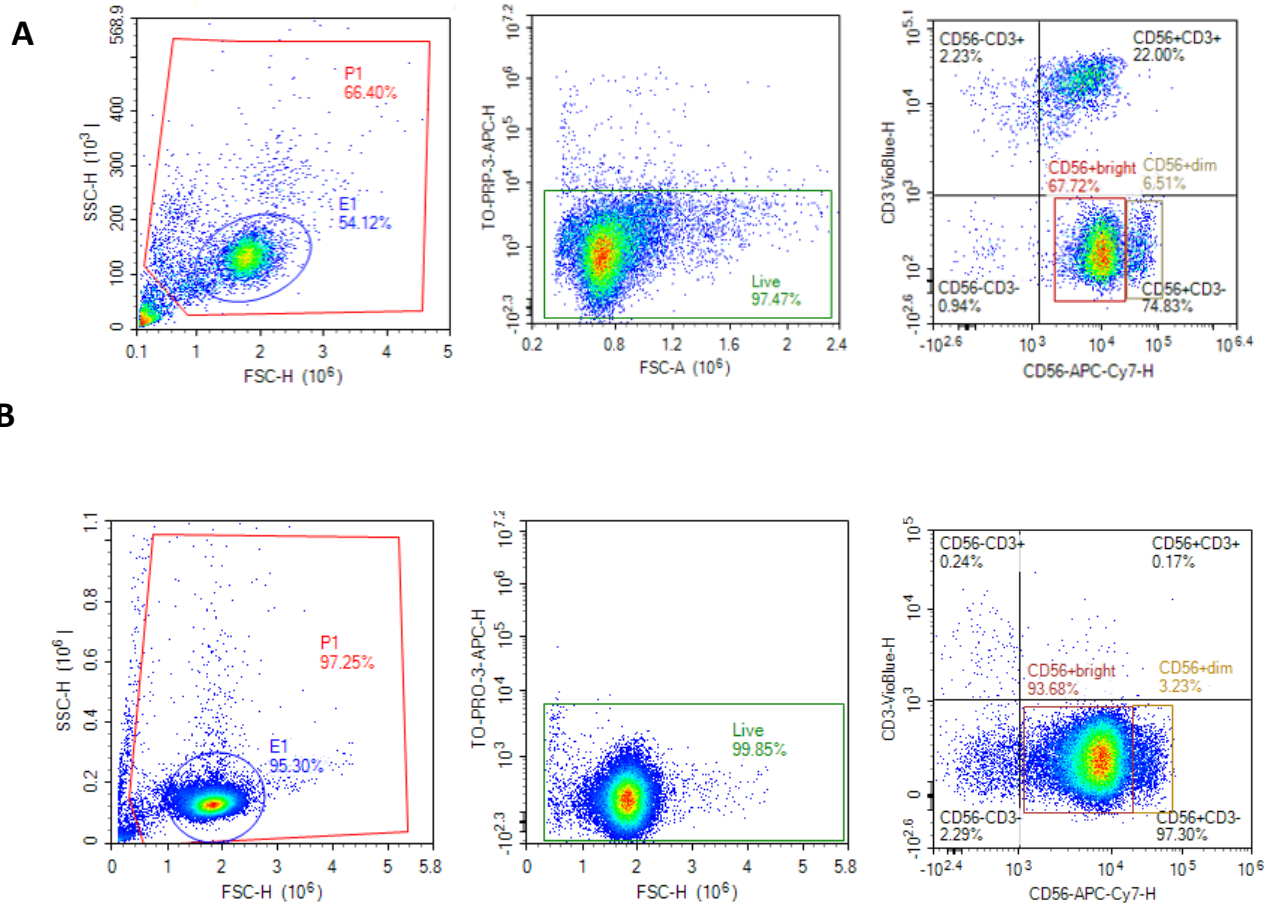
Figure 2-2: Gating Strategy of NK Cells to Identify Concentration and Purity

NK cells were isolated via either positive selection (A) or negative selection (B). TO-PRO-3 (APC) counterstain dye was used to assess the viability and purity was determined on the CD56$^+$/CD3$^-$ population after staining with CD3 (REA613) Vioblue and CD56 (NCAM16.2) APC-Cy7. All the experiments were performed as technical duplicates from biological triplicates (n=3).

2.2.1 Negative Selection

This technique relies on depletion of unwanted, non-NK cells through a tetrameric antibody complex and magnetic particles, using the EasySep NK Enrichment Kit (StemCell Technologies, UK). The sample is incubated in a magnet, where unwanted cells are depleted and the NK cells are poured off into a new tube. This method was performed per manufacture's protocol.

Initially, PBMCs were centrifuged at 300g for 5 minutes at RT and pelleted cells were resuspended in EasySep Buffer at a final concentration of 50×10^6/ml. Depending on the suspension volume, cells were transferred to either a 5ml round bottom tube or a 13ml round bottom tube. Enrichment Cocktail (50µl/ml) was added to the tube and the sample was incubated at RT for 10 minutes. Vortexed Magnetic Particles (100µl/ml) were subsequently added to the sample and incubated at RT for 5 minutes. EasySep buffer was added to result in a final volume of 2.5ml for the 5ml small round bottom tube or up to 5ml/10ml for the 13ml round bottom tube, depending on the initial sample volume (<2ml or ≥ 2ml respectively). Finally, the sample was inserted into the EasySep magnet and incubated at RT for 2.5 minutes. The sample was poured in a new Falcon tube by continuous inverted motion, then supplemented culture medium was added and sample was centrifuged at 300g for 5 minutes, RT. Supernatant was discarded, and pellet was resuspended in fresh supplemented culture medium for count. NK cell purity was validated by phenotyping using CD56 (NCAM16.2) APC-Cy7 (Becton Dickinson, UK) and CD3 (REA613) VioBlue (Miltenyi,UK)

monoclonal antibodies. An illustration of the NK negative selection technique can be seen in **Figure *2-3***.

```
┌─────────────────────────────────────┐
│  PBMC preparation in the recommended │
│  concentration within the volume     │
│  range using EasySep buffer          │
└─────────────────────────────────────┘
                 │
                 ▼   Transfer PBMC sample to a 5ml polystyrene round-
                     bottom tube
┌─────────────────────────────────────┐
│  Add Enrichment Cocktail 50µl/ml     │
│                                      │
└─────────────────────────────────────┘
                 │
                 ▼   Mix and incubate for 10 minutes at RT
┌─────────────────────────────────────┐
│  Add Magnetic Particles (after       │
│  vortex for 30 seconds)              │
│  100µl/ml                            │
└─────────────────────────────────────┘
                 │
                 ▼   Mix and incubate for 5 minutes at RT
┌─────────────────────────────────────┐
│  Add recommended EasySep buffer to   │
│  the sample for a final volume of    │
│  2.5ml and place the tube to the     │
│  magnet without lid                  │
└─────────────────────────────────────┘
                 │
                 ▼   Mix and incubate for 2.30 minutes at RT
┌─────────────────────────────────────┐
│  Pick up magnet and in a single      │
│  continuous motion, invert the       │
│  magnet with the tube and pour off   │
│  to a new tube                       │
└─────────────────────────────────────┘
```

Figure 2-3: EasySep Human NK Cell Isolation Kit

2.2.2 Positive Selection

In this method, the NK cells are selected via magnetic beads conjugated to a CD56 monoclonal antibody. . The sample is placed on a magnetic column attached to a magnetic separator and the unwanted cells are washed off. The desired cells (CD56$^+$) are collected into a new tube by removing the column from the magnetic separator. This protocol was conducted as per manufacturer's instructions.

Initially, PBMC cells were counted and washed with MACS buffer (PBS + 2Mm EDTA + 0.5% FBS) by centrifuging at 300g for 5 minutes, RT. Pelleted cells were resuspended in MACS buffer (80µl per 1x10^7 cells) and CD56 MicroBeads (Miltenyi Biotec) were added (20µl per 1x10^{7}cells). Sample was gently mixed and incubated at 4°C for 15 minutes. During this incubation time, an appropriate MACS magnetic column was selected according to the number of cells; MS column or LS column for a maximum of 1x10^7 or 1x10^8 cells/ml respectively, and then placed on the magnetic separator. For the MS column the magnetic separator used was the MiniMACS whereas for the LS column was either the MidiMACS, QuadroMACS or VarioMACS. The magnetic column was rinsed with MACS buffer (500µl for MS column and 3ml for LS column) and the incubated sample was added to the appropriate rinsed column. After, the sample was completely passed through the reservoir, the column was washed 3 times with MACS buffer in the same volume as mentioned before. Unlabeled cells (negative fraction) were washed off from the column at this point and the desired cells (positive fraction) were collected by removing the column from

the magnetic separator. MACS Buffer was added to the reservoir (1ml for MS column or 5ml for LS column) and firmly applied the plunger to collect the desired cells to a new tube. Finally, supplemented culture medium was added to the new tube and collected cells were centrifuged at 300g for 5 minutes, RT. An illustration of the NK cell positive selection method can be seen in Figure 2-4.

PBMC preparation in the recomended concetration using MACS buffer
(80µl per $1x10^7$ cells)

Addition of CD56 MicroBeads and incubation for 15 minutes at 4°C
(20µl per $1x10^7$ cells)

Preparation of MACS Magnetic column by placing to the appropriate magnetic seperator and rinse with MACS buffer

500µl for MS column on MiniMACS seperator and 3ml for LS column on MidiMACS/QuadroMACS/VarioMACS seperators

Load sample to the reservoir of the MACS magnetic column and wash 3 times with MACS buffer (same volume as above)

Removal of MACS magnetic column from the magnetic separator and use the plunger to collect the "positive fraction" consisting of the CD56 labelled cells

Figure 2-4: NK Cell Isolation via Positive Selection Using CD56 MicroBeads and Magnetic Separator

Pelleted cells were resuspended in culture medium for cell count and the purity of NK cells was determined using CD56 (NCAM16.2) APC-Cy7 (Becton Dickinson, UK) and CD3 (REA613) VioBlue (Miltenyi,UK) monoclonal antibodies as aforementioned.

2.2.3 Immunophenotyping of Natural Killer Cells

The sample of cells was washed by adding 2ml of staining buffer consisting of Phosphate Buffer Saline (PBS) and 2% FBS (Gibco, ThermoFisher Scientific, UK) and centrifuged for 5 minutes at 300g, RT. The pellet was then resuspended in 100µl of staining buffer and specific volume of the fluorochrome conjugated monoclonal antibodies were added to the pelleted cells as per manufacturer's instructions; 5µl for CD56 (NCAM16.2) APC/Cy7 (Becton Dickinson, UK) and 2µl for CD3 (REA613) Vioblue (Miltenyi, UK). Subsequently, the cells were incubated for 15 minutes at 4°C and then washed as mentioned above. Finally, supernatant was removed and pelleted cells were resuspended in 100µl of staining buffer and analysed by flow cytometry (NovoCyte, Agilent). An unstained sample was used as a control for the gating strategy.

Cells labelled as $CD56^+/CD3^-$ were addressed as the pure NK population and the final concentration of NK cells after isolation, was adjusted according to this population. The TO-PRO-3 (1:1000 in PBS) (ThermoFisher Scientific, UK) counterstain dye was used as a viability dye to permit the accurate quantification of the NK cell concentration.

2.3 Natural Killer Cytotoxic Assays

2.3.1 Flow Cytometric Assay for Non-Adherent Target Cells

The NK functional cytotoxic assay for the non-adherent target cell lines K562 and RAJI were assessed using flow cytometry (NovoCyte, Agilent). This technology allows a rapid, sensitive and quantitative analysis of single cells in a distinct population of cells. It consists of three systems; fluidics, optics and electronics. The fluidics system consists of a pressurised sheath fluid that hydrodynamically enables the cells to pass one at a time through the laser beam. The optical system encompasses of the excitation optics (lasers) and the emission optics (photomultiplier tubes or PMTs). The optics system can distinguish cells according to their size and granularity through light forward scatter (FSC) and side scatter (SSC) respectively or via fluorescently labelling of a protein of interest using a fluorochrome. Finally, the electronics system converts the signals to digital, in order to allow the visualisation of results on the computer.

2.3.1.1 PKH67 Membrane Dye Labelling of K562 and RAJI Target Cells

For this assay, the target cells were firstly fluorescently labelled using a cell membrane dye, PKH67. Initially, cells were washed with HBSS (no calcium and no magnesium) (ThermoFisher Scientific, UK) by centrifuging for 5 minutes at 300g, RT. The supernatant was discarded and pellet was resuspended in 500µl of Diluent C from the PKH67 Green Fluorescent Cell Linker Kit for General Cell Membrane Labeling (Sigma-Aldrich, UK). In a new 15ml polypropylene conical tube, the dye mixture was prepared by adding

4µl of PKH67 dye to 500µl of Diluent C and kept in the dark. Subsequently, target cell suspension was added to the dye mixture and incubated for 3 minutes at RT in the dark. Finally, 1ml of supplemented culture medium was added to the sample and incubated for 1 minute at RT to stop the reaction. The conical tube was then centrifuged for 5 minutes at 300g, RT. The pellet was resuspended in 10ml of fresh supplemented culture medium and transferred to a new 15ml polypropylene conical tube for an additional wash under the same conditions.

Finally, the pellet was resuspended in 3ml of supplemented culture medium and the cell concentration, viability and efficacy of labelling were evaluated using the flow cytometry (NovoCyte, Agilent). The PKH-labelled target cells were then resuspended in a final concentration of 0.2×10^6/ml for the following NK cell lysis assay.

Both target cells were PKH67 labelled in their exponential phase of growth, implying that cell culture media change was performed the day prior the initiation of the cytotoxic assay.

2.3.1.2 Killing Assay

For all the killing assays in this project, the ratio of effector to target (E:T) was 5:1. This ratio was based on previous optimisation studies performed by our group, in which several E:T ratios were investigated, using the same target cells, to establish the optimum ratio for killing assays. The E:T ratios tested were 1:1, 2:1, 5:1 and 10:1.

For this experiment, NK cells were isolated via NK Negative Selection as section 2.2.1 and purity was checked as section 2.2.3. Subsequently, the NK cells were resuspended at 2×10^6/ml.

There were three effector conditions for this assay; the non-primed resting NK (rNK), the cytokine-primed NK cells using 10 ng/ml of recombinant human IL-15 (rhIL-15) (R&D Systems, UK) and the tumour-primed NK (TpNK) cells using the previously identified priming leukaemic cancer cell line, INB16 in a ratio of NK:INB16 (1:2). All NK cell priming conditions were performed overnight.

For the cytokine priming of NK cells, the NK cells were co-incubated with 10ng/ml of rhIL-15 overnight. This ratio was established from previous studies in which different rhIL-15 concentrations were tested. These included 1, 2, 5, 10 and 20ng/ml and after the o/n co-interaction with the NK cells the efficacy of cytokine-primed NK cells was assessed in a cytotoxic killing assay against the aforementioned target cells.

For the tumour priming of NK cells, INB16 cells were used after mitomycin C (MMC) (Sigma-Aldrich) treatment. For this procedure, INB16 cells were transferred to a 50ml polypropylene conical tube and washed in HBSS (no calcium and no magnesium) (ThermoFisher Scientific, UK) by centrifuging for 5 minutes at 300g, RT. MMC powder stock (2mg) was reconstituted in 2ml of saline (1mg/ml) and subsequently filtered. The INB16 pellet was then resuspended in fresh supplemented culture medium at 5×10^6/ml and 10ng/ml of the reconstituted filtered MMC was added. The

sample was incubated for 2h at 37°C in the dark and then washed 3 times as mentioned above. Finally, the pelleted cells were resuspended in fresh supplemented culture medium in a concentration of 4×10^6/ml. The tumour priming was performed in a NK:INB16 (1:2) o/n. This ratio has been already established by our lab, after performing studies testing 1:1, 1:2 and 1:5 of NK:INB16 ratios. The mechanism behind the INB16:NK interaction and subsequently priming relies on the binding of CD15 on INB16 cell surface to the CD2 on the NK cells.

All corresponded, effector conditions and target cells were co-incubated at the appropriate ratios abovementioned.

For the hypoxic killing assays in this project, the experiment was prepared as mentioned above, however, the incubation of target cells and effector cells and subsequently the killing assay were performed in a converted cell culture incubator (Panasonic) with 5% CO_2 and 1% O_2 upon nitrogen purge. Both normoxia and hypoxia killing assays were performed simultaneously for each donor. All samples were performed as technical duplicates.

The viability of the labelled target cells, was assessed using a nuclear counterstain dye, TO-PRO-3 (1:1000 in PBS) (ThermoFisher Scientific, UK) that positively stains dead cells with APC fluorophore due to their disrupted membrane. Therefore, the viable, PKH67-labelled target cell population (FITC$^+$) was identified as TO-PRO-3 negative (APC$^-$) and the absolute number of cells from this FITC$^+$/APC$^-$ phenotype, was used to calculate the

percentage of lysis. Figure 2-4 illustrates the gating strategy for K562 (A) and RAJI (B) target cells.

For plotting the data, the percentage of specific lysis was defined after subtracting any spontaneous target cell lysis from the "control" labelled target cells, that was measured immediately after the initiation of the killing assay ("0h" of co-incubation). The killing assay was performed at E:T (5:1) in three different timepoints; 4h, 6h and 16h. For every timepoint tested, a "control" sample of target cells only was also included to evaluate any spontaneous cytolysis and determine the specific cytolysis for the corresponded timepoint.

The series of calculations to obtain the results of this assay can be seen below:

Equation 2-3:

$$Live\ target\ cells$$
$$= \frac{Absolute\ count\ of\ live\ PKH67\ target\ cells\ (for\ the\ specific\ timepoint)\ x\ 100}{Absolute\ count\ of\ live\ cells\ at\ 0h}$$

Equation 2-4:

$$Live\ cells\ after\ co-incubation\ with\ NK\ effector\ cells$$
$$= \frac{Absolute\ count\ of\ live\ PKH67\ target\ cells\ in\ each\ NK\ effector\ conditions\ x\ 100}{Absolute\ count\ of\ live\ cells\ at\ this\ specific\ timepoint}$$

Equation 2-5:

$$Specific\ Cytolysis\ (\%) = 100 - live\ cells$$
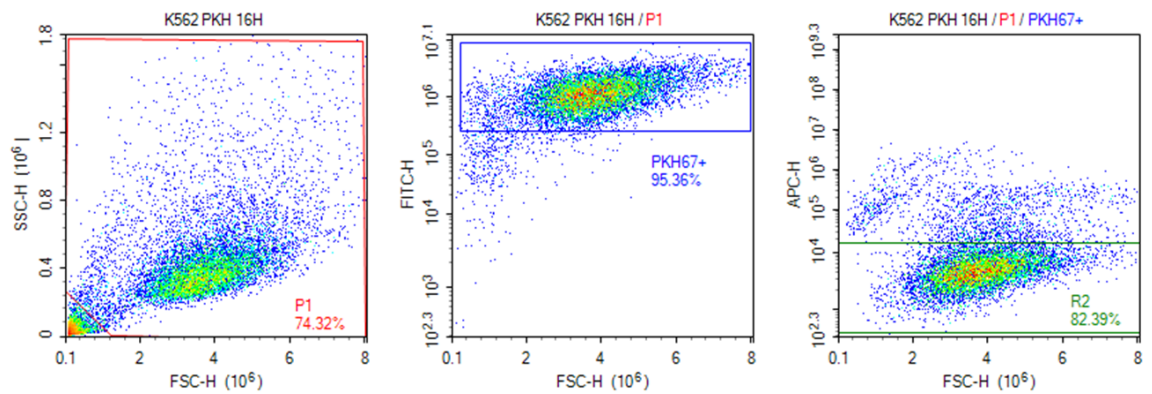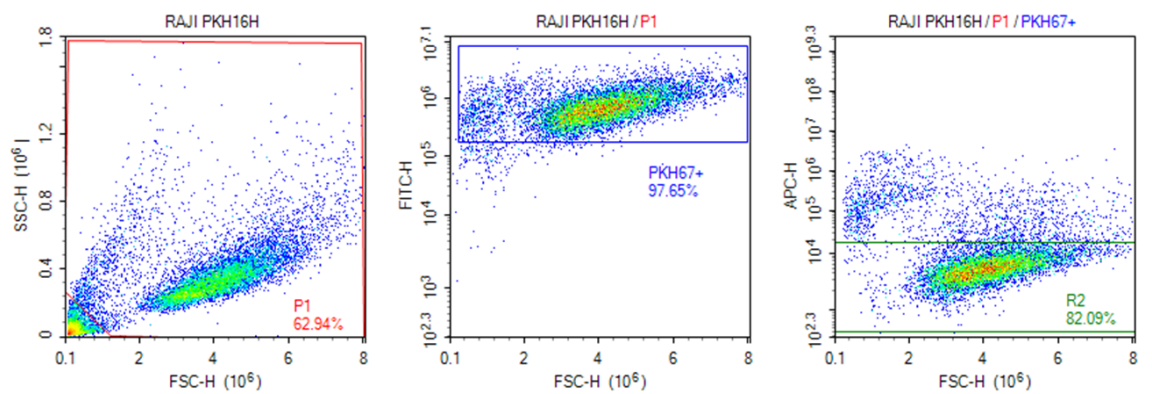
Figure 2-5: Gating Strategy of PKH67 Labelled K562 and RAJI Target Cells

Representative plot showing the gating strategy used for the cytotoxic assays of K562 (A) and RAJI (B) target cells against non-primed and primed NK cells. Target cells were PKH67 labelled (FITC) and TO-PRO-3 (1:1000) (APC) counterstain dye was used as viability dye. Timepoints tested; 4h, 6h and 16h. FITC+/APC- (R2 gate) was the one used to evaluate the target cell cytolysis. Experiment performed in technical duplicates and biological triplicates (n=3)

2.3.2 Electrical Impedance Assay for Adherent Target Cells

2.3.2.1 xCELLigence RTCA System

NK cell functional cytotoxic assay for the adherent target cell lines SKOV3 and OVCAR3 cell lines were performed in the xCELLigence Real-Time Cell Analysis (RTCA) system (Agilent). This equipment is a microelectronic biosensor using non-invasive electrical impedance to measure and monitor adherent cells in a continuous and quantitative readout. It requires the use of special microtiter e-plate where its bottom is fused with gold microelectrodes that allows the transmission of electrical impedance in the presence of an electrically conductive solution (supplemented culture medium). Two xCELLigence RTCA systems were used for this project, the DP RTCA and MP RTCA which consist of 3x16-well e-plate cradles and 6x96-well e-plate cradles respectively. The xCELLigence DP and MP stations are connected to an analyser and subsequently to a control unit (laptop). Figure 2-6. This technology works by measuring the changes in the interaction of the electrodes/solution via adhesion of adherent cells to the bottom of the microtiter plates. This impedance is translated in a unitless parameter known as Cell Index (CI). It is defined as:

Equation 2-6:

$$Cell\ Index\ (CI) = (Rtn - Rt0)/10$$

Rtn is the cell-electrode resistance measured at a time point Tn on the well, and Rt0 is the background resistance, of the supplemented culture medium alone, measured at time point t0. The Cell Index is directly correlated with the number of viable cells.

Control Unit

E-plate station
(3x 16-well e-plates)

E-plate station
(6x 96-well e-plates)

or

Analyser

electrode

electrode
without cell

cell

electrodes with one
cell attached

cells

electrode

electrode with two
cells attached

electrode with two
strongly-attached cells
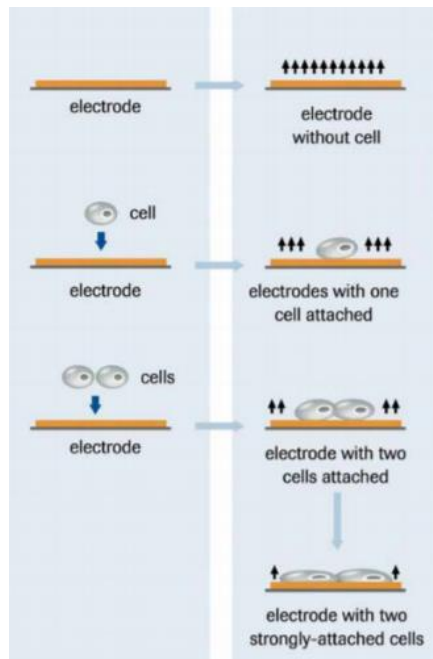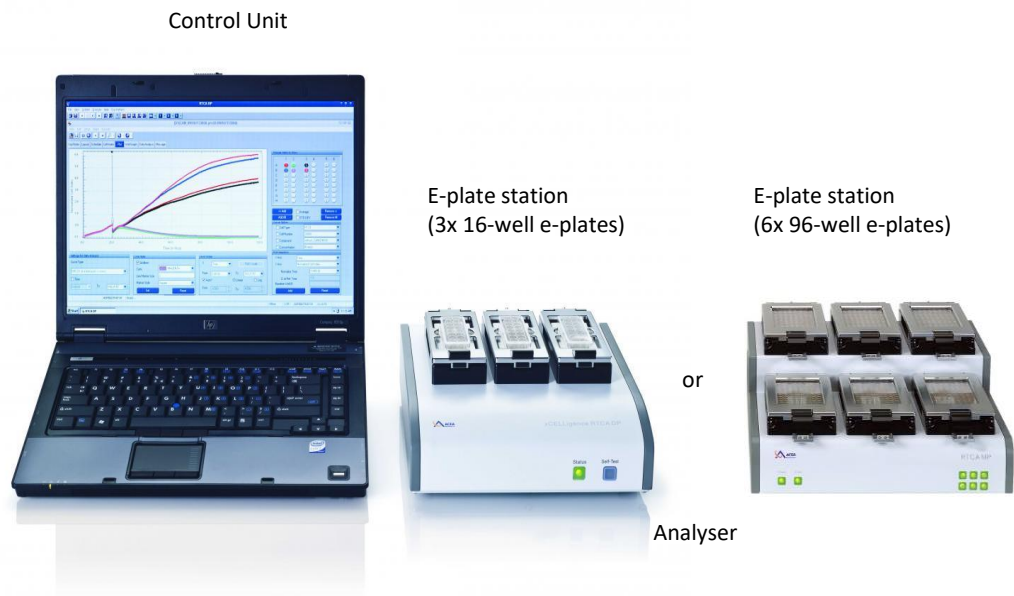
Figure 2-6: The xCELLigence RTCA Instrument and a Schematic Illustration of Electrical Impedance Generation (ACEA Biosciences)

The adherent epithelial ovarian cancer cell lines, SKOV3 and OVCAR3 were passaged the day before seeding on the xCELLigence e-plates (day 0). On the day of the experiment (day 1), SKOV3 and OVCAR3 cells were harvested and re-suspended in 0.1×10^6/ml and 0.2×10^6/ml working stocks correspondingly. In order to define the electrical impedance between the cells and the xCELLigence station, supplemented culture media (50µl/well) specific for each target cell line was added to all the wells of the e-plate, prior to the addition of the target cells, for background measurement (first step). Subsequently, target cells were seeded at 5,000/well for SKOV3 and 10,000/well for OVCAR3 and left in the biosafety cabinet for 30 minutes at RT. Finally, the e-plate was inserted in the xCELLigence RTCA instrument (Agilent) and the adhesion and growth rate of target cells were monitored overnight before the addition of any effector cells the next day (day 2).

The killing assay of the adherent cells was conducted at E:T (5:1). Briefly, NK cells were isolated from PBMCs via negative selection as section 2.2.1 and resuspended in a concentration of 0.5×10^6/ml for the SKOV3 target cells and 1×10^6/ml for OVCAR3 target cells. The NK effector conditions used for the cytotoxic functional killing assays against SKOV3 and OVCAR3 target cells, included rNK, cytokine-primed via human recombinant IL-15 (10ng/ml) (R&D Systems, UK), or TpNK using INB16 MMC treated: (NK:INB16, 1:2). All the NK effector conditions were left o/n at 37°C, 5% CO_2, 21% O_2 (day 1).

The next day (day 2), all the NK effector conditions were added to the corresponded wells of the e-plates that already contained the pre-seeded target cells at E:T (5:1). Finally, e-plates were placed back onto the

xCELLigence RTCA system and killing assay was measured every 15 minutes for a duration of 48h.

For the hypoxic cytotoxic assay, target cells and effector cells were pre-incubated in hypoxia 37°C, 5% CO_2, 1% O_2 prior any addition to the e-plates. Replicates of the plates, as in normoxia (5% CO_2, 21% O_2), were prepared and killing assay of the target cells was simultaneously performed under normoxic and hypoxic conditions. All samples were performed as technical duplicates.

2.3.3 Esight Live Cell Imaging

The eSight system (Agilent) combines the live cell imaging and the real-time electrical impedance measurements of the xCELLigence RTCA system. It allows the visualisation of biological cell functions under brightfield and fluorescence using 3 fluorescent channels; red, blue and green. For this experiment, the NK-insensitive SKOV3 target cell line was used against the three aforementioned NK cell effector conditions.

SKOV3 target cells were labelled with PKH67 as described in section 2.3.1.1. Subsequently, they were seeded on the e-plate at a concentration of 5,000 cells/well and left o/n to adhere and proliferate with readouts every 15 minutes. The next day NK cells were isolated from PBMCs and labelled with Cell Trace Violet 2Mm (ThermoFisher Scienticic, UK), a cell tracing reagent that covalently binds to intracellular amines of the cells. For this staining procedure, NK cells were transferred in a 15ml polypropylene conical tube and washed with PBS (ThermoFisher Scientific, UK) for 5 minutes at 300g,

RT. Supernatant was discarded and pellet was resuspended in PBS (ThermoFisher Scientific, UK) at 1×10^6/ml. Cell Trace Violet working concentration was prepared by adding 2μl of DMSO to the 5Mm stock concentration and 1μl of this stock was added to each ml of cell suspension to achieve a working concentration of 5 Mm. Subsequently, NK cells were incubated for 20 minutes at 37°C in the dark with gentle mixing every 5 minutes to allow the even distribution of the dye reagent. Incubation was stopped by adding 5 times the original volume of supplemented culture medium to the NK cells and left for 5 minutes at RT. Finally, cells were centrifuged for 5 minutes at 300 g, RT and resuspended in fresh supplemented culture medium. Viability of cells and efficacy of staining was assessed using flow cytometry (NovoCyte, Agilent) and TO-PRO-3 counterstain dye.

Finally, NK effector conditions were added to the SKOV3 target cell e-plate and target cell lysis was obtained using Caspase 3/7 red reagent, a nucleic acid binding dye that attaches to the DNA of apoptotic cells and produce a bright red signal.

2.4 RNA Extraction

RNA extraction of NK cells from PBMC and ascitic fluid samples of ovarian cancer patients (OCPs) was performed to identify differential gene expression. As the starting material was very small, three different RNA extraction methods were conducted, to establish the one that gives the highest RNA yield from small sample (less than 0.3×10^6 cells)

2.4.1 RNAqueous-Micro Kit

This kit (Applied Biosystems, UK) is used for isolating RNA from small samples including cultured cells (≤0.5x10^6), tissue samples (≤10 mg) and microdissected tissues. This procedure was performed as per manufacturer's instructions.

Cells were washed with PBS (ThermoFisher Scientific, UK) to remove any supplemented media residuals and pellet was resuspended in 100µl of lysis solution by vortexing vigorously. This lysis solution contains guanidium thiocyanate, which is a strong chaotropic agent that disrupts the cell membrane and affects ribonucleases. After this step, the sample was mixed with 50µl of 100% high grade ethanol and transferred to a MicroFilter Cartridge Assembly with the lid closed on top of a 2ml collection tube and centrifuged for 10 seconds at maximum speed. This filter selectively binds to the RNA. Subsequently, 180µl of Wash solution 1 were added to the MicroFilter, the lid was closed and centrifuged for 10 seconds at maximum speed. 180µl of Wash Solution 2/3 (working solution mixed with 100% ethanol) was then added to the MicroFilter and centrifuged again as before. The last two steps were repeated and the MicroFilter Cartridge was transferred to a new collection tube. Sample was centrifuged for 1 minute at maximum speed and the MicroFilter Cartridge was transferred to a MicroElution tube. Finally, 5-10µl of preheated at 75°C Elution solution were added to the center of the filter, cap was closed and incubated for 1 minute at RT prior centrifuging for 30 seconds at maximum speed. The last step of Elution solution addition and spinning was repeated.

A DNase I treatment and DNase inactivation step was performed after the RNA isolation to remove any traces of contamination by genomic DNA. Initially, 1/10 volume of 10x DNAse I buffer and 1µl of DNAse I enzyme (working stock reconstituted in 550µl of RNAse-free water) was added to the sample and incubated for 30 minutes at 37°C. During this incubation time, DNAse inactivation reagent was removed from -20°C to thaw and vigorously vortexed to completely resuspend it. 1/10 volume of DNAse inactivation reagent was subsequently added, incubated for 2 minutes at RT with vortex intervals and then centrifuged for 1,30 minutes at maximum speed. Finally, RNA was transferred to new RNA free tube and stored at -20°C.

2.4.2 RNeasy Micro Kit

This protocol is also designed to isolate RNA from small samples including cultured cells ($\leq 0.5 \times 10^6$) even as little as a single cell, tissue samples ($\leq$5mg), fibrous tissues ($\leq$5mg) and microdissected tissues. This procedure was conducted following manufacturer's instructions (Qiagen, UK). The initial principle of this method was the same as the RNAqueous Micro kit which involves the lysis of the sample in a lysis buffer containing the same agent.

Briefly, cells were washed with PBS by centrifuging for 5 minutes at 300g to remove any residues of supplemented culture medium. The supernatant was removed and pellet was resuspended with 350µl of Lysis Buffer RLT (working stock mixed with 4 volumes of 100% ethanol) and vortexed vigorously. An equivalent volume of 70% ethanol was added to the lysate and mixed well by gently pipetting. The sample was then transferred to

RNeasy MinElute Spin Column placed on top of a 2ml collection tube, cap was closed and centrifuged for 15 seconds at 8000g, RT. 350µl of Buffer RW1 were added to the RNeasy MinElute Spin Column, cap was closed and span for 15 seconds at 8000g, RT. Subsequently 10µl of DNAse I enzyme (working stock reconstitute in 550µl of RNAse-free water) were added to 70µl of Buffer RDD and mixed gently by inverting the tube. This mixture (final volume 80µl) was added to the center of the RNeasy MinElute Spin Column membrane and incubated for 15 minutes at RT. 350µl of Buffer RW1 was added and sample was centrifuged for 15 seconds at 8000g, RT. Then, the RNeasy MinElute Spin Column was placed on top of a new 2ml collection tube and 500µl of Buffer RPE was added, lid was closed and span for 15 seconds at 8000g, RT. Subsequently, 500µl of 80% ethanol was added and centrifuged for 3 minutes at 8000g , RT with closed lid. The RNeasy MinElute Spin Column was placed onto a new 2ml collection tube, cap remained open and span for 5 minutes at maximum spin to ensure any elimination of residual ethanol on the membrane of the column. Finally, the RNeasy MinElute Spin Column was transferred to a new 1.5ml collection tube, 14µl of RNAse-free water were added to the center of the membrane, lid was closed and centrifuged for 1 minute at maximum speed. The eluted RNA was collected on the 1,5ml collection tube and stored at -20ºC.

2.4.3 PicoPure RNA Isolation Kit

This protocol also enables the isolation of RNA from small samples including culture cells, even from a single cell and tissue samples (≤10 mg).

This procedure was performed according to manufacturer's protocol (Arcturus, ThermoFisher Scientific, UK).

Initially, cells were washed by centrifugation for 10 minutes at 3,000g, RT in 1ml of suspension medium. This medium consisted of 900µl 1Xpbs + 10% Bovine Serum Albumin (BSA) and 100µl of 0.5M ethylenediaminetetraacetic acid (EDTA). Subsequently, supernatant was discarded and pellet was resuspended in 1ml of suspension medium and mixed by gently pipetting. Sample was then centrifuged for 5 minutes at 3,000g, RT. 100µl of Extraction Buffer was added to the pellet by mixing gently and incubated for 30 minutes at 42°C. After this step, sample was centrifuged for 2 minutes at 3,000g, RT and the supernatant which contained the RNA, was carefully collected and transferred to a new RNA-free Eppendorf tube. 100µl of 70% ethanol was added to the extracted RNA and gently mixed. Subsequently, the mixture was inserted onto a pre-conditioned RNA Purification Column and centrifuged for 2 minutes at 100g, RT and then immediately after, for 30 seconds at 16,000g, RT. For the pre-condition of the column, 250µl of Conditioning Buffer were added directly to the membrane of the column and incubated for 5 minutes at RT, followed by centrifugation for 1 minute at 16,000g, RT. Finally, 100µl of Wash Buffer 1 were added to the sample on the column and centrifuged for 1 minute at 8000g, RT.

A DNase treatment was performed to remove any interference of genomic DNA from the eluted RNA sample. For this method, the RNAse-Free DNAse Set (Qiagen) was used, same as in RNeasy Micro kit protocol. Briefly, 5µl of DNAse I enzyme working stock (reconstitute as mentioned in

section 2.4.1.) and 3µl of Buffer RDD were mixed and subsequently added onto the membrane of the purification column. Sample was incubated for 15 minutes at RT. After this step, 40µl of Wash Buffer 1 were added to the membrane of the purification column and centrifuged for 15 seconds at 8,000g, RT. Then, 100µl of Wash Buffer 2 were added and centrifuged for 1 minute at 800g, RT. Addition of Wash Buffer 2 was repeated and sample was span for 2 minutes at 16,000g, RT. Finally, the purification column was transferred to a new 0.5ml microcentrifuge tube and 11µl of Elution Buffer were added directly onto the membrane. Sample was incubated for 1 minute at RT, centrifuged for 1 minute at 1000 g, RT followed by another centrifugation for 1 minute at 16,000g, RT. The eluted RNA was collected on the 0.5ml microcentrifuge tube and stored at -20°C.

The highest RNA yield was obtained from the RNeasy Micro Kit (Qiagen, UK) and, therefore it was selected for the consecutive RNA extraction experiments.

2.5 Immunophenotyping of NK Cell Receptors and Adhesion Molecules

2.5.1 PBMC and Ascites From Ovarian Cancer Patients

The expression of NK cell activating and inhibitory receptors, as well as, adhesion molecules from the PBMC and ascitic fluid derived from ovarian cancer patients was characterized and compared. For the completion of this

experiment 3 different panels were created and can be observed below in Table 2-1.

The cryopreserved samples were initially thawed as described in section 2.1.4. and left to recover for 2h in a cell culture incubator (Panasonic) (37°C, 5% CO_2, 21% O_2). After this incubation, the cell concentration and viability were determined using Flow Cytometry (NovoCyte, Agilent) and TO-PRO-3 counterstain viability dye (ThermoFisher Scientific, UK). Subsequently, $1x10^6$ cells from PBMCs and ascites samples of OCPs were added onto each FACS tubes for immunophenotyping. Samples were washed with 2ml of staining buffer (PBS+1%FBS), and pellet was resuspended in 100µl of staining buffer. A cocktail of the antibodies for each panel (Table 2-1) was added to the corresponded tubes and samples were incubated for 15 minutes, in the fridge at 4°C. Finally, the samples were washed with 2ml of staining buffer and centrifuged at 300g, 5 minutes, RT. Pellets were resuspended in 200µl of staining buffer and analysed by flow cytometry (NovoCyte, Agilent). An unstained sample was used as a control for gating strategy. All samples were acquired as technical duplicates.

For the design of all the panels in this project, the fluorophores chosen for the equivalent markers were based on the intensity of the fluorophores as well as the intensity of the markers. For instance, for markers that are normally highly expressed in cells the fluorophore used was of lower intensity and *vice versa*. This was conducted in order to avoid/limit spectral spill-over and discriminate between background signal and the actual signal from the markers.

In addition, to ensure that the expression of a marker did not intervene with the signal from another marker, fluorescence minus one (FMO) controls were used in these studies. The FMO control consists of all the fluorophores in the panel except for the one being measured and allows the correct gating strategy for every marker by excluding any spectral spillover of a fluorophore to another channel.

Moreover, compensation controls were also prepared every time the panels were run in the flow cytometer. This was important to ensure that any detection of signal was a result of the corresponded fluorophore and not due to any spectral spillover. In addition compensation controls enable the assessment of the flow cytometer performance by ensuring effective differentiation of negative and positive population for each of the fluorophores.

Table 2-1: Flow Cytometry Panels for Immunophenotyping of NK Cell Receptors and Adhesion Molecules

		Panel 1				
Excitation Laser (nm)	**Bandpass filter (nm)**	**Receptor**	**Fluorophore**	**Clone**	**Supplier**	**Catalogue #**
V405	585/40	L/D Zombie Yellow	BV570	n/a	BioLegend	423103
V405	675/30	CD3	BV650	SK7	BD	563999
V405	780/60	CD16	BV786	3G8	BD	563690
B488	530/30	NKp80	FITC	4A4.D10	Miltenyi	130-094-843
B488	585/40	NKp44	PE	P44-8	BD	558563
B488	780/60	NKp30	PE-Vio770	REA823	Miltenyi	130-116-393
R640	675/30	CD69	APC	FN50	BioLegend	310910
R640	780/60	CD56	APC-Cy7	HCD56	BioLegend	318332

		Panel 2				
Excitation Laser (nm)	**Bandpass filter (nm)**	**Receptor**	**Fluorophore**	**Clone**	**Supplier**	**Catalogue #**
V405	585/40	L/D Zombie Yellow	BV570	n/a	BioLegend	423103
V405	675/30	CD3	BV650	SK7	BD	563999
V405	780/60	CD2	BV786	RPA-2.10	BioLegend	300234
B488	530/30	CD57	FITC	TB01	Invitrogen	MA1-81071
B488	585/40	TRAIL	PE	RIK2	BioLegend	308206
B488	615/24	CD62L	PE-Vio615	REA828	Miltenyi	130-112-653
B488	675/30	CD27	PerCP-Vio700	REA499	Miltenyi	130-120-037
R640	675/30	KIR2DL1	APC	143211	R&D	FAB1844A-100
R640	780/60	CD56	APC-Cy7	HCD56	BioLegend	318332

		Panel 3				
Excitation Laser (nm)	**Bandpass filter (nm)**	**Receptor**	**Fluorophore**	**Clone**	**Supplier**	**Catalogue #**
V405	585/40	L/D Zombie Yellow	BV570	n/a	BioLegend	423103
V405	675/30	CD3	BV650	SK7	BD	563999
V405	780/60	CXCR4	BV786	12G5	BD	741001
B488	530/30	2B4	FITC	2-69	BD	550815
B488	585/40	NKG2D	PE	1D11	BioLegend	320806
B488	615/24	DNAM-1	PE-Vio615	REA1040	Miltenyi	130-117-491
B488	675/30	PD1	PerCP-Vio700	REA802	Miltenyi	130-111-957
B488	780/60	NKp46	PE-Vio770	REA808	Miltenyi	130-112-281
R640	675/30	NKG2A	APC	131411	R&D	FAB1059A-100
R640	780/60	CD56	APC-Cy7	HCD56	BioLegend	318332

2.5.2 Resting and Primed NK Cells From Healthy Donors

The characterization of the NK cells derived from PBMC of HDs for this study, was performed on non-primed rNK cells and primed NK cells via either hrIL-15 (10ng/ml) (R&D Systems), or TpNK (INB16 MMC:NK, 2:1) as described in 2.3.1.2. This was conducted after co-incubation of these effector conditions with pre-seeded OVCAR3 or SKOV3 target cells. Effector conditions without any contact with the epithelial ovarian cancer target cells were used as controls. The co-incubation of E:T (5:1) was performed in 12-well flat-bottom plates.

For this experiment, PBMC samples from HD were initially thawed as described in section 2.1.4 and left to recover for 2h in a cell culture incubator (Panasonic) (37°C, 5% CO_2, 21% O_2). After determining the cell concentration and viability using TO-PRO-3 counterstain dye in Flow Cytometry (NovoCyte, Agilent), 1×10^6 of PBMC was taken to immunophenotype for NK cells, to identify the concentration of NK cells in the PBMC sample. This was performed using CD56 APC/Cy7 (clone: NCAM 16.2, BD Bioscience) and CD3 Vioblue (clone: REA613, Miltenyi) monoclonal antibodies, as described in section 2.2.3.

All effector conditions were incubated o/n in a cell culture incubator (Panasonic) (37°C, 5% CO_2, 21% O_2). The next day, the effector conditions were added to the corresponded target cells according to the NK cell count. The seeded concentration of SKOV3 and OVCAR3 target cells was 0.1×10^6/well and therefore the concentration of the effector conditions added was 0.5×10^6/well to achieve an E:T (5:1).

Effector conditions alone, without any co-incubation with the target cells, were also added to different wells of the same 12-well flat-bottom plate vessel, as controls. The killing assay was performed for a total of 4h and subsequently the culture medium in each of the wells, that consisted of the NK effector and lysed target cells was collected to new sterile FACS tubes. For the adherent target cells along with the NK conjugated cells, non-enzymatic cell dissociation solution (Sigma-Aldrich, UK) was used to collect the cells.

The collected samples were centrifuged at 300g, 5 minutes, RT and pelleted cells were resuspended in 100µl of staining buffer. Cocktail mixture of NK cell antibodies from Table 2-1 was prepared and cells were incubated for 15 minutes at 4°C. Finally, cells were washed by centrifugation at 300g, 5 minutes, RT and analysed by Flow Cytometry (NovoCyte, Agilent). All samples were performed as technical duplicates.

In addition, the immunosuppressive NK cell phenotype in the ovarian cancer TME was also investigated. For these studies, the E:T ratio on the 12-well flat-bottom plate was 1:2, thus on the wells with the target seeded concentration of 0.1×10^6, the rNK cell concentration added was 0.05×10^6. For this experiment, the plates were incubated o/n in a cell culture incubator (Panasonic) (37°C, 5% CO_2) and the cells were collected and stained as described above.

2.6 Immunophenotyping of NK Cell Ligands on SKOV3 and OVCAR3 Epithelial Ovarian Cancer Target Cells

The expression of NK ligands on the surface of the NK cell-insensitive SKOV3 and NK cell-sensitive OVCAR3 target cell lines was evaluated to investigate the difference in relation to the NK cell sensitivity in ovarian cancer. For this experiments, SKOV3 and OVCAR3 target cells were harvested using Cell Detachment solution (amsbio, UK) as described in section 2.1.1. Subsequently cell concentration and viability were established using the Trypan Blue exclusion method as described in section 2.1.2 and target cells were stained with Cell Trace Violet (ThermoFisher Scientific, UK) as described in section 2.3.2.2. The labelled target cells were then resuspended at 0.1×10^6 and 1ml of each target ovarian cancer cell line was added to the appropriate wells of a 12-well flat-bottom plate and left to adhere o/n in a cell culture incubator (Panasonic) (37°C, 5% CO_2).

The next day, the primed and non-primed NK cell effector conditions, were added to SKOV3-labelled and OVCAR3-labelled target cells at E:T (5:1) and left either 4h or E:T (1:2) for o/n incubation in a cell culture incubator (Panasonic) (37°C, 5% CO_2). Wells with labelled target cells alone were used as controls for this experiment. After the o/n incubation, the adherent and non-adherent cells were collected as mentioned in 2.5.2. Finally, collected cells were washed with 2ml of staining buffer and stained with a cocktail mixture of NK cell ligands antibodies (Table 2-2). Samples were washed with staining buffer at 300g, 5 minutes, RT and analysed by Flow Cytometry (NovoCyte, Agilent).

Table 2-2 NK ligands and Cell Surface Expression Molecules on SKOV3 and OVCAR3 Epithelial Ovarian Cancer Target Cells

						Panel 1
Excitation Laser (nm)	**Bandpass filter (nm)**	**Receptor**	**Fluorophore**	**Clone**	**Supplier**	**Catalogue #**
V405	445/44	Cell Trace Violet	BV421	n/a	ThermoFisher	C34557
V405	780/60	CD15	BV786	HI98	BD	563838
B488	530/30	MICA/B	VioBright FITC	6D4	BioLegend	320912
B488	585/40	ULBP1	PE	170818	R&D	FAB1380P
B488	675/30	CD70	PerCP-Vio700	REA292	Miltenyi	130-104-312
B488	780/60	CD24	PE-Vio770	REA832	Miltenyi	130-112-658
R640	675/30	L/D TO-PRO-3	APC	n/a	ThermoFisher	T3605
R640	780/60	HLA-A/B/C	APC-Cy7	W6/32	BioLegend	311426

						Panel 2
Excitation Laser (nm)	**Bandpass filter (nm)**	**Receptor**	**Fluorophore**	**Clone**	**Supplier**	**Catalogue #**
V405	445/44	Cell Trace Violet	BV421	n/a	ThermoFisher	C34557
V405	780/60	ULBP-2/5/6	BV786	165903	BD	748134
B488	530/30	ULBP-3	AlexaFluor700	166510	R&D	FAB1517V-100UG
B488	585/40	MUC16	PE	EPSISR23	Abcam	ab215693
B488	675/30	HLA-DR	PerCP-Vio700	REA805	Miltenyi	130-111-793
R640	675/30	L/D TO-PRO-3	APC	n/a	ThermoFisher	T3605
R640	780/60	CD48	APC-Cy7	HM48-1	BioLegend	103432

						Panel 3
Excitation Laser (nm)	**Bandpass filter (nm)**	**Receptor**	**Fluorophore**	**Clone**	**Supplier**	**Catalogue #**
V405	445/44	Cell Trace Violet	BV421	n/a	ThermoFisher	C34557
V405	780/60	PDL-1	BV786	29E.2A3	BioLegend	329736
B488	585/40	CD112	PE	TX31	BioLegend	337410
B488	615/24	HLA-E	PE-Vio615	REA1031	Miltenyi	130-117-552
B488	675/30	B7-H6	PerCP-Vio700	JAM1EW	ThermoFisher	46-6526-42
B488	780/60	CD155	PE-Vio770	REA1081	Miltenyi	130-119-001
R640	675/30	L/D TO-PRO-3	APC	n/a	ThermoFisher	T3605

2.7 Statistical Analysis

There were three types of statistical analysis used in this project to analyse the results obtained. A two-tailed unpaired t-test to evaluate the comparison between HD- and OCP- derived samples, a two-tailed paired t-test to compare the efficacy of NK cell function derived from the same sample against the target cell lines and a one-way ANOVA with Dunnett's multiple comparisons follow up test to compare the differences between the control rNK effector cells to the two different types of primed NK effector cells.

It is important to note that the majority of the experiments were conducted during the 2020/2021 COVID-19 pandemic and lockdown. This has influenced the generation of results as it had detrimental effects on obtaining patient samples, access to facilities for the use of necessary equipment, and lack of consumables and reagents due to the high demand and priority for COVID laboratories.

Chapter 3   Natural Killer Cell Profiling in Ovarian Cancer

3.1 Introduction

Under physiological conditions, NK cells comprise 5-15% of the lymphocyte population in the peripheral blood (PB). In patients with advanced ovarian cancer the NK cell count in PB is lower compared to healthy individuals (~2-10%) (Lukesova *et al.*, 2015). A comparative study of the PB and ascitic fluid in ovarian cancer patients, demonstrated that the percentage of NK cell populations in these two compartments was equivalent (Lukesova *et al.*, 2015). However, the NK cells from ascites were primarily CD56^{bright} whereas the NK cells from the PB of both healthy donors and ovarian cancer patients were mainly CD56^{dim} (Nham *et al.*, 2018).

The phenotypic differences of the NK cells between ovarian cancer patients and healthy donor samples have been investigated by various studies. Comparison of the NK cell activating receptors, demonstrated higher expression of CD16 molecules on the PB of both healthy donors and ovarian cancer patients whereas expression of CD69 was higher in the ascitic fluid compared to the PB samples from both healthy donors and ovarian cancer patients samples (Nham *et al.*, 2018). NKG2D NK activating receptor expression was similar in all three groups of samples (Nham *et al.*, 2018) whereas DNAM-1 and 2B4 activating receptors were lower in the NK cells from ascites (Carlsten *et al.*, 2009). Differences on the expression levels of the NCRs (NKp30, NKp44, NKp46) on the NK cells from both healthy donors

and ovarian cancer patient samples, have shown controversial results (Carlsten *et al.*, 2009; Nham *et al.*, 2018; Pesce *et al.*, 2015). Comparison of the NK cell inhibitory receptors demonstrated higher but not significant expression of NKG2A in the ascites and downregulation of CD158a and CD158b, where CD158a was significantly lower on the NK cells in the ascitic fluid (Nham *et al.*, 2018).

The presence of NK cells in the ascitic fluid and their impact on the overall survival of patients has been contentious. Dong and colleagues showed no better outcome and predicted worse overall survival, whereas, Webb *et al* (2014) reported that tumour-infiltrating NK cells are linked to better clinical outcome (Dong *et al.*, 2006; Webb *et al.*, 2014).

The genomic differences of the NK cells from healthy individuals and ovarian cancer patients (OCP) samples have not yet been described. In this chapter, the genomic differences of the NK cells from these samples have been assessed and a more detailed phenotypic analysis of the NK cell receptors and adhesion molecules has been performed for the HD and OCP samples.

Herein, the NK cell characterisation in ovarian cancer was investigated, by comparing the NK cells derived from the ascites at the tumour site with the NK cells in circulation in ovarian cancer patients, in an endeavour to understand the mechanism behind NK cell function impairment at the presence of the tumour cells. Subsequently, NK cells derived from ovarian cancer patients were further compared with healthy volunteered donors to

examine in a broader approach, variations between donors with ovarian cancer and healthy individuals.

3.2 Aims

The aims of this Chapter were:

(i)   To determine variation on the specific phenotypes of NK cells in ovarian cancer patients by comparing NK cells derived from the site of the disease, the ascites against the circulating PB-derived NK cells, in a broader immunophenotyping panel;

(ii)   To determine immunophenotypic differences between the PB derived NK cells from HD and OCP samples;

(iii) To determine a potential immunosuppressive phenotype of infiltrated NK cells on the tumour site from the ascites and compare it with the NK cells derived from HDs;

(iv)   To determine the NK cell mediated lytic function in ovarian cancer, between HD-PB derived samples against NK cells derived from the tumour site, the ascites. This was performed in a flow-based and electrical-impedance based functional killing assays via Flow Cytometer and xCELLigence RTCA instrument respectively.

3.3 Methods

3.3.1 Isolation of Natural Killer Cells

The NK cells from HD were derived from either leukocyte cones or heparinised blood of healthy volunteers. The PBMCs from those samples

were obtained after isolation as described in Chapter 2 (section 2.2) and were either proceed immediately for NK isolation or cryopreserved in 10% DMSO/FBS and stored in vapour phase nitrogen. For patient samples, both PBMCs and ascitic fluid were cryopreserved in vapour phase nitrogen after collection. Upon thawing, the sample was placed in supplemented culture medium and incubated in a standard culture incubator (21% O_2, 5% CO_2, 37°C) for 2h to allow recovery of the cells prior any handling.

The NK cells from all biological samples were subsequently isolated via negative selection as described in section 2.2.1. and purity was assessed via immunophenotyping as explained in section 2.2.3. The viability was also determined using TO-PRO-3 viability dye (ThermoFisher Scientific).

3.3.2 RNA Extraction

The RNA extraction of NK cells from HD-PBMC and OCP-Ascites samples was performed following the RNeasy Micro Kit (Qiagen) protocol as defined in section 2.4.2. The RNA samples were subsequently sent to Eurofins Genomics to process and analyse.

3.3.3 Immunophenotyping of Natural Killer Cells

An extensive screening of NK cells comprising of immune-monitoring markers, activating, inhibitory and chemokine receptors as well as adhesion and other molecules had been designed and can be seen below on Table 2-1. This was performed for the thorough analysis of NK cells from HD-PBMC and OCP (both PBMC and ascites) samples. The staining procedure for the immunophenotyping was conducted as described in section 2.2.3.

Finally, samples were analysed using flow cytometry (NovoCyte, Agilent). A representative gating strategy of NK cells for all the 3 panels designed can be seen below (Figure 3-1).
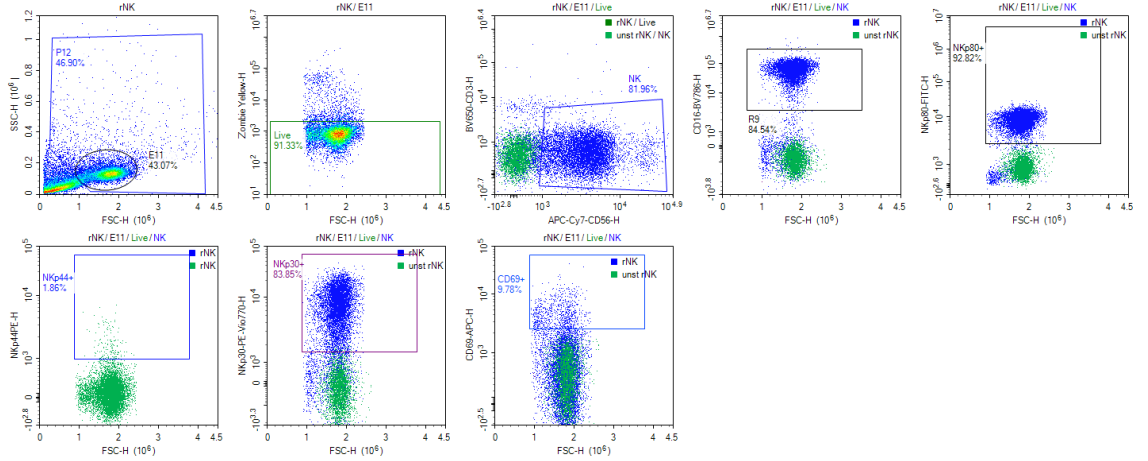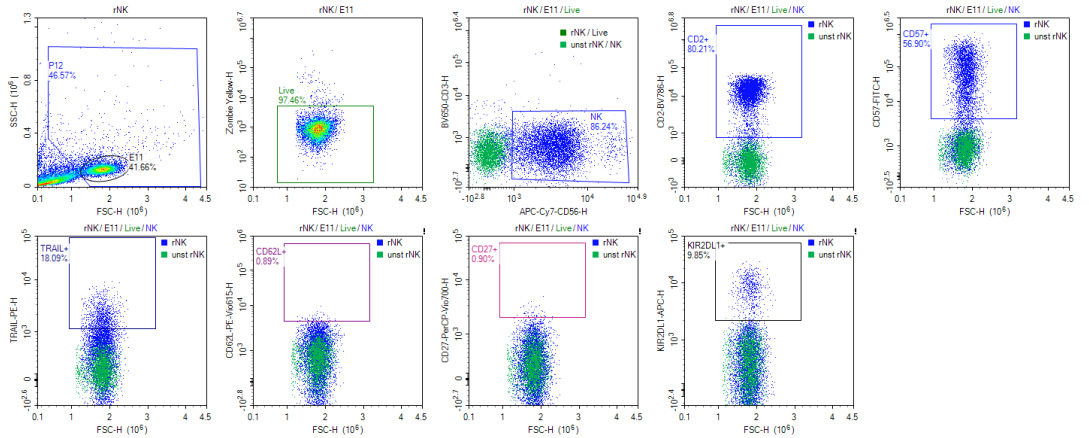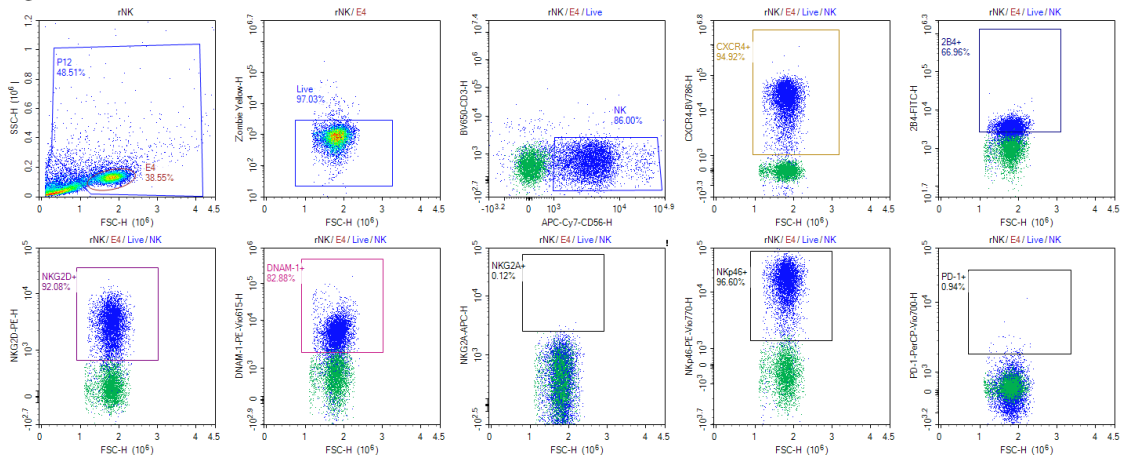
Figure 3-1: Representative Gating Strategy for NK Cell Receptors

Gating strategy of isolated NK cells via negative selection. Blue represents the stained NK cell population for the particular panel, overlayed with the equivalent unstained NK cell sample (green population) Zombie Yellow dye was used as viability dye. Experiment performed on biological triplicates (n=3) and run as technical duplicates.

3.3.4 Natural Killer Cell Cytotoxic Assays

3.3.4.1 K562 and OVCAR3 Target Cells

K562 target cells were first PKH67-labelled as described in section 2.3.1.1. Subsequently, they were resuspended in supplemented culture medium at $0.2x10^6$/ml working stock, placed in a 13ml polypropylene tube and incubated o/n at 37°C, 5% CO_2, 21% O_2. The next day, 200µl of each working stock solution were transferred to the corresponded FACS tubes that already contained 200µl of rNK effector cells ($1x10^6$/ml stock) to achieve an E:T (5:1). Finally, 100µl of supplemented culture medium was added to all the tubes to achieve a final volume of 500µl. FACS tubes containing only the target cells were also prepared as controls for establishing the specific lysis. Results were analysed by flow cytometry (NovoCyte, Agilent) after 4h, 6h and 16h of co-incubation. For the target cell viability, TO-PRO-3 nuclear counterstain dye was added (1/10 of total sample volume) to all the samples prior acquisition. Stop conditions in the flow cytometer were set to 10,000 events of interest from the PKH67 positive target cells. The number of live cells from the PKH67-labelled target cells was distinguished by TO-PRO-3 dye in which dead cells were positive for this dye. This assay was conducted for 3 biological replicates for both HD-derived and OCP-derived samples in technical duplicates.

For the OVCAR3 ovarian target cancer cell line, the NK cytotoxic assay was performed in the xCELLigence RTCA system (Agilent) as explained in section 2.3.2. OVCAR3 cells were passaged the day prior the experiment. The next day, they were harvested using Detachment solution

and resuspended in supplemented culture medium at 0.2×10^6/ml working stock. Subsequently, 50µl of OVCAR3 target cells were seeded to the e-plates that have been already calibrated for background measurement as mentioned in section 2.3.2.1. Upon OVCAR3 cells seeding, the e-plates were left for 30 minutes under the microbiological safety cabinet and then placed back into the xCELLigence RTCA system and incubated o/n at 37°C, 5% CO_2. The next day, 100µl of the NK effector cells (1×10^6/ml stock) were added to the corresponded wells to achieve the E:T (5:1). Wells containing solely the target cells were also prepared to facilitate the specific cytolysis establishment. Corresponded supplemented culture medium was added to the appropriate wells to reach an equal final volume of 200µl in all the wells (50µl background + 50µl target cells + 100µl effector cells/100µl supplemented culture medium). A continuous readout for a total duration of 48h was performed with 15 minutes intervals. This assay was conducted for 3 biological replicates for both HD-derived and OCP-derived samples in technical triplicates.

3.3.5 Statistical Analysis

A two-tailed unpaired t-test was used to compare the values between the pair of samples investigated in this chapter. The p-value was determined as *$p \leq 0.05$, **$p \leq 0.01$ and ***$p \leq 0.001$ (GraphPad Prism 9.0.0).

3.4 Results

3.4.1 Natural Killer Cell Antigen Profiling in Ovarian Cancer

The NK cell specific phenotypes among the OCP samples was investigated to determine differences between NK cells derived from the ascites that are located at the site of the disease and compared to the NK cells derived from the circulated PBMC of the ovarian cancer patients. Figure 3-2 represents the overlay bar charts with individual donor points of the NK cells derived from OCP-PBMC (blue bars) and OCP-Ascites (orange bars) as a percentage (Figure 3-1A) and MeFI (Figure 3-1B) of NK cell receptors (OCP-Ascites n=6; OCP-PBMC n=3).

For the majority of the NK cell receptors, their expression levels were downregulated on the NK cells found in the ascitic fluid compared to the NK cells in blood circulation. Downregulation on the percentage of expression was observed for the markers CD2, CD57, CXCR4, CD62L, CD27 and TRAIL, for the NK activating receptors CD16, NKp80, NKp30, NKp46 and DNAM-1 and for the NK inhibitory receptor KIR2DL1. From the aforementioned markers, only the downregulation of CD16 was statistically significant (*$p < 0.05$; $p = 0.0288$). This is possibly due to the conspicuous observation in which the OCP-Ascites samples resulted in two distinct populations for the expression levels of the markers among the donors investigated. Moreover, the reduction of expression of the aforesaid markers was mainly noticeable on the percentage levels compared to their MeFI

levels. Downregulation on the MeFI of NK receptors was observed only for CD16, NKp80, NKp30, CD57, CD62L, TRAIL and KIR2DL1.

On the contrary, NK cells derived from the ascites, exhibited upregulation of CD69 and 2B4 levels on both the percentage and MeFI of expression.

No difference was observed for the markers NKp44, NKG2A CTLA4 and PD1 due to the already very low levels of expression.

Figure 3-2: Levels of NK Cell Receptors on OCP Samples (PBMC and Ascites)

Bar chart showing the percentage (A) and MeFI (B) of the NK cell receptors between the two different OCP sample materials; Ascitic fluid samples (n=6) (orange bar) and PBMC samples (n=3) (blue bar). Error bars represent SD of the mean. Statistical analysis using unpaired t-test. * p<0.05

Figure 3-3 shows the percentage of frequency and MeFI expression levels of the NK cell receptors as bar charts displaying each individual donor between PBMC-derived NK cells from healthy individuals and ovarian cancer patients. All of the NK activating receptors tested such as CD16, NKp80, NKp30, NKp46, 2B4, NKG2D, DNAM-1, demonstrated decreased frequency on the PBMC of the ovarian cancer patients compared to the PBMC from HD. This reduction was statistically significant for NKp46 (*$p<0.05$; $p=0.0304$), 2B4 (****$p<0.0001$), DNAM-1 (*$p<0.05$; $p=0.0343$). No difference was observed for the NK activating receptor NKp44 levels. In addition, CD57 and CXCR4 markers were decreased on the OCP-PBMC samples compared to HD-PBMC samples without statistical significance though. On the contrary, CD69 and CD2 levels were significantly increased on OCP-PBMC samples compared to the HD-PBMC samples (*$p<0.05$; $p=0.0406$ for CD69 and $p=0.0179$ for CD2). Furthermore, increase expression levels on the OCP-derived samples was also observed for CD62L, CD27, KIRD2DL1 and TRAIL without statistical significance (OCP-PBMC and HD-PBMC, n=3).

There were no statistically significant differences in MeFI levels for all the markers tested.
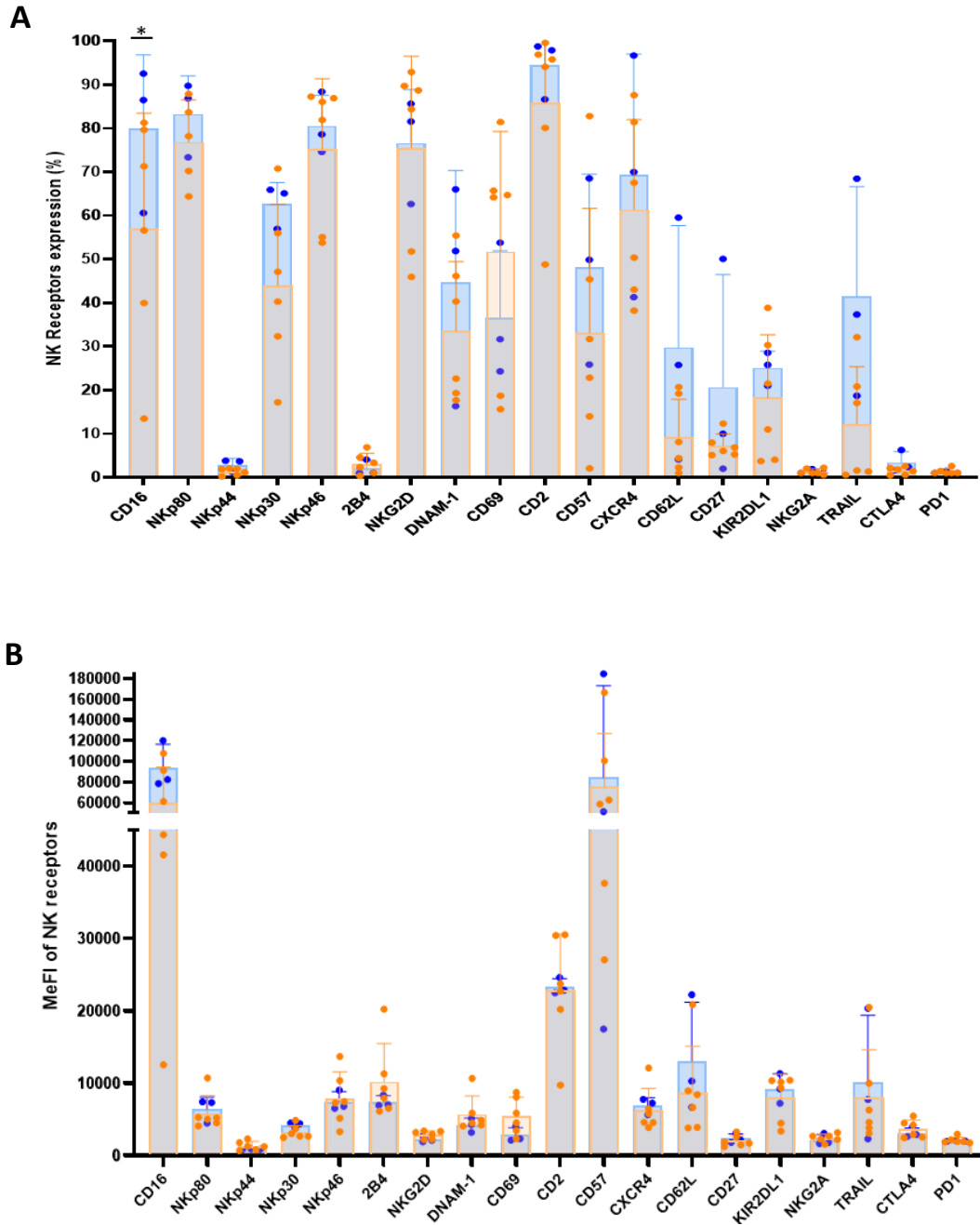
Figure 3-3: Levels of NK Cell Receptors on HD-PBMC and OCP-PBMC Samples

Bar chart showing the percentage (A) and MeFI (B) of the NK cell receptors between HD-PBMC samples (n=3) (grey bar) and OCP-PBMC samples (n=3) (blue bar). Error bars represent SD of the mean. Statistical analysis using unpaired t-test. *p≤0.05, **p≤0.01, ***p≤0.001 and ****p<0.0001.

Subsequently, after comparing the PB-NK cells between HD and OCP samples, further comparison was followed to evaluate immunophenotypic differences against HD-derived NK cells and impaired NK cells derived from the site of the disease, the ascites.

Figure 3-4 display bar chart plots with symbols of individual donors showing the NK immunophenotype comparison between HD-PBMC (grey bars) and OCP-Ascites (orange bars) samples both as a frequency of expression (Figure 3-3A) and MeFI (Figure 3-3B). NK cell activating receptor markers CD16, NKp30 and NKp46 levels significantly reduced in OCP-Ascites samples with $*p<0.05$ (CD16 p=0.0330, NKp30 p=0.0386 and NKp46 p=0.324). CD57 and CXCR4 percentage levels were also decreased in OCP samples compared to HD ($*p<0.05$; p=0.0363 for CD57 and p=0.0218 for CXCR4). In addition, DNAM-1 and 2B4 frequency levels in OCP Ascites samples were dramatically decreased ($***$ $p<0.001$; p=0.0002 for DNAM-1 and $****p<0.0001$ for 2B4) On the contrary, CD69 was significantly increased in OCP samples compared to HD ($*p<0.05$; p=0.0127). No statistical significance was observed for the other NK cell markers. Furthermore, in Figure 3-4A it is evident that the donors derived from OCP-Ascites form two distinct groups on the levels of expression for the NK receptors compared to the more consistent pattern on HDs (OCP-Ascites n=6; HD-PBMC n=3).

No significant difference was observed on the MeFI NK receptor expression levels between the HD and OCP-Ascites samples.
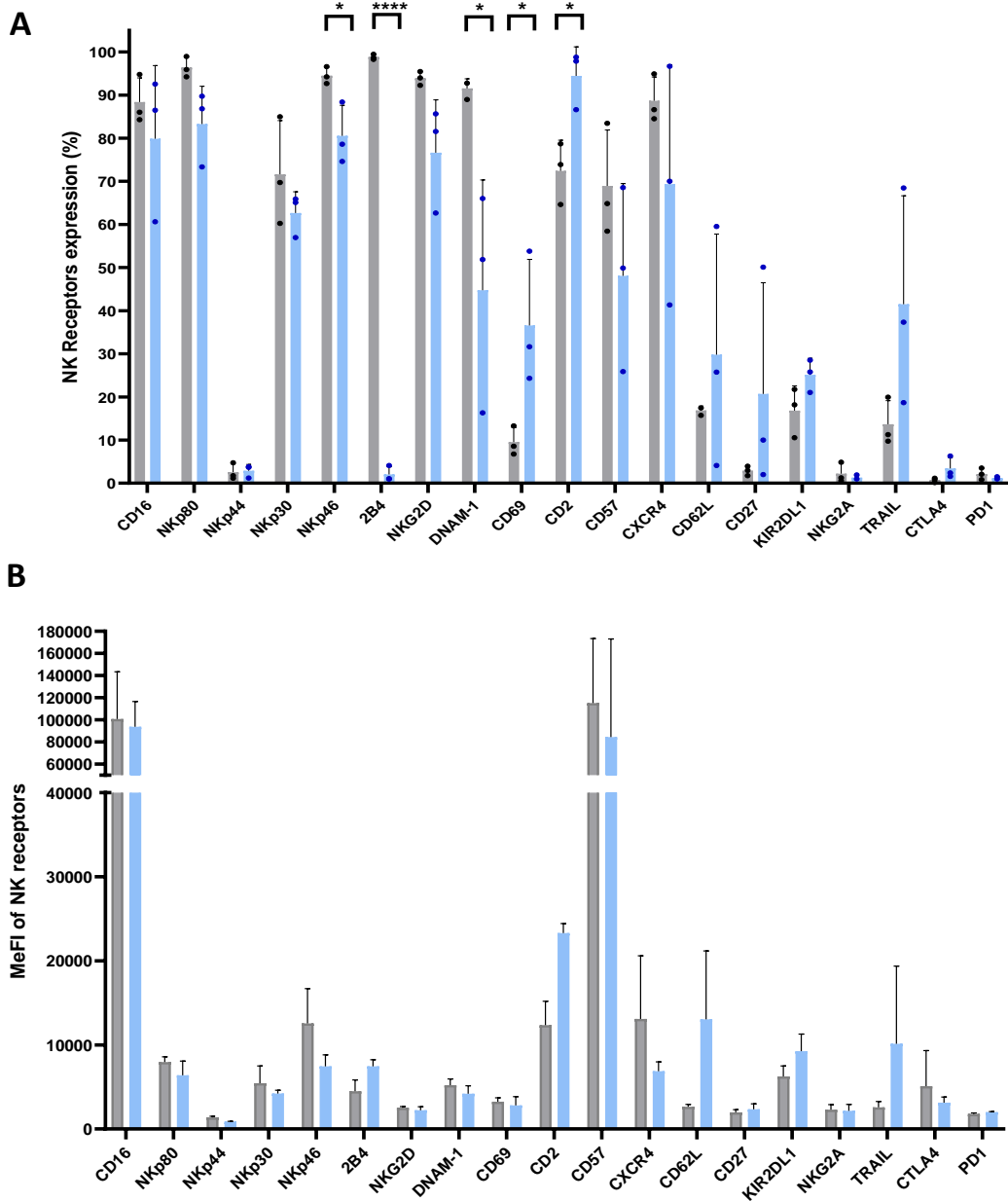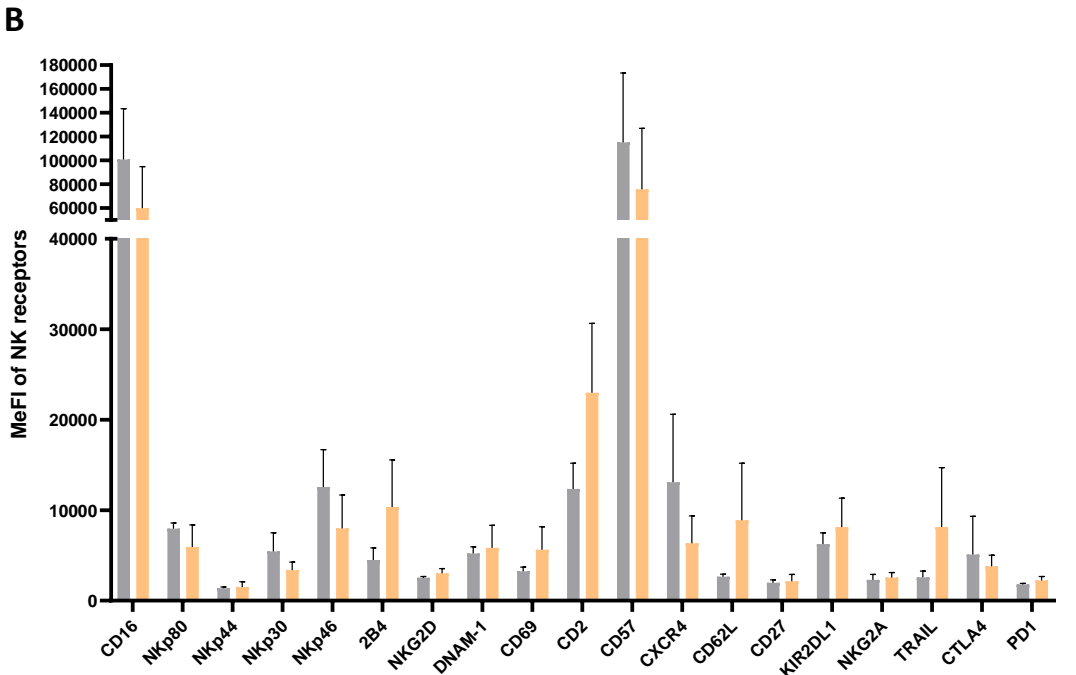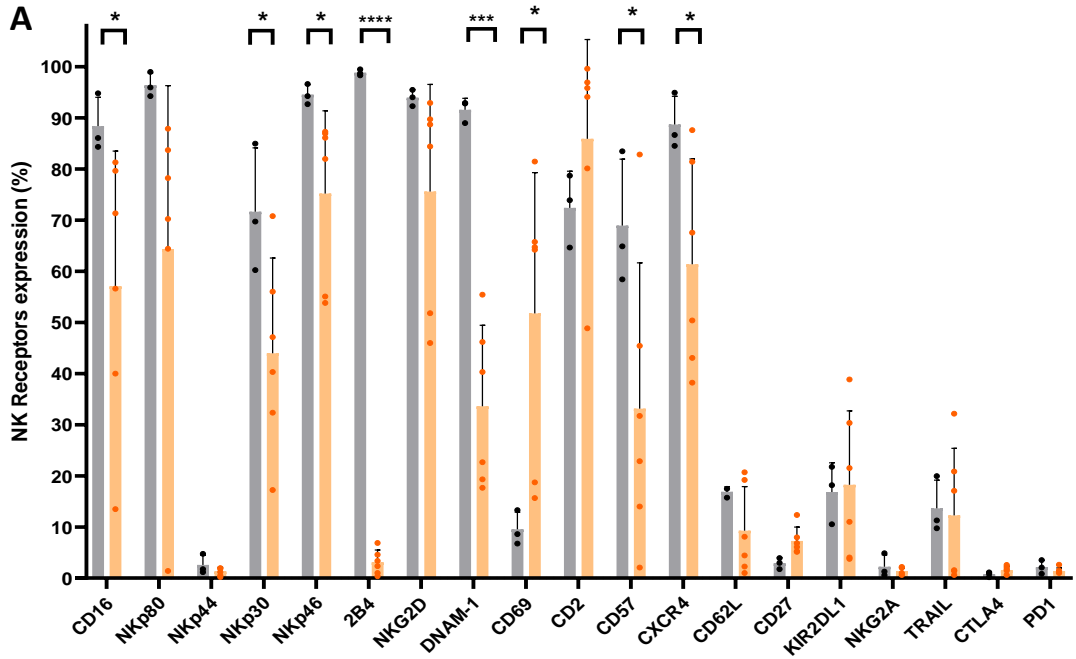
Figure 3-4: Levels of NK Cell Receptors on HD-PBMC and OCP-Ascites Samples

Bar chart showing the percentage (A) and MeFI (B) of the NK cell receptors between HD-PBMC samples (grey bar) (n=3) and OCP-Ascites samples (n=6) (orange bar). Error bars represent SD of the mean. Statistical analysis using unpaired t-test. *p≤0.05, **p≤0.01, ***p≤0.001 and ****p<0.0001.

3.4.2 Natural Killer Cell Cytotoxicity Assay

After investigating the immunophenotypic differences among the different samples, comparison of the NK cell cytotoxic function from HD-derived and OCP-derived NK cell functional capacity was assessed using an NK cell cytotoxicity assay.

Figure 3-5A represents the specific cytolysis of rNK effector cells against K562 and OVCAR3 respectively in an E:T ratio, 5:1. The NK cells for this assay, derived from HD-PBMC samples (clear box plots) and OCP-Ascites samples (orange dotted box plots). For the K562 target cells the results were plotted after 4h, 6h and 16h of effector-to-target co-incubation. No difference was observed between the two different NK cell origins after 4h of E:T interaction. However, after 6h and 16h the percentage of K562 specific cytolysis was significantly lower for the OCP-derived samples compared to the HD samples with *p<0.05 for both timepoints (p=0.0493 and p=0.0496 respectively).

Figure 3-5B displays the OVCAR3 ovarian cancer target specific cytolysis after 4h, 6h, 16h, 24h and 48h of co-incubation with rNK effector cells derived from HD-PBMC and OCP-Ascites samples. Similar to K562 cells, there was a statistically significant difference between the HD-PBMC and OCP-Ascites samples after 6h of effector-target co-interaction, onwards. OCP-derived NK cells resulted in significantly lower OVCAR3 specific cytolysis with *p<0.05 after 6h (p=0.0493) and 16h (p=0.0176). After 24h and 48h the significance was even higher with **p<0.01 (p=0.0086 and p=0.0070, correspondingly).
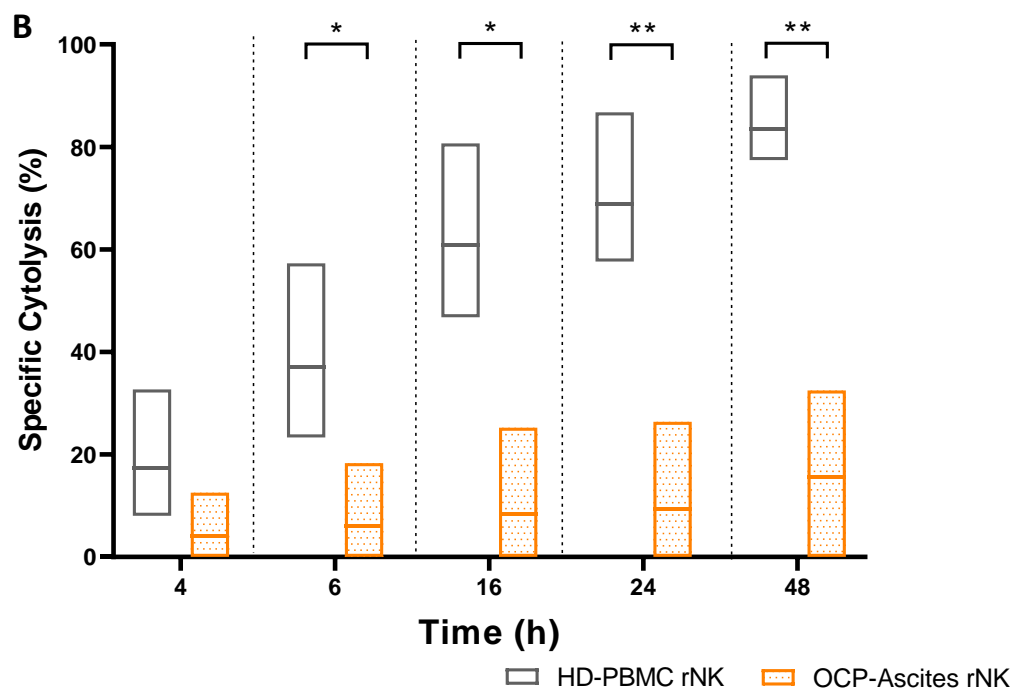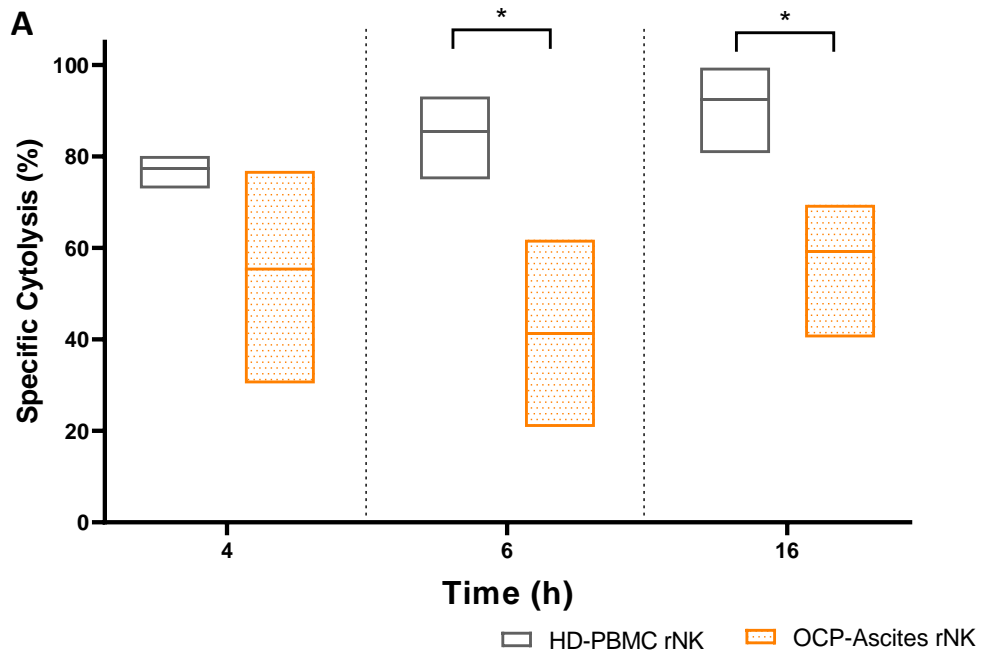
Figure 3-5: Percentage of Specific Cytolysis of HD-PBMC and OCP-Ascites Derived Samples Against K562 And OVCAR3 Target Cells

NK effector cells were co-incubated with K562 (A) and OVCAR3 (B) target cell lines in E:T (5:1). NK cells derived from HD-PBMC (clear box plot) and OCP-Ascites (orange dotted box plot). Line represents the mean. Statistical analysis using unpaired t-test with Welch's correction. * p<0.05, ** p<0.01.

3.5 Discussion

In this chapter the phenotype and cytotoxic function of NK cells derived from ovarian cancer patients were explored and compared to NK cells from healthy individuals. The phenotypic characterisation was attained using a vast immunophenotype panel for NK cell receptors to examine their expression levels between the HD-derived and OCP-derived samples, as well as, among the two different types of OCP-derived biological material; PBMC and ascites. This is the first time that such an extensive panel of NK cell receptors in ovarian has been investigated and presented.

Comparison of OCP-PBMC and OCP-Ascites samples, demonstrated downregulation of all the NK cell markers tested.CD16 was statistically lower in NK cells derived from OCP Ascites compared to OCP-PBMCs. This has been also reported by other groups (Belisle *et al.*, 2007; Carlsten *et al.*, 2009; Hoogstad-van Evert *et al.*, 2018). The NK cell activating receptor NKG2D levels were comparable in the OCP-derived samples, a result also observed in other studies (Belisle *et al.*, 2007; Hoogstad-van Evert *et al.*, 2018; Lukesova *et al.*, 2015; Nham *et al.*, 2018).

On the contrary, CD69 and 2B4 levels, were found to be upregulated on the NK cells derived from the ascites compared to the NK cells derived from the PBMC of the ovarian cancer patients, however without statistical significance. The reason behind the non-statistical difference was the low number of donors for the OCP-PBMC samples as well as the heterogeneity of the ascitic fluid samples that differentiates the donors into two distinct

populations of CD69 expression level. In addition, upregulation of 2B4 levels in ascites might be contribute to NK cell function impairment on the infiltrating NK cells at the site of the tumour. Chlewicki and colleagues reported that high levels of 2B4 exhibited inhibitory signals to NK cell cytotoxicity (Chlewicki, 2008).

Comparison of OCP- derived NK cells and HD-derived NK cells resulted in statistically significant differences on CD69 and 2B4 frequency and expression levels. CD69 was statistically higher in NK cells derived from the OCP samples compared to the HD-PBMC samples, while, 2B4 expression was significantly lower in OCP-derived NK cells compared to HDs. These results are aligned with Nham and colleagues (Nham *et al.*, 2018).

Findings from Belisle *et al* (2008) and Carlsten *et al* (2009) showed opposed conclusions compared to the results obtained in this project (Belisle *et al.*, 2007; Carlsten *et al.*, 2009). These studies demonstrated lower 2B4 expression levels in the ascites and no difference between PBMC-NK from HD and OCPs. However, in this project comparison of OCP (both PBMC and ascites) with HD samples resulted in great statistically significant reduction of 2B4 on the OCP samples compared to the HD-derived samples (****p<0.0001). A supposition behind these opposed results might rely on the format of presenting the data between the published reports and this study. Belisle and colleagues illustrated the Geometric mean (GeoMean) and Carlsten group the Mean Fluorescence Intensity (MFI) with the average at the Mean of the population without showing the percentage of expression

,(Belisle *et al.*, 2007; Carlsten *et al.*, 2009). Herein, the Median Fluorescence Intensity (MeFI) was used together with the percentage of expression. Median is more robust statistic and it is influenced the least, by skews or outliers compared to the GeoMean and MFI. Contemplating the heterogeneity within the individual donors from the OCP samples as also observed in this project, and that fluorescent intensity is logarithmic, the use of percentage and MeFI to plot the expression levels of the markers, are the most representable to allow the detection of these receptors and markers. In addition the different clones of the 2B4 may result in the differences between the results obtained here and the previous studies as Carslten and colleagues used different clone whereas for Belisle's group although the fluorochrome used was the same, there was no information on the clonality of the antibody in that report.

Further evaluation between circulating NK cells from OCP and HD samples, resulted in lower frequency levels of NK cell activating receptors in OCPs with the NKp46, 2B4, DNAM-1 demonstrating statistical significance on this reduction. CD16 between OCP-PBMC and HD-PBMC samples was the only NK cell activating receptor marker that was comparable. This was also observed by other groups (Belisle *et al.*, 2007; Carlsten *et al.*, 2009; Nham *et al.*, 2018). The rest of the NK cell activating receptors displayed downregulation on the OCP-derived samples compared to the HD-derived NK cells, nevertheless, without statistical significance. This is also supported by Nham *et al* (2008) report in which the NK cell activating receptors NKp80, NKp30, NKp44, NKp46 and DNAM-1 were investigated. In that study, the same statistical analysis tests were used as here, and no significant

difference for these NK cell activating receptors was observed. When the MeFI of these NK cell receptors was analysed, there was no difference between the samples (Nham *et al.*, 2018). On the contrary, results from this project, showed upregulation of CD69, CD2, CD62L, CD27 and TRAIL on the NK cells derived from the PBMC of OCPs. This increase of expression levels were statistically significant for CD69 and CD2.

Furthermore, investigation of NK cells derived from OCP-Ascites samples and HD-PBMC samples exhibited similar downregulation of the NK activating receptors in which the NK activating markers NKp30, NKp46, 2B4 and DNAM-1, expressed statistical significance. Moreover, the NK cell activating receptors NKp44, NKp80 and NKG2D demonstrated also lessen expression levels on the OCP-Ascites derived NK cells compared to the HD-PBMC derived NK cells. On the contrary, analogous to OCP-PBMC, the NK cells derived from the ascites, displayed higher levels of CD2, KIR2DL1 and CD69, with statistical significance for the latter.

Given that comparison of ascites between OCP and HD samples cannot occur, as the malignant ascites are only present in the cancer patients, reports investigating the NK cells in the peritoneal cavity in healthy like individuals, have been conducted for women with endometriosis. This is a benign gynaecological disease in which ectopic endometrium tissue is present outside the uterus resulting in pelvic pain and infertility (Jeung, 2016). It has been reported, that NK cells on the peritoneal fluid in endometriosis, also expressed an impaired immunophenotype with decreased NK cell cytotoxicity function that was associated with

downregulation of NK cell activating receptors and upregulation of NK cell inhibitory receptors (Jeung, 2016). Similar to the results obtained here for the NK cell characterisation on the malignant ascites from OCPs, NK cells in endometriosis also showed reduction of the NK cell activating receptors NKp44, NKp46, CD16 and NKG2D as well as upregulation of the NK cell inhibitory receptors KIR2DL1 and NKG2A (Jeung *et al.*, 2016). However, CD69 expression by NK cells in the malignant ascites and normal ascitic fluid were different, in that it was significantly upregulated in the OCP-Ascites whereas in the peritoneal fluid of individuals with endometriosis, CD69 expression was lower (Jeung *et al.*, 2016). The reason behind this might rely on the NK cell activation after interaction with the cancer cells and the tumour microenvironment (TME) at the site of the tumour that triggers CD69 upregulation. This supposition is also supported with the results obtained here that CD69 expression was higher in the ascites compared to the circulated NK cells in ovarian cancer patients. On the other hand, the downregulation of CD69 on the benign peritoneal fluid might be a result of the upregulation of NKG2A/CD94 levels that it has been demonstrated by Borrego and colleagues that increase of this NK cell inhibitory receptor counteracts the CD69 expression (Borrego *et al.,* 1999). Herein, NKG2A/CD94 expression on NK cells from OCP and HD samples were comparable as the levels for this NK cell inhibitory receptor were low.

CD2 molecule plays a significant role in NK-target adhesion and immunological synapse formation. Herein, its expression levels were found to be higher in the OCP-derived samples compared to HD-derived samples, with statistical significance between the PBMC sampled from HDs and

OCPs. This might be a result of the NK cell mechanism to enhance its conjugation with the tumour target cell and cause NK-mediated cytotoxicity. Comparison between the two OCP-derived samples showed a slight downregulation of CD2 levels in the ascitic fluid. This might be due to the immunosuppressive TME as well as the reduction of CD16 expression levels in the ascites that cause impairment in NK-target cell interaction efficacy.

The NK cell inhibitory receptors levels in NK cells from OCP- and HD-derived samples were also evaluated in this project. NKG2A expression was similar in all the samples and this observation was also aligned with the results from other groups (Belisle *et al.*, 2007; Hoogstad-van Evert *et al.*, 2018; Nham *et al.*, 2018). However, the percentage of cells expressing NKG2A was higher in those studies compared to the results obtained here. A possible reason might be the stage and OS of the patient-derived material collected as here the samples were from ovarian cancer patients after recurrence, at a late stage following palliative treatment. According to Hoogstad-van Ever and colleagues, the poorer the OS and progression of the disease the lower the NKG2A expression was found (Hoogstad-van Evert *et al.*, 2018). KIR receptor family exemplifies another category of NK inhibitory receptors. They are characterised by their long cytoplasmic tail that encompasses immunoreceptor tyrosine-based inhibition motifs (ITIMs).

Nevertheless, besides the inhibitory KIRs, NK cells also express activating KIRs, distinguished by their short cytoplasmic tail that contains immunoreceptor tyrosine activation motifs (ITAMs). Due to the great homology between different KIRs and the great heterogeneity of KIRs

expression in the NK cells, there is a current challenge on most KIR-specific monoclonal antibodies to be able to discriminate between inhibitory or activating KIRs. Therefore, here, only the KIR2DL1 NK inhibitory receptor was tested as it is currently the only one commercially available that can identify solely this inhibitory KIR without its activating counterpart. David and colleagues were the first to generate antibodies that can recognise separately inhibitory and activating KIRs and therefore facilitate the assessment of the expression levels of these receptors and their functional significance on NK cell responsiveness (David *et al*., 2009). Herein, KIR2DL1 was lower in the NK cells derived from the OCP-Ascites samples compared to the OCP-PBMCs. The expression level of this receptor was similar between ascitic fluid and HD-PBMCs, however, PBMCs derived from OCPs expressed higher KIR2DL1 level than PBMCs from HDs but was not statistically significant. The results obtained here were comparable with Nham *et al* (2018) findings (Nham *et al*., 2018).

Tumor necrosis factor (TNF)–related apoptosis-inducing ligand (TRAIL) is a key NK molecule that has been shown to prevent tumor growth, invasion and metastasis by inducing apoptosis in tumour target cells. In this project, TRAIL exhibited lower levels in the NK cells derived from OCP-Ascites compared to the OCP-PBMC derived samples. This might be due to the exposure of NK cells to cancer cells in the ascitic fluid, which is aligned with Hoogstad-Van-Evert and colleagues findings in which they reported downregulation of TRAIL percentage of expression upon tumour target co-incubation (Hoogstad-van Evert *et al*., 2018). However, no difference was observed between OCP-Ascites and HD-PBMC samples as the percentage

of expression levels was already low. Nonetheless, comparison of TRAIL expression levels between the NK cells from OCP-PBMC and HD-PBMC samples exhibited differences, as this marker was found to be upregulated on the patient-derived samples. This might be due to the immune surveillance in the PB of OCPs. The majority of the patient-derived samples that were obtained for this project were from a late stage of ovarian cancer, and consequently, tumour cells are present in the PB of the patients due to extravasation and metastasis of the tumour cells. TRAIL expression levels are low under normal physiological circumstances in HD donors as it does not induce apoptosis in normal cells, and thus, its upregulation in the PB of OCPs might be a result of an attempt of the NK cells in the blood to eliminate the circulating tumour cells via apoptosis.

Furthermore, for the first time, CD62L expression was investigated in ovarian cancer setting using NK cells derived from PBMC and ascites samples from OCPs. Evaluation of all the samples resulted in higher CD62L expression levels in the OCP-PBMC compared to ascites and HD-PBMC samples. This might be due to the predominant presence of CD56^{dim} NK subset on the patient-derived PBMCs as well the exposure of those NK cells to tumour target cells in the PB of OCPs. This CD56^{dim}/CD62L^{+} NK phenotype represents a unique polyfunctional mature subset that facilitates as an intermediate step upon NK cell maturation that combines both the ability to respond to cytokines and activate receptors stimulations (Juelke *et al.*, 2010). In addition, although Belisle and colleagues suggested that NK cells in ascites express CD62L due to their CD56^{bright}/CD16$^{-/low}$ phenotype that allows migration and trafficking of NK cells at the site of the tumour, they

have not tested it phenotypically. Here it was demonstrated that CD62L is also expressed in the ascites, supporting Belisle's hypothesis (Belisle *et al.*, 2007).

CXCR4 is an NK chemokine receptor mediating cell chemotaxis. It has been shown to be overexpressed relative to the stage in several malignancies including ovarian cancer and has been implicated directly in tumour progression via support in the tumour invasion and metastasis (Figueras *et al.*, 2018). Here, the CXCR4 expression was found to be lower in the ascites compared to the PBMCs of the OCP-derived samples. The higher CXCR4 levels in the OCP-PBMC samples might be possibly due to the greater ability of these circulating NK cell populations to migrate to other sites, compared to the NK cells that have been already localised in a single location, the ascites.

CD27 is another marker for defining NK cell responsiveness and maturation, as CD27 levels have been reported to be present exclusively on the most mature NK cell subpopulation (Vossen *et al.*, 2008). NK cells derived from OCP-Ascites samples expressed lower percentage compared to the NK cells derived from the OCP-PBMCs in this study. This might be a result of CD16 downregulation in ascites that was found in this project to be statistically significant as Vossen and colleagues had defined that NK cells expressing high CD16 levels are also expressing low or absent CD27 levels (Vossen *et al.*, 2008). When OCP samples were compared to NK cells derived from HDs, patient-derived samples expressed higher CD27 levels, especially the OCP-PBMC samples. This might ascribe to the NK cell

cytotoxic impairment on the ovarian cancer patients as high levels of CD27 expression is correlated to less perforin and granzyme B levels as well as lower cytotoxicity efficacy when investigated against K562 target cells (Vossen *et al.*, 2008). This impairment of NK cytotoxic function from NK cells derived from OCPs, against the same target cells as well as the OVCAR3 ovarian cancer target cells was also observed in this project after conducting functional killing assays.

CD57 is a marker of NK cell differentiation, maturation and functional response. Herein, evaluation of OCP samples resulted in a lower expression of CD57 molecule in the NK cells derived from OCP-ascites compared to OCP-PBMC derived NK cells. The overall CD57 expression from OCP-derived NK cells was lower compared to the HD-derived samples. A potential explanation for this, may be due to the amount of CD16 expression levels that signifies a higher level of NK cell maturation and ADCC cytotoxicity. Considering the fact that CD57 is predominantly expressed by the $CD56^{dim}/CD16^{+/high}$ NK subset (Lopez-Vergès *et al.*, 2010) as well as the results obtained here where CD16 was downregulated in ovarian cancer patients, might justify this CD57 downregulation. This is also supported by the fact that in this project the NK cells derived from the ascitic fluid exhibited statistically lower CD16 compared to the NK derived from the PBMC of both HDs and OCPs and as a consequence the levels of CD57 marker were statistically lower too in the ascites.

The PD-1 expression on the NK cells of patient and HD samples was also investigated here. Results obtained for HD-derived NK cells are aligned

with literature which states that NK cells from HD-PBMCs do not express PD-1, with the exception of a fraction of cytomegalovirus (CMV⁺) individuals (Pesce *et al.*,2017). However, PD-1 expression on NK cells has been detected in cancer patients in several malignancies, including multiple myeloma (Benson *et al.*, 2010), renal cell carcinoma (RCC) (MacFarlane *et al.*, 2014) as well as in peritoneal ascitic fluid from ovarian cancer patients (Pesce *et al.*, 2017). A supposition might be the necessity of NK cells to get activated either via cytokines or after encounter with cancer cells in order to express PD-1. This speculation has been also supported with the study from MacFarlane and colleagues (MacFarlane *et al.*, 2014). However, results obtained in this chapter did not demonstrate PD-1⁺ NK cells derived from OCP samples.

In conclusion, this chapter demonstrated the difference on the expression levels of various NK receptors and molecules between HD-derived PBMC samples as well as patient-derived samples from both circulating PBMC and ascites. Comparison between the two different sample materials from OCPs is currently limited reported, as only two previous studies have already investigated this (Belisle *et al.*, 2007; Nham *et al.*, 2018). However, herein, is the first time that an extensive panel comprising of several NK cell receptors and molecules has been studied and compared the circulated NK cells from the OCP and the NK cells at the site of the tumour from the ascites.

Notably, the ascitic fluid from the OCPs was used as patient-derived material for ensuing experiments to evaluate the NK cell function impairment

compared to HD samples. The rationale behind this relies upon copious factors including the absence of relatively statistically significant difference between the PBMC and Ascites samples, the logistics on the availability of the patient material to collect the required number of cells for conducting the experiments as well as the fact that ascites are located at the tumour site and hence it is a pertinent candidate to enhance understanding of the immunosuppressive mechanisms at the site of the TME. In addition, the NK cells in the PB of OCPs, it is highly likely that it does not entail a homogenous population of NK cells, however, it consists of a mixture of NK cells that have been already encountered cancer cells at the site of the tumour or have not yet been exposed to tumour cells.

Some conceivable reasons for the non-statistically significant differences in NK cell receptor expression as well as for the scattered individual points of the ascites samples that also resulted in two distinct groups, might be due to the heterogenous nature of ascites and the diversity of responses between the ascitic fluid derived from different stages of ovarian cancer and its correlation with different levels of OS.

Furthermore, the cytotoxic efficacy of the NK cells from OCPs was tested in a functional killing assay against the NK cell-sensitive cell lines K562 leukaemic cells and OVCAR3 ovarian cancer cells and were compared with the NK cells derived from HD-PBMCs. The results for this assay were acquired using flow cytometer for K562 target cells and xCELLigence RTCA system for OVCAR3 target cells. Herein is the first evaluation of NK cell functionality from biological sample of ovarian cancer patients and investigate

the ascites-derived NK cells that are found directly in the site of the tumour, using an electrical impedance non-invasive continuous real time cell analysis via the xCELLigence RTCA platform.

Chapter 4   Expression of Natural Killer Cell

Ligands in Ovarian Cancer

4.1 Introduction

The differential expression of key cell surface markers on ovarian cancer cells have been associated with NK cell-mediated lysis impairment. Patancar and colleagues demonstrated that MUC16 induced downregulation of CD16 causing impairment of the NK cell cytotoxicity (Patankar *et al*., 2005). In addition, Gubbels *et al* (2010) showed that MUC16 facilitated tumour survival via inhibition of the synapse between NK cells and ovarian cancer cells (Gubbels *et al*., 2010). Furthermore, Koh *et al* (2012) reported susceptibility of CD24+ ovarian cancer cells to NK-mediated cytotoxicity due to upregulation of NKG2D ligands (MICA/B, ULBP1 and ULBP3) and down-regulation of MHC-class I molecule expression (Koh *et al*., 2012).

In addition to the differential expression of cell surface molecules on ovarian cancer cells, alterations in the expression of NK cell ligands on tumour cells is also correlated to the susceptibility to NK cell-mediated lysis. In this regard, it was postulated that sensitivity of OVCAR3 and resistance of SKOV3 ovarian cancer cell lines by rNK cells, depends on the expression levels of cell surface markers and NK cell ligands. Few studies have investigated the NK cell ligands for the activating receptors NKG2D, DNAM-1 and NKp30 having heterogeneous expression on the two ovarian cancer target cells tested in this project. The ligands studied for the aforementioned NK cell activating receptors were the MICA/B and ULBP(1-6) for the NKG2D,

CD112 and CD155 for the DNAM-1 and B7-H6 for the NKp30 (Bjørnsen *et al.*, 2019; Huang *et al.*, 2011; Labani-Motlagh *et al.*, 2016).

Due to these controversial results and the fact that OVCAR3 has been shown to express high levels of MUC16 (Goodell *et al.*, 2009), a more thorough investigation on the different expression levels of cell surface markers and NK cell ligands on the NK cell-sensitive OVCAR3 and NK cell-resistant SKOV3 ovarian cancer cell lines has been performed and analysed in this chapter. In addition, differences on the NK cell function between the SKOV3 and OVCAR3 ovarian cancer cell lines using non-primed and primed NK cells has been determined and consequential changes on the expression levels of both NK cell receptors and ligands have been examined in this chapter. Finally, an immunosuppressive NK cell phenotype was investigated by co-incubation of the NK cells with either the NK cell-resistant SKOV3 or NK cell-sensitive OVCAR3 ovarian cancer cell lines in an E:T (1:2). This was performed in an endeavour to understand immunophenotypic changes on NK cells that exhibit impaired function in an environment where the target cells are in greater numbers compared to the effector immune cells as occur inside the body. This ratio was subsequently compared with the E:T (5:1) ratio that is been used for the functional killing assays.

Aims

The aims of this Chapter were:
  (i)　　To determine phenotypic differences on the NK ligands and surface molecules between the NK cell-resistant SKOV3 and NK

cell-sensitive OVCAR3 ovarian cancer cell lines using an extensive immunophenotypic panel;

(ii)   To determine variations on the NK cell receptors and ligands upon co-incubation of NK cells with each of the ovarian cancer target cell lines that display opposed NK cell mediated lysis sensitivity.

4.2 Methods

4.2.1 Isolation of Natural Killer Cells From Healthy Donors

NK cells were isolated as described previously in Chapter 2 (2.2.1.) The concentration and purity of the isolated NK cells were determined after immunostaining with CD56 APC/Cy7 (clone: NCAM 16.2, BD Bioscience) and CD3 Vioblue (clone: REA613, Miltenyi) monoclonal antibodies as explained in section 2.2.3.

4.2.2 SKOV3 and OVCAR3 Ovarian Cancer Target Cells

The ovarian cancer target cells were harvested using Detachment solution as described in section 2.1.1 and resuspended in supplemented culture medium at 0.1×10^6/ml . Subsequently, 1ml was seeded on 12-well plate and left o/n to adhere uniformly at the bottom of the wells. The next day NK effector cells from HD samples were added at E:T (1:2) and incubated o/n at a cell culture incubator at 37°C, 5% CO_2.

4.2.3 Immunophenotyping of Natural Killer Receptors and Ligands

After the o/n incubation all the cells were collected via non-enzymatic detachment solution. The NK effector cells were stained for the markers and receptors mentioned in Chapter 2 (2.6) and Chapter 3 (3.3.3) however, this time, without including CTLA-4 and PD-1 as results herein showed no expression of these markers on NK cells. This was also comparable with other studies, in which the NK cells expressed low (<15%) PD-1 expression (Benson *et al.*, 2010; MacFarlane *et al.*, 2014; Pesce *et al.*, 2017). Therefore these two markers were excluded from the large immunophenotyping panel to narrow it to the markers that display differences in expression and frequency.

Ovarian cancer target cells were stained for NK cell ligands and surface molecules before and after co-incubation with the NK effector cells E:T, 2:1. Target cells were stained with Cell Trace Violet (ThermoFisher Scientific, UK) as described in Chapter 2, section 2.3.3. and TO-PRO-3 counterstain viability dye was used. Finally, samples were analysed via flow cytometry (NovoCyte, Agilent). The purity of target cells after co-incubation with the NK cell effector conditions was between 20-40%. In order to enable a better investigation of NK cell ligand expression on the surface of the ovarian target cells, the gating strategy set was initially on Cell Trace Violet$^+$ which represents only the target cells and subsequently the live population from those Cell Trace Violet$^+$ target cell population. Representative graphs indicating the gating strategy for SKOV3 and OVCAR3 target cells for the 3 panels designed, can be seen below (1). For all of the NK effector cells used in these studies, the

purity of NK cells after negative isolation was >90%. Gating strategy for NK

effector cells was performed as shown above in Figure 3-1.

Panel 1: SKOV3
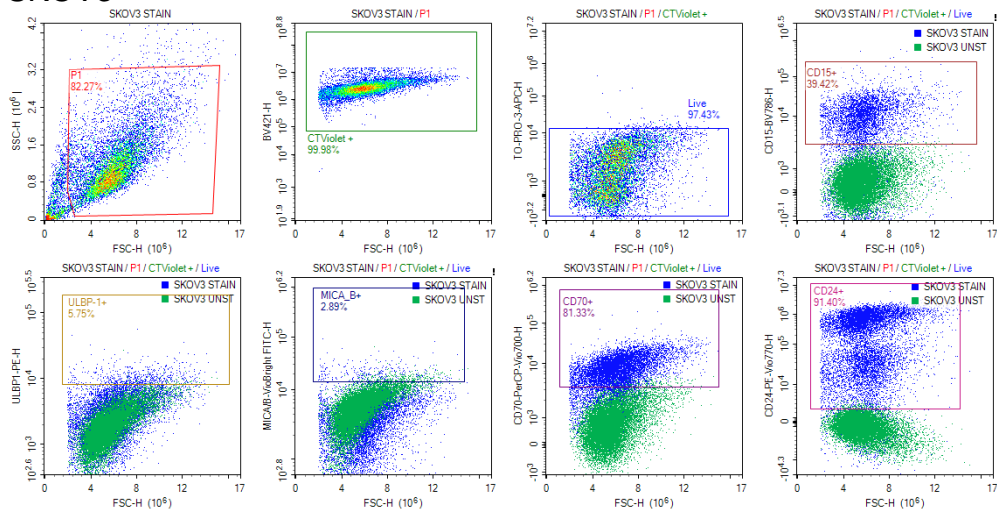
Panel 1: OVCAR3
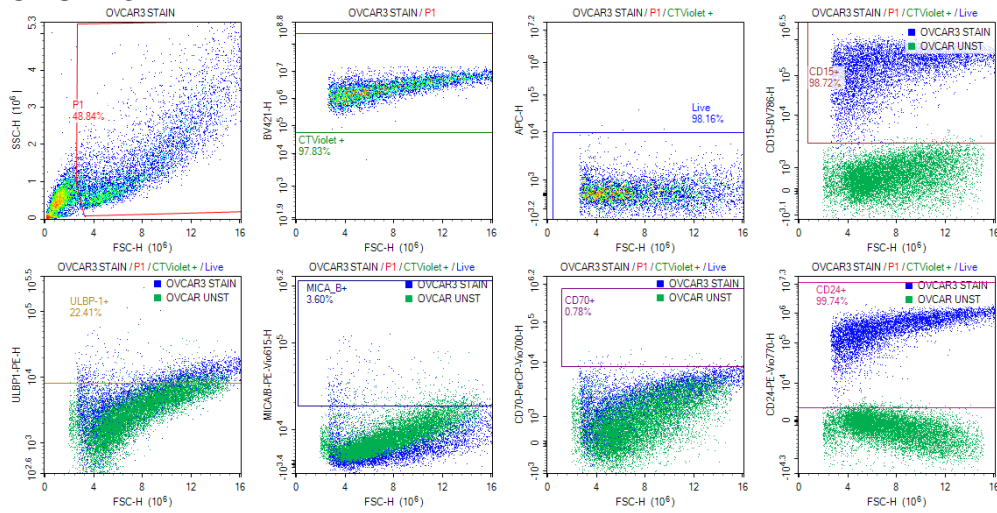
Panel 2: SKOV3
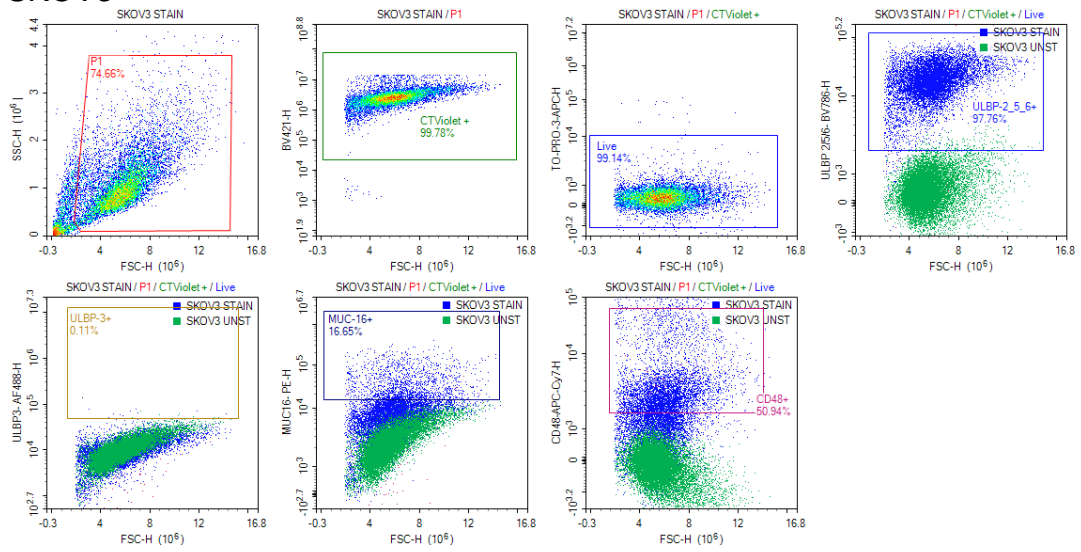
Panel 2: OVCAR3
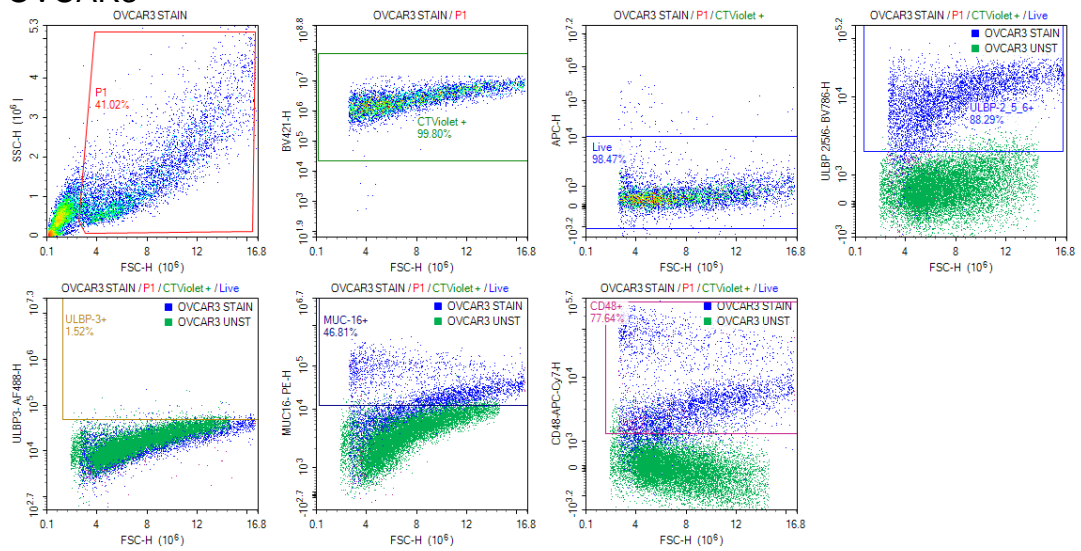
Panel 3:
SKOV3
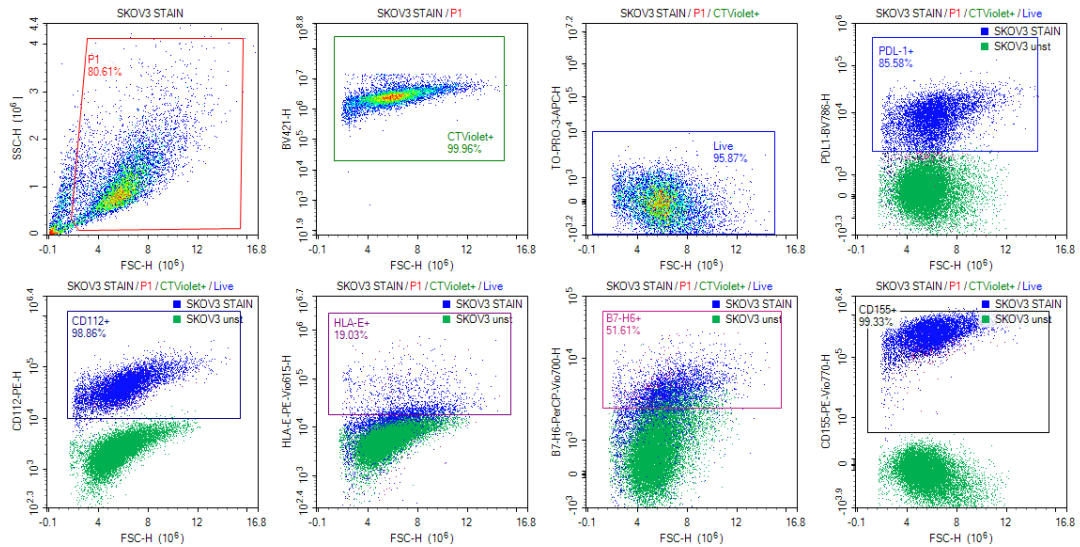
Panel 3:
OVCAR3
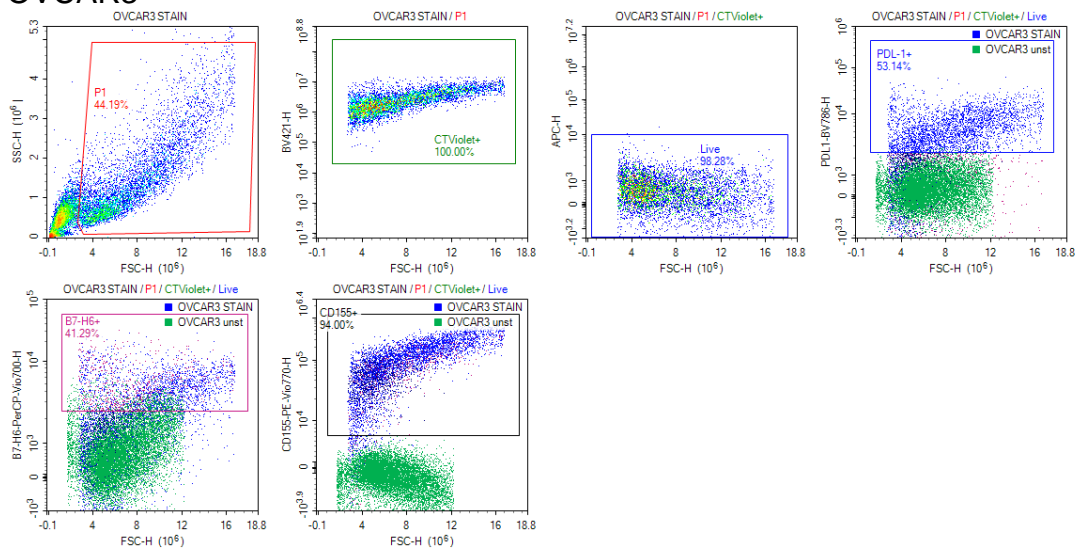
Figure 4-1: Representative Gating Strategy of NK Cell Ligand Panels For SKOV3 and OVCAR3 Target Cells

Gating strategy SKOV3 and OVCAR3 ovarian target cells. Blue represents the stained NK cell population for the particular panel, overlayed with the equivalent unstained target sample (green population). Target cells were pre-labelled with Cell Trace Violet and TO-PRO-3 (APC) counterstain dye was used as viability dye. Experiments performed on biological triplicates (n=3) and run as technical duplicates.

4.2.4 Statistical Analysis

A two-tailed paired t-test was used to compare the NK cell receptors and ligands levels between the two different SKOV3 and OVCAR3 ovarian cancer cell lines. The p-value was determined as $*p \leq 0.05$, $**p \leq 0.01$, $***p \leq 0.001$ and (GraphPad Prism 9.0.0).

4.3 Results

Figure 4-2 represents the percentage (A) and MeFI (B) expression levels of the NK ligands and surface molecules on SKOV3 and OVCAR3 ovarian cancer target cells. Comparison of the CD15 showed higher percentage levels of expression on the OVCAR3 target cells (95.70%) compared to SKOV3 cells (52.22%) with great statistical significance $(***p < 0.001; p = 0.0009)$. Statistical significance was also observed on the MeFI expression levels of the CD15 $(*p < 0.05; p = 0.0393)$. In addition, all the ULBPs ligands demonstrated statistically higher percentage levels on SKOV3 cells compared to OVCAR3. ULBP-1 expression levels were 29.14% on SKOV3 cells and 4.28% on OVCAR3 $(*p < 0.05; p = 0.0420)$. ULBP-3 and ULBP-2/5/6 ligands showed higher percentage of expression on SKOV3 cells (62.68% and 88.27% respectively) compared to OVCAR3 cells (7.83% and 71.94% respectively) with statistical significance of $*p < 0.05$ ($p = 0.0114$ and $p = 0.0105$ correspondingly). However, this was not analogous for the MeFI expression levels as no statistical significance was observed for the ULBP ligands. Moreover, CD155 ligand expression levels were higher on SKOV3

cells (99.33%) compared to OVCAR3 (87.25%) with great statistical significance (***p<0.001; p=0.0010). The MeFI levels of CD155 were also statistically higher on SKOV3 cells (*p<0.05; p=0.0136). CD48 levels were statistically higher on OVCAR3 (48.47%) compared to SKOV3 (23.59%) with **p<0.01; p=0.0018. MUC16 was also significantly higher in OVCAR3 (54.81%) compared to SKOV3 (24.92%) with *p<0.05; p=0.0224. However, CD48 and MUC16 did not demonstrate statistical significance on the MeFI expression levels between the two ovarian cancer cell lines. On the contrary, SKOV3 expressed significantly higher expression levels of CD70 (79.65%) in comparison to OVCAR3 (15.87%) (**p<0.01; p=0.0017). CD70 MeFI expression levels were also statistically higher on SKOV3 (*p<0.05; p=0.0161). Additionally, PDL-1 and the B7-H6 ligand were significantly higher on SKOV3 (83.02% and 75.54% respectively) compared to OVCAR3 (45.42% and 51.41% correspondingly) (**p<0.01; p=0.0040 and p=0.0026 respectively. Nevertheless, this statistical significance of PDL-1 and B7-H6 was not observed on the MeFI levels. The remaining ligands and surface molecules did not express significant difference between SKOV3 and OVCAR3 cells. MICA/B, CD112, CD24 and HLA A/B/C displayed high expression levels on both ovarian cell lines of >90%. In contrast, percentage expression levels of the HLA-E and HLA-DR were low for both SKOV3 and OVCAR3 cells (<16%). Although CD112 and HLA-A/B/C percentage expression was not significant, the MeFI expression of those ligands showed statistically higher levels on SKOV3 compared to OVCAR3 (*p<0.05; p=0.0127 for CD155 and **p<0.01; p=0.0031 for HLA-A/B/C).
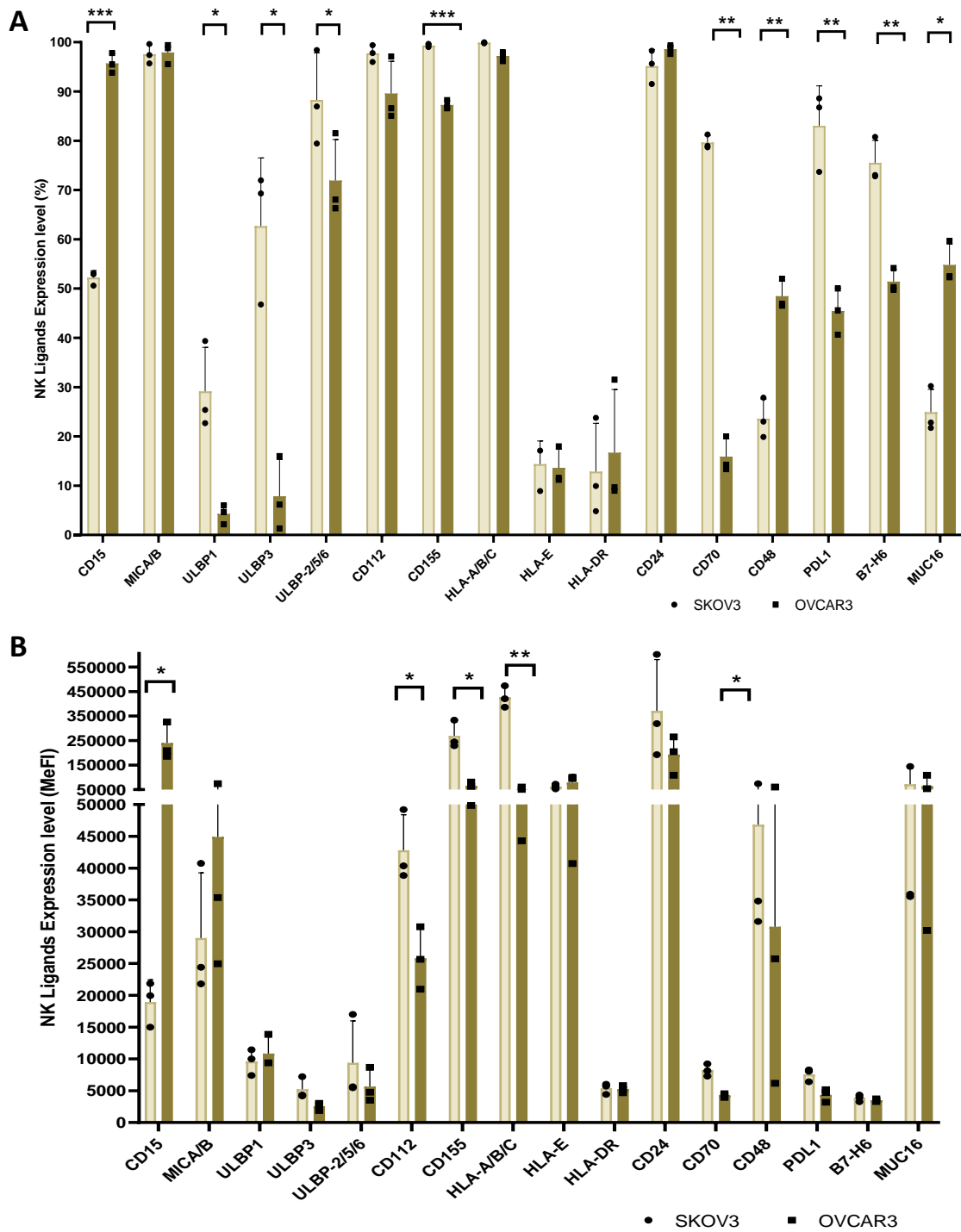
Figure 4-2: NK Cell Ligand and Surface Molecules Expression Levels on Ovarian Cancer Target Cell Lines

Bar charts showing symbols of the individual donors on the percentage (A) and MeFI (B) of the NK cell ligands and surface molecules on the NK cell-resistant SKOV3 (light brown) and NK cell-sensitive OVCAR3 (dark brown) ovarian cancer target cell lines. Error bars represent SD of the mean. Statistical analysis using paired t-test. Biological triplicates (n=3). * p<0.05, ** p<0.01, *** p <0.001.

Figure 4-3 demonstrates the percentage and the MeFI expression levels of the NK cell receptors respectively on the surface of NK cells without target cell interaction as well as upon overnight co-incubation at E:T (1:2) with either SKOV3 or OVCAR3 ovarian cancer target cells. The results obtained showed no difference on the NK cell receptors between the different conditions in both percentage and MeFI expression.
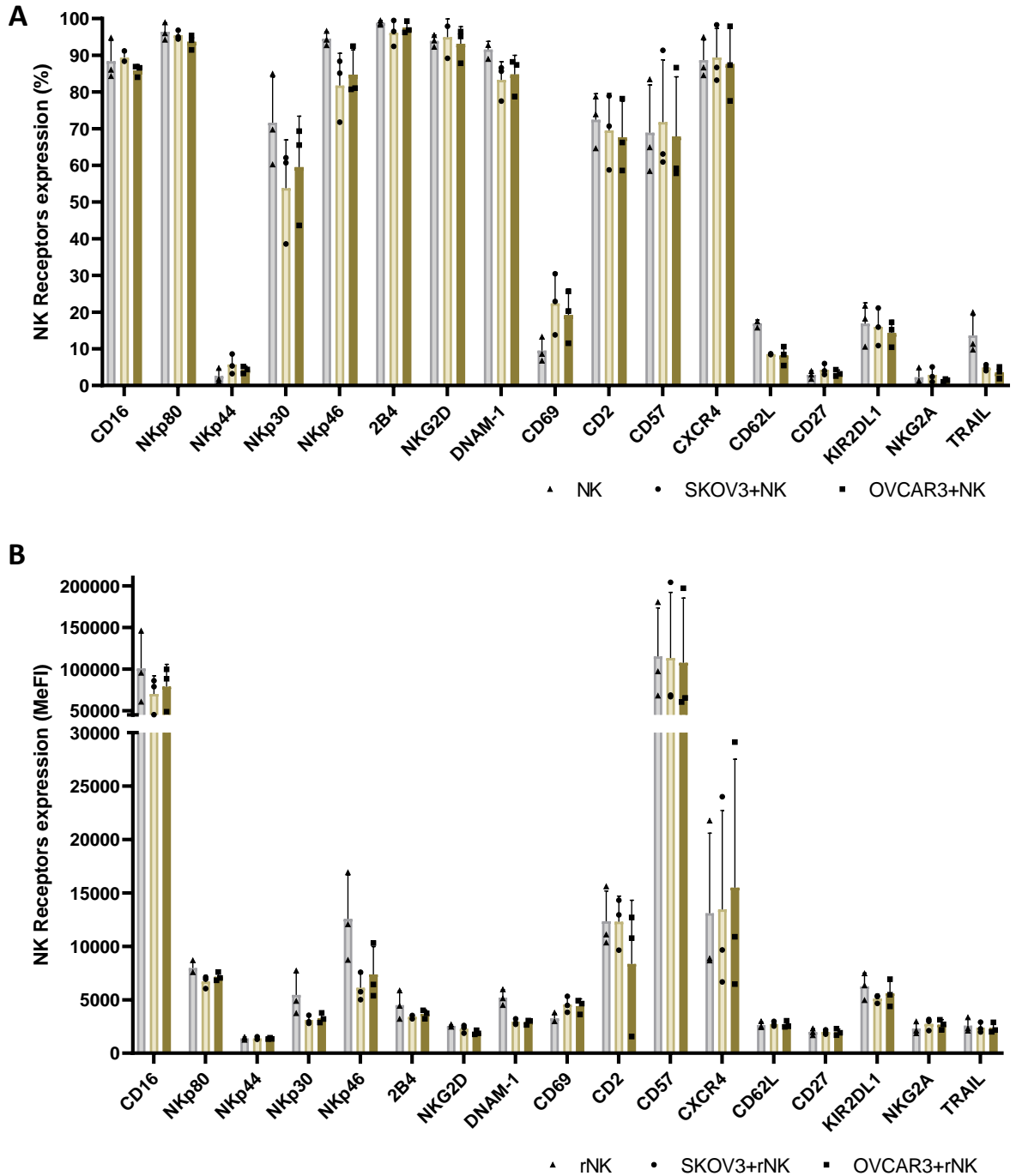
Figure 4-3:NK Cell Receptor Expression Levels by the Immunosuppressive Ovarian Cancer Phenotype

Bar chart showing symbols of individual donors on the percentage (A) and MeFI (B) of the NK cell receptors on the surface of NK cells (grey), on the NK cell-resistant SKOV3 (light brown) and NK cell-sensitive OVCAR3 (dark brown) ovarian cancer target cell lines. E:T (1:2). Error bars represent SD of the mean. Statistical analysis using paired t-test. Biological triplicates (n=3).

Subsequently, the immunosuppressive phenotypic ratio in which target cells are in superior number compared to the effector NK cells (E:T, 1:2) was compared with the conventional E:T ratio used in functional NK cell cytotoxicity assays (E:T, 5:1) These ratios were compared upon co-incubation with either the NK cell-resistant SKOV3 (Figure 4-4) or the NK cell-sensitive OVCAR3 (Figure 4-5) target cell lines. Results obtained, showed a disperse expression of NK cell receptors on E:T (5:1) among the HD samples, compared to the E:T (1:2).

Evaluation of the two E:T ratios against the NK cell-resistant SKOV3 target cells (Figure 4-4A) revealed that NKp44 levels, were significantly reduced in the E:T (5:1) compared to E:T (1:2) (*p<0.05; p=0.0498). In addition, DNAM-1 NK activating receptor levels were significantly increased (*p<0.05; p=0.0490) in the functional killing ratio of E:T (5:1) compared to the immunosuppressive ratio of E:T (1:2). Finally, CD62L levels exhibited increase on the NK cells co-incubated with SKOV3 in E:T (5:1) compared to E:T (1:2) (*p<0.05; p=0.0296). No statistical significance was observed for the MeFI Figure 4-4B) expression levels of the NK cell receptors.

Comparison of the E:T ratios against the NK cell-sensitive OVCAR3 cell line displayed also statistical significance on NKp44 and CD62L percentage levels Figure 4-5A. The NKp44 expression was downregulated also at E:T (5:1) ratio (*p<0.05; p=0.0208) compared to E:T (1:2) whereas CD62L expression levels were also found to be higher at E:T (5:1) ratio, however, with greater statistical significance, contrary to the NK cell-resistant SKOV3

target cells (*p<0.01; p=0.0050). No difference was observed on the MeFI

expression levels of the NK cell receptors and molecules (Figure 4-5B).
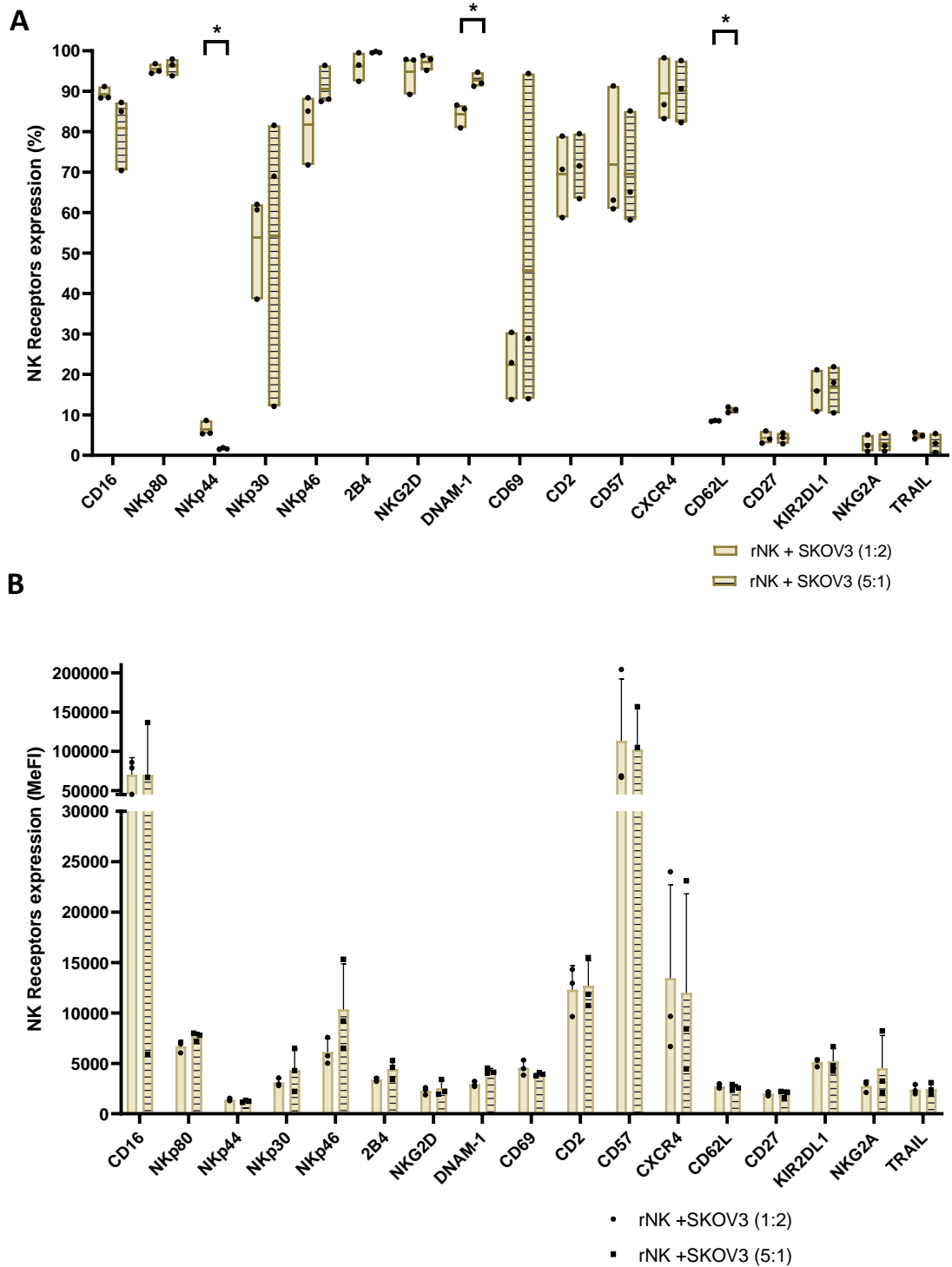
Figure 4-4: NK Cell Receptor Expression Levels on the NK Cell-Resistant SKOV3 Ovarian Cancer Target Cells at E:T (1:2) and (5:1)

Floating bars showing symbols on the percentage (A) and bar charts on the MeFI (B) with symbols for individual donors of the NK cell receptors on the surface of NK cells after co-incubation with the NK cell-resistant SKOV3 in E:T (1:2) (solid bar) and E:T (5:1) (patterned bar).Error bars represent SD of the mean. Statistical analysis using paired t-test. Biological triplicates (n=3). * p<0.05.
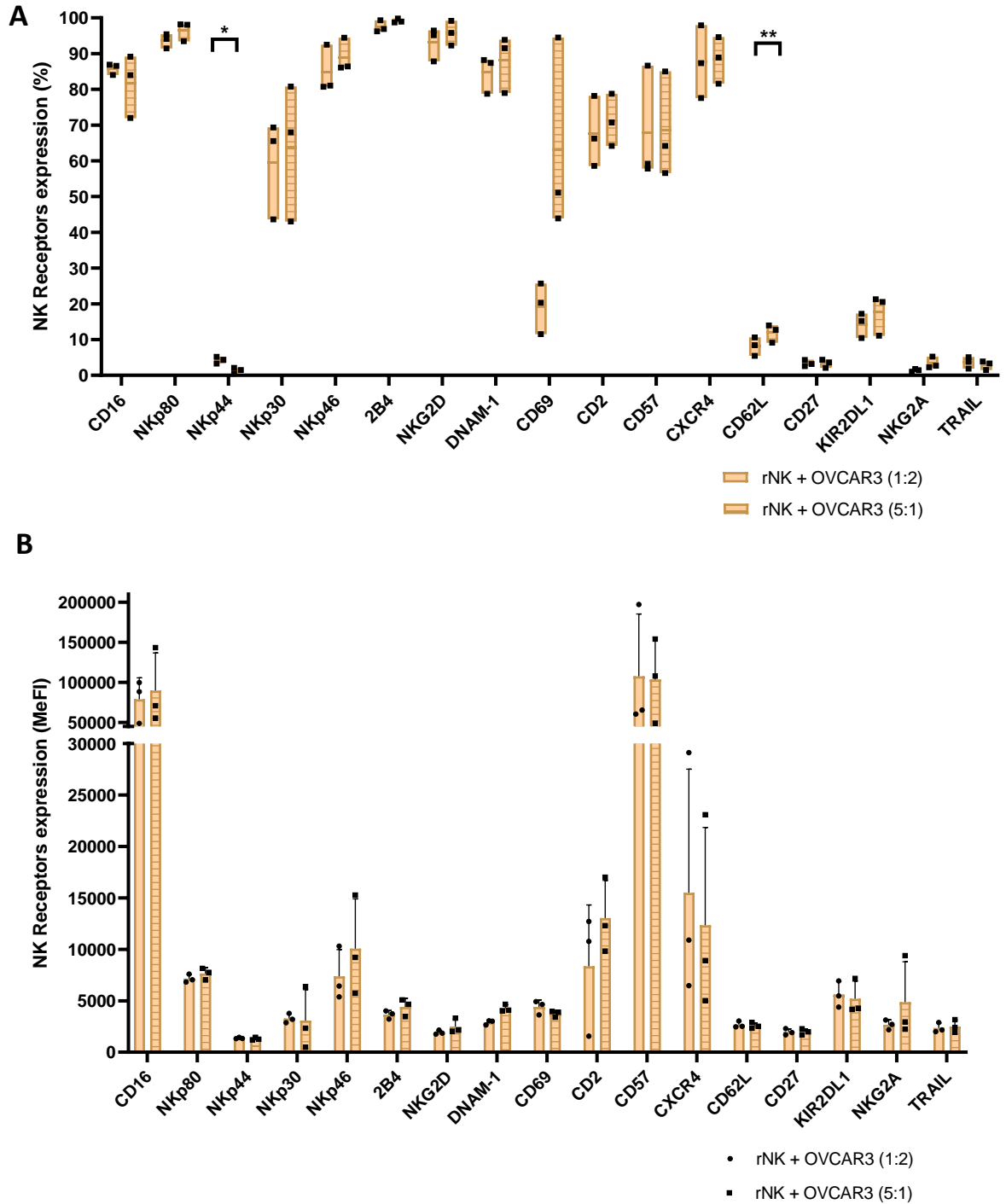
Figure 4-5: Natural Killer Receptor Expression on the NK Cell-Sensitive OVCAR3 Ovarian Cancer Target Cells at E:T (1:2) and (5:1)

Floating bars (min to max) and bar chart showing symbols of individual donors on the percentage (A) and MeFI (B) of the NK cell receptors on the surface of NK cells, on the NK cell-sensitive OVCAR3 ovarian cancer target cell. Comparison of E:T (1:2) (solid bar) and E:T (5:1) (patterned bar). Error bars represent SD of the mean. Line on Floating bars represent the mean. Statistical analysis using paired t-test. Biological triplicates (n=3). * $p<0.05$, **$p<0.01$.

4.4 Discussion

The NK cell responsiveness and deviations in sensitivity of ovarian cancer cell lines to NK cell-mediated lysis has been studied in this chapter. This was performed by comparing the expression levels of NK cell ligands and other surface molecules on the NK cell-resistant SKOV3 and NK cell-sensitive OVCAR3 ovarian cancer target tumour cell lines as well as of the NK cell receptors and molecules after interaction with the two different target cells. Comparison of MHC class I and MHC class II expression levels resulted in no difference between the two main ovarian cancer cell lines as the levels of the classical MHC class I HLA-A/B/C, the non-classical MHC class I HLA-E and the MHC class II HLA-DR molecules were similar. In addition, the expression of NK cell activating ligands on the surface of the SKOV3 and OVCAR3 cells was evaluated to investigate the mechanism behind their different sensitivities in the NK cell-mediated lysis.

The ligands of one of the main NK cell activation receptor NKG2D, MICA/B and ULBPs (1-6), have been tested in this chapter. The expression levels of MICA/B showed no difference with both cell lines expressing it in high levels. MICA/B is generally expressed in higher levels in cancer cells and to a lesser extent borderline/benign tumours whereas normal ovarian epithelium do not express MICA/B (Li *et al.*, 2009). The role of these ligands in ovarian cancer has been controversial as Huang and colleagues reported that MICA/B expression levels are correlated to an enhanced response to NK cell-mediated lysis whereas Roda-Navarro *et al* (2006) have reported a negative association of MICA/B expression and NK cell efficacy due to the

transfer of these ligands onto the NK cell surface, a process known as trogocytosis, which it causes downregulation of NKG2D to the surrounding NK cells (Roda-Navarro *et al.*, 2006). Comparison of ULBPs such as ULBP-1, ULBP-3 and ULBP2/5/6, revealed differences on their expression levels between the NK cell-resistant SKOV3 and NK cell-sensitive OVCAR3 cell lines as they were found to be expressed at a lower extent on OVCAR3 cells with statistical difference. This might be a result of the chronic exposure and contact of the NK cell-sensitive OVCAR3 target cells to the NK effector cells that it has been reported to cause downregulation or shedding of NK activating receptor ligands (Carlsten *et al.*, 2009; Pesce *et al.*, 2015). Understanding of NKG2D ligands in ovarian cancer setting is still limited and published reports demonstrate controversial significance of the NKG2D ligands on the prognosis in ovarian cancer patients. Sutherland and postulated that ULBPs facilitate the recruitment and infiltration of NK cells at the site of the tumour in several carcinomas, including ovarian cancer which this results in better prognosis, low recurrence rate and better OS (Sutherland *et al.*, 2006). However, Li *et al* (2009) demonstrated that increased expression of ULBPs, particularly the ULBP2 is an indicator of poor prognosis and OS (Li *et al.*, 2009).

Another important NK cell activating receptor that has key role in NK cell/target signalling pathway is DNAM-1. Therefore, its ligands, CD112 and CD155 were assessed here to identify the potential mechanism behind the opposed sensitivity between the two ovarian cancer cell lines against NK cell-mediated lysis. The expression level of these two ligands although it was found to be very high for both ovarian tumour cells, OVCAR3 exhibited lower

levels with statistical significance on the MeFI levels compared to SKOV3. The presence of CD112 and CD155 on these two ovarian tumour cell lines have also been reported in another study (Labani-Motlagh *et al.*, 2016). The high expression of CD112 and CD155 on the NK cell-resistant SKOV3 cells might postulate the impairment of NK cell response on this cell line as published studies have correlated the upregulation of DNAM-1 ligands both on the surface of the tumour target cells as well as on the TME as soluble molecules, to tumour progression and inhibition of NK cell activity due to downregulation of the DNAM-1 NK cell receptor expression via chronic ligand engagement (Carlsten *et al.*, 2009; Okumura *et al.*, 2020). This might also support and strengthen the results in chapter 3 where it was shown that DNAM-1 levels were lesser in OCP samples, particularly for the infiltrating NK cells derived from the ascites, that were in contact with the tumour.

Furthermore, CD48 the ligand for the NK activation marker 2B4 was found in this project to be upregulated in the OVCAR3 ovarian cells to almost doubled in comparison to SKOV3 cells with statistical significance. The role of this ligand on tumour progression and immunological surveillance efficacy has been disputable due to its dual capability to bind to 2B4 as well as to CD2. The CD48/2B4 interaction has been associated with tumour protection against immune responses, NK cell suppression and enhanced progression, invasion and metastasis (Belisle *et al.*, 2007). Nevertheless, other studies demonstrated that CD48/2B4 pairing is valuable as it prevents NK cell fratricide mainly in activated NK cells (Taniguchi *et al.*, 2007) as well as being able to promote NK cell activation and cytolytic function (McArdel *et al.*, 2016). This opposed role of CD48/2B4 on either activating or inhibiting NK

cell function might be correlated to the expression level of the 2B4 receptor as aforementioned here in Chapter 3 where 2B4 ability to activate or inhibit NK cell cytotoxicity was correlated to lower or higher levels of this receptor respectively (Chlewicki, 2008). Additionally CD48/CD2 conjugation is allied predominantly to immunological synapse formation, effective adhesion of NK cells to the target cells and supplemental NK cell activation (McArdel *et al.*, 2016). Herein, the higher CD48 expression levels on the NK cell-sensitive OVCAR3 ovarian cancer cell line may postulate its sensitivity to NK cell mediated lysis by portraying efficient amount of this ligand to bind to both 2B4 and CD2 on the NK cells and augment the NK cell-to-Target contact and NK cell responsiveness.

In addition, CD15 is the ligand for the CD2 molecule on the NK cells. CD15/CD2 conjugation facilitated immunological synapse between NK cells and target cells, prime rNK cells and enhance NK cell cytotoxicity response (Sabry *et al.*, 2011). In this project, OVCAR3 cell line expressed significantly higher levels of CD15 compared to SKOV3 cells. Similar levels of CD15 in OVCAR3 was also reported by Stuelten *et al* (2010) (Stuelten *et al.*, 2010). However, Stuelten and colleagues also reported analogous levels in SKOV3 cells which this was not observed here, as the CD15 expression in SKOV3 cells was significantly lower to nearly half compared to OVCAR3. Some postulations for this variance may be the difference in the fluorophore and clone of this antibody although it was purchased from the same company as well as the difference in the flow cytometer instrument that the samples were acquired as each instrument exhibit variances on their sensitivity and expression levels during sample acquisition. The panel of Stuelten *et al*

(2010) study comprised of 3 antibodies whereas the panel here was more extensive as it was encompassed of 8 antibodies (Stuelten *et al.*, 2010). Thus, the difference in the number of antibodies in the panel and the instrument sensitivity might contributed to the difference in CD15 expression level on SKOV3 ovarian cancer cells.

CD70 is a type 2 transmembrane surface protein of the TNF family and it is the ligand for CD27, a receptor that it is generally upregulated in several malignancies, including ovarian cancer and it was also shown in this project. Hence, the expression levels of its ligand, CD70 were assessed here and it was demonstrated that SKOV3 ovarian cancer cells displayed superior expression of CD70 compared to the OVCAR3 cells with statistical significance. This difference on the expression levels on these two cell lines were related to Ryan *et al* (2010) study (Ryan *et al.*, 2010). Liu and colleagues reported that upregulation of CD70 is correlated to drug resistance, poor prognosis and lower PFS and OS (Liu *et al.*, 2013). CD70 expression has been demonstrated to be associated with immunological escape and impairment of immune cell functions and even mediate apoptosis of lymphocytes and this might postulate the rationale of the SKOV3 resistance to NK cell-mediated lysis (Grewal, 2008).

PDL-1 expression levels have been reported to be upregulated in several cancers including ovarian cancer and it is related to lower PFS and OS. Wang and colleagues reported poor prognosis and OS in ovarian cancer patients after bioinformatics analysis and its expression was associated with immune evasion and tumour progression and metastasis (Wang, 2019).

Herein, PDL-1 levels were twice on the NK cell-resistant SKOV3 ovarian target cells compared to the NK cell-sensitive OVCAR3 ovarian target cells with statistical significance. This was also in line with Grenga and colleagues study (Grenga *et al.*, 2014). Therefore, the high levels of PDL-1 on the surface of the NK cell-resistant cell line SKOV3, might also be a potential mechanism of tumour evasion and metastasis.

CD24 is a molecule for cancer stem cells (CSCs) and its overexpression has been linked to poor prognosis as it is involved in tumour progression, invasion and metastasis. CD24 is expressed in several types of cancer, including ovarian cancer. Kristiansen and colleagues were the first to demonstrate its expression in a solid tumour and its correlation in prognosis and OS in ovarian cancer patients (Kristiansen *et al.*, 2002). Herein, both SKOV3 and OVCAR3 target cells, expressed analogous high CD24 levels. It has been reported that NK cell mediated lysis, preferentially target tumour cells that express CD24 via NKG2D-dependent signalling (Koh *et al.*, 2012). Although this might consolidate the sensitivity of OVCAR3 target cells to NK cell mediated cytotoxicity, it cannot similarly justify it for the NK cell-resistant SKOV3 cell line. Therefore, the controversial correlation of CD24 expression in clinical application and NK cell responses against the two opposed ovarian cancer cell lines, brings the necessity for further studies to be conducted in order to identify the exact mechanism of CD24 and enhance our understanding on its role behind NK cell responses upon immunosurveillance.

B7-H6 is the ligand for the NKp30 activating receptor on the NK cells. Herein, the NK cell-resistant SKOV3 target cell line, exhibited statistically higher levels of B7-H6 molecule, compared to the NK cell-sensitive OVCAR3 target cells. This postulates a potential resistance mechanism of SKOV3 to NK cell-mediated lysis, as it has been published that B7-H6 expression is associated with NK cell impairment by downregulation of the NKp30 and subsequently tumour escape. This is a result of chronic engagement of NKp30/B7-H6 by both B7-H6 expression on the surface of the target ovarian cancer cells or by soluble B7-H6 molecules on the TME (Pesce *et al*., 2015). This statement is also aligned with the results obtained in this project (Chapter 3), where the NK cell receptors immunophenotyping showed downregulation of the NKp30 on OCPs compared to HDs samples and primarily the NKp30 levels were reduced further on the infiltrated NK cells derived from the ascites at the site of the tumour, that might encompasses soluble B7-H6 molecules.

MUC16 is an ovarian cancer marker that has been variously reported for its role in prognosis of the disease as it is linked to tumour metastasis and immune protection of tumour target cells. MUC16 has been described by various studies to suppress NK cell responsiveness via inhibition of NK cell:Target immune synapse and subsequent NK cell mediated lysis impairment through its ADCC mediated pathway by CD16 downregulation (Carlsten *et al*., 2009; Gubbels *et al*., 2010; Patankar *et al*., 2005). Controversially, OVCAR3 ovarian cancer cell line although it is an NK cell-sensitive target cell, it is also the conventional cell line used in studies that expressed MUC16. Herein, OVCAR3 cells expressed significantly higher

MUC16 levels compared to SKOV3 which this is also reflected in the literature. However, the association between the high MUC16 levels and the sensitivity to NK cell lysis that the OVCAR3 cells exhibit is contradictory. A potential explanation behind this, might be that this CD16 downmodulation caused by MUC16 levels, can facilitate the disassemble of NK cell immune synapse and augment serial engagement and killing of target cells, enhancing the NK cell-mediated lysis efficacy and efficiency (Srpan *et al*., 2018).

In conclusion, this chapter compared the expression levels of NK cell ligands and surface molecules on the NK cell-resistant SKOV3 and NK cell-sensitive OVCAR3 ovarian cancer cell lines, with the objective to explain the differences on the sensitivity to NK cell mediated lysis. Although for the majority of the markers the differences in their expression levels were similar between the two ovarian tumour target cells, some differences might explain the opposed NK cell sensitivity they exhibit. SKOV3 cells expressed significantly higher levels of NK cell ligands from important NK cell activating receptors such NKG2D, DNAM-1 and NKp30. As a result, this upregulation of the NK cell ligands causes impairment of these receptors by chronic engagement and subsequently immune evasion of SKOV3 target cells. In contrast, OVCAR3 target cells expressed significantly higher levels of CD15 and CD48. CD15 binds to CD2 on the NK cells whereas CD48 exhibit dual recognition and bind to both CD2 as well as to 2B4. The interaction of both ligands to CD2, promote NK cell activation, recognition and engagement to tumour target cells. CD48:2B4 interaction stimulate NK cell responses and also protect NK cells from fratricide.

Herein it was the first time that such an extensive panel was used to establish the ovarian cancer resistance to NK cell cytotoxicity. This was also evaluated using a representative immunosuppressive environment where the tumour target cells are in greater numbers than the effector NK cells (E:T. 1:2) to establish a potential NK immunosuppressive phenotype in ovarian cancer setting. This immunosuppressive phenotype was compared against the NK cell-resistant SKOV3 and NK cell-sensitive OVCAR3 target cell lines and was further compared with the conventional E:T (5:1) ratio that is been used in a functional NK cell cytotoxicity assay. This comparison resulted in lower levels of CD16 and NKp44, with statistical significance, for the E:T (5:1) compared to the immunosuppressive E:T (1:2) after co-interaction with either ovarian cancer target cells. On the contrary, higher levels of NKp46, 2B4, NKG2D, DNAM-1 and CD62L were observed for the E:T (5:1) compared to the E:T (1:2). Statistical significance of this enhanced levels was detected for the CD62L after co-interaction with either ovarian cancer target cells and DNAM-1 after co-incubation with the NK cell-resistant SKOV3 target cell line.

Chapter 5   Priming of Natural Killer Cells in

Ovarian Cancer

5.1 Introduction

The cytokines that have been actively studied so far in the field of NK cell immunotherapy, to achieve NK cell-mediated induced priming, include the IL-2, IL-12, IL-15, IL-18 and IL-21 (Romee *et al.*, 2014) whereas the tumour cell lines studied to this point, that are required to achieve a tumour-induced priming of NK cells are the CTV-1 and NALM-16 tumour cells (North *et al.*, 2007) (Pal *et al.*, 2017).

The priming of NK cells was first reported almost four decades ago via cytokine-induced priming using IL-2. This stimulation is known as LAK and it facilitates NK cell-mediated lysis against previously resistant tumours to rNK cells (Grimm, 1982). Since its establishment as an NK cell priming agent, IL-2 has been extensively studied, both *in vitro* and *in vivo*, in cancer immunotherapy. However, its clinical outcome was controversial as it resulted in substantial toxicity and Treg cell induction, which restricts the NK cell function, even at low-dose of IL-2 administration in cancer patients (Romee *et al.*, 2014).

IL-15 is an additional cytokine that shares biological similarities and functions with IL-2 such as NK cell development, proliferation, survival and enhanced cytotoxicity. Together, these two cytokines represent the most studied priming agents of NK cells. However, IL-15 demonstrates better

clinical responses with less toxicity and an absence of Treg cell induction compared to IL-2. Therefore, several clinical trials using IL-15 are gaining momentum either as recombinant human IL-15 (rhIL-15) or as superagonist ALT-803 which has prolonged half-life than rhIL-15 and displays greater effects in NK cell functions (Romee *et al.*, 2014).

Other cytokines that have been studied for NK cell priming include IL-12, IL-18 and IL-21. IL-12 has antitumoral potential and IFN-γ dependent anti-tumour responses in advanced malignancies. However, rhIL-12 as a single agent showed poor clinical efficiency and severe toxicities. Combination of IL-12 with targeted therapies has been used in early phase studies with better clinical outcome (Romee *et al.*, 2014). Moreover, IL-18 either as a single NK cell priming agent or in combination with chemotherapeutic drugs, such as rituximab, demonstrated relative clinical safety without dose limiting toxicity, but, limited clinical response. Finally, IL-21 is another cytokine used for NK cell immunotherapy. *In vitro* studies revealed that IL-21 enhanced the ADCC NK cell activation mechanism (Gowda *et al.*, 2008). Clinical trials using rhIL-21 either as a single agent or in combination with cetuximab, exhibited promising clinical outcome with limited toxicity profile in ovarian cancer patients (Romee *et al.*, 2014).

Remarkably, NK cell priming using a combination of the aforementioned cytokines, such as IL-12, IL-15 and IL-18 results in memory-like NK cells, called cytokine-induced memory-like (CIML) NK cells as first described in murine studies by Cooper and colleagues (Cooper *et al.*, 2009). Subsequently, Romee *et al* (2012) were the first to report the induction of

human CIML-NK cells upon pre-activation with IL-12, IL-15 and IL-18 that resulted in long-lived (6 weeks) functionally activated NK cells (Romee *et al.*, 2012). In addition, Uppendahl *et al* (2019) recently published the CIML-NK cells against ovarian cancer cells as well as OCP ascitic fluid, in an attempt to examine the priming effectiveness against the immunosuppressive TME (Uppendahl *et al.*, 2019).

Alternatively to cytokine-primed NK cells, a pioneering study by our group, established the use of CTV-1, a previously resistant leukaemic cell line to rNK cell cytotoxicity, as an effective priming agent for NK cell immunotherapy (North *et al.*, 2007). The mechanism behind this approach relies on the type of evasion strategy that the CTV-1 cancer cells exploit against rNK cells that has been reported in this study. The majority of previously determined NK cell resistant cancer cells express type 1 evasion strategy that prevents the efficient priming of NK cells. However, the CTV-1 tumour cells convey type 2 evasion strategy as they are capable of priming but fail to trigger the NK cells. In this study North and colleagues co-incubated o/n CTV-1 cell lysates with freshly isolated NK cells in a ratio CTV-1:NK (2:1) prior the cytotoxicity assays. The target cells used in this study were from several cancer types such as lymphoma (RAJI and DAUDI), breast cancer (MCF7), leukaemia (K562) and primary leukaemic, ovarian and breast tumour cells from cancer patients. Functional killing assays were performed at either 1:1 or 5:1 E:T ratios. North and colleagues showed that tumour-primed NK cells effectively activated NK cells to kill previously resistant tumour cells to rNK lysis irrespective of HLA matching (North *et al.*, 2007). Additionally, Pal *et al* (2017) reported priming of NK cells with the

NALM-16 leukaemic cell line that resulted in tumour-induced memory-like (TIML) NK cells. These NK cells were capable to induce tumour-specific cytotoxicity and enhanced perforin synthesis (Pal *et al.*, 2017).

5.2 Aims

The aims of this Chapter were:

(i)   To perform functional killing assay to identify the effect of NK cell priming via either cytokine-induced using rhIL-15 or tumour-induced using INB16 leukaemic cell line in ovarian cancer, using HD-derived NK cells and SKOV3 and OVCAR3 target ovarian cancer cells. RAJI and K562 tumour cells were used as controls.

(ii) To perform functional killing assay to investigate the effect of cytokine- and tumour- primed NK effector cells in ovarian cancer setting using NK cells derived from OCP-Ascites samples against SKOV3 and OVCAR3 ovarian cancer cells. RAJI and K562 tumour cells were used as controls.

(iii) To determine the differences on the expression level of NK receptors and adhesion molecules of non-primed and primed NK cells as well as of the NK cell ligands after co-incubation with SKOV3 and OVCAR3, using extensive immunophenotypic panels.

5.3 Methods

5.3.1 Cytokine- and Tumour- Priming of Natural Killer Cells

The NK cells used as effector cells in this Chapter, derived from whole population HD-PBMC and OCP-Ascites. Isolation of NK cells was performed as described in Chapter 2 (section 2.2.1). The percentage of NK cells on these two populations was determined after immunostaining with CD56 APC/Cy7 (clone: NCAM 16.2, BD Bioscience) and CD3 Vioblue (clone: REA613, Miltenyi) monoclonal antibodies as in section 2.2.3. This was performed to achieve an E:T (5:1) ratio for the cytotoxic assays.

The NK cells were cytokine-primed o/n using recombinant human IL-15 (10ng/ml) (R&D Systems). For the tumour-primed NK cells (TpNK), INB16 tumour cells previously treated with mitomycin C (MMC) as explained in section 2.3.1.2at a NK:INB16 ratio (1:2). Non-primed resting NK cells (rNK) were also used as controls. All effector conditions were incubated o/n in a culture incubator (Panasonic) at 37°C, 5% CO_2, 21% O_2. The next day, the rNK and primed-NK cells were added to the corresponded target cells. The tumour target cells that were used in this chapter were the NK cell-sensitive K562 and OVCAR3 cell lines as well as the NK cell-resistant RAJI and SKOV3 cell lines. A summary of all priming conditions for each target cell can be observed at *Table 5-1*.

Table 5-1:Target Cells and Natural Killer Cells Effector Conditions

Target Cells			
K562	OVCAR3	RAJI	SKOV3
Conditions			
Targe*t al*one		Targe*t al*one	
rNK		rNK	
NK+rhIL-15(10ng/ml)		NK+rhIL-15(10ng/ml)	
		TpNK	

5.3.2   Natural Killer Cell Cytotoxic Assays

5.3.2.1 K562 and RAJI Target Cells

For the K562 and RAJI target cells, they were first PKH67-labelled as described in Chapter 2, section 2.3.1.1. Each of the target cells was resuspended in supplemented culture medium at 0.2×10^6/ml working stock, placed in a 13ml polypropylene tube and incubated o/n at 37°C, 5% CO_2, 21% O_2. The next day, 200µl of each working stock solution were transferred to the corresponded FACS tubes that already contained 200µl of either the primed or non-primed NK effector cells to achieve a final E:T (5:1) ratio. Finally, 100µl of supplemented culture medium was added to all the tubes to achieve a final volume of 500µl. FACS tubes containing target cells only were also prepared as controls for establishing the specific lysis.

The cytolysis of K562 and RAJI target cells was measured after 4h, 6h and 16h by flow cytometry (NovoCyte, Agilent). For the target cell viability, TO-PRO-3 nuclear counterstain dye was added (1/10 of total sample volume) to all the samples prior acquisition. The acquisition of samples in the flow

cytometry (NovoCyte, Agilent), was set to 10,000 events of the PKH67 positive target cells population. The number of live cells from the PKH67-labelled target cells was distinguished by TO-PRO-3 dye in which dead cells were positive for this dye. This assay was conducted for 3 biological replicates for both HD-derived and OCP-derived samples in technical duplicates.

5.3.2.2 SKOV3 and OVCAR3 Ovarian Cancer Target Cells

For the adherent ovarian cancer SKOV3 and OVCAR3 cell lines, the NK cytotoxic assay was performed in the xCELLigence RTCA system (Agilent) as mentioned in section 2.3.2.1. The ovarian cancer target cells were passaged the day prior the experiment. The next day, SKOV3 and OVCAR3 target cells were harvested using Detachment solution as described in section 2.1.1 and resuspended in supplemented culture medium at 0.1×10^6/ml and 0.2×10^6/ml working stocks respectively. Subsequently, 50µl of each target cell line were seeded to the already background calibrated e-plates, to achieve a concentration of 5,000 SKOV3 cells/well and 10,000 OVCAR3 cells/well. The e-plates were placed back into the xCELLigence RTCA system and incubated o/n at 37°C, 5% CO_2, 21% O_2.

The next day, 100µl of the working stock for primed and non-primed NK effector cells were added to the corresponded wells to achieve the E:T (5:1) ratio for each cell line. Wells containing solely the target cells were also prepared to facilitate the specific cytolysis establishment. Corresponded supplemented culture medium was added to the appropriate wells to reach an equal final volume of 200µl in all the wells for both ovarian cancer cell

lines (50µl background + 50µl target cells + 100µl effector cells or 100µl supplemented culture medium). A continuous readout for a total duration of 48h was performed with 15 minutes intervals. This assay was conducted for 3 biological replicates for both HD-derived and OCP-derived samples in technical triplicates.

5.3.3 eSIGHT Live Cell Imaging

The SKOV3 target cells were fluorescently labelled with PKH67 cell membrane dye (Sigma-Aldrich) following the manufacturer's protocol, as described in section 2.3.1.1. Subsequently, the ovarian cancer target cells were resuspended in stock concentration 0.1×10^6/ml and 5,000 cells were seeded on the e-plate and left o/n at 37°C, 5% CO_2, 21% O_2. Readouts were performed every 15 minutes. Additionally, the NK effector cells were labelled with Cell Trace Violet (ThermoFisher Scientific, UK) as explained in section 2.3.3 at working concentration 5µM and incubated o/n with either rhIL-15 (10ng/ml) or MMC treated INB16 (2:1). Non-primed rNK effector cells were used as a control in this assay. The next day all the effector conditions were added to the seeded SKOV3 target cells on the e-plate at an E:T (5:1) ratio. Caspase 3/7 red reagent (ThermoFisher Scientific, UK) was finally added to allow the observation of target cell lysis. Measurements were taken every 5 minutes for a duration of 48h.

5.3.4 Avidity

The total binding strength between cells including tumour and immune cells is known as avidity. Herein, this parameter was used to investigate the

interaction and engagement of NK cells to the different target cells that expose different sensitivity against NK cell mediated cytotoxicity. This was performed in an endeavor to understand better the mechanism behind this and facilitate the development of a more effective immunotherapeutic approach using a high-throughput, fast and reproducible technology.

The avidity assay was performed using the z-Movi Cell Avidity Analyser (Lumicks). This technology applies acoustic force ramps to measure the avidity using special z-Movi chips where the target cells and effector cells are added.

The NK cell-resistant SKOV3 ovarian cancer cell line was used for this experiment, and were passaged two days prior to the day of the experiment. On the day of the experiment, SKOV3 target cells were harvested using TryPLE Express (ThermoFisher Scientific, UK) and count. SKOV3 cells were subsequently, centrifuged at 200g for 5 minutes at RT and resuspended in a serum-free medium at a concentration of 100×10^6/ml. 20µl of this stock target cell concentration were added to the z-Movi chip reservoir and a syringe with 1,5ml of air cushion was used by pulling and releasing the plunger and slowly open the valve of the chip so it can create an optimum pressure flow of cells for a uniform layer of seeding. The valve was then closed and the chip was subsequently rinsed 5 times with 100µl of PBS using a pipet. The chip reservoir was refilled with 300µl of complete culture medium containing the serum and the monolayer of SKOV3 target cells was checked under a brightfield microscope and incubated at 37°C for 30 minutes in a dry incubator (ThermoFisher Scientific). After this incubation time, the culture

medium was exchanged by repeating the method of the syringe with a 1,5ml air cushion and valves and the chip was then incubated again for 2h at 37°C dry incubator (ThermoFisher Scientific).

The NK effector cells were derived from HD samples and were isolated and immunophenotyped as explained in Chapter 2 section 2.2. Consequently, NK effector cells were pre-labelled with CellTrace Far Red Dye (Invitrogen, Fisher Scientific, UK) by reconstituting the vial of dye in 10μl DMSO. 1μl of the dye stock solution was added in 1ml of pre-warmed PBS (1x solution). The NK cells were resuspended in $1x10^6$/ml and 1ml of the dye mixture solution was added and subsequently incubated at 37°C for 15 minutes by mixing every 5 minutes. After the incubation, 5ml of complete culture medium was added to the cells and washed by centrifuge at 200g for 5 minutes, at RT. Pellet was washed in 5ml of PBS and centrifuged again on the same aforementioned parameters.

Finally, the NK cells were resuspended in complete medium at $1x10^6$/ml and incubated o/n either with IL-2 (10ng/ml), IL-15 (10ng/ml), MMC treated INB16 (1:2) or rNK as a control. The next day, NK effector cell conditions were centrifuged, resuspended at $20x10^6$/ml and 20μl were added to each corresponded chip containing the pre-seeded SKOV3 target cells (total of 4 chips, 1 for every effector condition). The z-Movi chips were incubated for 5-10 minutes, rinsed to remove the excess floating labelled effector cells and 100μl of complete medium were added to the chips. Finally the z-Movi chips were placed into the z-Movi Cell Avidity Analyser (Lumicks) and acoustic force ramps were applied to measure the avidity.

5.3.5 Immunophenotyping of Primed Natural Killer Cell Receptors and Ligands

An extensive screening of NK cell receptors and ligands had been designed to investigate the effects of NK cell priming, as well as the NK cell sensitivity using the NK cell-resistant SKOV3 and NK cell-sensitive OVCAR3 ovarian target cell lines. The panels used are equal to the ones defined in Table 2-1 and Table 2-2. This was performed on NK effector cells and target cells before and after the co-incubation at E:T (5:1). The NK cells, derived from HD-PBMC samples and the effector conditions used here, consisted of non-primed rNK, cytokine-primed via rhIL-15 (10ng/ml, R&D Systems) NK cells and TpNK cells via MMC treated INB16 (NK:INB16, 1:2). The NK cells were incubated for the priming conditions o/n in a cell culture incubator (Panasonic) at 37°C, 5% CO_2, 21% O_2. Viability of NK effector cells was established using Zombie Yellow (Biolegend, UK). The purity of isolated NK cells prior priming conditions was >90% with around 75-80% of this population being CD56^{bright} subset and around 5% CD56^{dim}. After o/n priming the CD56^{bright} NK cell subset dropped to 65-75% and the CD56^{dim} NK cell population increased by 5%.

Target cells were stained with Cell Trace Violet (ThermoFisher Scientific, UK) as described in section 2.3.3 and viability was determined using TO-PRO-3 counterstain dye Finally, samples were analysed via flow cytometry (NovoCyte, Agilent).

5.3.6 Statistical Analysis

A two-tailed paired t-test was used to compare the values of rNK and cytokine-primed NK effector conditions from HD or OCP samples against the NK cell-sensitive cell lines.

A two-tailed unpaired t-test with Welch's correction, was used to compare the values between the HD-PBMC and OCP-Ascites samples.

One-way ANOVA and Dunnett's multiple comparisons follow up test with rNK cells used as the control column, was performed to compare the two different NK priming conditions (tumour or cytokine mediated NK cell priming) with the non-primed control rNK cells against the NK cell-resistant target cell lines.

The p-value was determined as *p≤0.05, **p≤0.01, ***p≤0.001 and ****p≤0.0001 (GraphPad Prism 9.0.0).

5.4 Results

5.4.1 Primed-Natural Killer Cell Receptor Levels in Ovarian Cancer

Figure 5-1 shows the extensive immunophenotyping panel for the NK cell receptor expression levels of non-primed and primed-NK cells. The priming was performed by either cytokine-induced using rhIL-15 (10ng/ml, R&D Systems) or an alternative priming approach, using INB16 tumour cells that had been already MMC treated in a priming ratio of NK:INB16 (1:2). The tumour-primed NK cells (TpNK) were compared to the negative control non-

primed rNK cells and the cytokine-primed NK effector cells via rhIL-15 were used as a positive control.

Results were plotted in a box plot showing individual donors for the percentage of frequency (A) and bar chart with individual points for the MeFI expression levels (B). The percentage levels for the NK cell activating receptors, NKp80, NKp30, 2B4 and DNAM-1 did not demonstrate significant difference between the rNK cells and the primed NK cells irrespective of the priming agent used. Similarly, the NK cell inhibitory receptors KIR2DL1 and NKG2A did not express differences among the NK effector conditions. Additionally, CD2, CD57, CD62L, CXCR4 and CD27 expression levels were not significant different between the NK conditions. However, expression of the NK cell activating receptors CD16, NKp46 and NKG2D was significantly reduced upon tumour priming compared to the control non-primed rNK cells with *$p < 0.05$. The CD16 and NKp46 levels on the rNK effector cells reduced from 88.37% and 94.5% respectively to 75.41% and 82.81% respectively ($p = 0.0131$ for CD16 and $p = 0.0341$ for NKp46). In addition, NKG2D levels were reduced from 93.71% in rNK cells to 87.20% in TpNK effector condition with *$p = 0.0464$. On the contrary, expression of NKp44 activating receptor and CD69 activating molecule was upregulated upon priming compared to the rNK cells with statistical significance. A greater proportion of cytokine-primed NK cells expressed NKp44 (7.10%) compared to the rNK cells (2.56%) with *$p < 0.05$; $p = 0.0283$. CD69 levels were significantly upregulated in both primed-NK cells compared to the rNK cells. CD69 expression was increased from 9.53% in rNK cells to 62.18% after cytokine priming (**$p < 0.01$; $p = 0.0014$) and 58.65% upon tumour-priming (**$p < 0.01$;

p=0.0035). Finally, the percentage of cells expressing TRAIL significantly downregulated on TpNK (3.73%) compared to the rNK cells (13.70%) with *p<0.05; p=0.0285. No significance was observed on the MeFI expression levels of these NK cell receptors and molecules upon priming either via cytokine- or tumour-induced mediated priming.
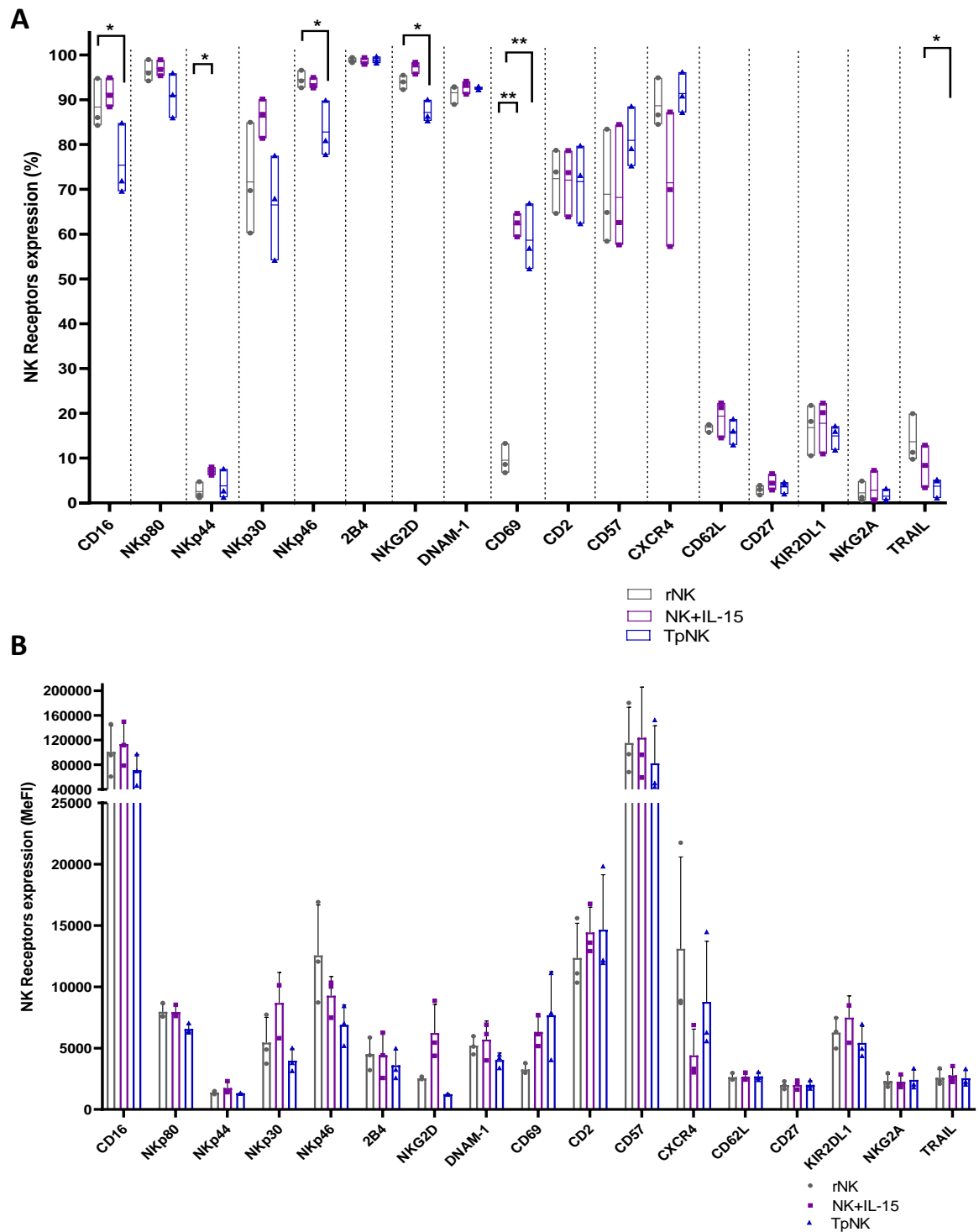
Figure 5-1: Natural Killer Cell Receptor Expression Levels after Cytokine- and Tumour Induced Priming

Percentage (A) and MeFI (B) expression levels of NK receptors and molecules between non-primed rNK (grey), cytokine-primed via rhIL-15 (10ng/ml) NK cells (purple) and tumour-primed via INB-16 MMC treated NK cells (NK:INB16,1:2) (blue). Error bars represent SD of the mean. Statistical analysis using paired t-test. . Biological triplicates (n=3). * p<0.05, **p<0.01.

After investigating the effects of priming on the NK cell receptors and molecules on the non-primed and primed NK effector cells, a further investigation was conducted to test the expression levels also upon co-incubation with the ovarian cancer target cells, the NK cell-resistant SKOV3 and NK cell-sensitive OVCAR3 cell lines.

Figure 5-2 illustrates the NK cell receptor expression levels of cytokine-primed NK effector cells upon interaction with SKOV3 and OVCAR3 target cells after 4h of co-incubation and an E:T (5:1). Cytokine-primed NK cells without any co-interaction with target cell were used as a control to plot the data. The only markers that resulted in significant difference were the CD16 and CD69 for both ovarian cancer target cells. The CD16 levels of the cytokine-primed NK effector cells were significantly downregulated upon the presence of the ovarian target cells in comparison with cytokine-primed NK effector cells alone with $*p<0.05$; $p=0.0343$ after co-incubation with SKOV3 and $**p<0.01$; $p=0.0060$ after co-incubation with OVCAR3. On the contrary, CD69 expression was significantly upregulated upon interaction with the ovarian tumour target cells with $*p<0.05$ for both target cell lines ($p=0.0188$ for SKOV3 and $p=0.0286$ for OVCAR3).

Figure 5-2: Natural Killer Cell Receptor Expression by Cytokine-Primed NK Cells in Ovarian Cancer

Percentage (A) and MeFI (B) expression levels of NK receptors of cytokine-primed NK effector cells via rhIL-15 (10ng/ml) after co-incubation with the NK cell-resistant SKOV3 (light purple) and NK cell-sensitive OVCAR3 (dark purple) ovarian cancer target cell lines. E:T (5:1), 4h co-incubation. Cytokine-primed NK cells without tumour target interaction (purple no-fill bar) was used as control. Error bars represent SD of the mean. Statistical analysis using paired t-test of each E:T primed condition against the cytokine-primed NK cells alone. Biological triplicates (n=3). * p<0.05, ** p<0.01.

The tumour priming of NK effector cells was also investigated as an additional priming agent against the NK cell-resistant SKOV3 ovarian cancer cell line and its effects on the NK cell receptors and molecules were also assessed here.

Figure 5-3 displays the effects of the tumour priming on the NK effector cells upon interaction with the ovarian cancer SKOV3 target cells after 4h co-incubation in a E:T (5:1). TpNK effector cells alone were used as a control.

Tumour priming demonstrated significant upregulation of the NKp80 NK activating receptor and the NK cell inhibitory receptor KIR2DL1 with *$p < 0.05$ ($p = 0.0492$ and $p = 0.0255$ for NKp80 and KIR2DL1 respectively) compared to the control TpNK effector cells without co-interaction with the SKOV3 target cells. No difference was observed on the frequency of expression on the other NK cell receptors and molecules. The MeFI expression levels for all the markers showed no statistical significance.
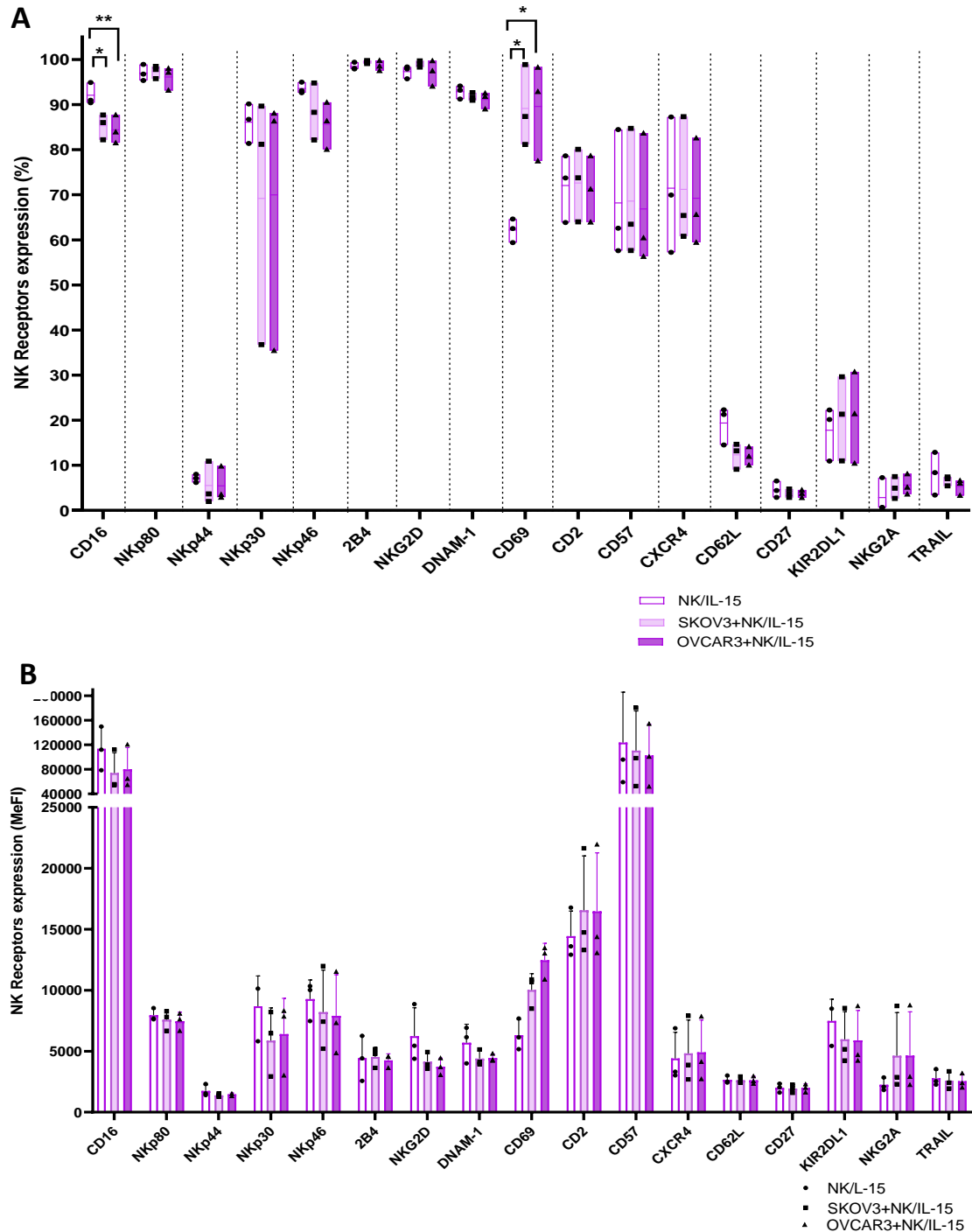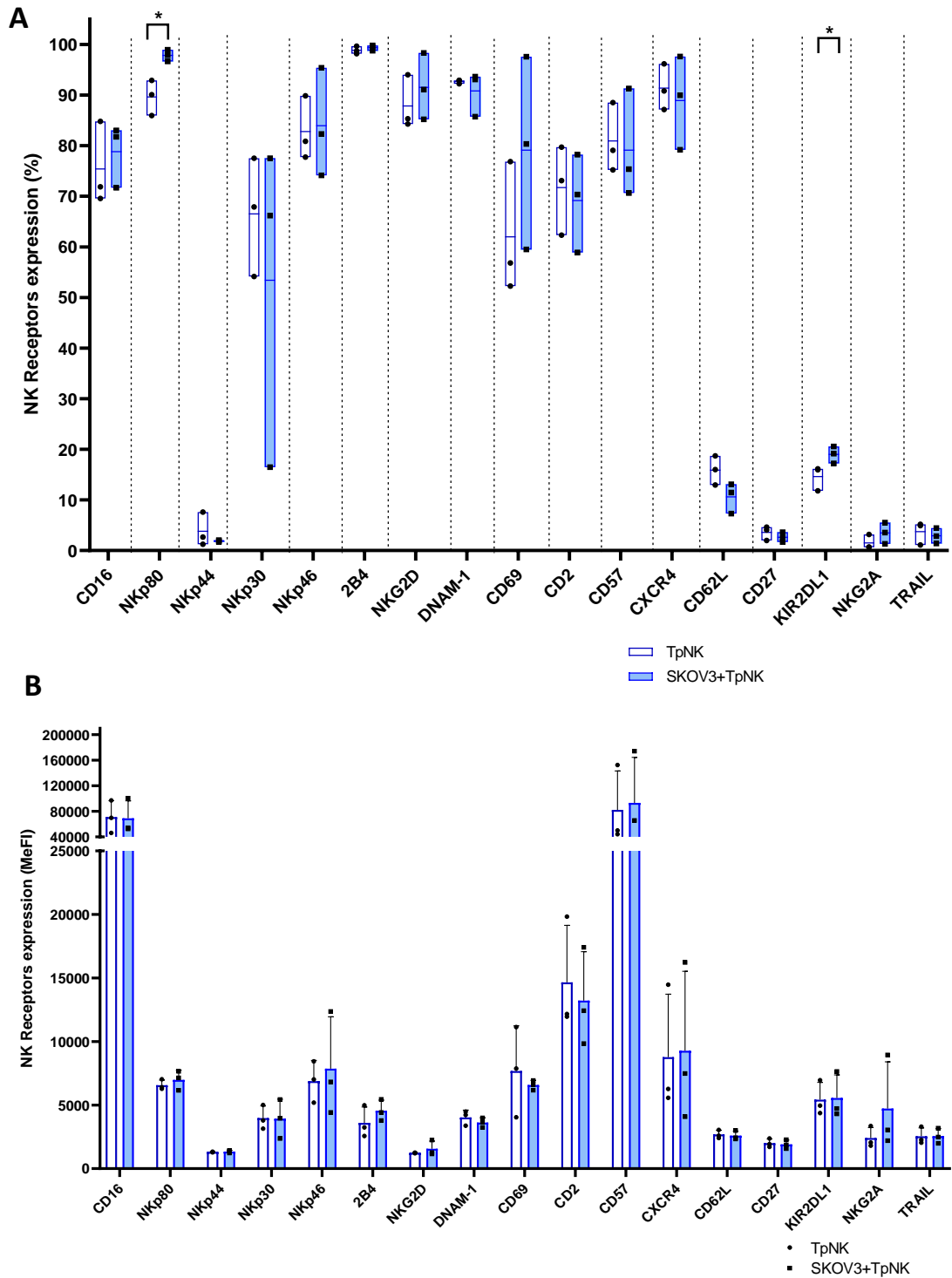
Figure 5-3: Natural Killer Cell Receptor Expression Levels on Tumour-Primed NK Cells in Ovarian Cancer

Percentage (A) and MeFI (B) expression levels of NK receptors of TpNK effector cells via INB16 MMC treated priming agent (NK:INB16, 1:2) before (blank) or after co-incubation with the NK cell-resistant SKOV3 ovarian cancer target cell line (blue). E:T (5:1), 4h co-incubation. Error bars represent SD of the mean. Statistical analysis using paired t-test of each E:T primed condition against the TpNK cells alone. Biological triplicates (n=3). * p<0.05.

5.4.2 Functional Cytotoxicity Assay of Primed-NK Cells in Ovarian Cancer

NK effector cells were either cytokine-primed via rhIL-15 (10ng/ml) or tumour primed via INB16 MMC treated cells o/n and subsequently added the next day to a functional killing assay (E:T, 5:1) against NK cell-sensitive and NK cell-insensitive cell lines in different time points. This was performed using NK cells derived from HD-PBMC samples and OCP-Ascites samples to establish the effectiveness of priming in NK cell function in ovarian cancer using the OCP derived samples.

Figure 5-4A shows the specific cytolysis of K562 target cells against the cytokine-primed NK effector cells derived from HD samples, after 4h, 6h and 16h of co-incubation. The primed NK effector cells compared to the control rNK cells exhibited statistically significant enhancement of cytotoxicity against the K562 target cells with *$p < 0.05$ after 4h ($p = 0.0251$) and 6h ($p = 0.455$). No difference was observed after 16h of E:T co-incubation as the target cell lysis percentage levels were already very high (95.69% for rNK effector condition and 99.48% for cytokine-primed NK effector cells).

Consequently, the efficacy of cytokine-primed NK effector cells was investigated on OCP samples (Figure 5-4B). After 4h of co-incubation, the cytokine priming, effectively enhanced the killing function efficacy of the NK cells from OCP samples with statistical significance (**$p < 0.01$; $p = 0.0016$). No difference was detected after 6h and 16h of E:T interaction.
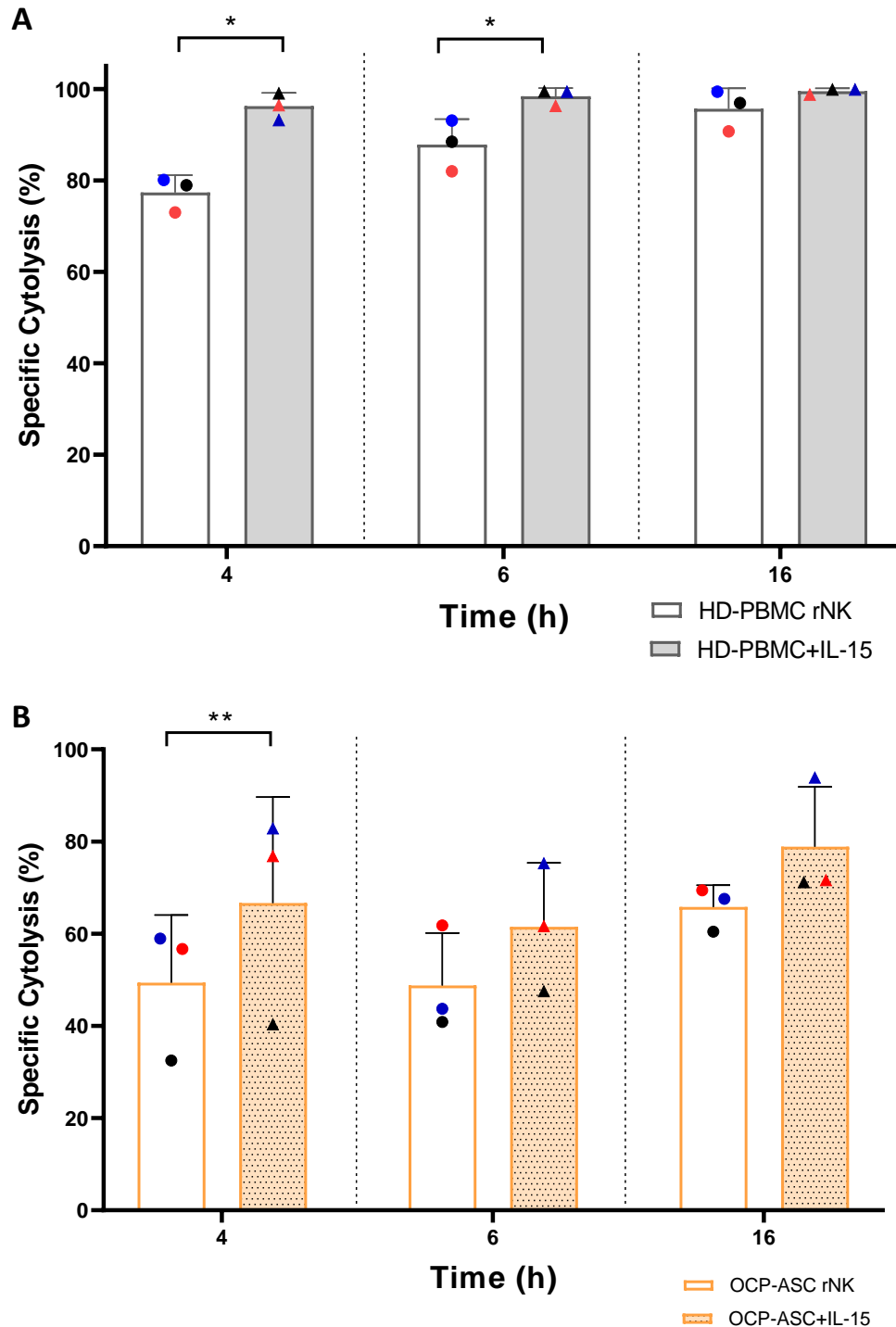
Figure 5-4: HD- and OCP-Derived Cytokine-Primed NK Cells Against K562 Target Cells

Bar chart with individual points of donors of K562 target cell specific cytolysis. rNK effector cells (white bars) and cytokine-primed NK cells (coloured bars) of HD-PBMC (A) and OCP-Ascites (B). Priming of NK cells via rhIL-15 (10ng/ml). Error bars represent SD of the mean. Statistical analysis using paired t-test. Biological triplicates (n=3). * p<0.05, ** p<0.01.

Figure 5-5 displays the cytokine-primed NK effector cells derived from HD (A) and OCP (B) samples against the NK cell-sensitive OVCAR3 ovarian cancer cell line. The assay was performed in the xCELLigence RTCA system that performs a continuous readout. A total of five timepoints were used to plot the data after E:T interaction; 4h, 6h, 16h, 24h and 48h.

The OVCAR3 lysis was statistically enhanced upon cytokine priming from the HD-derived samples (Figure 5-5A), for all the aforementioned timepoints. After 4h and 6h the p-value was **p<0.01 (p=0.0029 and p=0.0030 respectively) and after 16h, 24h and 48h there was a statistical significance of *p<0.05 (p=0.0355, p=0.0413 and p=0.0445 respectively).

In contrast, cytokine priming of NK cells derived from OCP samples (Figure 5-5B) did not augment the OVCAR3 target cell lysis throughout all the timepoints. However, increase in OVCAR3 cell cytolysis began at the very last timepoint (48h), and the cytokine-primed NK effector cells showed enhanced target cell cytolysis, specifically for one donor, without still any statistical significance.
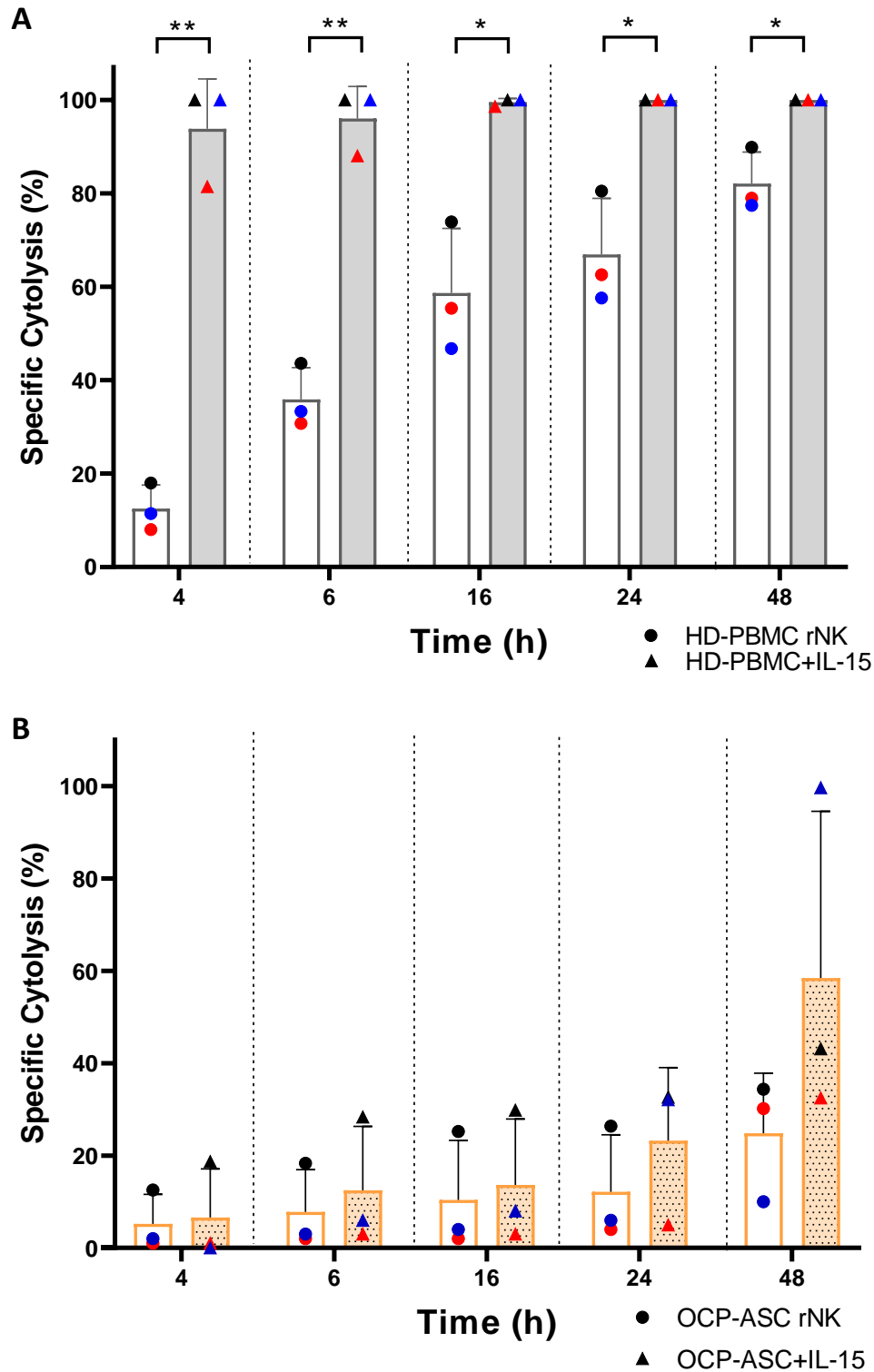
Figure 5-5: HD- and OCP-Derived Cytokine-Primed NK Cells Against OVCAR3 Target Cells

Bar chart with individual points of donors of OVCAR3 target cells specific cytolysis. rNK effector cells (white bars) and cytokine-primed NK cells (coloured bars) of HD-PBMC (A) (solid colours) and OCP-Ascites (B) (dotted pattern). Cytokine priming via rhIL-15 (10ng/ml). Error bars represent SD of the mean. Statistical analysis using paired t-test. . Biological triplicates (n=3). . * p<0.05, ** p<0.01.

After investigating the effects of cytokine priming of NK cells in ovarian cancer using OVCAR3 target cells as well as NK cells derived from OCP samples, the effects of tumour priming of the NK effector cells were also examined. This priming condition was conducted on the control NK cell-resistant target cells RAJI as well as the SKOV3 ovarian cancer target cells to assess it in an ovarian cancer setting.

Figure 5-6 demonstrates the specific cytolysis of RAJI target cells upon TpNK compared to the rNK negative control effector cells and the cytokine-primed (rhIL-15, 10ng/ml) NK positive control cells. The results were acquired after 4h, 6h and 16h of E:T (5:1) co-incubation.

Figure 5-6A displays the priming effects on the NK cells derived from HD-PBMC samples. RAJI target cell lysis by TpNK effector cells was statistically increased for all the timepoints with a p-value of *p<0.05 at 4h (p=0.0252) and **p<0.01 after 6h (p=0.0031) and 16h (p=0.0024).The cytokine-primed positive control NK effector cells also showed statistical significance for all the timepoints, with p-value ****p<0.0001.

The effects of TpNK against RAJI target cells were also tested on NK cells derived from OCP samples (Figure 5-6B). Statistical significance was only observed after 4h of E:T (5:1) co-interaction for both priming conditions (**p<0.01; p=0.0022 for TpNK and ***p<0.001; p=0.0008 for cytokine-primed NK cells).

Figure 5-6: Primed-NK Cells From HD and OCP Samples Against RAJI Target Cells

Bar chart with individual points of donors of RAJI target cells specific cytolysis. rNK effector cells (white bars) and cytokine-primed NK cells or TpNK cells (coloured bars) of HD-PBMC (A) (solid colours) and OCP-Ascites (B) (dotted pattern). Cytokine priming via rhIL-15 (10ng/ml) and tumour priming via INB16 MMC treated (NK:INB16 1:2). Error bars represent SD of the mean. Statistical analysis using paired t-test. Biological triplicates (n=3). * p<0.05, ** p<0.01, ***p<0.001, ****p<0.0001.

Subsequently, the effects of TpNK effector cells were investigated on the NK cell-resistant SKOV3 ovarian cancer cell line. The cytotoxic assay was conducted on the xCELLigence RTCA system in a continuous readout with 15 minutes intervals. Finally, five timepoints, 4h, 6h, 16h, 24h and 48h were selected to analyse and plot the results (Figure 5-6).

SKOV3 target cell lysis was significantly increased after 6h of incubation onwards for the NK cells derived from HD-PBMC samples (Figure 5-7A). After 6h the statistical significance for TpNK effector cells was equal to the positive control cytokine-primed NK (**p<0.01; p=0.0046 for TpNK and p=0.0014 for cytokine-primed NK cells respectively). After 16h of co-interaction onwards the p-value of TpNK effector cells was *p<0.05 (p=0.0170 after 16h, p=0.0241 after 24h and p=0.0128 after 48h). The cytokine-primed NK effector cells increased the SKOV3 specific cytolysis with a statistical significance of ****p<0.0001 after 16h of E:T interaction onwards.

Tumour-priming of NK cells that derived from OCP samples (Figure 5-6B) only expressed difference on the enhancement of SKOV3 target cell lysis with statistical significance after 48h of co-incubation with the target cells (*p<0.05; p=0.0422). Similarly, the cytokine-primed NK effector cells expressed significant difference at late co-incubation timepoints with the same p-value as TpNK effector cells, however here a statistically significant difference was observed after 24h (*p<0.05; p=0.0363) and 48h (**p<0.01; p=0.0032).
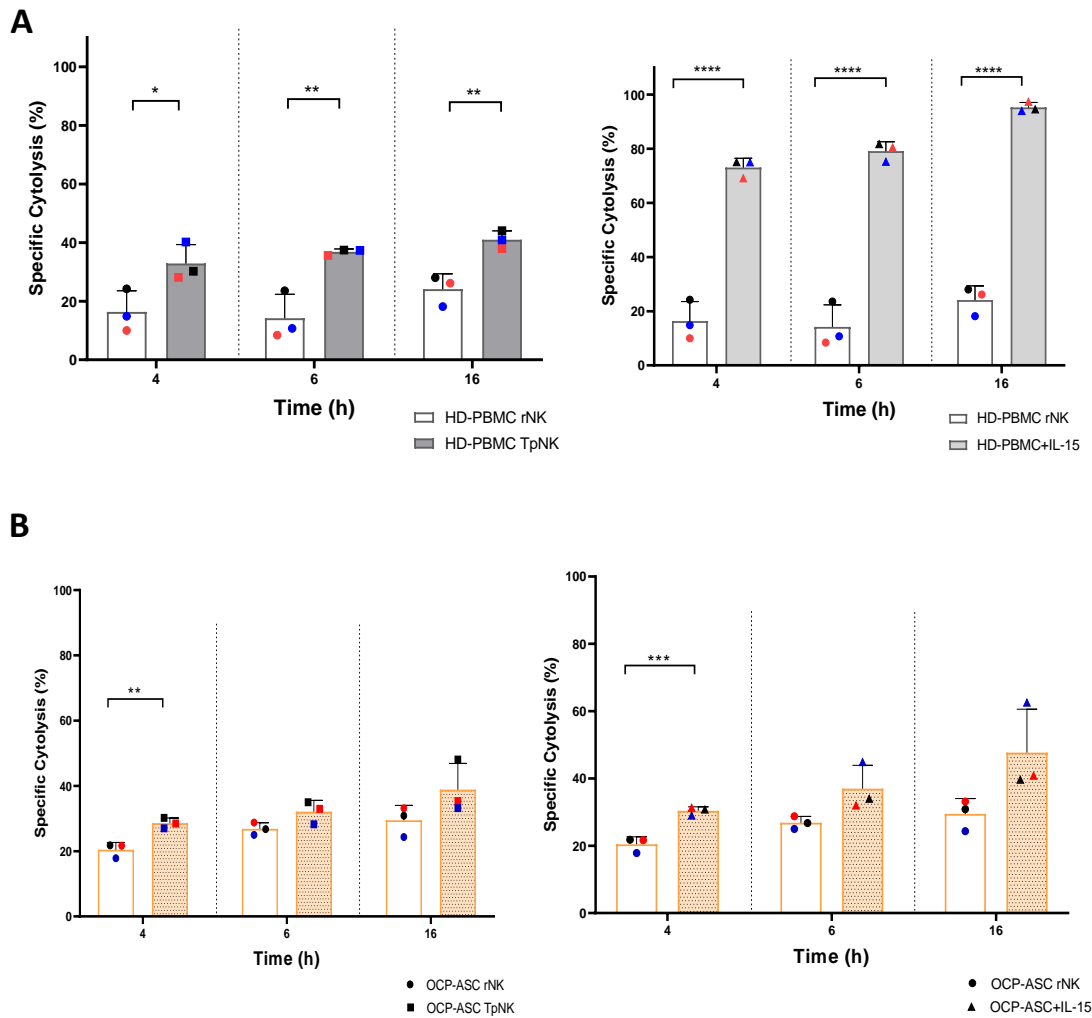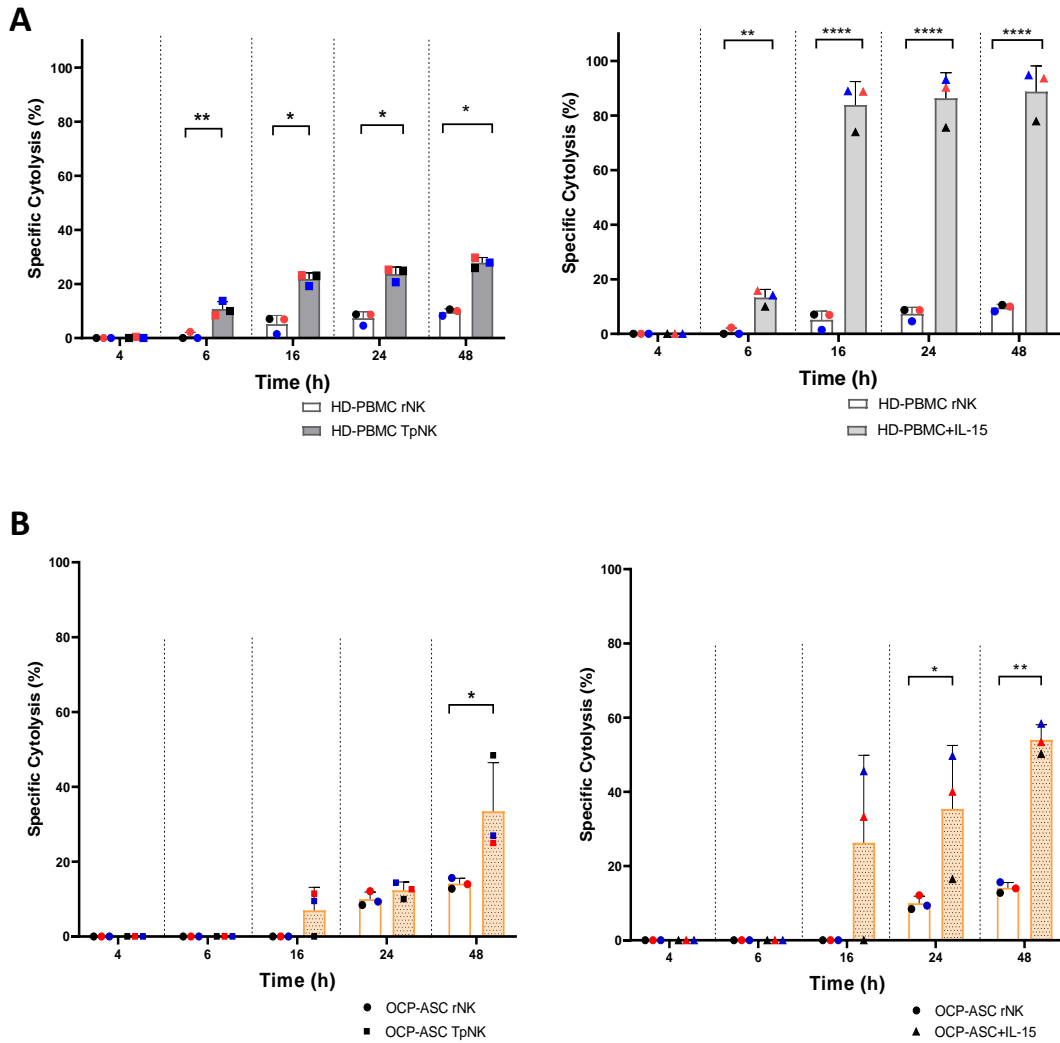
Figure 5-7: Primed-NK Cells From HD and OCP Samples Against SKOV3 Target Cells

Bar chart with individual points of donors of SKOV3 target cells specific cytolysis. rNK effector cells (white bars) and cytokine-primed NK cells or TpNK cells (coloured bars) of HD-PBMC (A) (solid colours) and OCP-Ascites (B) (dotted pattern). Cytokine priming via rhIL-15 (10ng/ml) and tumour priming via INB16 MMC treated (NK:INB16 1:2). Error bars represent SD of the mean. Statistical analysis using paired t-test. . Biological triplicates (n=3). * p<0.05, ** p<0.01, ***p<0.001, ****p<0.0001.

5.4.3 Natural Killer Cell Ligand Levels in Ovarian Cancer

The NK cell ligands frequency and expression levels and surface molecules on the surface of the ovarian cancer target cells were investigated to determine the mechanisms of action behind the enhancement of target cells lysis upon NK cell priming as well as the mechanisms behind the opposed NK cell sensitivity these ovarian cancer target cell lines exposed. This was performed in a 4h functional killing assay of E:T (5:1).

Figure 5-8 represents the percentage and expression levels on the NK cell-resistant SKOV3 ovarian cancer cell line. Control comprising of SKOV3 target cells alone without any co-interaction with the NK cell-primed effector cells was used and compared with either after co-incubation with the TpNK or cytokine-primed (rhIL-15, 10ng/ml) NK cells and results were plotted on a bar chart.

For the majority of the NK cell ligands and surface molecules, their levels were downregulated upon interaction with the primed-NK effector cells. The ULBP3, ULBP2/5/6, CD155, CD112, B7-H6, CD70 and PDL-1 percentage levels were downregulated after co-interaction with the NK-primed effector cells with statistical significance (*p<0.05) for the last four ligands abovementioned. Cytokine-primed NK effector cells resulted in reduction of expression levels of CD112 ligand from 97.73% to 83.75% (p=0.0492), B7-H6 levels from 72.20% to 41.89% (p=0.0142) and CD70 levels from 79.65% to 52.98% (p=0.0194). Although, lessened levelslower expression of the above ligands was observed, the differences were not of statistical significance. However, the PDL-1 levels on SKOV3 target cells,

were significantly downregulated in both NK cell priming conditions. Upon cytokine-primed NK effector cells, the PDL-1 levels reduced from 83.02% to 58.17% (*p<0.05; p=0.0357) and after TpNK to 60.09% (*p<0.05; p=0.0474).

On the contrary, the expression levels of CD15, CD48 and HLA-E on the SKOV3 target cells were upregulated upon interaction with the NK cell-primed effector cells with statistical significance. CD15 levels were significantly enhanced on SKOV3 cells upon exposure to the primed NK effector cells from 49.55% to 70.48% after TpNK (**p<0.01; p=0.0011) and 62.95% (*p<0.05; p=0.0103) after cytokine-primed NK effector cells respectively. Additionally, both priming conditions also significantly enhanced the expression levels of CD48 from 23.59% to 48.19% (**p<0.01; p=0.0095) with cytokine-primed NK cells and to 71.42% (***p<0.001; p=0.0003) with TpNK effector cells. The percentage of cells expressing HLA-E was significantly increased after co-incubation with the TpNK effector cells from 14.36% to 59.45% (***p<0.001; p=0.0007). Upregulation of HLA-E was also observed upon interaction with the cytokine-primed NK effector cells without, however, statistical significance.

No significant difference was observed for the MeFI expression levels of the NK cell ligands and surface molecules on the SKOV3 target cells for all the conditions tested.

Figure 5-8: NK Cell Ligand Expression Levels on SKOV3 Target Cells After Co-incubation With Primed-NK Cells

Bar chart with individual points of HD-derived donors of SKOV3 target cells before (control, light green) and after co-incubation with TpNK (light blue) and cytokine-primed NK effector (light purple) cells in E:T 5:1 in a 4h assay. Expression levels in percentage (A) and MeFI (B). Error bars represent SD of the mean. Statistical analysis using One-way ANOVA with Dunnett correction and rNK effector condition was selected as control group against each priming condition. Biological triplicates (n=3) * p<0.05, ** p<0.01, ***p<0.001.

Figure 5-9 displays the NK cell ligands and surface molecules on the NKcell-sensitive OVCAR3 ovarian cancer target cells after co-incubation with the primed NK effector cell conditions.

Both NK cell priming conditions induced significant upregulation of the ULBP-1 levels from 4.28% on OVCAR3 target cells alone to 14.62% (*$p < 0.05$; $p = 0.0218$) after co-incubation with cytokine-primed NK effector cells and 16.97% (**$p < 0.01$; $p = 0.0088$) after TpNK effector cells interaction. However, for ULBP-2/5/6 levels statistically significant downregulation was only observed upon cytokine-induced NK effector cells from 71.74% to 54.62% (*$p < 0.05$; $p = 0.0199$). Moreover, significant downregulation after OVCAR-3 co-incubation with the primed NK effector cells was seen on both CD112 and CD155 ligands of the DNAM-1 NK activating receptor. CD112 expression levels reduced from 89.59% to 75.39% (*$p < 0.05$; $p = 0.0191$) after co-incubation of OVCAR3 target cells with the cytokine-primed NK effector cells and 78.62% (*$p < 0.05$; $p = 0.0429$) upon TpNK cell interaction. The percentage of cells expressing CD155 reduced from 87.25% on OVCAR3 target cells to 30.32% (**$p < 0.01$; $p = 0.0029$) upon exposure to cytokine-induced NK effector cells and 46.89% (*$p < 0.05$; $p = 0.0150$) after TpNK co-incubation. Finally, the percentage of cells expressing CD70 was significantly reduced after exposure to primed-NK effector cells from 12.54% to 3.22% (**$p < 0.01$; 0.0019) and 6.99% (*$p < 0.05$; 0.0110) after cytokine-primed and TpNK effector cells correspondingly.

No statistical significance was observed on the MeFI levels for the aforementioned NK cell ligands and surface molecules on the OVCAR3 target cells.
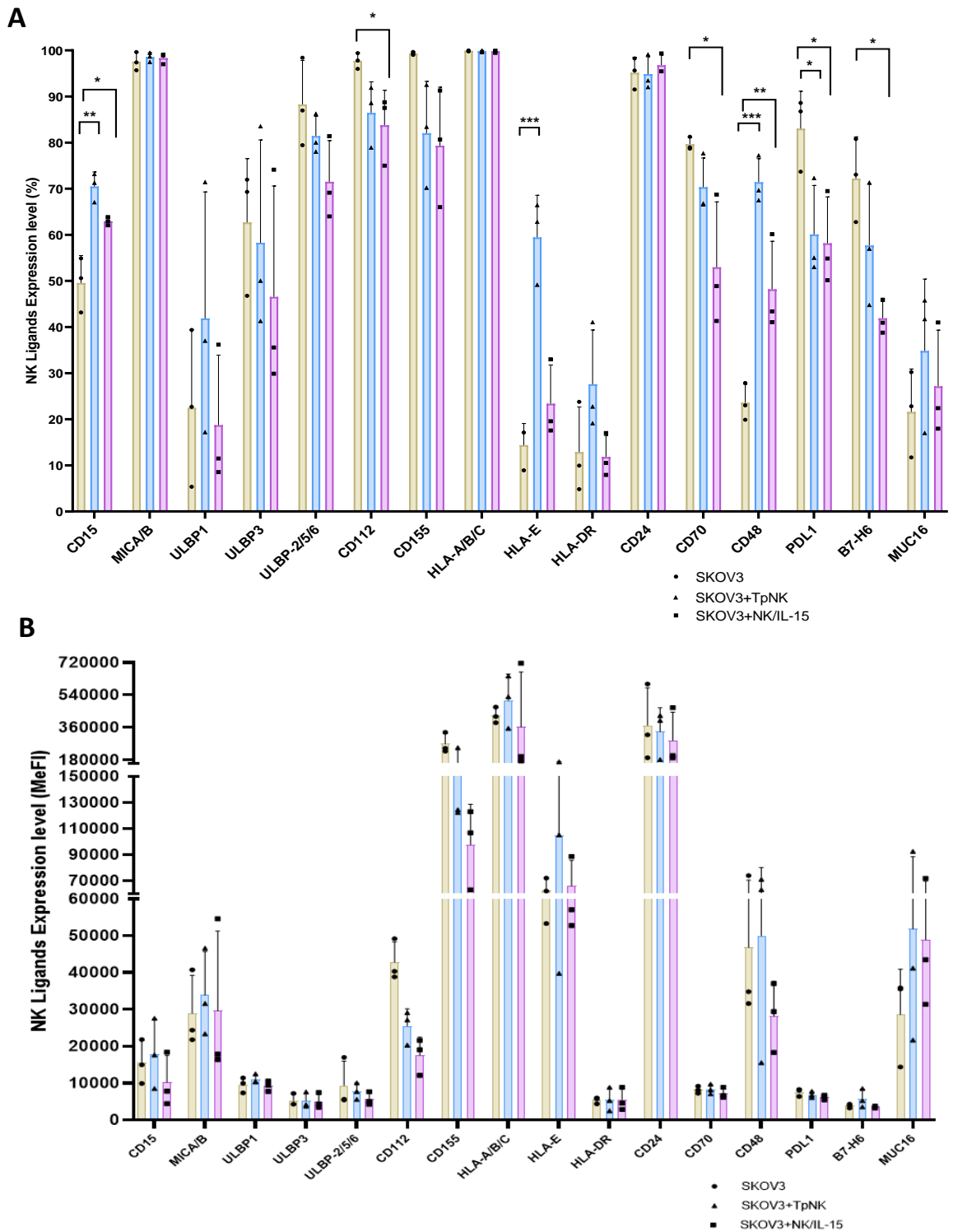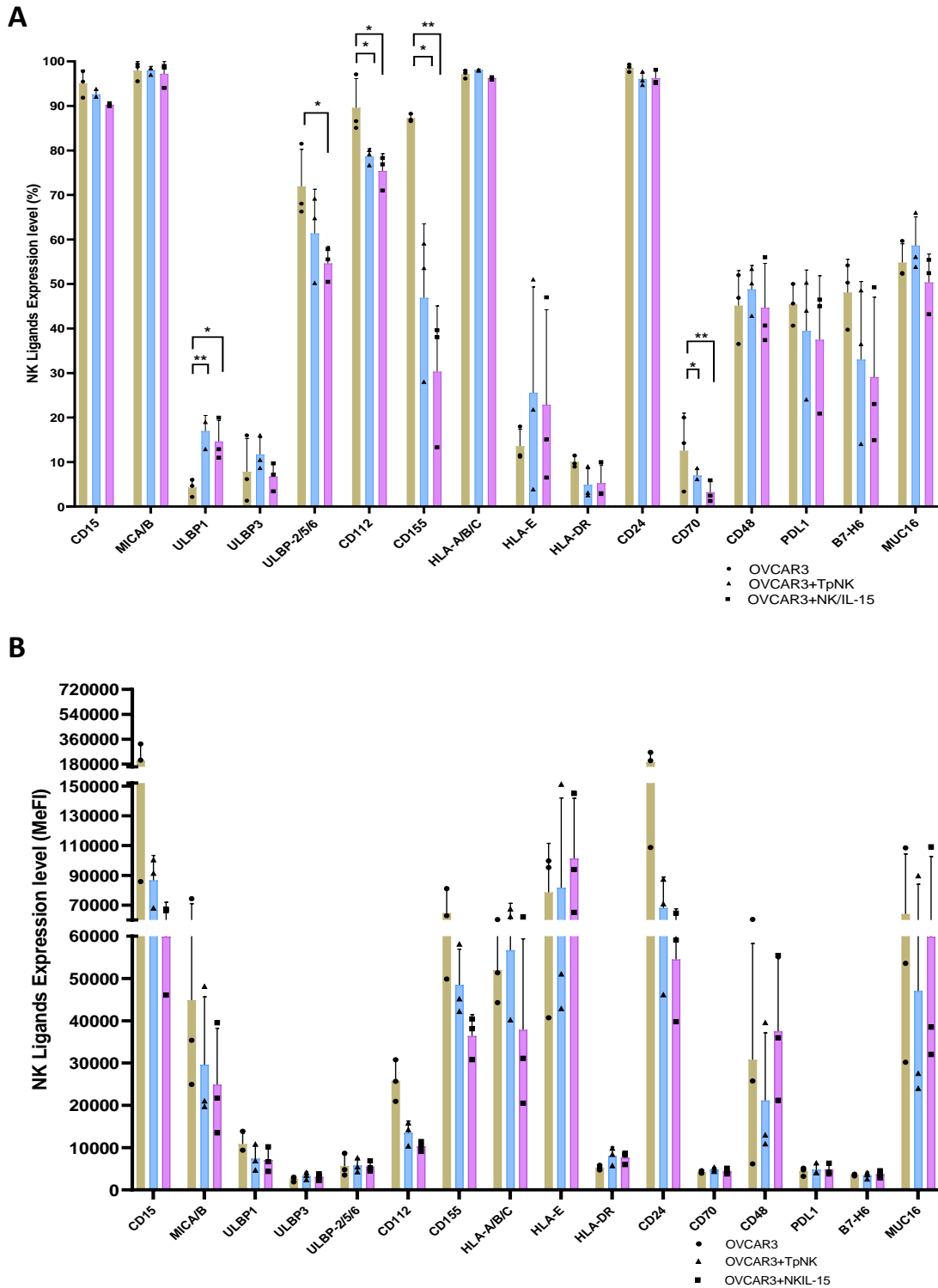
Figure 5-9: NK Cell Ligand Expression Levels on OVCAR3 Target Cells After Co-incubation With Primed-NK Cells

Bar chart with individual points of HD-derived donors of OVCAR3 target cells before (control, green) and after co-incubation with TpNK (blue) and cytokine-primed NK (purple) effector cells in E:T 5:1 in a 4h assay. Expression levels in percentage (A) and MeFI (B). Error bars represent SD of the mean. Statistical analysis using One-way ANOVA with Dunnett correction and control selected as control group against each priming condition. Biological triplicates (n=3). * $p < 0.05$, ** $p < 0.01$.

5.4.4 eSIGHT Live Cell Imaging Analysis

The eSIGHT Live Cell Imaging Analyser (Agilent) enabled the observation of interaction between the SKOV3 ovarian cancer target cell lysis upon co-incubation with three different NK effector conditions in a E:T (5:1). The effector conditions were the rNK, the cytokine-induced mediated primed NK cells (rhIL-15; 10ng/ml) and the TpNK via MMC treated INB16 (NK:INB16, 1:2). All the NK cells were pre-labelled with Cell Trace Violet (2µM) (ThermoFisher Scientific, UK), and Caspase 3/7 red reagent (ThermoFisher Scientific, UK) was added to determine the target cell lysis. All the figures display the NK cell-resistant SKOV3 target cells as the large spindle-like cells, the NK effector cells as small round violet cells and target cell death is shown as red due to the Caspase 3/7 Red Reagent.

Figure 5-10 (A-H) show the dynamic interaction between rNK effector cells and SKOV3 target cells. This figure illustrates the high numbers of recruited rNK cells against a single target cell without the ability to trigger killing (A-D). However, target cell lysis occurs once the recruited rNK cells have broken the bond between adjacent target cells, disabling the SKOV3 target cell to maintain its spindle-like phenotype and eventually go through apoptosis (E-H).
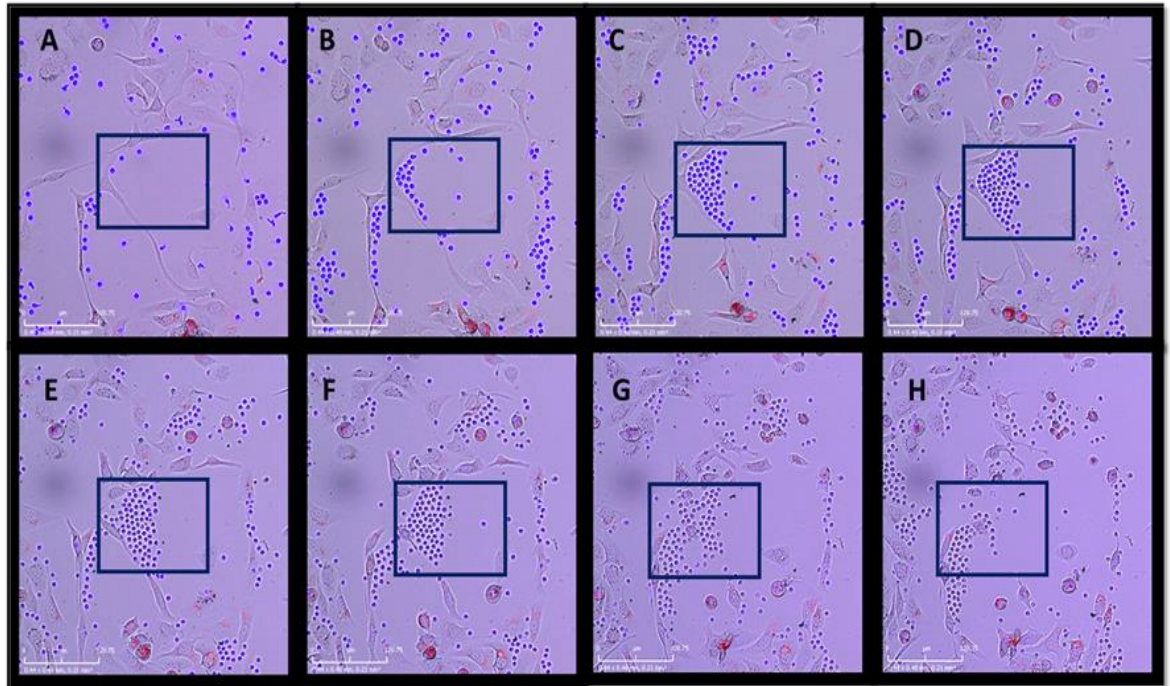
Figure 5-10: Representative images of non-primed rNK effector cells against SKOV3 ovarian target cells un eSIGHT Live Cell Imaging Analyser

Representative images from video analysis of rNK effector cells against SKOV3 ovarian cancer target cells. NK effector cells stained with Cell Trace Violet dye and target cytolysis was visualised via Caspase 3/7/ Red Reagent.

Figure 5-11 (A-H) demonstrate the interaction of cytokine-primed NK effector cells with rhIL-15 (10ng/ml) against SKOV3 target cells. Opposed to the rNK effector cells, herein, it is noticeable that fewer cells are recruited for the elimination of the SKOV3 target cells, as shown in the squares in Figure 5-11. Intriguingly, in Figure 5-11 (F-H), it is shown that even a single cytokine-primed NK cell is efficient to bind and lyse the SKOV3 target cell, as indicated by the release of Caspase 3/7 Red Reagent and the change of the cell shape towards circular phenotype before undergoing apoptosis.
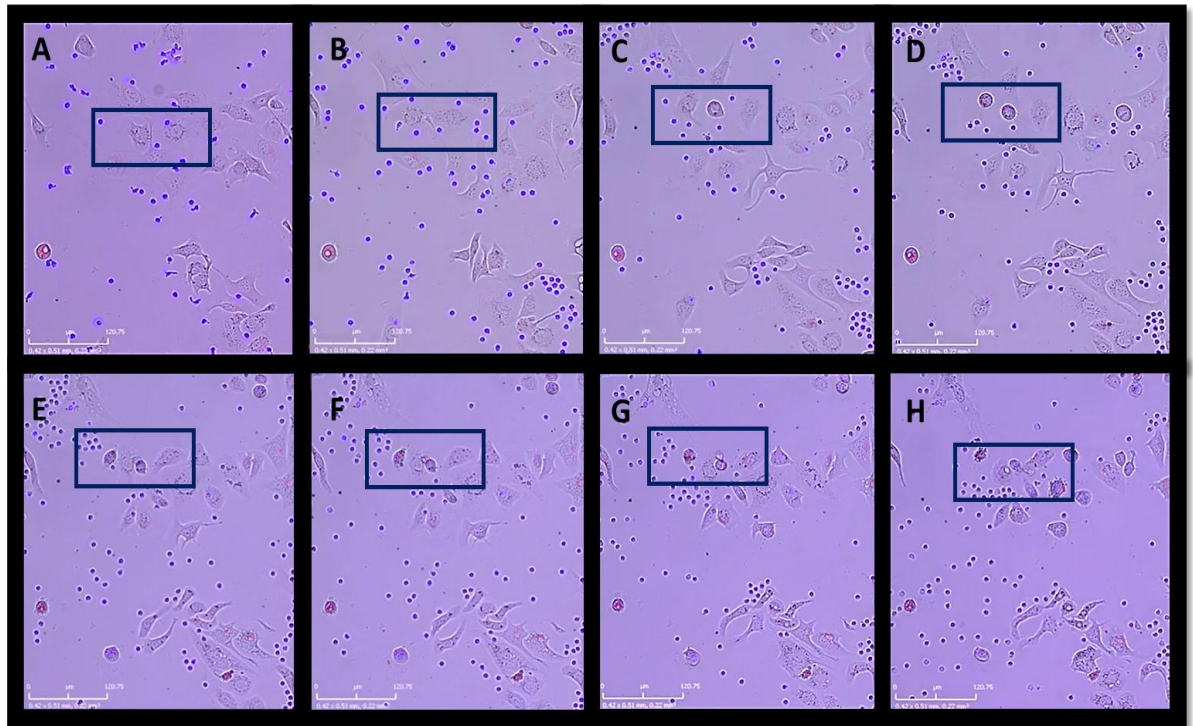
Figure 5-11: Representative images of cytokine-primed NK effector cells against SKOV3 ovarian target cells un eSIGHT Live Cell Imaging Analyser

Representative images from video analysis of cytokine-primed NK effector cells against SKOV3 ovarian cancer target cells. NK effector cells stained with Cell Trace Violet dye and target cytolysis was visualised via Caspase 3/7/ Red Reagent.

Figure 5-12 (A-H) illustrate the TpNK effector cells against SKOV3 target cells. MMC treated INB16 cells can be seen as the bigger circular cells found next to the small round Cell Trace Violet labelled NK effector cells. Similar to NK effector cells primed with rhIL-15 (10ng/ml), it involved less recruited TpNK effector cells against SKOV3 target cells compared to rNK effector cells. In this figure (from A-D) the INB16 MMC treated cells bind to the surface of the target cells and restrain their movement, allowing the TpNK effector cells to bind and trigger target cell lysis. Once the SKOV3 target cells go through apoptosis as indicated by the release of Caspase 3/7/ Red Reagent and change to a round-shaped, the INB16 MMC treated cells are detaching to move to the next target cell (E-H).
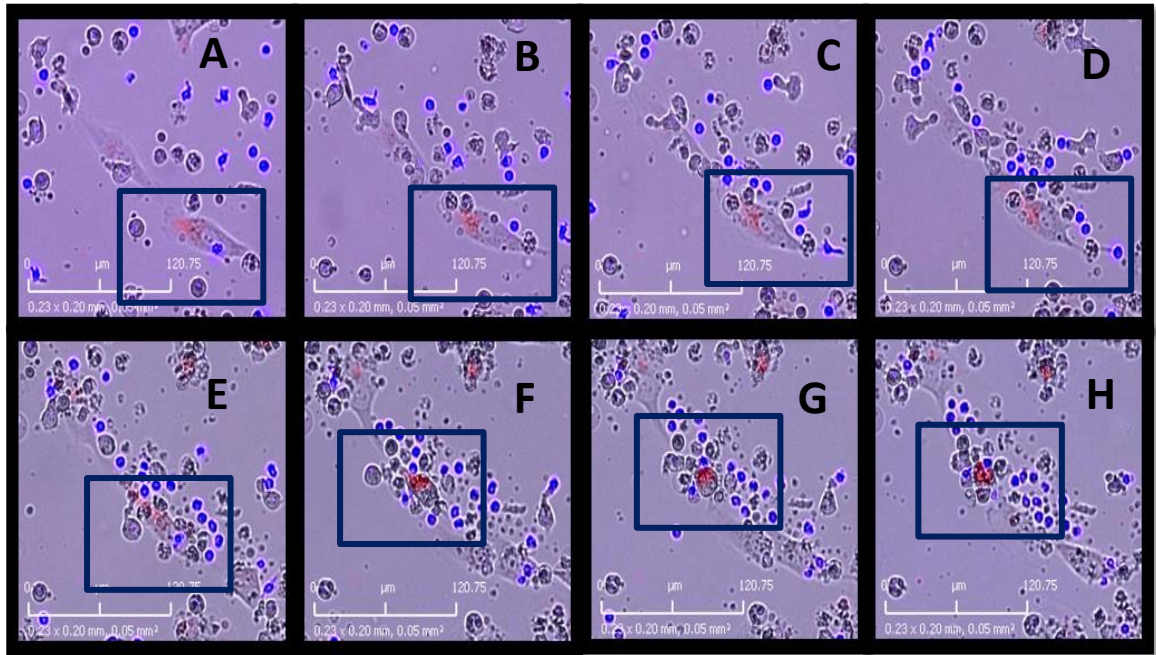
Figure 5-12: Representative images of tumour-primed NK effector cells against SKOV3 ovarian target cells un eSIGHT Live Cell Imaging Analyser

Representative images from video analysis of TpNK effector cells against SKOV3 ovarian cancer target cells. Priming agent used was the INB16 tumour target cells after MMC treatment. Priming ratio NK:INB16, 1:2. NK effector cells stained with Cell Trace Violet dye and target cytolysis was visualised via Caspase 3/7/ Red Reagent.

5.4.5 Avidity of Natural Killer Cells in Ovarian Cancer

Avidity of non-primed and primed NK cells against the NK cell-resistant SKOV3 ovarian target cell line was assessed using the z-Movi Cell Avidity Analyzer (Lumicks). Firstly, avidity of rNK cells that have been derived from different HD samples (n=3) was assessed to investigate any divergence of avidity among donors. The target cells used for this study were the NK cell-resistant SKOV3 ovarian cell line and the NK cell-sensitive K562 leukaemic cell line. NK effector cells were pre-labelled with CellTrace Far Red Dye (Invitrogen, Fisher Scientific, UK). Effector cells and target cells were co-incubated at E:T (5:1) and left for 5 minutes prior placing them onto the z-Movi Cell Avidity Analyser (Lumicks). Consequently, avidity readouts were obtained by applying acoustic force for 2,5 minutes.

Figure 5-13 indicates that avidity of rNK effector cells and target cells, is donor dependent and also that the sensitivity of the target cell to NK cell mediated lysis affects the avidity. SKOV3 target cells expressed significantly lower binding avidity against the rNK effector cells compared to the K562 targets for all the HD samples tested.
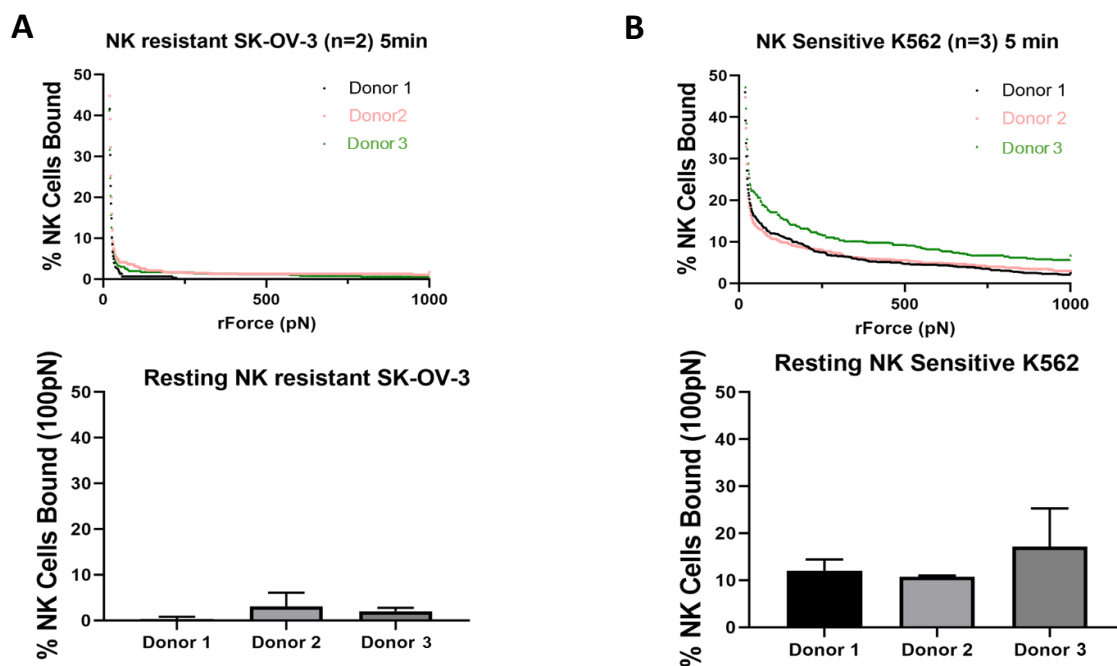
Figure 5-13: Avidity of rNK Cells Against the NK Cell-Resistant SKOV3 and NK Cell-Sensitive K562 Target Cells

SKOV3 (A) and K562 (B) target cells were seeded in the z-Movi Chip and incubated for 2h to uniformly attached at the bottom of the chip prior addition of effector cells. NK effector cells were labelled with Far Red dye. E:T (5:1), left for 5 minutes following acoustic force for 2.5 minutes for avidity readout in z-Movi Cell Avidity Analyser.

Subsequently, the avidity of primed-NK cells against NK cell-resistant cell lines was assessed. NK cells were pre-labelled with CellTrace Far Red Dye (Invitrogen, Fisher Scientific, UK) and were either cytokine-primed using rhIL-2 (10ng/ml) or rhIL-15 (10ng/ml), as well as tumour-primed using INB16 target cells pre-treated with MMC (NK:INB16, 1:2). Non-primed rNK effector cells were used as negative control and the NK cell-resistant target cells investigated were the SKOV3 ovarian tumour cells and RAJI lymphoma cells. Effector cells and target cells (E:T, 5:1) were incubated together for 5 minutes and subsequently placed on the z-Movi Cell Avidity Analyser (Lumicks) to apply acoustic force for 2,5 minutes and measure the avidity.

Figure 5-14 shows that rNK effector cells, exhibited the lowest avidity measurements against the two NK cell-resistant target cells. For SKOV3 cells, low binding avidity was similarly expressed against the cytokine-primed NK cells via rhIL-2 as these ovarian target cells display also resistance to rhIL-2 primed NK effector cells cytotoxic function. This was not observed against RAJI cells as cytokine priming of NK cells by either rhIL-2 or rhIL-15 results in comparable enhancement of NK cell killing efficacy against the RAJI target cells. Interestingly, TpNK cells demonstrated the higher avidity measurement against the SKOV3 target cells that was slightly superior than the rhIL-15 primed NK effector cells. However, this was not observed against RAJI target cells as although TpNK effector cells demonstrated prominent avidity compared to the rNK cells, its comparison with the cytokine-induced mediated NK cell priming showed lower percentage of NK cells bound to the target cells.

Overall, these results demonstrate the correlation of avidity and binding kinetics to NK cell cytotoxic responsiveness against tumour target cell lines that exhibit similar or opposed sensitivity to NK cell mediated lysis. Herein, it was the first time to show this in ovarian cancer setting.
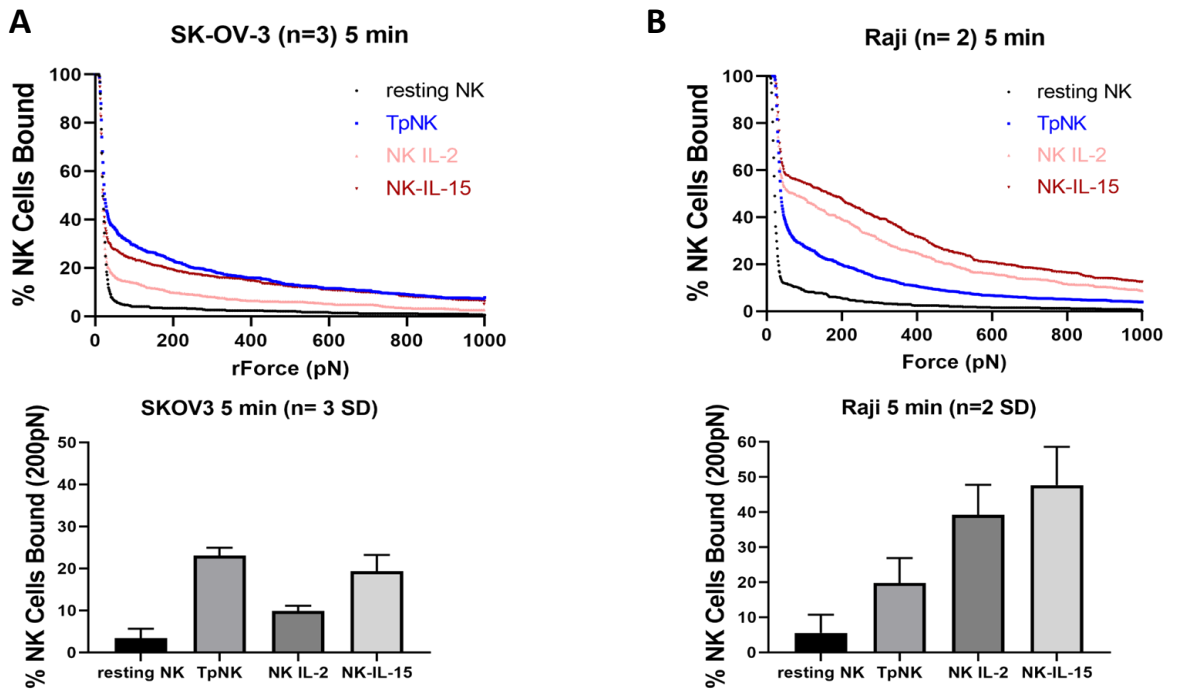
Figure 5-14: Avidity of Resting and Primed NK Cells Against the NK Cell-Resistant Target Cells SKOV3 and RAJI

SKOV3 (A) and RAJI (B) target cells were seeded in the z-Movi Chip and incubated for 2h prior addition of NK effector conditions. NK effector cells were labelled with Far Red dye. Effector conditions; NK, TpNK via INB16 pre-treated with MMC (NK:INB16, 1:2), cytokine-primed via rhIL-2 (10ng/ml) or rhIL-15 (10ng/ml). Co-incubation of E-T (5:1) for 5 minutes following acoustic force for 2.5 minutes in z-Movi Cell Avidity Analyser.

5.5 Discussion

The NK cell cytotoxicity resistance in ovarian cancer was assessed by comparing the expression levels of NK cell receptors upon co-incubation with the NK cell-resistant SKOV3 or NK cell-sensitive OVCAR3 target cells in a functional cytotoxicity assay of E:T (5:1). Subsequently, priming of NK cells by either rhIL-15 (10ng/ml) or tumour priming via INB16 MMC treated (NK:INB16, 1:2) was performed to investigate the rescue of NK cell responsiveness and NK cell lysis against the ovarian cancer target cells. Furthermore, the expression levels of the NK cell ligands on the surface of the target cells were examined after the co-interaction with the primed and non-primed NK effector cells in order to enhance the understanding on the NK cell function against these two target cell lines that expressed opposed sensitivity in NK responsiveness.

The priming effects on the NK cell receptor expression levels were evaluated to observe any variations on the surface of the NK cells before any encounter with the ovarian tumour target cells. Cytokine-primed NK cells with rhIL-15, compared to the rNK cells, resulted in upregulation on the NK activating receptors NKp30, NKp44, NKG2D as well as to the activation marker CD69, with statistical significance for the NKp44 and CD69 levels. On the other hand, downregulation of TRAIL expression levels with statistical significance as well as of the NK cell chemokine receptor CXCR4 was observed on the cytokine-primed NK cells compared to the control rNK cells.

Tumour-primed NK cells via INB16 MMC treated cells, resulted in significant downregulation of CD16, NKp46, NKG2D and TRAIL, compared to the control rNK cells. Additionally, NKp80 expression levels were lessen upon tumour priming compared to the rNK cells, without, however, statistical significance. However, tumour priming resulted in upregulation of CD57 and CD69 with statistical significance for CD69 expression levels.

After determining the expression levels of NK cell receptors and molecules upon either cytokine-induced or tumour-induced NK cell mediated priming, these expression levels were further evaluated after co-incubation with the two ovarian tumour target cell lines, SKOV3 and OVCAR3. Co-interaction of cytokine-primed NK effector cells with the ovarian cancer target cells, resulted in a comparable reduction of the NK activating receptors CD16, NKp30, NKp46, DNAM-1 as well as the adhesion molecule CD62L and TRAIL. The lessening of CD16 levels was statistical significance for both target cells compared to the control cytokine-primed NK cells that were not co-incubated with the targets. On the contrary, the only marker that was upregulated with statistical significance upon target co-incubation with either cell line, was the CD69 activation marker. No differences were observed for any of the other NK receptors.

Tumour-primed NK effector cells were co-incubated with the NK cell-resistant SKOV3 target cell line in an endeavour to overcome the NK cell function impairment using an alternative priming agent compared to the cytokines. Co-interaction of TpNK effector cells and SKOV3 cells in significant upregulation of the NK activating receptor NKp80 and the NK

inhibitory receptor KIR2DL1, compared to the TpNK effector cells without any co-interaction with target cells. On the contrary, downregulation of the NKp44 and CD62L of TpNK effector cells after co-incubation with SKOV3 target cells was observed, compared to the control TpNK cells. This reduction of NK activating receptor levels on the surface of NK cells upon tumour priming was also reported in Sabry *et al* (2019) study (Sabry *et al.*, 2019).

In addition, the levels of the NK cell ligands and surface molecules on the SKOV3 and OVCAR3 ovarian cancer cells were also assessed after co-incubation with the primed-NK effector cells. The CD15 and CD48 levels after co-incubation with the SKOV3 target cells were significantly upregulated for both types of primed-NK cells. Additionally, TpNK resulted in upregulation of HLA-DR and HLA-E with statistical significance for the HLA-E levels. On the contrary, reduction of ULBP3, ULBP-2/5/6, CD112, CD155, CD70, PDL-1 and B7-H6 was observed on the surface of SKOV3 target cells after co-incubation with the primed NK effector cells, compared to the control SKOV3 target cells. This decrease was significant for the CD112, CD70 and B7-H6 NK cell ligands, after co-interaction with the cytokine-primed NK effector cells, whereas HLA-E lessen levels were significant after SKOV3 co-interaction with the TpNK effector cells. The PDL-1 levels were significantly reduced after co-interaction with either of the primed-NK effector cells.

Moreover, the expression levels of the NK ligands and surface molecules on the NK cell-sensitive OVCAR3 ovarian cancer target cells resulted in significant upregulation of the ULBP1 NK cell ligand after co-incubation with either TpNK or cytokine-primed NK effector cells compared to

the control OVCAR3 target cells alone. On the contrary, significant reduction on the OVCAR3 target cells was observed on the CD112, CD155 and CD70 levels after co-interaction with either type of primed-NK effector cells. Down-modulation of ULBP-2/5/6 was also observed, however it was only statistically significant after OVCAR3 interaction with the cytokine-primed NK effector cells.

Comparison between the two ovarian cancer target cells, showed that the NK cell-sensitive OVCAR3 target cell line, opposed to the NK cell-resistant SKOV3 cells did not express differences on the expression level of CD15, ULBP-3 and CD48 in all of the three effector conditions co-incubated with the target cells compared to the control target cells alone. Upregulation was only observed in ULBP-1 and HLA-E ligands in similar levels for all effector conditions against the OVCAR3 target cells compared to SKOV3 cells that this upregulation was only observed upon co-incubation with TpNK effector cells. In addition, OVCAR3 cells exposed downregulation of HLA-DR ligand opposed to the SKOV3 target cells specifically upon primed both cytokine-induced and tumour-induced NK effector cells co-incubation.

Similar to SKOV3, OVCAR3 target cells exhibited downregulation of CD70 as well as of the DNAM-1 ligands CD112 and CD155, especially for the CD155, after co-interaction with the cytokine-primed NK effector cells. Additionally, PDL-1 and B7-H6 were also downmodulated similarly after co-incubation with either rNK or primed NK effector cells. Finally MUC16 expression levels on OVCAR3 target cells, were similar between the control target cells alone and the primed NK cells. However comparison of OVCAR3

target cells alone with the non-primed rNK effector cells, resulted in downregulation of MUC16 levels.

Overall, priming of NK cells resulted in augmented NK cell cytotoxicity efficacy in both NK cell-resistant and NK cell-sensitive cell lines. In this project, the NK effector cells were either cytokine-primed using rhIL-15 or tumour-primed using INB16 MMC treated (NK:INB16, 1:2) tumour cells.

Tumour-mediated priming, showed greater efficacy on the NK cell-resistant cell lines. This might be reliant on the priming mechanism of NK:INB16 interaction in which the CD15 on the INB16 tumour cells conjugate with CD2 on the NK cells. The NK cell-sensitive OVCAR3 ovarian cell line was shown here to express significantly higher levels of CD15 compared to the NK cell-resistant SKOV3 ovarian cancer cells which might interfere and compete with INB16 for NK cell contact and subsequently impairment in the priming and killing functions of the NK effector cells. Tumour priming of NK cells has been previously reported by North *et al* (2007) and Pal *et al* (2017) using CTV-1 or NALM-16 leukaemic tumour cell lines respectively as priming agents (North *et al.*, 2007; Pal *et al.*, 2017).

Herein, the TpNK cells using the leukaemic cell line INB16, resulted in enhanced SKOV3 tumour target cell lysis with statistical significance compared to the control rNK effector cells from 6h of E:T co-interaction onwards. The significant enhancement of target cell lysis after tumour-mediated NK cell priming from HD-derived NK cells, was observed in both ovarian cancer target cells for almost all the timepoints tested. However,

TpNK effector cells derived from OCP-Ascites samples, only displayed statistical significance at the late timepoints for SKOV3 target cells whereas no significance was observed for any of the timepoints tested against OVCAR3 target cells.

In conclusion, tumour priming of NK cells using the leukaemic cell line INB16 that had been previously MMC treated, displayed significant enhancement on lysis of the NK cell-resistant SKOV3 tumour target cells compared to the control rNK cells. Herein, it was the first time that TpNK cells were used to significantly overcome the NK cell cytotoxicity impairment and resistance in ovarian cancer. Following the aforementioned results, INB16 tumour priming agent, can be lucratively used in NK cell based immunotherapy in ovarian cancer without the restrictions and limitations of NK cells primed using rhIL-15. These include the cytotoxicity levels upon administration and the dependency of IL-15 cytokine to maintain the enhance NK cell responsiveness upon priming. On the contrary, CD2:CD15 expression levels that are required for the tumour priming were shown here that remain stable.

Chapter 6   Effects of the Hypoxic Tumour Microenvironment on Natural Killer Cells in Ovarian Cancer

6.1 Introduction

6.1.1 Hypoxic Tumour Microenvironment

Hypoxia is a prominent feature of the tumour microenvironment. During tumour development, there is inadequate oxygen and nutrients supply due to poor vascularisation of the growing cancer mass. The tumour and stromal cells can adapt to the hypoxic TME through regulation of the hypoxia-inducible factors (HIFs). This family entails three members; HIF-1, HIF-2 and HIF-3. These factors include an additional oxygen sensitive α-subunit (HIF-1α, HIF-2α and HIF-3α) which dimerises with the constitutively expressed HIF-1β. The HIF-1α and HIF-2α are the best studied among the α-subunit members. They are both regulated by oxygen-dependent hydroxylation and share structural similarities in their DNA-binding and dimerisation domains but differ in their transactivation domains. However, HIF-3α lacks the transactivation domain and may function as an inhibitor of HIF-1α and HIF-2α (Rankin & Giaccia, 2008).

Hypoxia induces impairment of the NK cell function via downregulation of the major activating NK receptors (NCRs and NKG2D). Although hypoxia affects NK cell natural cytotoxicity, the ADCC mechanism remains intact as

the expression levels of CD16 molecule was shown to be stabled even upon hypoxic conditions (Balsamo *et al*., 2013). A recent study by Parodi *et al* (2018) have demonstrated that hypoxia not only impaired the NK cell cytotoxicity, but also, alters the transcriptome, immunoregulation and migration properties of NK cells in the TME (Parodi *et al*., 2018). Reports from Sarkar *et al* (2013) and Velásquez *et al* (2018) had demonstrated that cytokine priming of NK cells using IL-2 or IL-15 overcomes the adverse effects of hypoxia on the NK cell function *in vitro* (Sarkar *et al.,* 2013; Velásquez *et al.,* 2016).

6.1.2 Natural Killer Cell Priming in Ovarian Cancer Tumour Microenvironment

The NK cell function impairment in the ovarian cancer TME, is a result of an orchestrating network consisting of the growing tumour mass, the ascites, the inhibitory immune cells such as MDSCs and Tregs and the secreted immunosuppressive cytokines including IL-10, TGF-β and IL-6. All these can alter NK cell function in different approaches. The production of the immunosuppressive cytokines can cause NK cell impairment both directly and indirectly via dysfunction of DCs which are required for the sufficient activation of NK cells (Nersesian *et al*., 2019).

Priming of NK cells, from ovarian cancer patients, via cytokines such as IL-12, IL-15 and IL-21 has demonstrated enhanced activation and NK cell cytotoxicity (Nersesian *et al*., 2019). However NK cells derived from ovarian cancer patient ascitic fluid, showed reduced response to IL-2 stimulation

primarily upon the presence of malignant cells in the ascites(da Silva *et al.*, 2017).

However, effects of hypoxia in TpNK cells against ovarian cancer, has not yet been investigated. In this chapter, functional killing assays using SKOV3 and OVCAR3 ovarian cancer target cells were conducted using non-primed (rNK), TpNK and cytokine-primed NK cells using rhIL-15 (10ng/ml) in both normoxia (21% O_2) and hypoxia (1% O_2).

6.1.3 Aims

The aims of this Chapter were:

(i)   To determine the effects of hypoxia (1% O_2) on rNK cell cytotoxicity against the NK cell-sensitive ovarian cancer cell line (OVCAR3) using HD-PBMC and OCP-Ascites samples. K562 target cells were used as control;

(ii)   To investigate the effects of NK cell priming in overcoming the NK cell function impairment of the hypoxic TME from HD-derived NK cells, in ovarian cancer against OVCAR3 and SKOV3 target cells. K562 and RAJI target cells were used as controls;

(iii)   To identify the NK cell priming in overcoming the NK cell function impairment of the hypoxic TME from OCP-derived NK cells, against OVCAR3 and SKOV3 target cell lines. K562 and RAJI target cells were used as controls.

6.2 Methods

6.2.1 Oxygen and Temperature Validation

The oxygen and temperature inside the vessels that were used for the experiments in this Chapter, were validated using the Fibox 4 single channel fiber optic oxygen transmitter (PreSens Precision Sensing). The vessels used were FACS tubes for the K562 and RAJI target cells and 96-well plates for the ovarian cancer target cells, SKOV3 and OVCAR3. A self-adhesive oxygen-sensitive spot (3mm diameter), was placed at the bottom of either vessel and 200µl or 100µl of corresponded culture medium was added to FACS tube and 96-well plate respectively to mimic the volume of the target cells addition. Subsequently, the vessels were placed into a multigas culture incubator that allows oxygen regulation via nitrogen gas purge (MCO-170M-PE, phcbi). The hypoxic conditions were set to 1% O_2, 5% CO_2, 37°C. The oxygen fibre optic sensor (type PSt3) and the temperature sensor (Pt100) were connected to the Fibox 4 whereas the other end of the sensors were placed inside the hypoxic incubator. The PSt3 was securely placed below the oxygen-sensitive spot and measurements were taken every 30 minutes. The next day, the vessels were removed from the hypoxic conditions and additional hypoxic culture medium was added to mimic the addition of effector cells for the cytotoxic assay. For FACS tubes 300µl were added (500µl total) and for the 96-well plate 100µl were added (200µl total). Finally the vessels were placed back into the hypoxic culture incubator and oxygen and temperature measurements continued with 30 minutes

intervals. Results were exported to the PreSens software to allow acquisition and analysis of the data.

6.2.2 Isolation of Natural Killer Cells

The NK cells from HD were derived from leucocyte cones or heparinised blood of healthy volunteers. The PBMCs from either starting material, were isolated as described in Chapter 2, section 2.2.1 and purity was assessed via immunophenotyping as described in section 2.2.3. The viability was also determined using TO-PRO-3 viability dye (ThermoFisher Scientific,UK).

6.2.3 Natural Killer Cell Cytotoxic Assay in Hypoxia against K562 and RAJI Target Cells

The K562 and RAJI cells were firstly fluorescently labelled using the PKH67 cell membrane dye (Sigma-Aldrich) as described in section 2.3.1.1. The PKH67-labelled target cells were resuspended at 0.2×10^6/ml in supplemented culture medium and were transferred into two 13ml polypropylene tubes. The first one was incubated in normoxic conditions (21% O_2, 5% CO_2, 37°C) and the second one in hypoxic conditions (1% O_2, 5% CO_2, 37°C) and left o/n.

The NK cell effector conditions include the non-primed rNK cells, the cytokine-mediated primed (rhIL-15, 10ng/ml) and the tumour-mediated primed NK cells via pre-treated INB16 cells (NK:INB16, 1:2). Subsequently, the NK effector cells were resuspended in a final volume of 200µl, transferred

in FACS tubes and incubated o/n in either normoxia or hypoxia prior addition to the corresponded cancer target cells.

The next day, viability of the PKH67-labelled target cells and NK cells was confirmed using TO-PRO-3 viability dye and 200µl of the target cells were transferred to the FACS tubes containing the corresponding effector conditions at a ratio E:T 5:1. The hypoxic PKH67-labelled target cells were transferred to the hypoxic effector cells whereas the normoxic PKH67-labelled target cells to the normoxic effector cells. 100µl of supplemented culture medium (either hypoxic or normoxic) was added to all the corresponded tubes to achieve a final volume of 500µl and the FACS tubes were transferred back to either normoxic or hypoxic incubators. The cytotoxic assay was measured after 4h, 6h and 16h in flow cytometry using TO-PRO-3 viability dye. This assay was performed for total of 5 biological replicates for both HD-derived and patient-derived samples in technical duplicates.

6.2.4 Natural Killer Cell Cytotoxic Assay in Hypoxia Against Ovarian Target Cancer Cells

The NK cell cytotoxic assay for the adherent epithelial ovarian cancer target cell lines, SKOV3 and OVCAR3 was performed in the xCELLigence RTCA system (Agilent) as described in section 2.3.2.1. The target cells were passaged the day before the experiment. The next day, target cells were harvested and resuspended in the corresponded supplemented culture medium at 0.1×10^6/ml and 0.2×10^6/ml for SKOV3 and OVCAR3

respectively. After conducting the background measurements on the e-plates using the corresponded supplemented culture medium (50µl), target cells were seeded (50µl) and left in the tissue culture cabinet for 30 minutes at RT. Two plates were used for this assay as one was placed in the xCELLigence RTCA system (Agilent) in normoxia (21% O_2, 5% CO_2, 37°C) and the second in the xCELLigence RTCA system (Agilent) in hypoxia (21% O_2, 5% CO_2, 37°C) so the assay in the two different oxygen concentrations could be performed in parallel. Finally the target plates were left o/n at the appropriate cell culture incubator.

For all the aforementioned conditions, NK effector cells were resuspended at a final volume of 100µl in 0.5×10^6/ml for the SKOV3 target cells and 1×10^6/ml for OVCAR3 target cells to achieve the E:T 5:1 and left o/n in either in normoxia or hypoxia.

The next day, 100µl of the appropriate NK effector conditions were added to the corresponded target cell wells in either normoxia or hypoxia and the assay was measured every 15 minutes for a duration of 48h. Finally, five timepoints, 4h, 6h, 16h, 24h and 48h were selected to analyse and plot the results. This assay was performed for a total of 3 biological replicates for both HD-derived and OCP-derived samples in technical triplicates.

6.2.5 Statistical Analysis

A two-tailed paired t-test was used to compare rNK and cytokine-primed NK effector conditions against the NK cell-sensitive cell lines K562 and OVCAR3 target cells from HD or OCP samples.

One-way ANOVA and Dunnett's multiple comparisons follow up test with rNK cells as the control column was performed to compare the two different NK priming conditions (tumour or cytokine mediated NK cell priming) with the non-primed control rNK cells against the NK cell-resistant RAJI and SKOV3 target cell lines.

The p-value was determined as $*p \leq 0.05$, $**p \leq 0.01$, $***p \leq 0.001$ and $****p \leq 0.0001$ (GraphPad Prism 9.0.0).

6.3 Results

6.3.1 Oxygen and Temperature Validation Under Hypoxic Conditions

The effect of hypoxia (1% O_2) on the NK cell cytotoxic function was tested using K562, RAJI, SKOV3 and OVCAR3 cancer target cell lines. The K562 and RAJI target cells were incubated in FACS tubes, whereas the ovarian cancer cell lines, SKOV3 and OVCAR3 were placed in 96-well plates. The oxygen and temperature inside these vessels were validated using the Fibox 4 single channel fibre optic oxygen transmitter (PreSens Precision Sensing) prior the experiments and measurements were recorded every 30 minutes. This was performed to

confirm that the NK cell cytotoxic assays were acquired under a pre-determined hypoxic environment of 1% O_2.

Firstly, the equivalent amount of supplemented culture medium was added to each vessel to mimic the addition of target cells (200µl for FACS tube and 100µl for 96-well plate). The oxygen measurements demonstrated that the culture medium inside the vessels had successfully reached 1% O_2 and maintained a temperature of 37°C after o/n incubation. Figure 6-1 (A & B). Subsequently, an equal amount of culture medium was added to each vessel to mimic the addition of the effector cells and the final volume (300µl for FACS tube and 100µl for 96-well plate). This validation was performed for a total of 24h.

For the FACS tube, the oxygen level increased to 4.2% and temperature dropped to 36°C after the second addition (Figure 6-1A). The oxygen concentration reached 1% after 4h and temperature was back to 37°C after 2.5h (Figure 6-1A).

For the 96-well plate, the oxygen level increased to 5.2% and fell back to 1% after 3.5h. The temperature remained relatively stable, as it dropped to 36.6°C and was steadied to 37°C after 1h (Figure 6-1B).
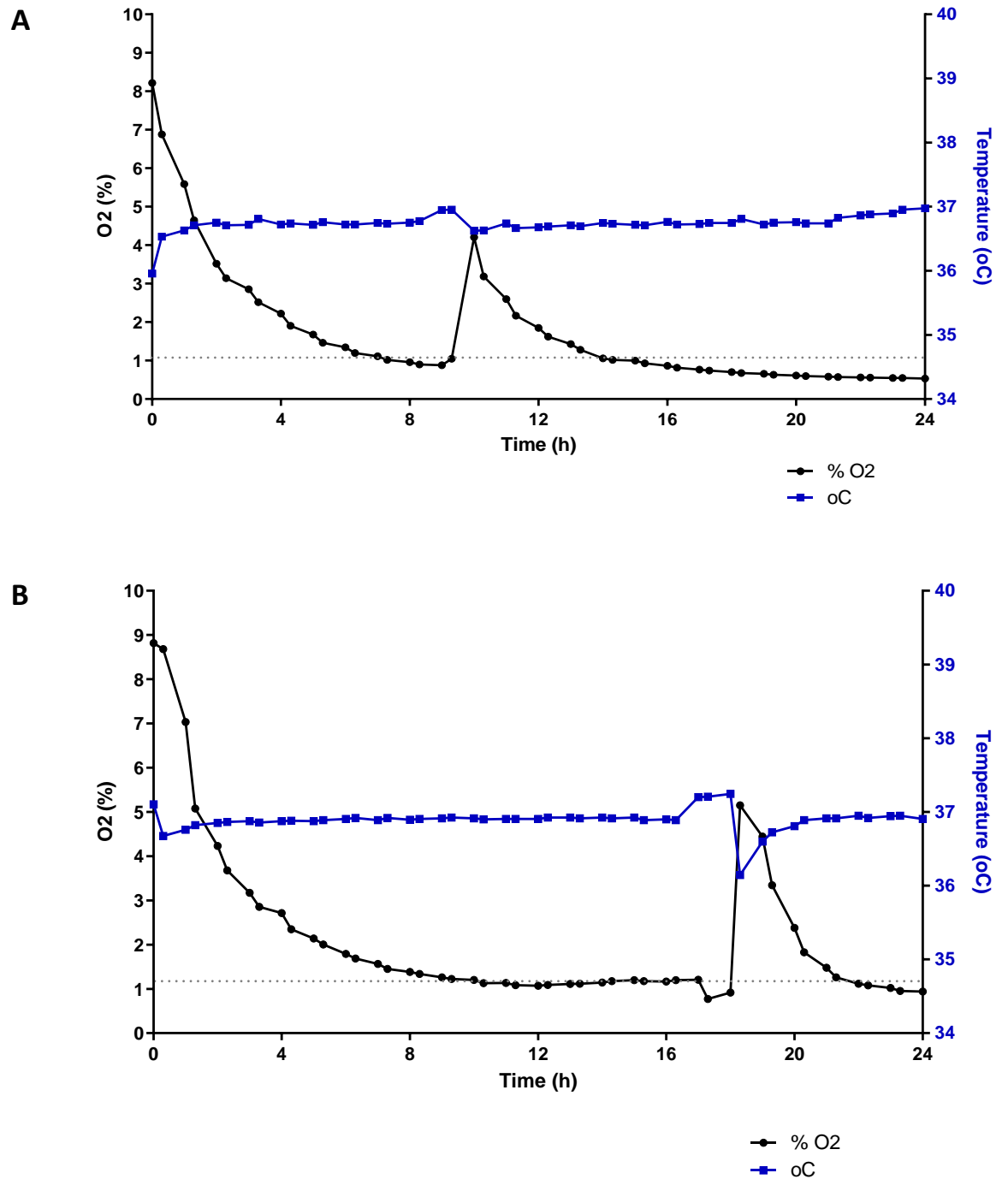
Figure 6-1: Oxygen Levels and Temperature Validation for Hypoxic Experiments

The oxygen level in FACS tubes (for K562 and RAJI experiments) (A) and 96-well plate (for SKOV3 and OVCAR3 experiments) were validated the Fibox 4 single channel fibre optic oxygen transmitter.

6.3.2 Hypoxic Functional Killing Assay of rNK Effector Cells Against OVCAR3 Ovarian Cancer Target Cells

The NK cell-mediated cytotoxicity impairment under hypoxia (1% O_2) was assessed for both HD- and OCP-derived samples. For this study, non-primed (resting) HD-PBMC and OCP-Ascites samples were used as effector cells in E:T (5:1) against the OVCAR3 NK cell-sensitive ovarian cancer target cell line. The xCELLigence RTCA system was used to measure the target cell lysis in a non-invasive continuous readout and the timepoints selected and plotted were after 6h, 16h, 24h and 48h.

Figure 6-2 illustrates a bar chart showing symbols of individual donors of non-primed rNK effector cells derived from HD-PBMC samples (A) and OCP-Ascites samples (B) under normoxic (solid bars) and hypoxic (pattern bars) conditions.

Figure 6-2A shows the hypoxic effects on the cytotoxicity function of rNK effector cells derived from HD-PBMC samples against the NK cell-sensitive OVCAR3 ovarian target cells after 4h, 6h, 16h, 24h and 48h of co-incubation. Reduction of target cell lysis was observed in hypoxia compared to normoxia for all the aforementioned timepoints, with statistical significance after 6h onwards. After 6h the OVCAR3 specific cytolysis decreased from 32.57% to 18.21% (*p<0.05; 0.0294). After 16h the target cell lysis dropped from 60.95% in normoxia to 43.73% in hypoxia (**p<0.01; 0.0043). After 24h the percentage of target cell specific cytolysis dropped from 68.98% to

59.30% upon hypoxia (**p<0.01; 0.0085) and from 82.47% to 61.68% after 48h in hypoxia (*p<0.01; 0.0410).

Figure 6-2B displays the comparison of rNK effector cells derived from OCP-Ascites samples in normoxia and hypoxia against the OVCAR3 target cell line. Opposed to HD samples in Figure 6-2A, hypoxic conditions enhanced the target cell lysis compared to normoxia for all the timepoints. This increase of OCP-derived NK cells in hypoxia was statistically significant for the two last timepoints with *p<0.05 (p=0.0488 after 24h and p=0.0446 after 48h). Comparison of the average percentages of OVCAR3 specific cytolysis for these timepoints were 13.74% in normoxia and 40.75% in hypoxia after 24h and 23.29% in normoxia and 50.25% in hypoxia after 48h of E:T co-incubation.

No statistical significance was observed on the previous two timepoints despite the enhanced NK cell function under hypoxia, due to the heterogeneity of patient samples. Interestingly, for one OCP-derived sample (red symbol), the NK cell killing efficacy was completely impaired under normoxia, whereas the same OCP donor exposed the highest OVCAR3 target cell cytolysis in hypoxia, for all the 3 donors tested throughout all the timepoints plotted. The average percentage of OVCAR3 specific cytolysis after 6h was 4.78% in normoxia and 26.04% in hypoxia and after 16h it was 7.11% and 37.70% in normoxic and hypoxic conditions correspondingly.
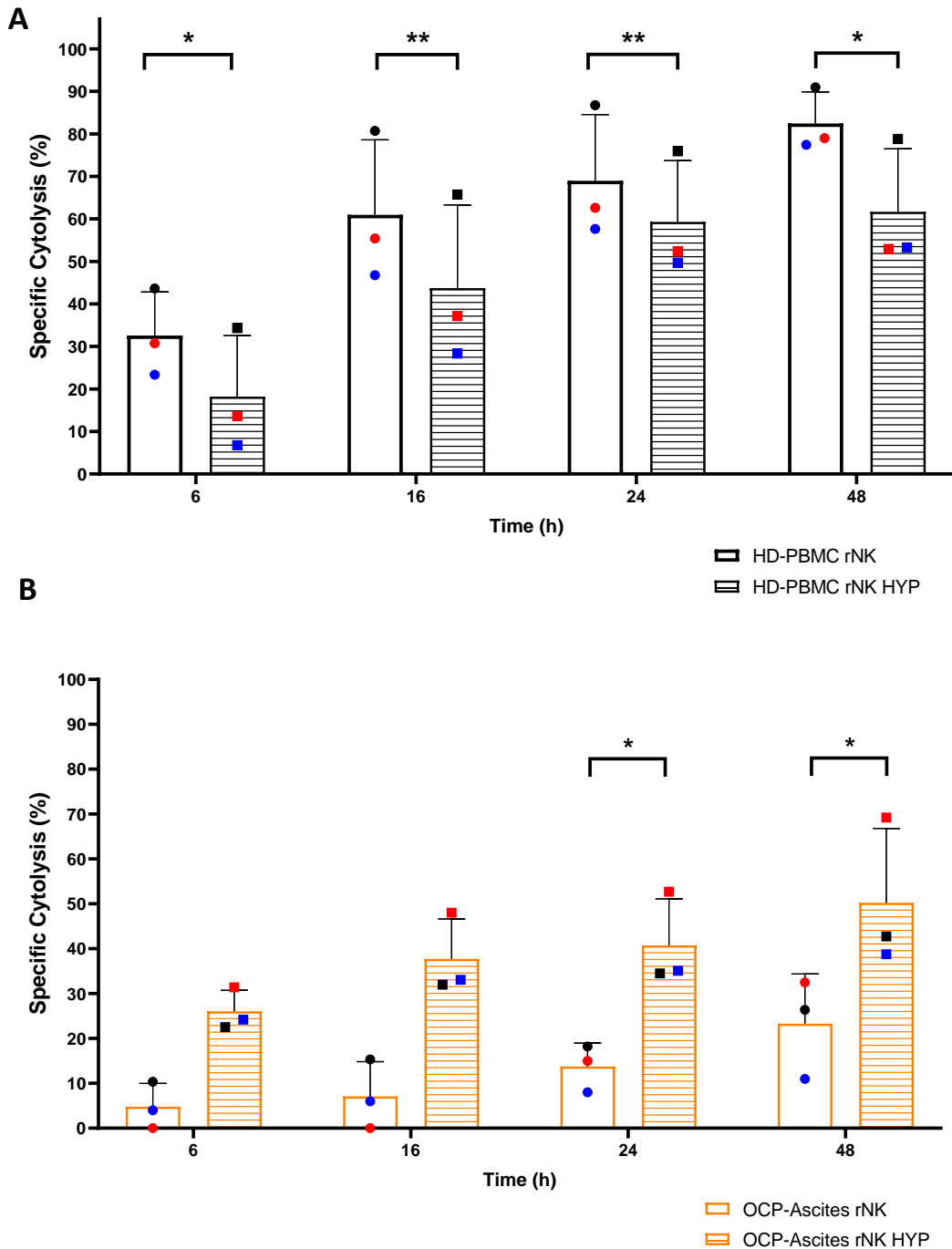
Figure 6-2: rNK Cells against OVCAR3 Ovarian Cancer Cells in Normoxia and Hypoxia

Bar chart with individual points of Non-primed NK effector cells derived from PBMC samples of HD (A) and Ascites from ovarian cancer patients (B) against the NK cell-sensitive OVCAR3 ovarian cancer target cell line, E:T (5:1). Error bars represent the SD of the mean. Statistical analysis using paired t-test between normoxia (21% O_2) vs hypoxia (1% O_2) of the same sample origin for each timepoint (4h, 6h, 16h, 24h and 48h). Biological triplicates (n=3). * $p < 0.05$, ** $p < 0.01$.

6.3.3 Cytokine Primed-NK Cells in Hypoxia Against OVCAR3 Target Cells

After identifying the effects of the hypoxic environment on the killing efficacy of non-primed rNK cells from HD-derived and OCP-derived samples, the NK effector cells were cytokine-primed via rhIL-15 (10ng/ml) to examine the restoration of NK cell function in hypoxia for HD samples and the enhancement of killing efficacy for OCP-derived samples in hypoxia against the OVCAR3 target cell line. The E:T was 5:1 for these experiments and the functional killing assays were performed in parallel in normoxia (21% O_2. 5% CO_2, 37°C) and hypoxia (1% O_2. 5% CO_2, 37°C). The xCELLigence RTCA system was used to measure the target cell lysis in a non-invasive continuous readout and the timepoints selected and plotted were after 6h, 16h, 24h and 48h.

Figure 6-3 illustrates a bar chart with symbols of individual donors the effects of cytokine priming of NK effector cells derived from HD-PBMC samples (A) and OCP-Ascites samples (B) in both normoxia (solid bars) and hypoxia (pattern bars) against the control rNK effector cells after 6h, 16h, 24h and 48h of E:T interaction.

Figure 6-3A represents the effects of the different oxygen conditions of cytokine primed NK effector cells derived from the HD-PBMC samples. There was significant increase of OVCAR3 target cell lysis upon cytokine priming in hypoxia for all the timepoints tested. After 6h the average percentage of target cell lysis in hypoxia increased from 18.21% to 95.61% on cytokine-

primed NK effector condition (**p<0.01; p=0.0098). This enhancement was comparable to normoxic conditions (**p<0.01; p=0.0079) where the average percentage of OVCAR3 lysis increased from 32.57% for rNK effector cells to 98.50% after cytokine priming.

For the last three timepoints, cytokine-primed NK effector cells improved significantly the percentage of OVCAR3 specific lysis only under hypoxic environment with *p<0.05 (16h from 43.73% to 99.85%, p=0.0379; 24h from 59.30% to 99.98%, p=0.0394 and 48h from 62.68% to 100%, p=0.0464).

Figure 6-3B shows the effects of cytokine-primed NK effector cells upon hypoxia from OCP-Ascites derived samples. Similarly to the effects of hypoxia on the cytotoxic function of non-primed rNK cells described in Figure 6-2B, cytokine-mediated NK cell priming, was superior under hypoxic environment compared to normoxia. Cytokine-primed NK effector cells in normoxic condition resulted in similar levels ofOVCAR3 target cell lysis except for the last timepoint of 48h where the percentage of specific cytolysis by cytokine-primed NK effector cells improved from 22.95% to 58.43%. No statistical significance was observed for all the timepoints due to variation of responses from the OCP donors.

Intriguingly, although cytokine mediated priming on the NK effector cells in normoxia, resulted in higher OVCAR3 target cell cytolysis, it exhibited lower target cell lysis compared to both rNK and cytokine-primed NK effector

conditions in hypoxia. Only after 48h the normoxic cytokine-primed NK effector cells expressed higher killing efficacy compared to the rNK cells in hypoxia but did not exceed the cytotoxicity improvement of hypoxic cytokine-primed NK cells for all the timepoints.

In hypoxia, an improvement of OVCAR3 specific cytolysis was followed upon cytokine priming compared to the control rNK effector cells throughout all the timepoints for all the OCP donors. No statistical significance was observed due to the heterogeneity of cytokine induced responses to the individual patient donors.
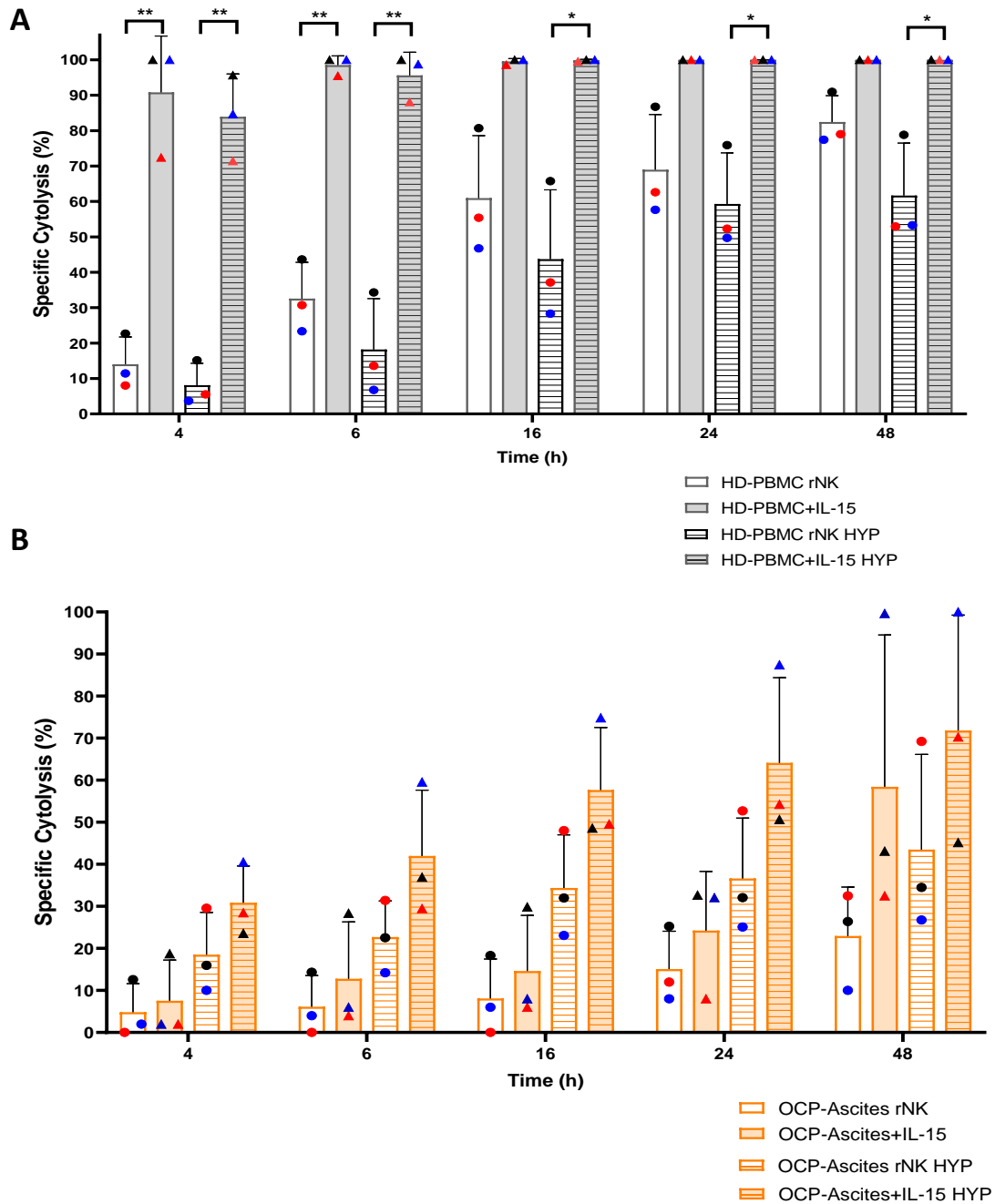
Figure 6-3: rNK and Cytokine-Primed Effector Cells Against OVCAR3 Ovarian Cancer Cell Line in Normoxia And Hypoxia

Bar chart with individual points of HD-PBMC samples (A) and OCP-Ascites derived samples (B). Solid bars represent normoxic conditions (21% O_2) and patterned bars represent hypoxic conditions (1% O_2). Effector conditions: rNK and cytokine-primed via rhIL-15 (10ng/ml). No-filled bars are for rNK effector cells and colour-filled bars correspond to cytokine-primed NK effector cells. Error bars signify the SD of the mean. Statistical analysis using paired t-test for non-primed and cytokine primed NK effector cells in either normoxia or hypoxia. Biological triplicates (n=3). * p<0.05, ** p<0.01.

6.3.4 Tumour Primed-NK Cells in Hypoxia Against NK Cell-Resistant Target Cells

The effects of hypoxia (1% O_2) on the NK cytotoxicity function for both HD-PBMC and OCP-Ascites samples was also investigated against the NK cell-resistant ovarian target cell line, SKOV3. The NK effector cell conditions used for these experiments were the control non-primed rNK cells, cytokine-primed via rhIL-15 (10ng/ml, R&D Systems) NK cells and TpNK cells via INB16 MMC treated cells (NK:INB16, 1:2). All the functional killing assays were performed in parallel in normoxic and hypoxic conditions in an E:T (5:1). Experiments were run in the xCELLigence RTCA system and the timepoints plotted were after 16h, 24h and 48h of E:T co-interaction.

Figure 6-4 displays the effects of the hypoxic environment (1% O_2) on the effectiveness of either cytokine-mediated or tumour-mediated NK cell priming against the SKOV3 target cells.

Comparison of HD-derived NK cells for the same priming conditions between normoxia and hypoxia, resulted in opposed observations with statistical significance (Figure 6-4). The cytokine-primed NK effector cells in hypoxia (blue bars), displayed less enhancement of SKOV3 target cell lysis compared to normoxic conditions with statistical significance for all the timepoints tested. The average percentage of SKOV3 target cytolysis in normoxia after 16h of co-incubation with the cytokine-primed NK effector cells was 83.88% compared to 43.27% in hypoxia (*p<0.05; p=0.0486). Similarly, after 24h the average percentage of target lysis in normoxia was

87.97% compared to 50.45% in hypoxia (*p<0.05; p=0.0485). Finally, after 48h there was statistical significance of **p<0.01; p=0.0053 (88.76% in normoxia and 58.16% in hypoxia) (Figure 6-4A).

In contrast, TpNK effector cells from HD-derived samples, expressed superior enhancement upon hypoxic environment compared to normoxia, with significant difference after 16h onwards of co-incubation with the SKOV3 target cells (Figure 6-4A) (purple bars). After 16h the average percentage of target cell lysis was 21.83% in normoxia whereas in hypoxia it was 29.62% (*p<0.05; p=0.0428). After 24h the average percentage in normoxia was 23.64% and 32.12% in hypoxia (*p<0.05; p=0.0425). Finally, after 48h the TpNK effector cells improved the SKOV3 cytolysis to 27.85% in normoxia and 38.33% in hypoxia with statistical significance of **p<0.01; p=0.0058.

Figure 6-4B shows the effects of cytokine-induced and tumour-induced priming of NK cells derived from OCP samples, against SKOV3 target cells upon normoxic and hypoxic conditions. Although the overall target cell killing was lower compared to the HD-derived samples, the effects of hypoxia on the cytokine priming and tumour priming NK effector cells were equivalent between HD-PBMC and OCP-Ascites samples, as in hypoxic conditions the improvement of cytokine-primed NK effector cells (orange bars) was lessened whereas for TpNK cells it was augmented (brown bars). No statistical significance was observed due to the heterogenous responses of OCP derived samples upon NK cell priming.
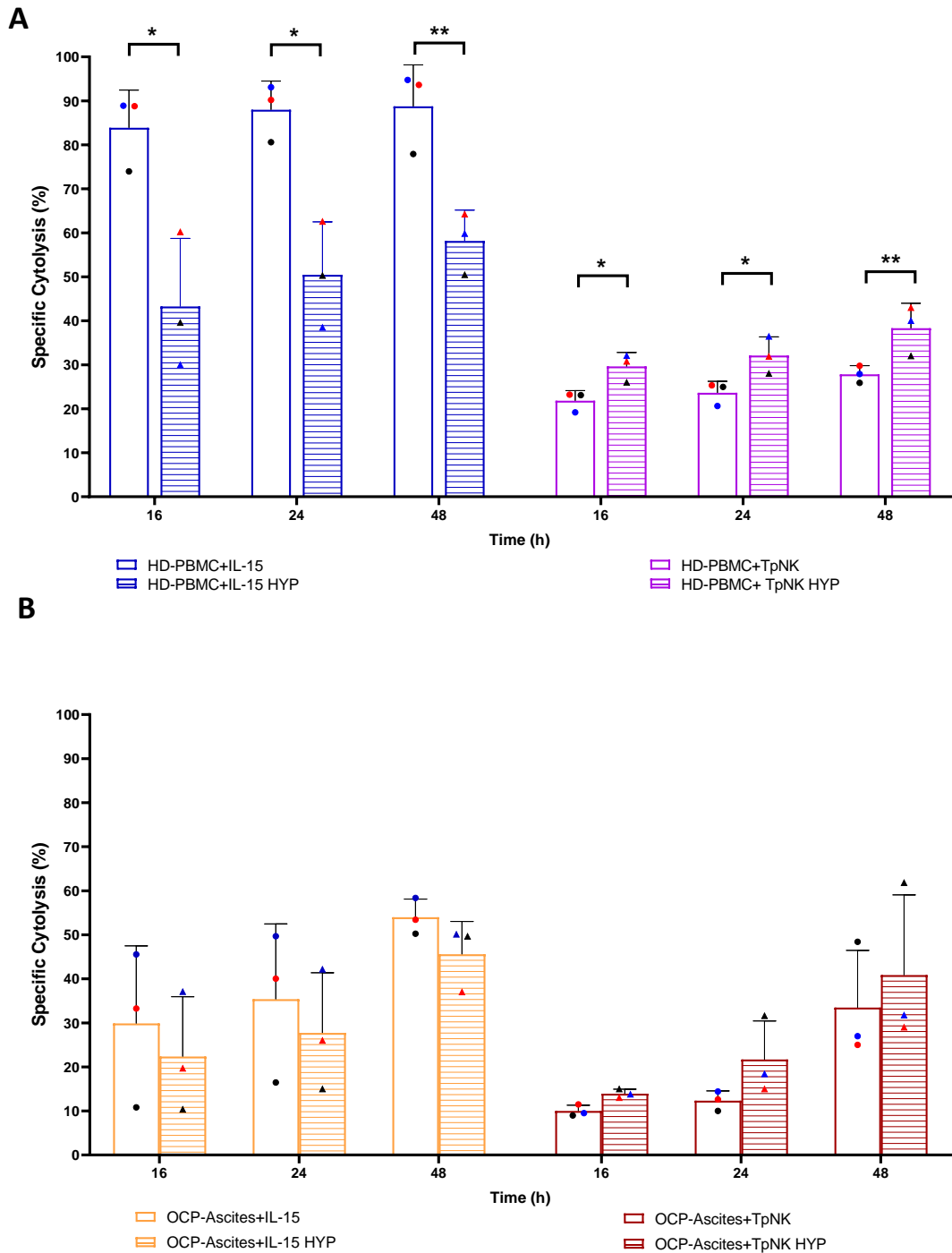
Figure 6-4: Comparison of Cytokine-Primed and Tumour-Primed NK Effector Cells Against SKOV3 Target Cells in Normoxia And Hypoxia

Three-way Bar Chart with symbols for individual donors for HD-PBMC (A) and OCP-Ascites (B) derived samples against SKOV3 ovarian cancer target cells. Percentage of SKOV3 specific cytolysis plotted after 16h, 24h and 48h of E:T co-incubation. E:T (5:1). Solid bars represent normoxic conditions (21% O_2) and patterned bars represent hypoxic conditions (1% O_2). Error bars signify the SD of the mean. Statistical analysis using paired t-test for the same effector condition in normoxia and hypoxia. Biological triplicates (n=3). * $p<0.05$, ** $p<0.01$.

The effects of the hypoxic environment on the priming efficacy of TpNK and cytokine-primed NK cells against the SKOV3 target cell line, through evaluation of each NK cell priming condition in normoxia and hypoxia have been plotted and described in Figure 6-4. Following, these observations, functional NK cell cytotoxicity assays were performed, comparing all the NK effector conditions against the SKOV3 target cells in normoxic, as well as, in hypoxic conditions.

Overall, priming of NK effector cells with either priming agent, improved SKOV3 target specific cytolysis in both normoxia and hypoxia for HD- and OCP- derived samples Figure 6-5.

For the HD-PBMC samples (Figure 6-5A) this increase was significant for all the timepoints investigated. Under normoxic conditions (21% O_2), cytokine-primed NK effector cells enhanced the percentage of SKOV3 target cells specific cytolysis with ****$p<0.0001$ for all the three timepoints. In addition, TpNK effector cells also significantly increased the SKOV3 target cell lysis with *$p<0.05$ for all the three timepoints ($p=0.0497$ after 16h, $p=0.0371$ after 24h and $p=0.0426$ after 48h).

Under hypoxic conditions (1% O_2) the average percentage of SKOV3 specific cytolysis was lessen for the cytokine-primed NK effector cells derived from HD samples (Figure 6-5A). After 16h the average percentage improved from 5.16% with rNK effector cells to 43.27% (**$p<0.01$; $p=0.0042$) upon cytokine priming and gradually this significance was increasing for the next

timepoints. After 24h of co-incubation the SKOV3 target cell lysis increased from 7.35% upon rNK effector cells to 50.45% upon cytokine-primed NK effector cells (***p<0.001; p=0.0007) and after 48h it was enhanced from 9.62% on rNK effector condition to 58.16% on cytokine-primed NK effector cells (****p<0.0001).

On the contrary, TpNK effector condition on HD-derived NK cells exposed superior cytotoxicity function in hypoxic conditions with greater statistical significance compared to normoxia. TpNK effector cells enhanced the SKOV3 specific cytolysis to 29.95% (*p<0.05; p=0.0292) after 16h, subsequently increased to 32.45% (*p<0.05; p=0.0107) after 24h and finally enhanced to 39.00% after 48h (***p<0.01; p=0.0006) compared to the control rNK effector cells.

This pattern of adverse effects on the NK cell function of cytokine-primed NK effector cells and the augmented effects on the NK cytotoxicity of the TpNK effector cells upon hypoxia, were similar for NK cells derived from the OCP-Ascites samples (Figure 6-5B). However, the overall target cell killing was lower compared to the HD-PBMC derived samples.

Cytokine-mediated NK cell priming of OCP-derived samples, resulted in an enhancement of SKOV3 target cell cytolysis, and was statistically significant for the last two timepoints, 24h and 48h both in normoxia and hypoxia.

After 24h of E:T co-interaction, the cytokine-primed NK effector cells improved significantly the average percentage of SKOV3 target cell lysis from 11.65% for the control rNK effector cells to 35.40% (*p<0.05; p=0.0489) under normoxic conditions. After 48h, the cytokine-primed NK effector cells improve SKOV3 target cell lysis from 14.14% of co-incubation with the rNK cells to 54.00% in normoxia with greater statistical significance of **p<0.001; p=0.0015.

TpNK effector cells enhanced SKOV3 target cell cytotoxicity with statistical significance after 48h of effector-target co-incubation (*p<0.05; p=0.0422).

Under hypoxia, cytokine-primed NK effector cells and TpNK effector cells derived from OCP samples, exhibited a heightened cytotoxicity against SKOV3 target cells after 24h and 48h of co-interaction with statistical significance (*p<0.05). After 24h, the target cell cytolysis increased from 4.91% upon co-interaction with rNK effector cells to 27.73% (p=0.0493) and 25.59% (p=0.0499) upon cytokine-primed NK cells and TpNK effector cells respectively. Additionally, after 48h, the SKOV3 target cell lysis augmented from 7.33% upon rNK effector cells addition, to 45.59% (p=0.0138) and 40.87% (p=0.0243) after co-incubation with cytokine-induced primed NK cells and TpNK correspondingly.
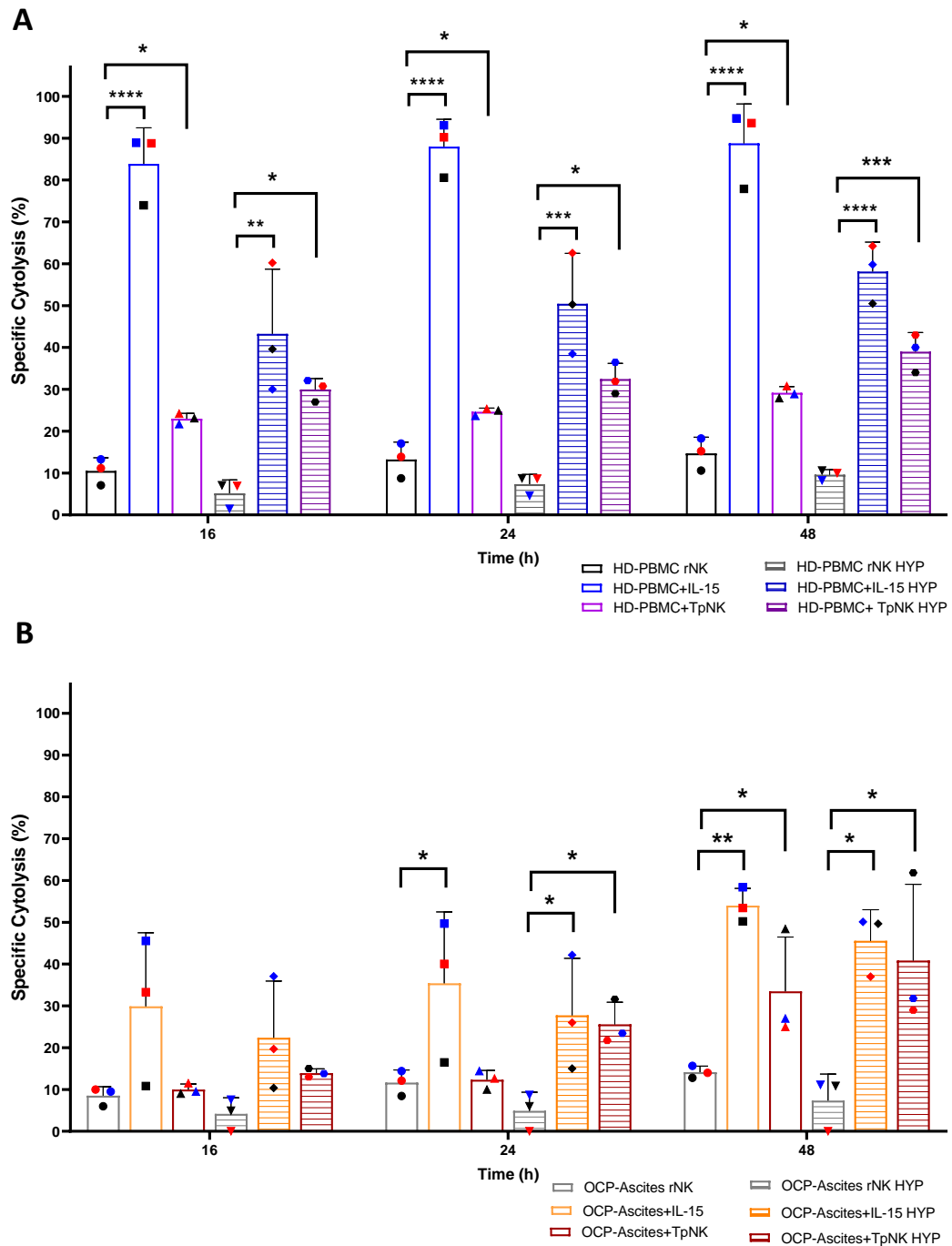
Figure 6-5: rNK and Primed NK Effector Cells Against SKOV3 Ovarian Cancer Cell Line In Normoxia And Hypoxia

Bar chart with individual points for each donor of HD-PBMC samples (A) and OCP-Ascites derived samples (B). Solid bars represent normoxic conditions (21% O_2) and patterned bars represent hypoxic conditions (1% O_2). Effector conditions: rNK, cytokine-primed via rhIL-15 (10ng/ml) and TpNK via INB16 MMC treated (NK:INB16 1:2). Error bars represent the SD of the mean. Statistical analysis using One-way ANOVA with Dunnett correction and rNK effector condition was selected as control group against each priming condition. Biological triplicates (n=3). * p<0.05, ** p<0.01, ***p<0.001, **** p<0.0001.

6.4 Discussion

Hypoxia, which is one of the key characteristics of the TME, contributes to the impairment of the NK cell function and subsequently facilitates tumour escape from immunosurveillance. In this chapter, these hypoxic conditions were reproduced in our laboratory using a multigas culture incubator that includes a nitrogen gas purge to create a hypoxic environment of 1% O_2. The hypoxic oxygen level concentration was validated using the Fibox 4 single channel fibre-optic oxygen transmitter (PreSens Precision Sensing) prior commencing these experiments. Herein, the adverse effects of hypoxia was assessed in ovarian cancer setting using the NK cell-resistant SKOV3 and NK cell-sensitive OVCAR3 ovarian tumour cell lines as target cells and the NK effector cells were derived from either HD-PBMC or OCP-Ascites samples. The NK cell cytotoxic efficacy was further evaluated by performing parallel functional potency assays against the two ovarian cancer target cell lines that expressed opposed NK cell sensitivity under hypoxia and normoxia. Finally, priming of NK effector cells was conducted either via cytokine-induced (rhIL-15, 10ng/ml) or tumour-induced (INB16 MMC treated, NK:INB16 1:2) priming agents in an endeavour to investigate the recovery of the NK cell function impairment upon hypoxia.

Herein, the hypoxic conditions caused NK cell impairment of the non-primed rNK effector cells against the OVCAR3 ovarian target cells with statistical significance for all the timepoints investigated (6h, 16h, 24h and 48h) for the NK cells derived from HD-PBMC samples. Interestingly, opposed results were observed for the NK cells derived from the OCP-Ascites, for

which the NK cell responsiveness was greater under hypoxia compared to the normoxia for all the timepoints tested (6h, 16h, 24h and 48h), with statistical significance for the last two timepoints. Considering the fact that NK cells from OCP samples derived from the ascites, which is already an immunosuppressive and hypoxic environment, this suggests a distinction between the effects of the chronic NK cell exposure to hypoxia and the acute NK cell exposure to artificially created hypoxic conditions. This adaptation of OCP-derived NK cells to perform better in hypoxia, might be a result of post-translational modifications of NK cells derived from the ascites tumour environment and herein is the first time that this has been demonstrated.

Furthermore, restoration or enhancement of NK cell function was investigated, via either cytokine- or tumour- induced mediated priming of NK cells. Cytokine-induced priming of NK cells restored the NK cell function and enhanced tumour cell lysis in both ovarian target cell lines. Comparison of the cytokine-primed NK effector cells in normoxia and hypoxia against the OVCAR3 target cells was similar, however, this improvement was significant only under hypoxic conditions throughout all the timepoints tested, compared to the control rNK cells for the HD-PBMC derived samples. This enhancement in NK cell function upon cytokine priming was also observed in OCP-derived NK cells, where the OVCAR3 target cell lysis of cytokine-primed NK effector cells was superior in hypoxia compared to normoxia. These observations are in accordance with Sarkar *et al* (2013) and Velásquez *et al* (2016) reports in which they published that IL-15 synergises with hypoxia and augments the NK cell responsiveness against

tumour target cells including ovarian cancer (Sarkar *et al.*, 2013; Velásquez *et al.*, 2016).

In contrast,, cytokine primed NK effector cells against SKOV3 target cells exhibited opposed results in comparison to OVCAR3 cells, as the percentage of target cell lysis was lower in hypoxia compared to normoxia for both HD- and OCP-derived samples. This reduction was statistically significant for all the timepoints tested for the HD-PBMC samples.

The NK cells against the SKOV3 target cell line were also tumour-primed as an alternative NK cell priming approach against the NK cell-resistant ovarian cancer cell line. Remarkably, the TpNK cells expressed superior killing in hypoxia compared to normoxia, in both HD- and OCP-derived samples, with statistical significance for the HD-derived NK cells. The improvement of SKOV3 target cell lysis upon cytokine- or tumour- primed NK effector cells was statistically significant in both normoxic and hypoxic conditions for both HD- and OCP- derived samples.

In conclusion, the results obtained in this chapter showed for the first time the use of tumour primed NK cells in ovarian cancer against the hypoxic immunosuppressive TME. TpNK cells demonstrated effectiveness to restore NK cell responsiveness against the NK cell-resistant SKOV3 ovarian cancer cell line under hypoxic conditions, from HD-PBMCs and OCP-Ascites samples. TpNK cells resulted in superior enhancement of NK cell function under hypoxia compared to normoxia and may postulate the importance of tumour-priming on NK cells found in circulation in the PB as well as in the

hypoxic TME. Herein, it was the first time to show the encouraging effects of tumour priming on the NK cells that derived directly from the site of the tumour, the peritoneal fluid/ascites of ovarian cancer patients. These results can enhance further the understanding of the NK cells derived directly from the hypoxic TME and suggest a novel efficacious translational immunotherapeutic approach upon the typical intraperitoneal administration against ovarian cancer.

Chapter 7   DISCUSSION

NK cells are encouraging multifaceted applicants in cancer immunotherapy as a result of their distinctive recognition and response mechanisms. They have the ability to interact and kill a wide range of tumour cells without prior sensitisation. This is due to the dual NK cell recognition responses that comprises of an array of activating and inhibitory receptors as well as the presence of FcγRIII receptor on the NK cell surface that results in natural cytotoxicity and ADCC response respectively. Additionally, NK cell function is not limited to the presence of specific MHC class I molecules on the target cells.

NK cell cytotoxicity can be reinvigorating by several approaches, both *in vivo* and *ex vivo. In vivo* approaches, involve the priming of NK cells via cytokine-mediated or tumour-mediated priming agents. IL-2 is the first cytokine approved and used clinically to produce lymphokine-activated killer (LAK) cells since its discovery in mid 1980s (Rosenberg *et al*., 1985). However, high doses of IL-2 administration can cause toxicities such as systemic capillary leak syndrome, a hypovolemic state and plasma leakage in the extravascular space (Rosenberg *et al*., 1985). A current focus on cytokine-based immunomodulatory NK immunotherapies including ovarian cancer is the substitution of IL-2 with IL-15. IL-15 was found to express less toxicity-related issues compared to the use of IL-2 and did not result in Treg cell stimulation that causes NK cell function impairment. Moreover, IL-15 enhanced further the NK cell proliferation and cytotoxicity as it binds with greater specificity to the cytotoxic T cells and non-terminally differentiated NK

cells (Waldmann, 2015). Few studies have investigated the ability of IL-15 and IL-15 super-agonist ALT-083 to improve the NK cell function against ovarian cancer. Results showed that the NK cell responsiveness from the ascites was restored with IL-15 or ALT-803 both *in vitro* against several ovarian cancer target cells (including SKOV3 and OVCAR3) and *in vivo* using NSG xenogeneic mouse model. These findings suggest the use of the IL-15 super-agonist ALT-083 in clinical trials for the treatment of ovarian cancer (Felices *et al.*, 2017; Hoogstad-van Evert *et al.*, 2018). Furthermore, Cooper and colleagues reported that combination of IL-12/IL-15/IL-18 resulted in successfully activated NK cells with memory-like properties that persisted enhanced cytotoxic responses for weeks (Cooper *et al.*, 2009). In addition to the cytokine-induced mediated NK cell priming, tumour cell lines have been used to enhance NK cell cytotoxicity *in vivo*. Herein, it was the first time to use the leukaemic INB16 tumour cell line to prime NK cells and compare it with the standard priming cytokine agent, IL-15. Results from our group have demonstrated the use of CTV-1 a leukemic cell line to prime NK cells and subsequently enhance cytotoxicity (North *et al.*, 2007; Sabry *et al.*, 2019). It was also shown that these two different NK-mediated priming agents exhibit distinct transcriptomic, phenotypic and NK cytokine secretion profiles (Sabry *et al.*, 2019). Furthermore Pal *et al* (2017) reported the use of leukaemic cell line (NALM-16) and primary leukaemia specimens (P3B, P31G, P18R and P84D) to augment NK cell activity (Pal *et al.*, 2017). The results obtained from Pal and colleagues showed successful improvement of NK cell responses, though this was specific only to the tumour cells that were also used to prime the NK effector cells. In contrast, previously findings from our

group as well as results obtained from this project, showed that tumour-induced mediated NK cell priming was not tumour specific, and it enhanced NK cell activity against leukaemic, lymphoma, breast and ovarian cancer target cells (North *et al.*, 2007).

Moreover, an additional *in vivo* strategy used to activate NK cell responses is immune-checkpoints inhibitors (ICIs). This antibody-based immunotherapy, can be against the NK cell inhibitory receptors (KIRs, NKG2A) and the typical immune checkpoints (PD-1, CTL-4). Combination of those two types of ICIs are used in clinical trials for several solid tumours including head and neck cancer (NCT03341936), non-small cell lung (NSCL) (NCT04145193 and NCT05061550), pancreatic (NCT03983057) and colorectal cancer (NCT04301557) (Lian *et al.*, 2022). An alternative approach of NK antibody-based immunotherapy to improve NK cell efficacy in antitumour treatment, is via targeting the NK activating receptors to enhance recognition of specific TAAs as well as activation and enhancement of the ADCC mechanism on NK cells. In ovarian cancer, engineered BiKEs, TriKEs and TetraKEs that crosslink ovarian tumour-associated antigens (TAAs) with CD16 on NK cells have shown encouraging results in both *in vitro* and *in vivo* studies. The BiKE construct, comprises of EpCAM and CD16 whereas the TriKE also includes the IL-15 cross-linker that not only enhances and sustains NK cell ADCC activity as the BiKEs, but also it facilitates NK cell expansion, proliferation, activation and survival both *in vitro* and *in vivo* (Vallera *et al.*, 2016). A TetraKE construct additionally encompasses CD133, a TAA on cancer stem cells (CSCs). The CSCs are highly drug refractory cells upon disease relapse and also the basal root of tumour cells. This

CD16/EpCAM/CD133/IL-15 design express dual antigen ADCC that augments the targeting ability against tumour cells and CSCs equally (Schmohl *et al.*, 2016b).

Furthermore, there are also *ex vivo* strategies to augment expansion and function of NK cells. There are several NK cell sources for *ex vivo* adoptive NK cell therapies, including predominantly the peripheral blood (PB) derived NK cells as well as "off-the-shelf" alternatives such as umbilical cord blood (UCB) derived NK cells, NK cell line (NK92) and induced pluripotent stem cells (iPSCs) (Du *et al.*, 2021). Adoptive transfer of PBNK cells can be either autologous or allogeneic. Although, autologous NK cells are easier to obtain directly from the cancer patient and expose low risk of graft versus host disease (GvHD), they are usually derived from already heavily pre-treated cancer patients with limited NK cell amount, expansion efficacy and cytotoxicity function against the current tumour (Du *et al.*, 2021). In contrast, the use of allogeneic NK cells is particularly beneficial and demonstrate greater antitumour efficacy compared to the autologous NK cells. This is due to the fact that allogeneic NK cells derived from healthy donors, exhibit normal function and also, they enhance NK cell mediated cytotoxicity via donor-recipient incompatibility with KIR mismatch on donor NK cells and MCH-class I on recipient tissues which subsequently trigger alloreactivity of NK cells (Ruggeri *et al.*, 2002).

In situations of inadequate availability of PBNK cells, the "off-the-shelf" NK cell sources can serve as alternative candidates. Umbilical cord blood (UCB) could act as an abundant source of NK cells for adoptive therapy, as it

accounts for a higher percentage of NK cells (~30%) compared to the PB (~10%). There are several clinical trials investigating UCB-NK cell derived therapy against haematologic malignancies (NCT02727803, NCT01729091 and NCT02280525, NCT04347616) (Lian *et al.*, 2022) as well as solid tumours, including ovarian cancer (NCT03539406). However, all the aforementioned clinical trials are still ongoing and no results have been reported yet. An investigation conducted by Luevano and colleagues after conducting to compare UCB-NK and PBNK cells both *in vitro* and *in vivo*, demonstrated that UCB-NK cells exhibited less NK cell cytotoxic function although IFN-γ, TNF and perforin levels were analogous to PBNK cells (Luevano *et al.*, 2012). This was possibly due to significantly higher expression levels of the NK cell inhibitory receptor NKG2A and low expression of granzyme B on UCB-NK cells. Nevertheless, the lower cytotoxicity of the UCB-derived NK effector cells was reversable upon IL-2 administration (Luevano *et al.*, 2012).

In addition, NK92 is another "off-the-shelf" candidate and it is readily available from current Good Manufacturing Practice (c-GMP) compliant master cell banks which this allows its clinical use. There are several advantages using a cell line for *in vitro* studies, including, homogenous population, clonal expansion, generation of large cell number through passages and result in reproducible and consistent data. NK92 is an IL-2 dependent NK cell line that has been established in early 1990s from a patient with non-Hodgkins lymphoma (Gong *et al.*, 1994). Since its discovery, NK92 exposed high cytotoxicity against a wide spectrum of tumour cells. This might be due to the presence of NK activating receptors including NKG2D

and some NCRs such as NKp30, NKp46 as well as the absence of KIRs NK inhibitory receptors on the surface of NK92 cells (Suck *et al.*, 2016). Several clinical trials have been currently running using NK92 that have already been irradiated (10Gy) prior administration. The first clinical application has been reported in 2001 where irradiated NK92 cells were administrated intravenously (IV) to patients with advanced solid tumours (Tonn *et al.*, 2001). Further clinical trials have followed against refractory metastatic renal cell carcinoma (RCC) and melanoma (NCT00900809) (Arai *et al.*, 2008) as well as haematological malignancies (NCT00990717) (Tonn *et al.*, 2013).

Moreover, iPSC-NK cells are also an alternative "off-the-shelf" candidates for NK adoptive immunotherapy. Cichocki *et al* (2020) reported that iPSC-NK cells displayed similar characteristics to PBNK cells, however they exhibit enhance potential for cell expansion *ex vivo* (Cichocki *et al.*, 2020). In addition it was demonstrated that the resultant immune responses included the recruitment and activation of T cells and postulate the combination of iPSC-NK cells with checkpoint inhibitor therapies (Cichocki *et al.*, 2020). Clinical trials using PSC-derived NK cells are currently running for advanced solid tumours including ovarian cancer (NCT04630769) (Lian *et al.*, 2022).

Following the generation of NK cells from the aforementioned different *ex vivo* sources, the expansion and functional augmentation of NK cells can be performed via incubation with cytokines such as IL-2, IL-15 and IL-18 to ensure survival, expansion and enhance cytotoxicity and IFN-γ production. In addition Fujisaki *et al* (2009) reported the use of modified K562 cancer

cells as feeder cells that expressed membrane bound IL-15, 41BB ligand to induce NK cell expansion and proliferation with higher responsiveness in *in vitro*, *in vivo* and clinical studies against leukaemia setting. (Fujisaki *et al.*, 2009). The generated K562-mb15-41BBL cells were irradiated (100 Gy) prior co-incubation with PBMCs or administration to the patients with AML. Fujisaki and colleagues compared NK cell expansion stimulated by K562-mb15-41BBL cells, to the control stimulation with IL-2 (10-6,000 IU/mL), IL-12 (1-10 ng/mL; R&D Systems), IL-15 (1-100 ng/mL; R&D Systems), and/or IL-21 (1-10 ng/mL; BioSource International) and cytokines were added daily to the NK cell culture. It was reported that this method resulted in greater NK cell expansion and cytotoxicity and exhibited distinct genetic and phenotypic profile compared to the control method of NK cell expansion (Fujisaki *et al.*, 2009).

Finally, NK cells can be modified ex vivo to express CARs that enhance TAA specificity and therefore enhance NK cell activity. This may be a better and safer alternative to CAR-T cells as the NK cells can derived from allogeneic sources resulting in readily availability, relatively more cost-effectiveness and independence to graft vs host disease (GvHD). Therefore, these can provide a potential safe and effective source of allogeneic "off-the-shelf" engineered cell therapy due to their robust tumour recognition compared to T-cells and the relatively short NK cell lifespan (Mehta & Rezvani, 2018). Clinical trials that use CAR-NK cells include anti-HER2 CAR-NK effector cells against advanced HER2+ solid tumours (NCT04319757) (Lian *et al.*, 2022). However, genetic modifications of primary NK cells are still impeded by low and variable transfection efficacies.

Therefore, UCB-derived NK cells can be used instead, as they exhibit greater genetical stability. Liu *et al* (2020) had generated CAR-NK cells derived from UCB transduced with a retroviral vector expressing anti-CD19 against CD19+ lymphoid tumours (NCT03056339) (Liu *et al.*, 2020). In addition, the NK92 cell line can also be used for genetic modification and generation of NK92-CAR cells due to the clonal expansion and genetic stability. However, the irradiation required before NK92 cell administration impairs NK cell proliferation and persistence *in vivo*. Experiments using engineered NK cells against ovarian cancer have been conducted and published with great effectiveness both *in vitro* against ovarian tumour target cells and *in vivo* using NSG xenogeneic mouse model. Klapdor and colleagues generated CAR-NK cells against CD24, a cancer stem cell marker that is linked with poor prognosis and clinical outcome in ovarian cancer. They also reported *in vitro* effective cytotoxic response against the ovarian cancer tumour target cells SKOV3 and OVCAR3, using CAR-NK92 against CD24 (Klapdor *et al.*, 2019). In addition, Li and colleagues generated a homogeneous CAR-NK cells using iPSCs (against tumours that express mesothelin, a receptor for CA125 (MUC16) that is overexpressed in more than 80% of the cases in ovarian cancer setting (Li *et al.*, 2018). Findings from Li *et al* (2018), demonstrated improved antitumour activity compared to CAR-T and non-CAR expressing cells *in vitro* and significantly reduced tumour size and increased survival *in vivo* similarly to CAR-T cells, but, with less toxicity (Li *et al.*, 2018). Based on early success in both *in vitro* and *in vivo* experiments, a phase I clinical trial has started (NCT03692637) to evaluate CAR-NK cells against mesothelin.

Numerous clinical trials have investigated the potential of NK cell immunotherapy using different sources for NK cells (Lian *et al.*, 2022)

Although NK cell-based immunotherapy is broadly studied against haematological malignancies and some solid tumours, there is yet limited information against ovarian cancer. The most robust studies implicated cytokine-based immunomodulation to enhance NK cell cytotoxic activity. Geller *et al* (2011), performed the largest clinical study including 14 OCPs that have already received chemotherapy. In this Phase II study, allogeneic NK cell adoptive transfer in combination with IL-2 were infused to the OCP intravenously (IV), however, although partial response was achieved, no sustained *in vivo* NK cell expansion was attained (Geller *et al.*, 2011). A current phase I clinical trial investigates the *ex vivo* expanded adaptive NK cell population isolated from cytomegalovirus-seropositive donors in platinum-resistant ovarian cancer patients. These NK cells were administrated in combination with IL-2 intraperitoneally (IP). The preliminary results from two patients, demonstrated NK cell *in vivo* persistence after 2 weeks in one patient that resulted in tumour size reduction and no disease progression after repeated NK cell infusions (NCT03213964).

7.1 Open Questions

There are some questions that still remain ambiguous on the NK cell immunological mechanism in ovarian cancer. These include the coherent understanding on NK cell recognition and responses, the mechanisms behind NK cell suppression and subsequent ovarian cancer cell evasion, the

differences in NK cell cytotoxicity sensitivity on ovarian tumour target cells as well as the role of the immunosuppressive ovarian TME on the NK cell function. Further studies on NK cell phenotypic and genomic level, as well as on its biological mechanism of action against ovarian cancer cells and the ovarian TME are still required to provide a better and deeper comprehension in the NK cell immunotherapy in ovarian cancer field.

7.2 Thesis Aims and Objectives

The aim of this project was to provide a deeper understanding of the NK cell function in ovarian cancer and establish potential approaches to overcome NK cell function impairment.

This was performed by firstly addressing the differences on the NK cells within the ovarian cancer patients by comparing the circulating NK cells found in the PBMC and the NK cells at the tumour site found in the ascites. Secondly, NK cell function efficacy was assessed between NK cells derived from healthy donors and ovarian cancer patients. This was investigated on a phenotypic level via immunophenotyping of NK cell receptors, on a genomic level via RNA sequencing and functionally through cytotoxic assays.

Furthermore, the NK cell-mediated cytotoxicity resistance in ovarian cancer was studied to evaluate the mechanisms behind the difference in the sensitivity of ovarian tumour target cells against NK effector cells. This was investigated using the NK cell-resistant ovarian cancer SKOV3 and NK cell-sensitive ovarian cancer OVCAR3 target cell lines. For these studies, the

expression levels of the NK cell ligands on the surface of those two ovarian cancer target cell lines were established, before and after their co-incubation with the NK effector cells (E:T, 5:1). The NK cell-mediated cytotoxic assays were performed in a flow-based and real-time electrical impedance-based platforms and the dynamic interaction between NK cell and target cells was also evaluated via live cell imaging.

Additionally, the effects of the immunosuppressive ovarian TME on the NK cells were also examined in this project in two different approaches. The first method, was to imitate the lower ratio of effector cells compared to the target cancer cells in the site of the tumour. This was achieved by co-incubating the NK effector cells and ovarian cancer target cells in an E:T ratio of 1:2 and subsequently investigate the expression levels of NK receptors and NK ligands. The second approach focused on the key characteristic of the TME which is that it is a hypoxic environment. Therefore, to emulate this, functional NK cell based cytotoxic assays were conducted in hypoxia (1% O_2) to study the effects of the hypoxic TME in NK cell function.

Finally, priming of NK cells derived from healthy donors as well as ovarian cancer patients, was studied in this project to assess its efficacy to overcome the NK-cell mediated cytotoxicity impairment in ovarian cancer. The NK cell mediated priming was achieved via either rhIL-15 (10ng/ml, R&D System) or via the previously identified leukemic cell line INB16 in a ratio NK:INB16 (1:2). The effects of NK cell mediated priming were investigated against the two ovarian cancer target cell lines abovementioned, that display opposed sensitivity to NK cell mediated cytotoxicity. These experiments were

also investigated in parallel in hypoxic conditions to assess the effectiveness of NK cell mediated priming to overcome the impairment of NK cell function caused by the hypoxic immunosuppressive TME.

7.3 Thesis Results

Herein, the experiments conducted have enhanced the comprehension on the NK cell responsiveness and functions as well as on the ovarian cancer resistance to NK cell mediated lysis. The results obtained in this project provided new-found and thorough insights on the NK cell receptors and molecules in ovarian cancer and gave answers on the potential mechanisms behind the ovarian tumour cell evasion and escape from NK immunosurveillance using for the first time such an extensive immunophenotyping panel. This also allowed a thorough characterisation of NK cells within the ovarian cancer patients by comparing circulated PBNK and ascites-NK cells from the tumour site as well as by comparing NK cells from OCP-derived and HD-derived samples.

Moreover, the genomic profile of NK cells in ovarian cancer has been attempted to be investigated in this project. For the completion of these experiments, the samples used, derived from PB and ascites of ovarian cancer patients as well as from PB of HDs. The NK cells were isolated from all the samples using the RNeasy Micro Kit (Qiagen, UK) RNA isolation method as specified in section 2.4.2 and the samples were subsequently sent to Eurofins Genomics to be processed and analysed. High throughput RNAseq was generated and Cufflinks processing was performed to allow a

final transcriptome assembly. TopHat, Bowtie and CummerRbund programs were used to analyse and generate various plots, such as Heat map and volcano plots, that were performed by Eurofins Genomics. Unfortunately, due to the very small RNA concentration obtained from OCP samples, only two samples derived from the ascites passed the threshold criteria for RNAseq processing and therefore the results for the NK cell genomic profiling in ovarian cancer and its comparison with HD-derived samples were not included in the Results section of this thesis. The main biological functions of the top genes obtained from the two OCP samples as well as the HD -PBMC samples included cell-to-cell signaling, cell adhesion, cell trafficking, cellular growth, differentiation and proliferation, cellular development and cellular metabolism. For the OCP derived samples some of the top genes found (such as CA8, CALB2, CASC9, MUC4), are associated with tumourigenesis and angiogenesis, the formation of new blood vessels that facilitates tumour metastasis.

In addition, here it is the first time to demonstrate tumour-priming of NK cells against solid tumours and primarily in ovarian cancer setting. The importance and effects of TpNK cells was signified in overcoming and improving the NK cell function against both NK cell-resistant ovarian cancer target cells as well as against the immunosuppressive hypoxic ovarian TME.

Furthermore, the dynamic interaction between non-primed and primed NK effector cells against the ovarian tumour target cells were also shown visually using the eSight live cell analysis (Agilent) and performing avidity tests using the z-Movi instrument (Lumicks). Both methods have not been

previously reported in ovarian cancer setting and they have facilitated the understanding behind the interaction and engagement of NK effector cells and ovarian cancer target cells.

Herein, it is the first time to address the effects of the hypoxic environment between the NK cells derived from HD-PBMCs and OCP-ascites. The results obtained, revealed the concept of acute and chronic hypoxia that speculated the reasons behind the differences on the priming and cytotoxicity effectiveness between the two different NK-derived effector cells. The HD-derived NK cells expressed superior cytotoxicity and priming efficacy in normoxia compared to the OCP-derived NK cells. However, when the HD-derived NK effector cells were exposed in hypoxic conditions (acute hypoxia) to mimic the NK cells in the hypoxic TME they failed to be effectively primed and, interestingly, under hypoxic conditions their cytotoxic function was lesser compared to the NK effector cells derived from the ascites which are found already in the hypoxic TME in OCPs (chronic hypoxia). This might also propose a post translational modification of the NK cells that have been infiltrated at the tumour site and are present in the immunosuppressive hypoxic ascitic fluid.

7.4 Future Studies

Following all the experimental procedures and the results obtained in this project, future studies could include blockade studies on the NK cell receptors and ligands that variations were observed. In addition quantification of cytokine secretion by the NK cells upon co-incubation with the ovarian

cancer target cells that display opposed sensitivity against NK cell lysis could be performed to enhance the comprehension behind the mechanisms for this resistance in ovarian cancer. Furthermore, a thorough genomic profiling between the PBMC and ascites samples derived from OCP samples could also enhance the characterisation of NK cell profiling in ovarian cancer. Moreover, better understanding on the hypoxic immunosuppressive ovarian TME could be evaluated by additionally investigating other immunosuppressive components and soluble modulators of the TME such as Tregs, MDSCs and TGFβ. Finally, subsequent to the investigation of NK cell responsiveness in ovarian cancer in a 2D-setting, 3D spheroids of ovarian tumour target cells could be created to examine the NK cell function efficacy and NK mobility and infiltration ability and aim to provide better understanding of the NK mechanisms against cancer target cells at the site of the tumour. This can assist to a better prognostic and predictive value in ovarian cancer.

7.5 Conclusions

There are several challenges in ovarian cancer therapeutic approaches, including the complexity of the ovarian cancer immunosuppressive TME, the limitation in treatment options and screening strategies, the heterogeneity among ovarian cancer patients and the high recurrence rate. All these, amplify the need for the development of effective and efficient therapeutic advances. The NK cells can be a promising multifaceted candidate to meet the current challenges in ovarian cancer. This is due to the ability of NK cells to migrate to the tumour site, as well as, to express both ADCC and natural

cytotoxicity without prior sensitisation or necessity of MHC class I presence, in comparison to the cytotoxic T-cells.

In this project, it was unveiled the successful priming of NK cells using a tumour-cell mediated priming agent, INB16, rather than only the typical cytokine-priming agent against ovarian cancer cells. This was effective to overcome the inhibitory signals of the NK cell-resistant ovarian cancer cell line, SKOV3, as well as to enhance the NK killing potential in samples derived from ovarian cancer patients even at the presence of a hypoxic immunosuppressive TME. In addition, this project offered a better understanding in ovarian cancer resistance against NK cell cytotoxicity. This was accomplished by the use of extensive immunophenotypic panels of NK cell receptors before and after exposure to the NK cell-resistant SKOV3 and NK cell-sensitive OVCAR3 ovarian target cells, as well as, through an exhaustive immunophenotypic screening for the first time, on NK cell ligands on the surface of the two ovarian tumour cells to determine the potential mechanism behind the difference on the NK cell sensitivity. These results have enabled a better understanding behind NK cells in ovarian cancer and the evasion of ovarian tumour cells against NK cell mediated cytotoxicity and postulate a multifaceted approach to meet the challenges of the great heterogeneity on ovarian cancer cell lines and ascites as demonstrated here.

Several questions still remain regarding NK cell function and responses in ovarian cancer. Therefore, this project has created the foundation data to design further research on NK cell immunotherapy in ovarian cancer and even broadly to other types of cancer. This can

encourage the development of an optimal therapeutic approach in ovarian cancer by targeting NK cells either alone or in combination with other therapies.

Chapter 8 BIBLIOGRAPHY

Akatsuka, A., Ito, M., Yamauchi, C., Ochiai, A., Yamamoto, K., & Matsumoto, N. (2010). Tumor cells of non-hematopoietic and hematopoietic origins express activation-induced C-type lectin, the ligand for killer cell lectin-like receptor F1. *International Immunology*, *22*(9), 783-790. https://doi.org/10.1093/intimm/dxq430

Anfossi, N., André, P., Guia, S., Falk, C. S., Roetynck, S., Stewart, C. A., Breso, V., Frassati, C., Reviron, D., Middleton, D., Romagné, F., Ugolini, S., & Vivier, E. (2006). Human NK Cell Education by Inhibitory Receptors for MHC Class I. *Immunity*, *25*(2), 331-342. https://doi.org/10.1016/j.immuni.2006.06.013

Arai, S., Meagher, R., Swearingen, M., Myint, H., Rich, E., Martinson, J., & Klingemann, H. (2008). Infusion of the allogeneic cell line NK-92 in patients with advanced renal cell cancer or melanoma: a phase I trial. *Cytotherapy*, *10*(6), 625-632.

Balsamo, M., Manzini, C., Pietra, G., Raggi, F., Blengio, F., Mingari, M. C., Varesio, L., Moretta, L., Bosco, M. C., & Vitale, M. (2013). Hypoxia downregulates the expression of activating receptors involved in NK-cell-mediated target cell killing without affecting ADCC. *43*(10), 2756-2764. https://doi.org/10.1002/eji.201343448

Bauer, S. (1999). Activation of NK Cells and T Cells by NKG2D, a Receptor for Stress-Inducible MICA. *Science*, *285*(5428), 727-729. https://doi.org/10.1126/science.285.5428.727

Belisle, J. A., Gubbels, J. A., Raphael, C. A., Migneault, M., Rancourt, C., Connor, J. P., & Patankar, M. S. (2007). Peritoneal natural killer cells from epithelial ovarian cancer patients show an altered phenotype and bind to the tumour marker MUC16 (CA125). *Immunology*, *122*(3), 418-429. https://doi.org/10.1111/j.1365-2567.2007.02660.x

Benson, D. M., Jr., Bakan, C. E., Mishra, A., Hofmeister, C. C., Efebera, Y., Becknell, B., Baiocchi, R. A., Zhang, J., Yu, J., Smith, M. K., Greenfield, C. N., Porcu, P., Devine, S. M., Rotem-Yehudar, R., Lozanski, G., Byrd, J. C., & Caligiuri, M. A. (2010). The PD-1/PD-L1 axis modulates the natural killer cell versus multiple myeloma effect: a therapeutic target for CT-011, a novel monoclonal anti-PD-1 antibody. *Blood*, *116*(13), 2286-2294. https://doi.org/10.1182/blood-2010-02-271874

Bhat, J., Dubin, S., Dananberg, A., Quabius, E. S., Fritsch, J., Dowds, C. M., Saxena, A., Chitadze, G., Lettau, M., & Kabelitz, D. (2019). Histone Deacetylase Inhibitor Modulates NKG2D Receptor Expression and Memory Phenotype of Human Gamma/Delta T Cells Upon Interaction With Tumor Cells [Original Research]. *Frontiers in Immunology*, *10*(569). https://doi.org/10.3389/fimmu.2019.00569

Biassoni, R., Cantoni, C., Pende, D., Sivori, S., Parolini, S., Vitale, M., Bottino, C., & Moretta, A. (2001). Human natural killer cell receptors and co-receptors. *Immunological Reviews*, *181*(1), 203-214. https://doi.org/10.1034/j.1600-065x.2001.1810117.x

Bjorkstrom, N. K., Riese, P., Heuts, F., Andersson, S., Fauriat, C., Ivarsson, M. A., Bjorklund, A. T., Flodstrom-Tullberg, M., Michaelsson, J., Rottenberg, M. E., Guzman, C. A., Ljunggren, H. G., & Malmberg, K. J. (2010). Expression patterns of NKG2A, KIR, and CD57 define a process of CD56dim NK-cell differentiation uncoupled from NK-cell education. *Blood*, *116*(19), 3853-3864. https://doi.org/10.1182/blood-2010-04-281675

Bjørnsen, E. G., Thiruchelvam-Kyle, L., Hoelsbrekken, S. E., Henden, C., Saether, P. C., Boysen, P., Daws, M. R., & Dissen, E. (2019). B7H6 is a functional ligand for NKp30 in rat and cattle and determines NKp30 reactivity toward human cancer cell lines. *Eur J Immunol*, *49*(1), 54-65. https://doi.org/10.1002/eji.201847746

Borrego, F., Robertson, M. J., Ritz, J., Peña, J., & Solana, R. (1999). CD69 is a stimulatory receptor for natural killer cell and its cytotoxic effect is blocked by CD94 inhibitory receptor. Immunology, 97(1), 159–165. https://doi.org/10.1046/j.1365-2567.1999.00738.x

Bottino, C., Castriconi, R., Pende, D., Rivera, P., Nanni, M., Carnemolla, B., Cantoni, C., Grassi, J., Marcenaro, S., Reymond, N., Vitale, M., Moretta, L., Lopez, M., & Moretta, A. (2003). Identification of PVR (CD155) and Nectin-2 (CD112) as Cell Surface Ligands for the Human DNAM-1 (CD226) Activating Molecule. *The Journal of Experimental Medicine*, *198*(4), 557-567. https://doi.org/10.1084/jem.20030788

Bryceson, Y. T. (2006). Synergy among receptors on resting NK cells for the activation of natural cytotoxicity and cytokine secretion. *Blood*, *107*(1), 159-166. https://doi.org/10.1182/blood-2005-04-1351

Caligiuri, M. A. (1990). Functional consequences of interleukin 2 receptor expression on resting human lymphocytes. Identification of a novel natural killer cell subset with high affinity receptors. *171*(5), 1509-1526. https://doi.org/10.1084/jem.171.5.1509

Carlsten, M., Norell, H., Bryceson, Y. T., Poschke, I., Schedvins, K., Ljunggren, H. G., Kiessling, R., & Malmberg, K. J. (2009). Primary human tumor cells expressing CD155 impair tumor targeting by down-regulating DNAM-1 on NK cells. *J Immunol*, *183*(8), 4921-4930. https://doi.org/10.4049/jimmunol.0901226

Carrega, P., & Ferlazzo, G. (2012). Natural killer cell distribution and trafficking in human tissues. *Front Immunol*, *3*, 347. https://doi.org/10.3389/fimmu.2012.00347

Cerwenka, A., & Lanier, L. L. (2016). Natural killer cell memory in infection, inflammation and cancer. *Nature Reviews Immunology*, *16*(2), 112-123. https://doi.org/10.1038/nri.2015.9

Chaplin, D. D. (2010). Overview of the immune response. *Journal of Allergy and Clinical Immunology*, *125*(2), S3-S23. https://doi.org/10.1016/j.jaci.2009.12.980

Chlewicki, L. (2008). Response to Comment on "Molecular Basis of the Dual Functions of 2B4 (CD244)". *The Journal of Immunology*, *181*, 5181-5181. https://doi.org/10.4049/jimmunol.181.8.5181-a

Cichocki, F., Bjordahl, R., Gaidarova, S., Mahmood, S., Abujarour, R., Wang, H., Tuininga, K., Felices, M., Davis, Z. B., Bendzick, L., Clarke, R., Stokely, L.,

Rogers, P., Ge, M., Robinson, M., Rezner, B., Robbins, D. L., Lee, T. T., Kaufman, D. S., Miller, J. S. (2020). iPSC-derived NK cells maintain high cytotoxicity and enhance in vivo tumor control in concert with T cells and anti–PD-1 therapy. *Science Translational Medicine*, *12*(568), eaaz5618. https://doi.org/doi:10.1126/scitranslmed.aaz5618

Cichocki, F., Valamehr, B., Bjordahl, R., Zhang, B., Rezner, B., Rogers, P., Gaidarova, S., Moreno, S., Tuininga, K., Dougherty, P., McCullar, V., Howard, P., Sarhan, D., Taras, E., Schlums, H., Abbot, S., Shoemaker, D., Bryceson, Y. T., Blazar, B. R., . . . Miller, J. S. (2017). GSK3 Inhibition Drives Maturation of NK Cells and Enhances Their Antitumor Activity. *Cancer Res*, *77*(20), 5664-5675. https://doi.org/10.1158/0008-5472.Can-17-0799

Cooper, M. A., Elliott, J. M., Keyel, P. A., Yang, L., Carrero, J. A., & Yokoyama, W. M. (2009). Cytokine-induced memory-like natural killer cells. *Proceedings of the National Academy of Sciences*, *106*(6), 1915-1919. https://doi.org/10.1073/pnas.0813192106

Cooper, M. A., Fehniger, T. A., & Caligiuri, M. A. (2001). The biology of human natural killer-cell subsets. *Trends Immunol*, *22*(11), 633-640.

Cortez, A. J., Tudrej, P., Kujawa, K. A., & Lisowska, K. M. (2018). Advances in ovarian cancer therapy. *Cancer Chemotherapy and Pharmacology*, *81*(1), 17-38. https://doi.org/10.1007/s00280-017-3501-8

da Silva, R. F., Yoshida, A., Cardozo, D. M., Jales, R. M., Paust, S., Derchain, S., & Guimarães, F. (2017). Natural Killer Cells Response to IL-2 Stimulation Is Distinct between Ascites with the Presence or Absence of Malignant Cells in Ovarian Cancer Patients. *Int J Mol Sci*, *18*(5). https://doi.org/10.3390/ijms18050856

David, G., Morvan, M., Gagne, K., Kerdudou, N., Willem, C., Devys, A., Bonneville, M., Folléa, G., Bignon, J.-D., & Retière, C. (2009). Discrimination between the main activating and inhibitory killer cell immunoglobulin-like receptor positive natural killer cell subsets using newly characterized monoclonal antibodies. *Immunology*, *128*(2), 172-184. https://doi.org/10.1111/j.1365-2567.2009.03085.x

Decker, D. G., Fleming, T. R., Malkasian, G. D., Jr., Webb, M. J., Jeffries, J. A., & Edmonson, J. H. (1982). Cyclophosphamide plus cis-platinum in combination: treatment program for stage III or IV ovarian carcinoma. *Obstet Gynecol*, *60*(4), 481-487.

Dong, H. P., Elstrand, M. B., Holth, A., Silins, I., Berner, A., Trope, C. G., Davidson, B., & Risberg, B. (2006). NK- and B-Cell Infiltration Correlates With Worse Outcome in Metastatic Ovarian Carcinoma. *American Journal of Clinical Pathology*, *125*(3), 451-458. https://doi.org/10.1309/15b66dqmfyym78cj

Du, N., Guo, F., Wang, Y., & Cui, J. (2021). NK Cell Therapy: A Rising Star in Cancer Treatment. *Cancers (Basel)*, *13*(16). https://doi.org/10.3390/cancers13164129

Dunn, G. P., Old, L. J., & Schreiber, R. D. (2004). The Three Es of Cancer Immunoediting. *Annual Review of Immunology*, *22*(1), 329-360. https://doi.org/10.1146/annurev.immunol.22.012703.104803

Fauriat, C., Long, E. O., Ljunggren, H. G., & Bryceson, Y. T. (2010). Regulation of human NK-cell cytokine and chemokine production by target cell

recognition. *Blood*, *115*(11), 2167-2176. https://doi.org/10.1182/blood-2009-08-238469

Felices, M., Chu, S., Kodal, B., Bendzick, L., Ryan, C., Lenvik, A. J., Boylan, K. L. M., Wong, H. C., Skubitz, A. P. N., Miller, J. S., & Geller, M. A. (2017). IL-15 super-agonist (ALT-803) enhances natural killer (NK) cell function against ovarian cancer. *Gynecologic oncology*, *145*(3), 453-461. https://doi.org/10.1016/j.ygyno.2017.02.028

Figueras, A., Alsina-Sanchís, E., Lahiguera, Á., Abreu, M., Muinelo-Romay, L., Moreno-Bueno, G., Casanovas, O., Graupera, M., Matias-Guiu, X., Vidal, A., Villanueva, A., & Viñals, F. (2018). A Role for CXCR4 in Peritoneal and Hematogenous Ovarian Cancer Dissemination. *Mol Cancer Ther*, *17*(2), 532-543. https://doi.org/10.1158/1535-7163.Mct-17-0643

Freud, A. G., Becknell, B., Roychowdhury, S., Mao, H. C., Ferketich, A. K., Nuovo, G. J., Hughes, T. L., Marburger, T. B., Sung, J., Baiocchi, R. A., Guimond, M., & Caligiuri, M. A. (2005). A Human CD34(+) Subset Resides in Lymph Nodes and Differentiates into CD56bright Natural Killer Cells. *Immunity*, *22*(3), 295-304. https://doi.org/https://doi.org/10.1016/j.immuni.2005.01.013

Freud, A. G., & Caligiuri, M. A. (2006). Human natural killer cell development. *Immunological Reviews*, *214*(1), 56-72. https://doi.org/10.1111/j.1600-065x.2006.00451.x

Fujisaki, H., Kakuda, H., Shimasaki, N., Imai, C., Ma, J., Lockey, T., Eldridge, P., Leung, W. H., & Campana, D. (2009). Expansion of Highly Cytotoxic Human Natural Killer Cells for Cancer Cell Therapy. *Cancer Research*, *69*(9), 4010-4017. https://doi.org/10.1158/0008-5472.Can-08-3712

Galy, A., Travis, M., Cen, D., & Chen, B. (1995). Human T, B, natural killer, and dendritic cells arise from a common bone marrow progenitor cell subset. *3*(4), 459-473. https://doi.org/10.1016/1074-7613(95)90175-2

Geller, M. A., Cooley, S., Judson, P. L., Ghebre, R., Carson, L. F., Argenta, P. A., Jonson, A. L., Panoskaltsis-Mortari, A., Curtsinger, J., McKenna, D., Dusenbery, K., Bliss, R., Downs, L. S., & Miller, J. S. (2011). A phase II study of allogeneic natural killer cell therapy to treat patients with recurrent ovarian and breast cancer. *Cytotherapy*, *13*(1), 98-107. https://doi.org/10.3109/14653249.2010.515582

Glozak, M. A., & Seto, E. (2007). Histone deacetylases and cancer. *Oncogene*, *26*(37), 5420-5432. https://doi.org/10.1038/sj.onc.1210610

Gong, J. H., Maki, G., & Klingemann, H. G. (1994). Characterization of a human cell line (NK-92) with phenotypical and functional characteristics of activated natural killer cells. *Leukemia*, *8*(4), 652-658.

Gonzalez, V. D., Falconer, K., Bjorkstrom, N. K., Blom, K. G., Weiland, O., Ljunggren, H. G., Alaeus, A., & Sandberg, J. K. (2009). Expansion of functionally skewed CD56-negative NK cells in chronic hepatitis C virus infection: correlation with outcome of pegylated IFN-alpha and ribavirin treatment. *J Immunol*, *183*(10), 6612-6618. https://doi.org/10.4049/jimmunol.0901437

Goodell, C. A., Belisle, J. A., Gubbels, J. A., Migneault, M., Rancourt, C., Connor, J., Kunnimalaiyaan, M., Kravitz, R., Tucker, W., Zwick, M., & Patankar, M. S. (2009). Characterization of the tumor marker muc16 (ca125) expressed by murine ovarian tumor cell lines and identification of a panel of cross-reactive

monoclonal antibodies. *J Ovarian Res*, *2*(1), 8. https://doi.org/10.1186/1757-2215-2-8

Gowda, A., Roda, J., Hussain, S. R., Ramanunni, A., Joshi, T., Schmidt, S., Zhang, X., Lehman, A., Jarjoura, D., Carson, W. E., Kindsvogel, W., Cheney, C., Caligiuri, M. A., Tridandapani, S., Muthusamy, N., & Byrd, J. C. (2008). IL-21 mediates apoptosis through up-regulation of the BH3 family member BIM and enhances both direct and antibody-dependent cellular cytotoxicity in primary chronic lymphocytic leukemia cells in vitro. *Blood*, *111*(9), 4723-4730. https://doi.org/10.1182/blood-2007-07-099531

Grenga, I., Donahue, R. N., Lepone, L., Bame, J., Schlom, J., & Farsaci, B. (2014). PD-L1 and MHC-I expression in 19 human tumor cell lines and modulation by interferon-gamma treatment. *Journal for ImmunoTherapy of Cancer*, *2*(Suppl 3), P102. https://doi.org/10.1186/2051-1426-2-s3-p102

Greppi, M., Tabellini, G., Patrizi, O., Candiani, S., Decensi, A., Parolini, S., Sivori, S., Pesce, S., Paleari, L., & Marcenaro, E. (2019). Strengthening the AntiTumor NK Cell Function for the Treatment of Ovarian Cancer. *International Journal of Molecular Sciences*, *20*(4), 890. https://doi.org/10.3390/ijms20040890

Grewal, I. S. (2008). CD70 as a therapeutic target in human malignancies. *Expert Opin Ther Targets*, *12*(3), 341-351. https://doi.org/10.1517/14728222.12.3.341

Grimm, E. A. (1982). Lymphokine-activated killer cell phenomenon. Lysis of natural killer- resistant fresh solid tumor cells by interleukin 2-activated autologous human peripheral blood lymphocytes. *155*(6), 1823-1841. https://doi.org/10.1084/jem.155.6.1823

Groth, A., Klöss, S., Pogge Von Strandmann, E., Koehl, U., & Koch, J. (2011). Mechanisms of Tumor and Viral Immune Escape from Natural Killer Cell-Mediated Surveillance. *Journal of Innate Immunity*, *3*(4), 344-354. https://doi.org/10.1159/000327014

Gubbels, J. A. A., Felder, M., Horibata, S., Belisle, J. A., Kapur, A., Holden, H., Petrie, S., Migneault, M., Rancourt, C., Connor, J. P., & Patankar, M. S. (2010). MUC16 provides immune protection by inhibiting synapse formation between NK and ovarian tumor cells. *Molecular Cancer*, *9*(1), 11. https://doi.org/10.1186/1476-4598-9-11

Guma, M. (2004). Imprint of human cytomegalovirus infection on the NK cell receptor repertoire. *104*(12), 3664-3671. https://doi.org/10.1182/blood-2004-05-2058

Haller, O., & Wigzell, H. (1977). Suppression of natural killer cell activity with radioactive strontium: effector cells are marrow dependent. *J Immunol*, *118*(4), 1503-1506.

Hanahan, D., & Robert. (2011). Hallmarks of Cancer: The Next Generation. *Cell*, *144*(5), 646-674. https://doi.org/10.1016/j.cell.2011.02.013

He, Y., & Tian, Z. (2017). NK cell education via nonclassical MHC and non-MHC ligands. *Cellular & Molecular Immunology*, *14*(4), 321-330. https://doi.org/10.1038/cmi.2016.26

Herberman, R. B., Nunn, M. E., Holden, H. T., & Lavrin, D. H. (1975). Natural cytotoxic reactivity of mouse lymphoid cells against syngeneic and allogeneic

tumors. II. Characterization of effector cells. *International Journal of Cancer*, *16*(2), 230-239. https://doi.org/10.1002/ijc.2910160205

Hermanson, D. L., & Kaufman, D. S. (2015). Utilizing Chimeric Antigen Receptors to Direct Natural Killer Cell Activity. *6*. https://doi.org/10.3389/fimmu.2015.00195

Hoogstad-van Evert, J. S., Maas, R. J., van der Meer, J., Cany, J., van der Steen, S., Jansen, J. H., Miller, J. S., Bekkers, R., Hobo, W., Massuger, L., & Dolstra, H. (2018). Peritoneal NK cells are responsive to IL-15 and percentages are correlated with outcome in advanced ovarian cancer patients. *Oncotarget*, *9*(78), 34810-34820. https://doi.org/10.18632/oncotarget.26199

Horowitz, A., Strauss-Albee, D. M., Leipold, M., Kubo, J., Nemat-Gorgani, N., Dogan, O. C., Dekker, C. L., Mackey, S., Maecker, H., Swan, G. E., Davis, M. M., Norman, P. J., Guethlein, L. A., Desai, M., Parham, P., & Blish, C. A. (2013). Genetic and Environmental Determinants of Human NK Cell Diversity Revealed by Mass Cytometry. *Science Translational Medicine*, *5*(208), 208ra145-208ra145. https://doi.org/10.1126/scitranslmed.3006702

Hu, P.-F., Hultin, L. E., Hultin, P., Hausner, M. A., Hirji, K., Jewett, A., Bonavida, B., Detels, R., & Giorgi, J. V. (1995). Natural Killer Cell Immunodeficiency in HIV Disease is Manifest by Profoundly Decreased Numbers of CD16 + CD56+ Cells and Expansion of a Population of CD16dim CD56- Cells with Low Lytic Activity. *JAIDS Journal of Acquired Immune Deficiency Syndromes*, *10*(3), 331-340. https://journals.lww.com/jaids/Fulltext/1995/11000/Natural_Killer_Cell_Immunodeficiency_in_HIV.5.aspx

Huang, B., Sikorski, R., Sampath, P., & Thorne, S. H. (2011). Modulation of NKG2D-ligand cell surface expression enhances immune cell therapy of cancer. *Journal of immunotherapy (Hagerstown, Md. : 1997)*, *34*(3), 289-296. https://doi.org/10.1097/CJI.0b013e31820e1b0d

Iizuka, K., Naidenko, O. V., Plougastel, B. F. M., Fremont, D. H., & Yokoyama, W. M. (2003). Genetically linked C-type lectin-related ligands for the NKRP1 family of natural killer cell receptors. *4*(8), 801-807. https://doi.org/10.1038/ni954

Jacobs, R., Hintzen, G., Kemper, A., Beul, K., Kempf, S., Behrens, G., Sykora, K.-W., & Schmidt, R. E. (2001). CD56bright cells differ in their KIR repertoire and cytotoxic features from CD56dim NK cells. *European Journal of Immunology*, *31*(10), 3121-3126. https://doi.org/10.1002/1521-4141(2001010)31:10

Jacobs, R., Stoll, M., Stratmann, G., Leo, R., Link, H., & Schmidt, R. E. (1992). CD16-CD56+ natural killer cells after bone marrow transplantation. *Blood*, *79*(12), 3239-3244.

Jeung, I., Cheon, K., & Kim, M. R. (2016). Decreased Cytotoxicity of Peripheral and Peritoneal Natural Killer Cell in Endometriosis. BioMed research international, 2016, 2916070. https://doi.org/10.1155/2016/2916070

Juelke, K., Killig, M., Luetke-Eversloh, M., Parente, E., Gruen, J., Morandi, B., Ferlazzo, G., Thiel, A., Schmitt-Knosalla, I., & Romagnani, C. (2010). CD62L expression identifies a unique subset of polyfunctional CD56dim NK cells. *Blood*, *116*(8), 1299-1307. https://doi.org/10.1182/blood-2009-11-253286

Kaifu, T., Escalière, B., Gastinel, L. N., Vivier, E., & Baratin, M. (2011). B7-H6/NKp30 interaction: a mechanism of alerting NK cells against tumors. *Cellular and*

Molecular Life Sciences, *68*(21), 3531. https://doi.org/10.1007/s00018-011-0802-7

Kärre, K., Ljunggren, H. G., Piontek, G., & Kiessling, R. (1986). Selective rejection of H–2-deficient lymphoma variants suggests alternative immune defence strategy. *319*(6055), 675-678. https://doi.org/10.1038/319675a0

Kiessling, R., Klein, E., & Wigzell, H. (1975). „Natural" killer cells in the mouse. I. Cytotoxic cells with specificity for mouse Moloney leukemia cells. Specificity and distribution according to genotype. *European Journal of Immunology*, *5*(2), 112-117. https://doi.org/10.1002/eji.1830050208

Klapdor, R., Wang, S., Morgan, M., Dörk, T., Hacker, U., Hillemanns, P., Büning, H., & Schambach, A. (2019). Characterization of a Novel Third-Generation Anti-CD24-CAR against Ovarian Cancer. *Int J Mol Sci*, *20*(3). https://doi.org/10.3390/ijms20030660

Koh, J., Lee, S. B., Park, H., Lee, H. J., Cho, N. H., & Kim, J. (2012). Susceptibility of CD24(+) ovarian cancer cells to anti-cancer drugs and natural killer cells. *Biochem Biophys Res Commun*, *427*(2), 373-378. https://doi.org/10.1016/j.bbrc.2012.09.067

Kristiansen, G., Denkert, C., Schlüns, K., Dahl, E., Pilarsky, C., & Hauptmann, S. (2002). CD24 is expressed in ovarian cancer and is a new independent prognostic marker of patient survival. *Am J Pathol*, *161*(4), 1215-1221. https://doi.org/10.1016/s0002-9440(10)64398-2

Kumar, S. (2018). Natural killer cell cytotoxicity and its regulation by inhibitory receptors. *Immunology*, *154*(3), 383-393. https://doi.org/10.1111/imm.12921

Kumar, V. (1978). Mechanisms of genetic resistance to Friend virus leukemia in mice. IV. Identification of a gene (Fv-3) regulating immunosuppression in vitro, and its distinction from Fv-2 and genes regulating marrow allograft reactivity. *147*(2), 422-433. https://doi.org/10.1084/jem.147.2.422

Kweon, S., Phan, M.-T. T., Chun, S., Yu, H., Kim, J., Kim, S., Lee, J., Ali, A. K., Lee, S.-H., Kim, S.-K., Doh, J., & Cho, D. (2019). Expansion of Human NK Cells Using K562 Cells Expressing OX40 Ligand and Short Exposure to IL-21. *Frontiers in Immunology*, *10*. https://doi.org/10.3389/fimmu.2019.00879

Labani-Motlagh, A., Israelsson, P., Ottander, U., Lundin, E., Nagaev, I., Nagaeva, O., Dehlin, E., Baranov, V., & Mincheva-Nilsson, L. (2016). Differential expression of ligands for NKG2D and DNAM-1 receptors by epithelial ovarian cancer-derived exosomes and its influence on NK cell cytotoxicity. *Tumor Biology*, *37*(4), 5455-5466. https://doi.org/10.1007/s13277-015-4313-2

Lanier, L. L. (2005). NK cell recognition. *Annual Review of Immunology*, *23*(1), 225-274. https://doi.org/10.1146/annurev.immunol.23.021704.115526

Lanier, L. L. (2015). NKG2D Receptor and Its Ligands in Host Defense. *Cancer Immunology Research*, *3*(6), 575-582. https://doi.org/10.1158/2326-6066.cir-15-0098

Lanier, L. L., Le, A. M., Civin, C. I., Loken, M. R., & Phillips, J. H. (1986). The relationship of CD16 (Leu-11) and Leu-19 (NKH-1) antigen expression on human peripheral blood NK cells and cytotoxic T lymphocytes. *The Journal of Immunology*, *136*(12), 4480-4486. https://www.jimmunol.org/content/jimmunol/136/12/4480.full.pdf

Lanier, L. L., Le, A. M., Civin, C. I., Loken, M. R., & Phillips, J. H. (1986). The relationship of CD16 (Leu-11) and Leu-19 (NKH-1) antigen expression on human peripheral blood NK cells and cytotoxic T lymphocytes. *J Immunol*, *136*(12), 4480-4486. https://www.jimmunol.org/content/jimmunol/136/12/4480.full.pdf

Li, K., Mandai, M., Hamanishi, J., Matsumura, N., Suzuki, A., Yagi, H., Yamaguchi, K., Baba, T., Fujii, S., & Konishi, I. (2009). Clinical significance of the NKG2D ligands, MICA/B and ULBP2 in ovarian cancer: high expression of ULBP2 is an indicator of poor prognosis. *Cancer Immunology, Immunotherapy*, *58*(5), 641-652. https://doi.org/10.1007/s00262-008-0585-3

Li, Y., Hermanson, D. L., Moriarity, B. S., & Kaufman, D. S. (2018). Human iPSC-Derived Natural Killer Cells Engineered with Chimeric Antigen Receptors Enhance Anti-tumor Activity. *Cell Stem Cell*, *23*(2), 181-192.e185. https://doi.org/10.1016/j.stem.2018.06.002

Lian, G., Mak, T. S.-K., Yu, X., & Lan, H.-Y. (2022). Challenges and Recent Advances in NK Cell-Targeted Immunotherapies in Solid Tumors. *International Journal of Molecular Sciences*, *23*(1), 164. https://www.mdpi.com/1422-0067/23/1/164

Liu, B., Nash, J., Runowicz, C., Swede, H., Stevens, R., & Li, Z. (2010). Ovarian cancer immunotherapy: opportunities, progresses and challenges. *Journal of Hematology & Oncology*, *3*(1), 7. https://doi.org/10.1186/1756-8722-3-7

Liu, E., Marin, D., Banerjee, P., Macapinlac, H. A., Thompson, P., Basar, R., Nassif Kerbauy, L., Overman, B., Thall, P., Kaplan, M., Nandivada, V., Kaur, I., Nunez Cortes, A., Cao, K., Daher, M., Hosing, C., Cohen, E. N., Kebriaei, P., Mehta, R., . . . Rezvani, K. (2020). Use of CAR-Transduced Natural Killer Cells in CD19-Positive Lymphoid Tumors. *New England Journal of Medicine*, *382*(6), 545-553. https://doi.org/10.1056/NEJMoa1910607

Liu, N., Sheng, X., Liu, Y., Zhang, X., & Yu, J. (2013). Increased CD70 expression is associated with clinical resistance to cisplatin-based chemotherapy and poor survival in advanced ovarian carcinomas. *Onco Targets Ther*, *6*, 615-619. https://doi.org/10.2147/ott.S44445

Ljunggren, H.-G., & Kärre, K. (1990). In search of the 'missing self': MHC molecules and NK cell recognition. *11*, 237-244. https://doi.org/10.1016/0167-5699(90)90097-s

Lopez-Vergès, S., Milush, J. M., Pandey, S., York, V. A., Arakawa-Hoyt, J., Pircher, H., Norris, P. J., Nixon, D. F., & Lanier, L. L. (2010). CD57 defines a functionally distinct population of mature NK cells in the human CD56dimCD16+ NK-cell subset. *Blood*, *116*(19), 3865-3874. https://doi.org/10.1182/blood-2010-04-282301

Luevano, M., Daryouzeh, M., Alnabhan, R., Querol, S., Khakoo, S., Madrigal, A., & Saudemont, A. (2012). The unique profile of cord blood natural killer cells balances incomplete maturation and effective killing function upon activation. *Hum Immunol*, *73*(3), 248-257. https://doi.org/10.1016/j.humimm.2011.12.015

Lukesova, S., Vroblova, V., Tosner, J., Kopecky, J., Sedlakova, I., Čermáková, E., Vokurkova, D., & Kopecky, O. (2015). Comparative study of various subpopulations of cytotoxic cells in blood and ascites from patients with

ovarian carcinoma. *Contemporary oncology (Poznan, Poland)*, *19*(4), 290-299. https://doi.org/10.5114/wo.2015.54388

MacFarlane, A. W. t., Jillab, M., Plimack, E. R., Hudes, G. R., Uzzo, R. G., Litwin, S., Dulaimi, E., Al-Saleem, T., & Campbell, K. S. (2014). PD-1 expression on peripheral blood cells increases with stage in renal cell carcinoma patients and is rapidly reduced after surgical tumor resection. *Cancer Immunol Res*, *2*(4), 320-331. https://doi.org/10.1158/2326-6066.Cir-13-0133

Matos, M. E. (1993). Expression of a functional c-kit receptor on a subset of natural killer cells. *178*(3), 1079-1084. https://doi.org/10.1084/jem.178.3.1079

McArdel, S. L., Terhorst, C., & Sharpe, A. H. (2016). Roles of CD48 in regulating immunity and tolerance. *Clin Immunol*, *164*, 10-20. https://doi.org/10.1016/j.clim.2016.01.008

McGuire, W. P., Hoskins, W. J., Brady, M. F., Kucera, P. R., Partridge, E. E., Look, K. Y., Clarke-Pearson, D. L., & Davidson, M. (1996). Cyclophosphamide and cisplatin compared with paclitaxel and cisplatin in patients with stage III and stage IV ovarian cancer. *N Engl J Med*, *334*(1), 1-6. https://doi.org/10.1056/nejm199601043340101

Mehta, R. S., & Rezvani, K. (2018). Chimeric Antigen Receptor Expressing Natural Killer Cells for the Immunotherapy of Cancer. *Frontiers in Immunology*, *9*, 283-283. https://doi.org/10.3389/fimmu.2018.00283

Mingari, M. C., Vitale, C., Cantoni, C., Bellomo, R., Ponte, M., Schiavetti, F., Bertone, S., Moretta, A., & Moretta, L. (1997). Interleukin-15-induced maturation of human natural killer cells from early thymic precursors: selective expression of CD94/NKG2-A as the only HLA class I-specific inhibitory receptor. *27*(6), 1374-1380. https://doi.org/10.1002/eji.1830270612

Moretta, A., Bottino, C., Vitale, M., Pende, D., Cantoni, C., Mingari, M. C., Biassoni, R., & Moretta, L. (2001). Activating receptors and co-receptors involved in human natural killer cell-mediated cytolysis. *Annual Review of Immunology*, *19*(1), 197-223. https://doi.org/10.1146/annurev.immunol.19.1.197

Munger, W., Dejoy, S. Q., Jeyaseelan, R., Torley, L. W., Grabstein, K. H., Eisenmann, J., Paxton, R., Cox, T., Wick, M. M., & Kerwar, S. S. (1995). Studies Evaluating the Antitumor Activity and Toxicity of Interleukin-15, a New T Cell Growth Factor: Comparison with Interleukin-2. *Cellular Immunology*, *165*(2), 289-293. https://doi.org/https://doi.org/10.1006/cimm.1995.1216

Nersesian, S., Glazebrook, H., Toulany, J., Grantham, S. R., & Boudreau, J. E. (2019). Naturally Killing the Silent Killer: NK Cell-Based Immunotherapy for Ovarian Cancer. *Frontiers in Immunology*, *10*, 1782-1782. https://doi.org/10.3389/fimmu.2019.01782

Nham, T., Poznanski, S. M., Fan, I. Y., Shenouda, M. M., Chew, M. V., Lee, A. J., Vahedi, F., Karimi, Y., Butcher, M., Lee, D. A., Hirte, H., & Ashkar, A. A. (2018). Ex vivo-expanded NK cells from blood and ascites of ovarian cancer patients are cytotoxic against autologous primary ovarian cancer cells. *Cancer Immunol Immunother*, *67*(4), 575-587. https://doi.org/10.1007/s00262-017-2112-x

North, J., Bakhsh, I., Marden, C., Pittman, H., Addison, E., Navarrete, C., Anderson, R., & Lowdell, M. W. (2007). Tumor-Primed Human Natural Killer Cells Lyse NK-Resistant Tumor Targets: Evidence of a Two-Stage Process in Resting NK

Cell Activation. *The Journal of Immunology*, *178*(1), 85-94. https://doi.org/10.4049/jimmunol.178.1.85

O'Leary, J. G., Goodarzi, M., Drayton, D. L., & Von Andrian, U. H. (2006). T cell– and B cell–independent adaptive immunity mediated by natural killer cells. *7*(5), 507-516. https://doi.org/10.1038/ni1332

Okumura, G., Iguchi-Manaka, A., Murata, R., Yamashita-Kanemaru, Y., Shibuya, A., & Shibuya, K. (2020). Tumor-derived soluble CD155 inhibits DNAM-1-mediated antitumor activity of natural killer cells. *J Exp Med*, *217*(4), 1. https://doi.org/10.1084/jem.20191290

Oppenheim, D. E., Roberts, S. J., Clarke, S. L., Filler, R., Lewis, J. M., Tigelaar, R. E., Girardi, M., & Hayday, A. C. (2005). Sustained localized expression of ligand for the activating NKG2D receptor impairs natural cytotoxicity in vivo and reduces tumor immunosurveillance. *Nat Immunol*, *6*(9), 928-937. https://doi.org/10.1038/ni1239

Orange, J. S. (2008). Formation and function of the lytic NK-cell immunological synapse. *Nature reviews. Immunology*, *8*(9), 713-725. https://doi.org/10.1038/nri2381

Pal, M., Schwab, L., Yermakova, A., Mace, E. M., Claus, R., Krahl, A.-C., Woiterski, J., Hartwig, U. F., Orange, J. S., Handgretinger, R., & André, M. C. (2017). Tumor-priming converts NK cells to memory-like NK cells. *Oncoimmunology*, *6*(6), e1317411. https://doi.org/10.1080/2162402X.2017.1317411

Parodi, M., Raggi, F., Cangelosi, D., Manzini, C., Balsamo, M., Blengio, F., Eva, A., Varesio, L., Pietra, G., Moretta, L., Mingari, M. C., Vitale, M., & Bosco, M. C. (2018). Hypoxia Modifies the Transcriptome of Human NK Cells, Modulates Their Immunoregulatory Profile, and Influences NK Cell Subset Migration. *Frontiers in Immunology*, *9*. https://doi.org/10.3389/fimmu.2018.02358

Patankar, M. S., Jing, Y., Morrison, J. C., Belisle, J. A., Lattanzio, F. A., Deng, Y., Wong, N. K., Morris, H. R., Dell, A., & Clark, G. F. (2005). Potent suppression of natural killer cell response mediated by the ovarian tumor marker CA125. *Gynecologic oncology*, *99*(3), 704-713. https://doi.org/10.1016/j.ygyno.2005.07.030

Paust, S., Gill, H. S., Wang, B.-Z., Flynn, M. P., Moseman, E. A., Senman, B., Szczepanik, M., Telenti, A., Askenase, P. W., Compans, R. W., & Von Andrian, U. H. (2010). Critical role for the chemokine receptor CXCR6 in NK cell–mediated antigen-specific memory of haptens and viruses. *11*(12), 1127-1135. https://doi.org/10.1038/ni.1953

Pegram, H. J., Andrews, D. M., Smyth, M. J., Darcy, P. K., & Kershaw, M. H. (2011). Activating and inhibitory receptors of natural killer cells. *Immunology & Cell Biology*, *89*(2), 216-224. https://doi.org/https://doi.org/10.1038/icb.2010.78

Pende, D., Cantoni, C., Rivera, P., Vitale, M., Castriconi, R., Marcenaro, S., Nanni, M., Biassoni, R., Bottino, C., Moretta, A., & Moretta, L. (2001). Role of NKG2D in tumor cell lysis mediated by human NK cells: cooperation with natural cytotoxicity receptors and capability of recognizing tumors of nonepithelial origin. *European Journal of Immunology*, *31*(4), 1076-1086. https://doi.org/10.1002/1521-4141(200104)31:4<1076::Aid-immu1076>3.0.Co;2-y

Pesce, S., Greppi, M., Tabellini, G., Rampinelli, F., Parolini, S., Olive, D., Moretta, L., Moretta, A., & Marcenaro, E. (2017). Identification of a subset of human natural killer cells expressing high levels of programmed death 1: A phenotypic and functional characterization. *J Allergy Clin Immunol*, *139*(1), 335-346.e333. https://doi.org/10.1016/j.jaci.2016.04.025

Pesce, S., Tabellini, G., Cantoni, C., Patrizi, O., Coltrini, D., Rampinelli, F., Matta, J., Vivier, E., Moretta, A., Parolini, S., & Marcenaro, E. (2015). B7-H6-mediated downregulation of NKp30 in NK cells contributes to ovarian carcinoma immune escape. *Oncoimmunology*, *4*(4), e1001224. https://doi.org/10.1080/2162402x.2014.1001224

Poli, A., Michel, T., Theresine, M., Andres, E., Hentges, F., & Zimmer, J. (2009). CD56bright natural killer (NK) cells: an important NK cell subset. *Immunology*, *126*(4), 458-465. https://doi.org/10.1111/j.1365-2567.2008.03027.x

Rankin, E. B., & Giaccia, A. J. (2008). The role of hypoxia-inducible factors in tumorigenesis. *Cell Death & Differentiation*, *15*(4), 678-685. https://doi.org/10.1038/cdd.2008.21

Roda-Navarro, P., Vales-Gomez, M., Chisholm, S. E., & Reyburn, H. T. (2006). Transfer of NKG2D and MICB at the cytotoxic NK cell immune synapse correlates with a reduction in NK cell cytotoxic function. *Proceedings of the National Academy of Sciences*, *103*(30), 11258-11263. https://doi.org/doi:10.1073/pnas.0600721103

Romagnani, C., Juelke, K., Falco, M., Morandi, B., D'Agostino, A., Costa, R., Ratto, G., Forte, G., Carrega, P., Lui, G., Conte, R., Strowig, T., Moretta, A., Munz, C., Thiel, A., Moretta, L., & Ferlazzo, G. (2007). CD56brightCD16- Killer Ig-Like Receptor- NK Cells Display Longer Telomeres and Acquire Features of CD56dim NK Cells upon Activation. *178*(8), 4947-4955. https://doi.org/10.4049/jimmunol.178.8.4947

Romee, R., Leong, J. W., & Fehniger, T. A. (2014). Utilizing Cytokines to Function-Enable Human NK Cells for the Immunotherapy of Cancer. *Scientifica*, *2014*, 1-18. https://doi.org/10.1155/2014/205796

Romee, R., Schneider, S. E., Leong, J. W., Chase, J. M., Keppel, C. R., Sullivan, R. P., Cooper, M. A., & Fehniger, T. A. (2012). Cytokine activation induces human memory-like NK cells. *Blood*, *120*(24), 4751-4760. https://doi.org/10.1182/blood-2012-04-419283

Rosenberg, S. A., Lotze, M. T., Muul, L. M., Leitman, S., Chang, A. E., Ettinghausen, S. E., Matory, Y. L., Skibber, J. M., Shiloni, E., Vetto, J. T., Seipp, C. A., Simpson, C., & Reichert, C. M. (1985). Observations on the Systemic Administration of Autologous Lymphokine-Activated Killer Cells and Recombinant Interleukin-2 to Patients with Metastatic Cancer. *313*(23), 1485-1492. https://doi.org/10.1056/nejm198512053132327

Rossof, A. H., Talley, R. W., Stephens, R., Thigpen, T., Samson, M. K., Groppe, C., Jr., Eyre, H. J., & Fisher, R. (1979). Phase II evaluation of cis-dichlorodiammineplatinum(II) in advanced malignancies of the genitourinary and gynecologic organs: a Southwest Oncology Group Study. *Cancer Treat Rep*, *63*(9-10), 1557-1564.

Ruggeri, L., Capanni, M., Urbani, E., Perruccio, K., Shlomchik, W. D., Tosti, A., Posati, S., Rogaia, D., Frassoni, F., Aversa, F., Martelli, M. F., & Velardi, A. (2002). Effectiveness of Donor Natural Killer Cell Alloreactivity in Mismatched Hematopoietic Transplants. *Science*, *295*(5562), 2097-2100. https://doi.org/doi:10.1126/science.1068440

Ryan, M. C., Kostner, H., Gordon, K. A., Duniho, S., Sutherland, M. K., Yu, C., Kim, K. M., Nesterova, A., Anderson, M., McEarchern, J. A., Law, C. L., & Smith, L. M. (2010). Targeting pancreatic and ovarian carcinomas using the auristatin-based anti-CD70 antibody-drug conjugate SGN-75. *Br J Cancer*, *103*(5), 676-684. https://doi.org/10.1038/sj.bjc.6605816

Sabry, M., Tsirogianni, M., Bakhsh, I. A., North, J., Sivakumaran, J., Giannopoulos, K., Anderson, R., Mackinnon, S., & Lowdell, M. W. (2011). Leukemic priming of resting NK cells is killer Ig-like receptor independent but requires CD15-mediated CD2 ligation and natural cytotoxicity receptors. *J Immunol*, *187*(12), 6227-6234. https://doi.org/10.4049/jimmunol.1101640

Sabry, M., Zubiak, A., Hood, S. P., Simmonds, P., Arellano-Ballestero, H., Cournoyer, E., Mashar, M., Pockley, A. G., & Lowdell, M. W. (2019). Tumor- and cytokine-primed human natural killer cells exhibit distinct phenotypic and transcriptional signatures. *PLOS ONE*, *14*(6), e0218674. https://doi.org/10.1371/journal.pone.0218674

Sarkar, S., Germeraad, W. T. V., Rouschop, K. M. A., Steeghs, E. M. P., Gelder, M. V., Bos, G. M. J., & Wieten, L. (2013). Hypoxia Induced Impairment of NK Cell Cytotoxicity against Multiple Myeloma Can Be Overcome by IL-2 Activation of the NK Cells. *PLOS ONE*, *8*(5), e64835. https://doi.org/10.1371/journal.pone.0064835

Schmohl, J. U., Felices, M., Todhunter, D., Taras, E., Miller, J. S., & Vallera, D. A. (2016a). Tetraspecific scFv construct provides NK cell mediated ADCC and self-sustaining stimuli via insertion of IL-15 as a cross-linker. *Oncotarget; Vol 7, No 45*. https://www.oncotarget.com/article/12073/

Schmohl, J. U., Felices, M., Todhunter, D., Taras, E., Miller, J. S., & Vallera, D. A. (2016b). Tetraspecific scFv construct provides NK cell mediated ADCC and self-sustaining stimuli via insertion of IL-15 as a cross-linker. *Oncotarget*, *7*(45), 73830-73844. https://doi.org/10.18632/oncotarget.12073

Spits, H., Artis, D., Colonna, M., Diefenbach, A., Di Santo, J. P., Eberl, G., Koyasu, S., Locksley, R. M., McKenzie, A. N., Mebius, R. E., Powrie, F., & Vivier, E. (2013). Innate lymphoid cells--a proposal for uniform nomenclature. *Nat Rev Immunol*, *13*(2), 145-149. https://doi.org/10.1038/nri3365

Srpan, K., Ambrose, A., Karampatzakis, A., Saeed, M., Cartwright, A. N. R., Guldevall, K., De Matos, G., Önfelt, B., & Davis, D. M. (2018). Shedding of CD16 disassembles the NK cell immune synapse and boosts serial engagement of target cells. *J Cell Biol*, *217*(9), 3267-3283. https://doi.org/10.1083/jcb.201712085

Stewart, J. A., Belinson, J. L., Moore, A. L., Dorighi, J. A., Grant, B. W., Haugh, L. D., Roberts, J. D., Albertini, R. J., & Branda, R. F. (1990). Phase I trial of intraperitoneal recombinant interleukin-2/lymphokine-activated killer cells in patients with ovarian cancer. *Cancer Res*, *50*(19), 6302-6310.

Stuelten, C. H., Mertins, S. D., Busch, J. I., Gowens, M., Scudiero, D. A., Burkett, M. W., Hite, K. M., Alley, M., Hollingshead, M., Shoemaker, R. H., & Niederhuber, J. E. (2010). Complex Display of Putative Tumor Stem Cell Markers in the NCI60 Tumor Cell Line Panel. *Stem Cells*, *28*(4), 649-660. https://doi.org/https://doi.org/10.1002/stem.324

Suck, G., Odendahl, M., Nowakowska, P., Seidl, C., Wels, W. S., Klingemann, H. G., & Tonn, T. (2016). NK-92: an 'off-the-shelf therapeutic' for adoptive natural killer cell-based cancer immunotherapy. *Cancer Immunology, Immunotherapy*, *65*(4), 485-492. https://doi.org/10.1007/s00262-015-1761-x

Sun, J. C., Beilke, J. N., Bezman, N. A., & Lanier, L. L. (2011). Homeostatic proliferation generates long-lived natural killer cells that respond against viral infection. *The Journal of Experimental Medicine*, *208*(2), 357-368. https://doi.org/10.1084/jem.20100479

Sutherland, C. L., Rabinovich, B., Chalupny, N. J., Brawand, P., Miller, R., & Cosman, D. (2006). ULBPs, human ligands of the NKG2D receptor, stimulate tumor immunity with enhancement by IL-15. *Blood*, *108*(4), 1313-1319. https://doi.org/10.1182/blood-2005-11-011320

Taniguchi, R. T., Guzior, D., & Kumar, V. (2007). 2B4 inhibits NK-cell fratricide. *Blood*, *110*(6), 2020-2023. https://doi.org/10.1182/blood-2007-02-076927

Thigpen, T., Shingleton, H., Homesley, H., LaGasse, L., & Blessing, J. (1979). cis-Dichlorodiammineplatinum(II) in the treatment of gynecologic malignancies: phase II trials by the Gynecologic Oncology Group. *Cancer Treat Rep*, *63*(9-10), 1549-1555.

Tonn, T., Becker, S., Esser, R., Schwabe, D., & Seifried, E. (2001). Cellular immunotherapy of malignancies using the clonal natural killer cell line NK-92. *J Hematother Stem Cell Res*, *10*(4), 535-544. https://doi.org/10.1089/15258160152509145

Tonn, T., Schwabe, D., Klingemann, H. G., Becker, S., Esser, R., Koehl, U., Suttorp, M., Seifried, E., Ottmann, O. G., & Bug, G. (2013). Treatment of patients with advanced cancer with the natural killer cell line NK-92. *Cytotherapy*, *15*(12), 1563-1570.

Uppendahl, L. D., Felices, M., Bendzick, L., Ryan, C., Kodal, B., Hinderlie, P., Boylan, K. L. M., Skubitz, A. P. N., Miller, J. S., & Geller, M. A. (2019). Cytokine-induced memory-like natural killer cells have enhanced function, proliferation, and in vivo expansion against ovarian cancer cells. *Gynecologic oncology*, *153*(1), 149-157. https://doi.org/10.1016/j.ygyno.2019.01.006

Vallera, D. A., Felices, M., McElmurry, R., McCullar, V., Zhou, X., Schmohl, J. U., Zhang, B., Lenvik, A. J., Panoskaltsis-Mortari, A., Verneris, M. R., Tolar, J., Cooley, S., Weisdorf, D. J., Blazar, B. R., & Miller, J. S. (2016). IL15 Trispecific Killer Engagers (TriKE) Make Natural Killer Cells Specific to CD33+ Targets While Also Inducing Persistence, In Vivo Expansion, and Enhanced Function. *Clin Cancer Res*, *22*(14), 3440-3450. https://doi.org/10.1158/1078-0432.Ccr-15-2710

Velásquez, S. Y., Killian, D., Schulte, J., Sticht, C., Thiel, M., & Lindner, H. A. (2016). Short Term Hypoxia Synergizes with Interleukin 15 Priming in Driving Glycolytic Gene Transcription and Supports Human Natural Killer Cell

Activities. *Journal of Biological Chemistry*, *291*(25), 12960-12977. https://doi.org/10.1074/jbc.m116.721753

Vesely, M. D., Kershaw, M. H., Schreiber, R. D., & Smyth, M. J. (2011). Natural Innate and Adaptive Immunity to Cancer. *Annual Review of Immunology*, *29*(1), 235-271. https://doi.org/10.1146/annurev-immunol-031210-101324

Vilgelm, A. E., & Richmond, A. (2019). Chemokines Modulate Immune Surveillance in Tumorigenesis, Metastasis, and Response to Immunotherapy [Review]. *Frontiers in Immunology*, *10*. https://doi.org/10.3389/fimmu.2019.00333

Vossen, M. T., Matmati, M., Hertoghs, K. M., Baars, P. A., Gent, M. R., Leclercq, G., Hamann, J., Kuijpers, T. W., & van Lier, R. A. (2008). CD27 defines phenotypically and functionally different human NK cell subsets. *J Immunol*, *180*(6), 3739-3745. https://doi.org/10.4049/jimmunol.180.6.3739

Waldmann, T. A. (2015). The shared and contrasting roles of IL2 and IL15 in the life and death of normal and neoplastic lymphocytes: implications for cancer therapy. *Cancer Immunol Res*, *3*(3), 219-227. https://doi.org/10.1158/2326-6066.Cir-15-0009

Wang, L. (2019). Prognostic effect of programmed death-ligand 1 (PD-L1) in ovarian cancer: a systematic review, meta-analysis and bioinformatics study. *Journal of Ovarian Research*, *12*(1), 37. https://doi.org/10.1186/s13048-019-0512-6

Webb, J. R., Milne, K., Watson, P., deLeeuw, R. J., & Nelson, B. H. (2014). Tumor-Infiltrating Lymphocytes Expressing the Tissue Resident Memory Marker CD103 Are Associated with Increased Survival in High-Grade Serous Ovarian Cancer. *Clinical Cancer Research*, *20*(2), 434-444. https://doi.org/10.1158/1078-0432.Ccr-13-1877

Welte, S., Kuttruff, S., Waldhauer, I., & Steinle, A. (2006). Mutual activation of natural killer cells and monocytes mediated by NKp80-AICL interaction. *7*(12), 1334-1342. https://doi.org/10.1038/ni1402

Wendt, K., Wilk, E., Buyny, S., Buer, J., Schmidt, R. E., & Jacobs, R. (2006). Gene and protein characteristics reflect functional diversity of CD56dim and CD56bright NK cells. *Journal of Leukocyte Biology*, *80*(6), 1529-1541. https://doi.org/10.1189/jlb.0306191

Wiltshaw, E., Evans, B., Jones, A., Baker, J., & Calvert, A. H. (1983). JM8, successor to cisplatin in advanced ovarian carcinoma? *The Lancet*, *321*(8324), 587.

Zhang, L., Conejo-Garcia, J. R., Katsaros, D., Gimotty, P. A., Massobrio, M., Regnani, G., Makrigiannakis, A., Gray, H., Schlienger, K., Liebman, M. N., Rubin, S. C., & Coukos, G. (2003). Intratumoral T Cells, Recurrence, and Survival in Epithelial Ovarian Cancer. *New England Journal of Medicine*, *348*(3), 203-213. https://doi.org/10.1056/nejmoa020177

Zhang, T., Scott, J. M., Hwang, I., & Kim, S. (2013). Cutting Edge: Antibody-Dependent Memory-like NK Cells Distinguished by FcR Deficiency. *190*(4), 1402-1406. https://doi.org/10.4049/jimmunol.1203034